The Role of eEF1A2 in the Pathogenesis of Motor Neurone Disease in Wasted Mice

Permphan Dharmasaroja

Doctor of Philosophy

The University of Edinburgh

2007

Contents

List of Figures

List of Tables

Declaration

I declare that this thesis has been composed by myself, and that all the work is my own unless otherwise clearly stated.

Permphan Dharmasaroja.

Acknowledgements

I wish to express my sincere gratitude to everyone who has helped and contributed to this thesis in one way or another. I would especially like to thank my supervisor, Dr. Cathy Abbott, for taking me on as a PhD student at Medical Genetics Section, Molecular Medicine Centre. Her contribution to this thesis has been incredible valuable due to her continuous support and important scientific input. I would like to thank my second supervisor, Professor Richard Ribchester for his expertise in fluorescence imaging and analysis, and giving me the opportunity to do experiments at the Division of Neuroscience. I would like to thank Helen Newbery for teaching me several laboratory methods and animal handling at the animal house. Also, I would like to thank Julia Boyd for her considerable assistance in cloning methods.

I would like to thank Tom Gillingwater at the Division of Neurosciene for his assistance, with great skill, in microdissection and a confocal microscope. For all work at the Transgenic unit, I would like to thank Brendan Doe for all helps, and would particularly like to thank all staff. I would also like to thank Laura Lettice for her equipment in preparation of DNA constructs.

I would particularly like to thank all the members of Abbott's group – Jean, Vicky, Vicki, Miriam, Jan, especially You-Ying for sharing experience and her creating a cheerful atmosphere; all former and present colleagues at Medical Genetics Section – Launa McClaren, Sebby, Ann, Susan, Heather, Helen, and Rosemary. Thanks to Dr. Ben Pickard for technical assistance in fluorescence microscope, and to Abby for using a cryostat. I would like to thank Professor David Porteous, Head of the Centre, for his suggestion on my project. Also many thanks to everyone on the third floor, Sir Alastair Curie Cancer Research Laboratories, including Professor David Melton, Professor Martin Hooper, Scott, Rebecca, and others for scientific discussion, and particularly to Alexey for interesting discussions and answering my questions about real-time RT-PCR.

Thanks to all other former and present PhD students for informal scientific discussions and for creating a great work environment – Simon, Jennifer, Andrea,

Ian, Launa, Nicola, Kristina, Oliver, and Song, also thanks to all members of Molecular Medicine Centre for their non-scientific contribution and all pleasant time inside the building.

In addition to Cathy's grant, this work was supported by a grant from the Office of Educational Affairs of Thailand. I personally thank to Associate Professor Jittipan Chavadej of Department of Anatomy, Faculty of Science, Mahidol University, Thailand, for her effort to find this scholarship for me.

Abstract

Motor neurone disease (MND) or amyotrophic lateral sclerosis (ALS) is a devastating disorder of the anterior horn cells of the spinal cord and the motor cranial nuclei that leads to progressive muscle weakness and atrophy. Involvement of both upper and lower motor neurons is characteristic. Major recent advances have shed light on its etiology, the key mechanisms in both familial and sporadic ALS, however, remain unknown. Although the SOD1 (G93A) mutant transgenic mouse model is widely used as a tool to study the pathogenesis and investigate therapeutic strategy, cure for ALS has not been discovered. More mouse models of ALS are needed. Mice with the autosomal recessive gene wasted (*wst*) develop a set of neurological features that include progressive muscle wasting, weight loss, progressive paralysis, and degeneration of motor neurones in spinal cord and brainstem. The wasted mutation is caused by a 15.8-kilobase deletion that completely abolishes the detectable expression of eukaryotic elongation factor 1A2 (eEF1A2), a tissue-specific protein that expresses only in nervous system, heart and skeletal muscle. In this PhD thesis, I describe the characterization of neuromuscular abnormalities of wasted mice and study expression of nerve-regulated genes using real-time RT-PCR. Muscle of wasted mice showed evidence of denervation atrophy, and the patterns of gene expression were characteristic for the type of denervation. I have constructed an epitope-tagged eEF1A2 plasmid and studied colocalisation of eEF1A2 and spinal motor neurone (SMN) protein in HeLa cells, using quantitative immunocolocalisation analysis. I have shown that a proportion of cytoplasmic eEF1A2 colocalises with SMN. To study the role or eEF1A2, I have constructed a muscle-specific transgene and generated transgenic homozygous wasted mice that specifically express human eEF1A2 in skeletal muscle, but not in neurones. Transgenic wasted mice showed the same phenotype as spontaneous mutant wasted mice. Muscle pathology and the patterns of gene expression were compatible with denervation. These findings suggest that the loss of eEF1A2 in motor neurone, but not muscle, leads to muscle atrophy in wasted mice.

Abbreviations and Symbols

AGE	advanced glycated end products
ALS	amyotrophic lateral sclerosis
AMPA	α-amino-3-hydroxy-5-methyl-4-isoxazole propionic acid
AMPS	ammonium persulphate
AMV	avian myeloblastosis virus
APEX	apurinic/apyrimidine endonuclease
APOE	apolipoprotein E
ATPase	adenosine triphosphatase
bp	base pair
BSA	bovine serum albumin
BTX	botulinum toxin
CCS	copper chaperone for SOD1
Cdks	Cyclin-dependent kinases
ClC-1	muscular chloride channel type 1
CNS	central nervous system
DAB	diaminobenzidene
DAPI	4',6-Diamino-2-phenylindole dihydrochloride
DEPC	diethyl pyrocarbonate
DHPLC	denaturing high performance liquid chromatography
DMEM	Dulbecco's Modified Eagle Medium
DMSO	dimethyl sulphoxide
dNTPs	deoxynucleotide triphosphates
DNA	deoxyribonucleic acid
EAAT	excitatory amino acid transporter
ECL	enhanced chemiluminesence
EDTA	ethylenediamenetetraacetic acid
Eef1a1	eukaryotic elongation factor 1A1 (mouse gene)
EEF1A1	eukaryotic elongation factor 1A1 (human gene)
Eef1a2	eukaryotic elongation factor 1A2 (mouse gene)
EEF1A2	eukaryotic elongation factor 1A2 (human gene)
eEF1A1	eukaryotic elongation factor 1A1 (protein)
eEF1A2	eukaryotic elongation factor 1A2 (protein)
EGF	epidermal growth factor
eIF2B	eukaryotic initiation factor 2B
ELISA	enzyme-linked immunosorbent assay
FITC	fluorescein isothiocyanate
FKHR	forkhead
FOXO	fork-head box O
FTD	frontotemporal dementia
g	gram
Gapdh	glyceraldehyde-3-phosphate dehydrogenase (mouse gene)
GAPDH	glyceraldehyde-3-phosphate dehydrogenase (protein)
GDP	guanosine diphosphate
GEF	guanine exchange factor
GFAP	glial fibrillary acidic protein

GTP	guanosine triphosphate
H&E	haematoxylin and eosin
HRP	horse radish peroxidase
HSA	human alpha-skeletal actin
HSP	hereditary spastic paraplegia
ICA	intensity correlation analysis
ICQ	intensity correlation quotient
IGF-1	insulin-like growth factor-1
kb	kilobase pair
kDa	kilodaltons
mAChR	muscarinic acetylcholine receptor
MAFbx	muscle atrophy F box
MAP2	microtubule-associated protein 2
MAPT	microtubule-associated protein tau
mg	milligram
MND	motor neuron(e) disease
mnd	motor neuron degeneration
MRF	myogenic regulatory factor
mRNA	messenger ribonucleic acid
mTOR	mammalian target of rapamycin
MuRF	muscle ring finger-1
NA	not available
nAchR	nicotinic acetylcholine receptor
NADH	nicotinamide adenine dinucleotide
NAIP	neuronal apoptosis inhibitory protein
NF-H	neurofilament (heavy chain) (protein)
NF-L	neurofilament (light chain)
NF-M	neurofilament (medium chain)
ng	nanogram
NGF	nerve growth factor
NIH	National Institutes of Health
NMDA	N-methyl-D-aspartate
NMJ	neuromuscular junction
nmd	neuromuscular degeneration
NSE	neuron-specific enolase
OXPHOS	oxidative phosphorylation
PBS	phosphate-buffered saline
PCR	polymerase chain reaction
PDM	product of the differences from mean
PI3-K	phosphoinositide-3 kinase
PKB	protein kinase B
PKCa	protein kinase C alpha
pmn	progressive motor neuronopathy
PLS	primary lateral sclerosis
PMA	progressive muscular atrophy
PVDF	polyvinylidene difluoride
rpm	revolutions per minute
RNP	ribonucleoprotein
RT	reverse transcriptase
SD	standard deviation

SDH	succinic dehydrogenase
SDS	sodium dodecyl sulphate
SEM	standard error of mean
SHIRPA	SmithKline/Harwell/Imperial College/Royal/ Hospital/Phynotye Assessment
SMA	spinal muscular atrophy
SMN	survival motor neuron
SOD1	superoxide dismutase
SV2	synaptic vesicle protein
TA	tibialis anterior muscle
Taq	*Thermus aquaticus*
TBE	tris-borate-EDTA
TBS	tris buffered saline
TEAA	triethylammonium acetate
TEMED	N,N,N',N'-tetramethylethylenediamine
TRITC	tetramethylrhodamine isothiocyanate
UTR	untranslated region
VDAC	voltage-dependent anion channel
VEGF	vascular endothelial growth factor
wr	wobbler
wst	wasted
ZPR1	zinc finger protein

Chapter 1 Introduction

1.1 Introduction

1.1.1 Motor Neurone Disease

Motor neurone disease (MND) is also known as Lou Gehrig's disease or amyotrophic lateral sclerosis (ALS). The progressive degeneration of upper and lower motor neurones is the pathological hallmark of this disease and clinical signs reflect this. When cortical (upper) motor neurones are involved, the weakness is associated with spasticity and stiffness of movement. When spinal (lower) motor neurones are first involved, the weakness arises from denervation of the affected muscles and is associated with muscle twitching (fasciculations) and then muscle atrophy. Regardless of the site of onset, the striking and devastating aspect of the illness is that it migrates ultimately to involve virtually all of the motor neurones. Upper motor neurone signs may disappear as the lower motor neurone weakness progresses. Sensory and cognitive functions are not affected and certain motor neurone groups, including those in the oculomotor (Hughes, 1982) and Onuf's nuclei (Mannen *et al.*, 1977), are also spared. Progressive motor neurone degeneration leads to paralysis and death, usually from respiratory failure, after around three years. Up to 50% of motor neurones may have degenerated before clinical signs appear (Hansen and Ballantyne, 1978). Roland suggested using the plural form, "motor neurone diseases", to describe all of the diseases of the motor system and the anterior horn cells, including spinal muscular atrophy (SMA) (Rowland, 1982). Spinal muscular atrophy is clinically and pathologically distinct from ALS itself.

1.1.2 Spinal Muscular Atrophy

Current classification of the form of SMA that has been mapped to chromosome 5q13 is based on clinical criteria, although the genotype-phenotype correlation is close to being established (Brahe, 2000). Severe SMA (SMA type I, Werdnig-Hoffmann disease, acute

SMA) is characterized by onset before 6 months of age, failure to achieve sitting without support, and life expectancy of 2 years or less. SMA type II (chronic SMA) is usually symptomatic between ages 6 months and 18 months, but may start earlier. SMA type III (juvenile SMA, Kugelberg-Welander disease) becomes symptomatic after 18 months. Life expectancy is into the sixth decade of life. Some forms of MND are linked to chromosome 5 and, thus, have been labelled SMA type IV (Moulard *et al.*, 1998). Poor muscle tone, muscle weakness, and lack of motor development are major clinical manifestations of SMA type I. Ocular muscles are spared. The heart is normal. Fasciculations are also present. A postural tremor of fingers is seen inevitably in SMA type II, but only occasionally in SMA type I. SMA type III shows proximal muscle weakness; the legs are more severely affected than the arms. As with SMA type I and type II, the absence of tendon reflexes in most cases completes the clinical picture. SMA type IV refers to "adult" onset of muscle weakness. The physical examination is similar to that described for SMA type III.

1.1.3 Epidemiology

ALS has a prevalence rate of about 4 per 100,000 and an annual incidence rate of about 1 to 1.5 per 100,000. The incidence increases with age with a peak occurrence between 55 to 75 years of age, and occurs predominantly in men with a male-to-female ratio of about 2:1. The average survival period after onset of symptoms is about 3 to 5 years. The incidence of ALS is higher in the Western Pacific than in other areas of the world. There are 3 major foci: the Chamorro people on the Islands of Guam, Rota, and Tinian; Japanese villagers on the Kii Peninsula of Honshu Island in Japan; the people living in West New Guinea in Indonesia. Genetic factors did not play a role in the Western Pacific ALS, and now the environmental factors, including excitotoxin from the cycad seed and mineral imbalances in the soil and water, are being studied as possible causes (Yanagihara *et al.*, 1984; Spencer *et al.*, 1987a; Spencer *et al.*, 1987a). Based on the genetic information available, ALS has been grossly divided into 2 categories: sporadic

ALS (SALS) and familial ALS (FALS). Up to 10% of all ALS cases are familial (Mulder *et al.*, 1986).

For SMA, rigorous epidemiological studies reveal that the gene frequency is higher than originally thought. In Italy the incidence was 7.8 per 100,000 live births, giving a carrier frequency of 1 in 57. The acute or severe form occurred in 4.1 per 100,000 live births (Mostacciuolo *et al.*, 1992). A 1992 study from Germany showed that the incidence was 10 per 100,000 with a carrier rate of 1 in 50 (Thieme *et al.*, 1993). Data from Iceland is consistent with the above studies (Ludvigsson *et al.*, 1999).

1.1.4 Pathology

The pathological hallmark of ALS is degeneration of large pyramidal neurones in the motor cortex and associated corticospinal tracts (Wong *et al.*, 1998). Lower motor neurones originating in the brainstem nuclei and spinal cord anterior horn are also affected. In most cases, motor neurones appear to undergo a process of involution or shrinkage, losing volume in both cytoplasm and nucleus. Muscle biopsy reveals denervation atrophy (Martin *et al.*, 2000). "Amyotrophy" refers to neurogenic atrophy of affected muscle groups; "lateral sclerosis" refers to the hardness to palpation of the lateral columns of the spinal cord, where gliosis follows degeneration of the lateral corticospinal tracts. Weakness and muscle atrophy are a consequence of large α motor neurones in the brainstem and spinal cord. Among the earliest pathological changes in the dying motor neurones is the appearance of fine wisps of ubiquitin-positive threads or skeins (Leigh *et al.*, 1988). Other intraneuronal inclusions are also seen in degenerating neurones and glia. These are Bunina bodies, Lewy-like bodies, congomerate hyaline inclusions, and advanced glycated end products (AGE) (Chou *et al.*, 1998; Kikuchi *et al.*, 2000). Phosphorylated and nonphosphorylated neurofilaments are components of congomerate hyaline inclusions. AGEs contain ubiquitin, phosphorylated neurofilament, and superoxide dismutase I (SOD I). Mitochondrial abnormalities have been found in

ALS patients (Borthwick *et al.*, 1999; Beal, 2000). A case of MND that was associated with mutations in mitochondrial DNA has been reported (Comi *et al.*, 1998). Fragmentation of Golgi apparatus is also found in some patients with ALS (Gonatas *et al.*, 1998).

SMA selectively affects the α motor neurones in the spinal cord (Davies *et al.*, 1991). The brain cortex is unaffected. Autopsy reveals a decreased number of motor neurones and gliosis in the anterior horn of the spinal cord as well as decreased numbers of lower cranial motor neurones, and changes in muscle biopsy are also of acute and chronic denervation (Hausmanowa-Petrusewicz *et al.*, 1980). In addition, muscle biopsy reveals group atrophy of type 1 and type 2 muscle fibres as opposed to the normal checkerboard pattern, and shows features of muscle immaturity, suggesting an arrest in development (Engel, 1970; Fidzianska, 1971). Rare angulated and large type 1 fibres are scattered throughout. In the early stages of the disease, the biopsy may show universally small fibres, with type 1 fibres being smaller than type 2, making the histological diagnosis difficult (Iannaccone *et al.*, 1987; Dubowitz, 1991).

1.2 Aetiology

1.2.1 Aetiology of Amyotrophic Lateral Sclerosis

The causes of ALS have been elusive. These include the involvement of environmental factors, viral infection, autoimmune phenomena, cytoskeletal abnormalities, loss of trophic factors, oxidative stress and excitotoxicity. Genetic factors also contribute to its causes.

1.2.1.1 Genetic Factors

Familial clustering of ALS has been recognized for many years. In some of these families, there is clear evidence of autosomal dominant inheritance and rarely of autosomal recessive inheritance. Identification of mutations in the gene encoding Cu/Zn superoxide dismutase 1 (SOD1) on chromosome 21 in 1993 is a breakthrough (Rosen *et al.*, 1993). SOD1, accounting for approximately 1% of total brain protein, is a copper and zinc dependent, cytoplasmic enzyme. The structural gene is located on chromosome 21q22.1 (Siddique *et al.*, 1991).Linkage studies performed in families with ALS led to a peak multipoint lod score of 6.1 for a subset of 23 families linked to chromosome 21 (Figlewicz *et al.*, 1994b). More than 100 different mutations have been identified in the SOD gene (Parton *et al.*, 2002), which may account for around 20% of all FALS (Siddique *et al.*, 1996). Most of the mutations are missense point mutation. A4V-SOD1 is the most common SOD1 mutation. Almost all of SOD1 mutations are dominant, except for D90A-SOD1, which can be either recessive or dominant (Andersen *et al.*, 1997; Al-Chalabi *et al.*, 1998). The remaining 80% are caused by mutations in other genes. Five per cent of SALS also have SOD1 mutations. Different heterozygous mutations in SOD1 gene cause distinct clinical manifestations and histopathology. For example, in patients with A4V-SOD1 mutation, the corticospinal tracts are spared (Cudkowicz *et al.*, 1998; Rowland, 1998).

1.2.1.1.1 Molecular Genetics of Autosomal Dominant ALS

Autosomal dominant forms of ALS include ALS1, ALS3, and ALS4. SOD1 mutation in the region 21q22, causing ALS1 (Siddique *et al.*, 1991), only accounts for approximately 20% of all FALS and about 3% of SALS (Jackson *et al.*, 1997; Shaw *et al.*, 1998). However, dominant mutations are unlikely to cause enzyme deficiencies due to the compensatory allele, and a correlation between disease severity and the level of enzyme activity has not been established (Esteban *et al.*, 1994; Sjalander *et al.*, 1995). Knock-out mice, homozygous for SOD1 deletions, are unaffected by motor neurone disease (Reaume *et al.*, 1996), while mice overexpressing human SOD1 mutations

develop motor neurone disease despite having higher SOD1 enzyme activity than their nontransgenic littermates (Gurney *et al.*, 1994). These evidences suggest that SOD1 mutations might produce an unknown toxic gain of function rather than an enzymatic deficiency in the pathogenesis of ALS. Adult-onset autosomal dominant FALS neither linked to chromosome 21 nor associated with SOD1 mutations is designated as ALS3 (Siddique *et al.*, 1991), and its locus is identified on chromosome 18q (Hand *et al.*, 2002). Juvenile-onset ALS with dominant inheritance and no bulbar involvement, ALS4, has been mapped to chromosome 9q34 (Chance *et al.*, 1998). Patients with ALS4 are associated with slowly progressive distal muscle weakness and atrophy and their life expectancy can be very long (Rabin *et al.*, 1999).

Dominant ALS with frontotemporal dementia (ALS/FTD) has been mapped to chromosome 9q21-22 (Hosler *et al.*, 2000). Another ALS/FTD, which includes parkinsonism, is caused by mutations in the tau gene on chromosome 17q21 (Lynch *et al.*, 1994). X-linked dominant ALS is mapped to chromosome Xp11-Xq12 (Cole and Siddique, 1999).

1.2.1.1.2 Molecular Genetics of Autosomal Recessive ALS

There are three forms of autosomal recessive, juvenile-onset ALS. Type 1 (ALS5) is the most prevalent form and has been linked to chromosome 15q15.1-q21.1 (Hentati *et al.*, 1998). Families with ALS5 have onset between 8 and 18 years, with both upper and lower motor neurone signs, fasciculations and atrophy of tongue, and occasionally, mild mental retardation. Type 3 recessive ALS (ALS2) is linked to chromosome 2q33-q34 (Hentati *et al.*, 1994; Hadano *et al.*, 2001b). The gene has been identified and its 184 kD protein product is call alsin, encoded by gene designated ALS2CR6 (Hadano *et al.*, 2001b; Yang *et al.*, 2001). Patients with ALS2 have onset between 3 and 23 years, and are characterized by spastic gait, distal muscle weakness and atrophy. Due to structural similarity with other proteins, alsin is speculated to act as a regulator/activator of

particular proteins that modulate microtubule assembly, membrane organization and trafficking in cells, including neurones (Hadano *et al.*, 2001a). ALS2CR6 is found in neuronal cells throughout the brain and spinal cord, particularly in neurones in the hippocampus and dentate gyrus, cerebellum, Purkinje cells, neurones in the cerebral cortex and spinal grey matter including anterior horn cells. Two independent deletion mutations in ALS2 result in frameshifts that generate premature stop codons (Hadano *et al.*, 2001b). In this form of ALS, two copies of mutant gene must be present, and therefore these mutations are likely to result in loss of function. The protein product of this gene is found in all cell types, including motor neurones, however its normal function is currently unknown. Families that are not linked to chromosome 15q or 2q are classified as type 2 (Hentati *et al.*, 1998).

1.2.1.1.3 Other candidate genes in ALS

Other candidate genes have been tested for a role in ALS pathogenesis. The other isoforms of SOD, SOD2 and SOD3, are not linked to ALS (de Belleroche *et al.*, 1995; Siddique and Deng, 1996). The neurofilament heavy subunit tail domain has been shown to harbor a small set of in-frame deletions and insertions in SALS patients, and one FALS patient also had a 14-amino-acid deletion (Al-Chalabi *et al.*, 1999). But because only 1% of ALS patients have these mutations, mutations in neurofilament heavy chain subunit are considered to be a risk factor rather than a major cause of disease (Figlewicz *et al.*, 1994a; Al-Chalabi *et al.*, 1999). Overexpression of peripherin, a component of intermediate filament protein associated with degenerating motor neurones in SALS, in mice provokes degeneration of motor axons (Beaulieu *et al.*, 1999; Beaulieu and Julien, 2003; Robertson *et al.*, 2003). Apolipoprotein E (APOE) genotypes have been studied as a risk factor, with a suggestion of APOE4 being more common in bulbar onset and with early onset of disease (Al-Chalabi *et al.*, 1996). An out-of-frame mutations of the mitochondrial DNA-encoded subunit I of cytochrome c oxidase has been reported in a patient with motor neurone-like degeneration (Comi *et al.*, 1998). A homozygous neuronal apoptosis inhibitory polypeptide (NAIP) mutation on chromosome 5q13 has

been reported in a sporadic case of ALS (Jackson *et al.*, 1996). Mutations in the apurinic/apyrimidine endonuclease (APEX nuclease) gene are also reported in ALS patients (Olkowski, 1998). The APEX nuclease is a DNA repair enzyme. A significant linkage disequilibrium for one common polymorphic locus in the APEX nuclease gene between ALS and control subjects has been shown (Hayward *et al.*, 1999). Mutant glial glutamate transporter (EAAT2) mRNA was reported in brain, spinal cord, and cerebrospinal fluid of up to 60% of patients with SALS, and was suggested as a result of abnormal RNA processing (Lin *et al.*, 1998). However, reports of similar splice variants in normal subjects make this difficult to interpret (Nagai *et al.*, 1998; Meyer *et al.*,1999). The survival motor neurone (SMN) locus has been implicated in the modification of mutant SOD1 disease in a transgenic mouse, a modification that delays disease onset significantly (Kunst *et al.*, 2000). Sixteen per cent of ALS patients have an abnormal number of SMN1 gene (1 or 3 copies), compared with 4% in controls, suggesting an abnormal SMN1 gene locus may be a susceptibility factor for ALS (Corcia *et al.*, 2002).

Vascular endothelial growth factor (VEGF) has been reported to be a modifier of $SOD1^{G93A}$ mice, and protects motor neurones against ischemic death (Lambrechts *et al.*, 2003). VEGF is an important angiogenesis factor expressed in several tissues and is rapidly upregulated during hypoxia (Carmeliet, 2000). A discrete deletion in the *VEGF* 5'-UTR predisposed a subset of the knockout mice to adult-onset progressive motor neurone degeneration, with some neuropathologic and clinical signs reminiscent of human motor neurone degeneration (Oosthuyse *et al.*, 2001). A case-control meta-analysis of four European populations demonstrated an association of three polymorphisms in the 5'-UTR, known to affect *VEGF* expression, with SALS (Lambrechts *et al.*, 2003). However, a recent study, comprising a large number of family-based and case-control samples, demonstrated a lack of association of the *VEGF* polymorphisms with SALS (Chen *et al.*, 2006).

1.2.2 Aetiology of Spinal Muscular Atrophy

All cases of SMA linked to chromosome 5 are genetic. Many of the variants are also genetic but linked to other chromosome. The gene locus of SMA type I, II, and III was mapped to chromosome 5q in 1990, using linkage studies (Brzustowicz *et al.*, 1990). A first gene of SMA was isolated in 1995 and was given the name SMN gene (Lefebvre *et al.*, 1995). The second gene known as NAIP gene was found to be deleted in 68% of SMA type I, but in only 2% in cases of SMA type II and III (Roy *et al.*, 1995). The third gene, BTF2p44 which encodes a subunit of the basal transcription factor TFIIH (Burglen *et al.*, 1997), has been shown to be missing in 15% of SMA patients, compared to only 1% of controls (Carter *et al.*, 1997). There are two copies of the SMN gene on each chromosome 5q, designated centromeric (SMN^C or SMN2) and telomeric (SMN^T or SMN1) depending on their placement. The disease-causing mutations are found in the telemetric copy. Only 5 nucleotides distinguish SMN1 from SMN2 genes without any effect on the amino acid sequence. One of these nucleotides is located in exon 7 and is responsible for the alternative splicing of exon 7 which is specific to the SMN2 transcripts (Lorson *et al.*, 1999). More than 95% of patients with SMA have a homozygous deletion of SMN1 (Monani *et al.*, 1999). SMN2 produces mostly transcript lacking the C-terminal 16 residues in exon 7 (SMNΔ7) (Lefebvre *et al.*, 1995). This is translated into an unstable protein, which is degraded rapidly. Thus, SMA patients produce reduced levels of SMN. SMA type II and III patients produce more protein than type I patients (Coovert *et al.*, 1997; Lefebvre *et al.*, 1997). The SMN2 copy number would be predicted to be important in determining phenotype. More copies are found in the milder SMA patients than in the severe cases (Campbell *et al.*, 1997; McAndrew *et al.*, 1997). However, siblings harboring identical SMN2 copy number but markedly different clinical manifestations have been reported (Hahnen *et al.*, 1995; Wang *et al.*, 1996; DiDonato *et al.*, 1997). This indicates the existing of modifier loci lying outside the SMN locus. The NAIP and SERF-1 have been suggested to act as phenotypic modifiers (Roy *et al.*, 1995; Scharf *et al.*, 1998). Adult-onset forms of proximal SMA

are also associated with SMN1 deletions on chromosome 5q11.2-13.3 (Clermont *et al.*, 1995).

1.3 Pathogenesis and Pathophysiology

1.3.1 Biological Properties of Motor Neurones

In order to consider possible causes of MND and roles of elongation factor 1A2 (eEF1A2) in the pathogenesis of MND, it is useful to briefly review some of the salient anatomical and biological properties of motor neurones.

Critical to early motor neurone formation is the protein Sonic hedgehog that activates transcription factors to induce formation of motor neurones (Tanabe and Jessell, 1996). Additional proteins, such as Isl-1, are critical for initial spinal motor neurone formation and identity (Pfaff *et al.*, 1996). During developmental period, axons elongate from newly specified motor neurones to seek and innervate target muscles. Axonal elongation and guidance are driven by a combination of extrinsic, local chemical cues and endogenously expressed molecules. Then, synapse formation with muscles occurs. At about the time that synaptic structures are formed, nearly half of all spinal motor neurones undergo a dramatic process of natural, programmed cell death. This step in spinal cord development may precisely match numbers of motor neurones to the available target muscle cells (Kandel and Schwartz, 2000).

1.3.2 Selective Vulnerability

Several biochemical features distinguish the lower motor neurone from other neural cells. This must account for the reasons why only motor neurones are affected in ALS or SMA, and why there is variation in the site of disease onset and in the relative degree of upper versus lower motor neurones. The spinal and bulbar motor neurones release

acetylcholine (Ach) as the neurotransmitter at the neuromuscular junction (NMJ). This is synthesized by choline acetyltransferase, an intracellular enzyme that is a biological marker for these cells in the spinal cord. The lower motor neurones are also distinguished by cell surface molecules, such as the low-affinity neuronal growth factor (NGF) receptor (p75) (McKay *et al.*, 1996). The large ALS-susceptible neurones in the anterior horn of the spinal cord bear androgen receptors (Matsuura *et al.*,1993). By contrast, smaller motor neurones that innervate extraocular muscles and are largely spared in ALS do not express surface androgen receptors (Rocha *et al.*, 2000; Tachibana *et al.*, 2000; Wickham *et al.*,2000). Motor neurones are unusual in not containing the Ca2+-buffering proteins parvalbumin and calbindin D-28K, with the exception of those in the oculomotor tracts and Onuf's nucleus (Ince *et al.*, 1993). Both proteins can protect neurones from AMPA/kainate receptor-mediated (but not from NMDA receptor-mediated) excitotoxicity (Waldvogel *et al.*, 1991).

1.3.3 Hypotheses of the Pathogenesis of ALS

SALS and FALS are clinically and pathologically similar, suggesting a common pathogenesis. An understanding of the mechanism of motor neurone injury and cell loss in ALS is still limited. However, several hypotheses have been proposed. These are immune or inflammatory mechanisms, free-radical-mediated oxidative stress, excitotoxicity, disorganization of intermediate filaments, and impaired mitochondrial function.

1.3.3.1 Immune or Inflammatory Mechanisms

Evidence for immune mechanisms include a higher incidence of immune disorders in patients (Haverkamp *et al.*, 1995), the presence of the CD4 and CD8 in the degenerating anterior horn of the spinal cord (Engelhardt *et al.*, 1993), the presence of paraproteinemias and lymphomas (Younger *et al.*, 1991), and the presence of IgG in motor neurones (Engelhardt and Appel, 1990). Immune or inflammatory reactions may

trigger increased intracellular calcium and motor neurone degeneration (Engelhardt *et al.*, 1997; Siklos *et al.*, 1998). In addition, antibodies directed against GM1 gangliosides and against voltage-dependent Ca2+ channels have been identified in sera from ALS patients (Smith *et al.*,1996). However, these antibodies have not been demonstrated to be toxic to motor neurones in culture. Moreover, treatment with immunosuppressant drugs has not been shown to modify the course of the disease in ALS patients.

1.3.3.2 Free-radical-mediated Oxidative Stress

1.3.3.2.1 SOD1-induced neuroneal injury

Mutant SOD1 may catalyze aberrant biochemical reactions, resulting in the production of potentially damaging reactive oxygen species, such as the superoxide anion ($O2\bullet^-$), the hydroxyl radical ($OH\bullet$), hydrogen peroxide (H_2O_2), and peroxynitrite ($ONOO^-$). SOD1 catalyzes the conversion of $O2\bullet^-$ to H_2O_2 and oxygen. Copper atom at active site mediates catalysis. SOD1 also involves in the generation of $OH\bullet$. $ONOO^-$ is generated non-enzymatically by the reaction between $O2\bullet^-$ and nitric oxide (NO). NO is generated by Ca2+-dependent nitric oxide synthase (NOS).

However, the loss-of-function hypothesis was disproved because the overexpression of mutant SOD1 [G93A] in mice caused MND despite the presence of elevated SOD1 activity (Gurney *et al.*,1994). In addition, the total elimination of SOD1 did not cause MND in SOD1 knocked-out mice (Reaume *et al.*, 1996). These evidence suggest that SOD1 mutations must cause MND by a toxic gain of function.

1.3.3.2.2 Impaired ability to bind to copper

Cu3+, the cupric ion, is cytotoxic when it is not bound to protein. Cells have mechanisms that chaperone it until it can be incorporated into enzyme. A copper

chaperone protein for SOD1 (CCS) incorporates copper ions into both wild-type and mutant mice SOD1 (Corson *et al.*, 1998; Subramaniam *et al.*, 2002). Copper chelation was shown to improve spinal motor neurone survival in G93A mutant SOD1 transgenic mice by more than 200% and to promote neurite outgrowth compared with that seen in untreated animals (Azzouz *et al.*, 2000). These studies raise a hypothesis that a reduced ability of mutant SOD1 to bind the ion may be a possible mechanism of neurotoxicity in ALS. However, although the absence of CCS led to a significant reduction of amount of copper-loaded mutant SOD1, it did not modify an onset and progression of MND in SOD1-mutant mice (Subramaniam *et al.*, 2002).

1.3.3.2.3 Impaired ability of SOD1 to bind zinc

Impairing the ability of the SOD1 to bind zinc may cause oxidative damage (Estevez *et al.*, 1999). Reduced affinity of mutant SOD1 for zinc enhances conversion of $ONOO^-$ into nitronium ions, compared with wild-type SOD1 (Crow *et al.*, 1997). The neurofilament light subunit has been implicated as a potential target of aberrant nitrosylation or as a high affinity-binding partner for zinc ions that may deplete the SOD1 enzyme. Elevated levels of free nitrotyrosine have been detected in the spinal cords in both SALS and FALS patients (Beal *et al.*, 1997), as well as in SOD1-knockout mice (Ferrante *et al.*, 1997). Nitrotyrosine may interfere with normal protein phosphorylation and phosphorylation mediated signaling.

1.3.3.3 Glutamate Excitotoxicity

Glutamate is a prime candidate as a cause of motor neurone excitotoxicity because it is a principle excitatory neurotransmitter in the motor system. In addition, the concentration of glutamate is about 20,000-fold higher intracellularly than extracellularly. Tightly regulated-dependent system ensures that extracellular glutamate concentrations remain very low to prevent cell injury. A precise idea of the proposed glutamate-mediated defect in ALS has come from the work of Rothstein and co-workers (Rothstein *et al.*,

1992). They first showed that glutamic acid uptake was impaired in post-mortem spinal cord and motor cortex of ALS patients (Rothstein *et al.*, 1992), and the suggested that this deficit could be explained by the selective loss of one of the subtypes of the glutamic acid transporter protein, EAAT2, that is expressed uniquely in glial cells (Rothstein *et al.*, 1995). Reduced levels of EAAT2 have been described in both SALS postmortem specimens (Bristol and Rothstein, 1996) and in transgenic mice with G85R SOD1 mutation (Bruijn *et al.*, 1997). The level of EAAT2 mRNA is not modified, suggesting the anomaly is post-translational (Bristol and Rothstein, 1996). The specific loss of EAAT2 could not be attributed simply to cell injury, because no significant astroglial loss was observed (Rothstein *et al.*, 1995). Multiple aberrant EAAT2 mRNA species arising from exon skipping and intron retention have been detected in SALS brains specimens and in the CSF of living patients (Lin *et al.*, 1998). However, these aberrant mutations are relatively infrequent (Lin *et al.*, 1998; Meyer *et al.*, 1998). Moreover, other reports indicated that splice variants were not associated with ALS (Aoki *et al.*,1998; Meyer *et al.*, 1999; Flowers *et al.*,2001).

The AMPA (α-amino-3-hydroxy-5-methyl-4-isoxazole propionic acid) subtype of glutamate receptor is responsible for most fast excitatory transmission in the central nervous system (CNS). Most of AMPA receptors in the CNS incorporate the GluR2 subunit (Terro *et al.*,1998). The GluR2 subunit I is impermeable to calcium, while others AMPA subunits and NMDA (N-methyl-D-aspartate) receptor are calcium-permeable. The activity of the GluR2 subunit depends on post-transcriptional editing of GluR mRNA (Sommer *et al.*, 1991). The selective vulnerability of motor neurones to AMPA could be explained either by the fact that the expression of GluR2 in motor neurones is normally lower than in other neurones (Williams *et al.*, 1997) or by an impairment in the editing of GluR2 mRNA in patients with ALS (Takuma *et al.*, 1999).

1.3.3.4 Disorganization of Intermediate Filaments

Neurofilaments are cytoskeletal proteins made up of three associated subunits: light (NF-L), medium (NF-M), and heavy (NF-H). They play a particular important role in maintaining axonal integrity in motor neurones and in axonal transport. In both human ALS patients and mutant SOD1 transgenic mice, neurofilament-rich, large-diameter axons have been shown to be the targets for degeneration (Kawamura *et al.*, 1981; Bruijn *et al.*, 1997). An intact neurofilament network is not required for SOD1 mediated disease (Eyer *et al.*, 1998). G37R SOD1 mice crossed with transgenic mice overexpressing the human NF-H subunit led to a 65% increase in the mean lifespan of these mice (Couillard-Despres *et al.*, 1998). Crossing with NF-L null mice also extended the lifespan of G85R mice by approximately 15% (Williamson *et al.*, 1998). Therefore, the overexpression of NF-H or lack of NF-L, which tends to result in perikaryal neurofilament accumulations, appears to be well tolerated by neurones and indeed is even neuroprotective. However, having reduced the total neurofilament content in mutant SOD1 mice by 40% has not been shown to find any change in the disease onset or progression of the mutant SOD1-mediated MND (Nguyen *et al.*, 2000). Also, there is no change in the survival of the mutant SOD1 mice by increasing the neurofilament density in an axon. This could be due to usage of two different mutant SOD1 transgenic mice.

Another intermediate filament, which has been found in almost 90% of motor neurone inclusion in SALS (Corbo and Hays, 1992) and SOD1 mutant mice (Tu *et al.*, 1996), is peripherin. Peripherin is a type III intermediate filament with molecular weight of 57 kD and normally expressed in autonomic nerves and peripheral sensory neurones, with only low amount in spinal motor neurones (Beaulieu *et al.*, 1999a). Levels of peripherin increase in response to cellular injury or inflammation (Troy *et al.*, 1990). Overexpression of peripherin in a transgenic mouse model which is deficient for NF-L caused late onset and selective motor neurone degeneration (Beaulieu *et al.*, 1999b). Studies of interactions between peripherin and neurofilament in SW13 cell line, which

lack endogenous intermediate filament proteins, have shown that peripherin may self assembly to establish an intermediate filament network or heterodimerise with each of the neurofilament subunits, resulting in a disorganized network and protein aggregation (Beaulieu *et al.*, 1999b). Recently, studies have shown that peripherin-mediated death of motor neurones can be rescued by the overexpression of NF-H (Beaulieu and Julien, 2003).

1.3.3.5 Impaired Mitochondrial Function

Mitochondrial function is known to decline with increasing age, which is the most robust risk factor for neurodegenerative diseases. Mitochondrial degeneration has been reported in ALS motor neurones (Wong *et al.*,1995)and is an early pathological feature in mutant SOD1 transgenic mice (Dal Canto and Gurney, 1994; Gurney *et al.*, 1994), preceding the onset of motor weakness (Kong and Xu, 1998). Abnormalities of mitochondrial electron transfer chain, in addition to reduced or damaged mitochondrial DNA, have been detected in muscle and liver biopsies from patients with SALS (Wiedemann *et al.*, 1998; Vielhaber *et al.*, 1999; Vielhaber *et al.*, 2000; Vielhaber *et al.*,2003). Impaired mitochondrial function may lead to a cellular energy deficit. There is a decrease in cytochrome-oxidase activity of individuals with SALS (Borthwick *et al.*, 1999). A study of ALS cybrids showed a significant decrease in complex-I activity and increases in activities of free-radical-scavenging enzymes (Swerdlow *et al.*, 1998). Metabolically compromised neurones may be unable to maintain membrane potential, resulting in opening of voltage dependent NMDA receptors and calcium influx. Therefore, a much lower concentration of extracellular glutamate may initiate the cascade of events leading to cell death.

1.3.3.6 Other Hypotheses

Motor neurones of SOD1-mediated ALS most likely die as a result of apoptosis (Martin, 1999). In mice expressing G39A SOD1 mutation, the expression of anti-apoptotic Bcl-2

delayed the onset of MND and prolonged life (Kostic *et al.*, 1997). However, some studies have shown that motor neurone death in ALS is not apoptotic (He and Strong, 2000). Cyclin-dependent kinases (Cdks) are proline-directed Ser-Thr kinase phosphorylating cell cycle and cytoskeletal proteins. The p35/Cdk5 complex is essential for neurite outgrowth, cell adhesion, cortical development, neuronal adaptive changes, and motor functions(Dhavan and Tsai, 2001; Smith *et al.*, 2001). Mislocalization and deregulation of Cdk5 activity by association with p25, a toxic capain-truncated form of p35, also participate in the pathogenesis of ALS (Nguyen *et al.*, 2001). Recently, a study reports the detection of abnormal cell cycling signaling associated with Cdk5 deregulation in mice expressing a mutant G37R SOD1 linked to human ALS and its potential involvement in motor neurone death (Nguyen *et al.*, 2003).

1.3.4 Pathogenesis of Spinal Muscular Atrophy

SMN protein is found in both cytoplasm and nucleus of all tissues, with the greatest expression in the brain, spinal cord and muscle, and the lowest expression in the lymphocytes and fibroblasts (Coovert *et al.*, 1997; Lefebvre *et al.*, 1997). SMN forms a complex with a series of proteins: Gemin 2 (Liu *et al.*, 1997), Gemin 3 (a DEAD box putative RNA helicase) (Charroux *et al.*, 1999; Campbell *et al.*, 2000), Gemin 5 (Gubitz *et al.*, 2002), the spliceosomal small nuclear ribonucleoprotein (RNP) Sm and Lsm protein (Fischer *et al.*, 1997), the small nucleolar RNP proteins including fibrillarin and GAR1 (Jones *et al.*, 2001; Pellizzoni *et al.*, 2001a), heterogeneous nuclear RNP-Q and coilin (Hebert *et al.*, 2001). Another two proteins which are components of the SMN complex with are Gemin 4 and Gemin 6, two novel proteins of unknown function (Charroux *et al.*, 2000; Pellizzoni *et al.*, 2002). SMN can also interact directly or indirectly with the FUSE-binding protein (Williams *et al.*, 2000), transcription factor E2 (Strasswimmer *et al.*, 1999), profilins (PFN-1 and 2) (Giesemann *et al.*, 1999), a zinc-finger protein called ZPR1 (Gangwani *et al.*, 2001), RNA helicase A, RNA polymerase II (Pellizzoni *et al.*, 2001b), and RNA (Bertrandy *et al.*, 1999). The complex has been shown to function in snRNP biogenesis, cycling between the cytoplasm and nucleus. In

the nucleus, it is involved in pre-mRNA splicing. PFN-2 is neurone specific and functions in the depolymerization of actin filaments, suggesting a possible role for the SMN-PFN-2 complex in neural transport (Giesemann *et al.*, 1999).SMN has also been reported to interact with the anti-apoptotic protein Bcl-2 (Iwahashi *et al.*, 1997), suggesting an interesting perspective for a role of the SMN protein in regulation of cellular survival and with NAIP-mediated anti-apoptotic activity (Liston *et al.*, 1996; Roy *et al.*, 1997). However, some studies do not show this interaction (Coovert *et al.*, 2000). The function of SMN protein is not fully understood and further studies will help in elucidate the tissue specificity of the disease. The creation of an animal model using conditional mutagenesis of the SMN gene should contribute to an understanding of the pathogenesis of SMA.

1.4 Eukaryotic Translation Elongation Factor 1A2

1.4.1 An Overview of Translational Elongation

Eukaryotic protein synthesis is a highly complex process and uses large quantities of cellular energy. The process comprises three steps: initiation, elongation, and termination, followed by folding and, in many cases by post-translational modifications, which give the protein a functional tertiary structure. After initiation, the formation of the 80S initiation complex is followed by the repetitive cyclic event of peptide chain elongation, which is a series of reactions catalyzed by elongation factors (in eukaryotes denoted as eEFs). Aminoacylated tRNA (aa-tRNA) is placed in the A (acceptor) site of the ribosome prior to peptide bond formation with an amino acid or peptide attached to the tRNA in the ribosomal P site. In eukaryotes, the factors involved in aa-tRNA recruitment are eEF1A and eEF1B (EE-Tu and EF-Ts in prokaryotes respectively), while translocation requires eEF2. In humans, eEF1B is composed of three subunits: eEF1Bα, eEF1Bβ and eEF1Bγ, and these subunits form a complex with eEF1A into a 'heavy' complex (eEF1H) (Janssen *et al.*, 1994). In mammalian cells, eEF1A exists in

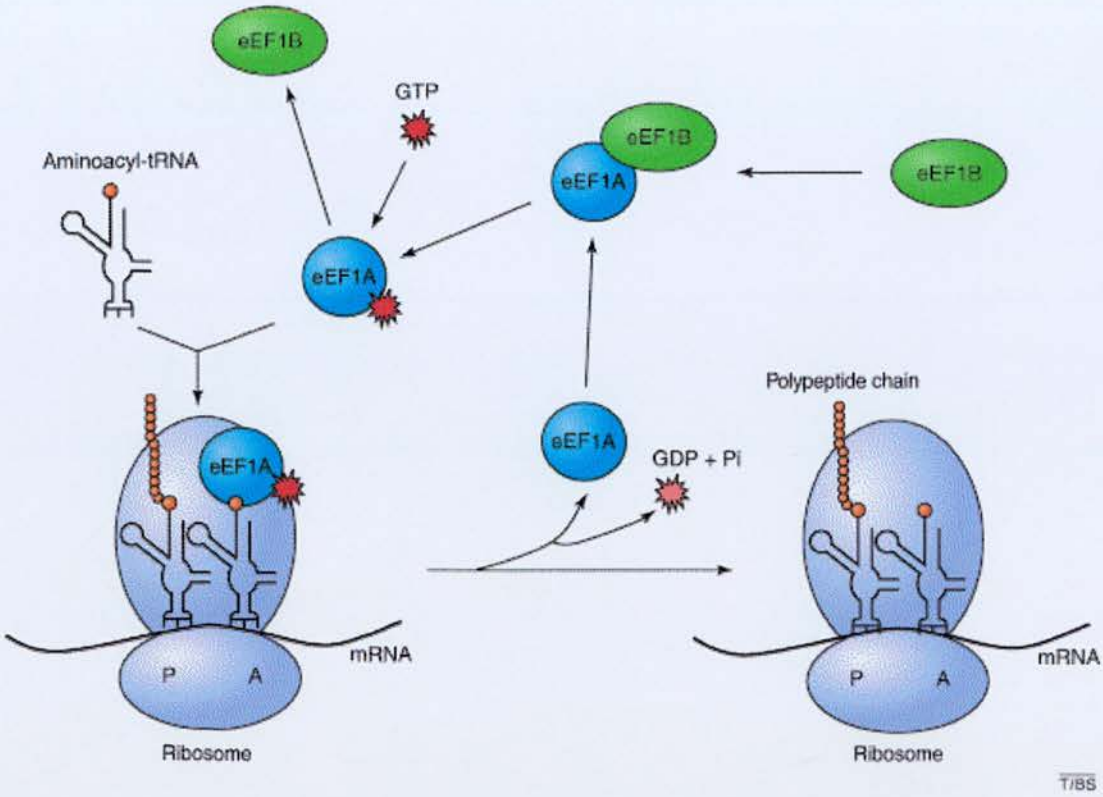

Figure 1-1 Translation elongation. Reproduced from Abbott and Proud (2004).

two different isoforms: the ubiquitous eEF1A1 and the tissue-specific eEF1A2 (Knudsen *et al.*, 1993). eEF1A binds GTP in the active form and then forms a complex with aa-tRNA, which is carried to the A site. The ribosome triggers the hydrolysis of GTP, and inactive eEF1A:GDP leaves the ribosome. The inactive GDP form is recycled to the GTP conformation by guanine nucleotide exchange factor (GEF) eEF1B (Edmonds *et al.*, 1998). eEF1Bα and eEF1Bβ, but not eEF1Bγ, have nucleotide exchange activity, particularly at their C-terminal regions. The ribosome acts as a GTPase-activating protein for eEF1A. The regulation of eEF1A activity by GTPase-activating proteins and GEFs is critically important in efficient and accurate protein synthesis. However, translational elongation activity is inversely related to translational fidelity (Carr-Schmid *et al.*, 1999). Abnormal high levels of elongation activity may result in premature termination or missense errors.

1.4.2 eEF1A2 as an isoform of eEF1A

The mouse *Eef1a* and human *EEF1A* belong to a multigene family, which are often expressed in a developmental- or tissue-specific manner. In mammalian genome, many *Eef1a*-like sequences exist and most of these are suspected to be pseudogenes, which all originate from *Eef1a1* (Uetsuki *et al.*, 1989; Madsen *et al.*, 1990; Ann *et al.*, 1991; Lund *et al.*, 1996). The cDNAs of two actively transcribed isoforms of *EEF1A* in human, and *Eef1a* in rat and mouse have been cloned, with extensive homology to each other but with a different 3'-UTR region (Brands *et al.*, 1986; Lu and Werner, 1989; Ann *et al.*, 1991; Shirasawa *et al.*, 1992; Knudsen *et al.*, 1993; Lee *et al.*, 1994). The two isoforms are 92.4% identical at the amino acid level (Knudsen *et al.*, 1993),and display equal activities in an in vitro translation assay (Kahns *et al.*, 1998). However, eEF1A1 is expressed ubiquitously (Lee *et al.*, 1993b; Lee, *et al.*, 1995), whereas eEF1A2 is expressed tissue-specifically in terminally differentiated cells in brain, heart and skeletal muscle (Lee *et al.*, 1992; Knudsen *et al.*, 1993; Lee *et al.*, 1993b). Upregulation of *Eef1a2* in brain, heart and muscle is shown to coincide with down-regulation of *Eef1a1* (Lee *et al.*, 1992; Lee *et al.*, 1993b; Lee et al., 1995), indicating that eEF1A2 takes over the function of eEF1A1 in protein synthesis in a tissue-specific manner. Human *EEF1A1* has been mapped to chromosome 6q14 by combined fluorescence in situ hybridization (FISH) and PCR analysis of a somatic cell hybrid panel, and *EEF1A2* has been mapped to chromosome 20q13.3 by FISH (Lund *et al.*, 1996). Both human *EEF1A1* and *EEF1A2* have been cloned and sequenced, and the structure of each gene has been analyzed (Uetsuki *et al.*, 1989; Bischoff *et al.*, 2000).

1.4.3 A Switch of Expression

Eef1a1 and *Eef1a2* are independent genes under different developmental control (Lee *et al.*, 1993b). In brain, heart and skeletal muscle, *Eef1a1* mRNA levels are significantly higher in developing embryos compared to those observed in adult tissues and stay relatively constant throughout embryonic life. However, *Eef1a1* expression is regulated in a different manner in these different tissues. Its expression is downregulated but at a

different time during development. The most dramatic decrease is in muscle and heart, where levels of *Eef1a1* diminish by 95% within the first month of postnatal life and coincide with the termination of the myogenic process (Lee *et al.*, 1993b). *Eef1a2* mRNA is detected late during embryonic period in brain and muscle, and steadily increased to reach a plateau early during postnatal life. During in vivo neurogenesis and myogenesis, *Eef1a2* mRNA accumulation correlates with the formation of postmitotic neurones and myocytes. Both *Eef1a1* and *Eef1a2* mRNA levels are remain steady after 1 month postnatal, indicating that their expression are independent of the aging process (Lee *et al.*, 1992). The switch of expression most likely occurs once *Eef1a2* mRNA has accumulated to levels capable of compensating for the reduction in the amount of *Eef1a1* (Lee *et al.*, 1995). In the brain, Rnase protection analysis of total RNA isolated from primary cultures of neonatal rat neurones, astrocyte and microglia demonstrates that *Eef1a2* expression is strictly limited to terminally differentiated neurones (Lee *et al.*, 1995). Using in situ hybridization, *Eef1a2* mRNA has been shown to localize in certain neurones, such as motor neuronees of the brain stem and Purkinje neurones in the cerebellum (Lee *et al.*, 1993a). In the brain of adult mice, eEF1A2 protein is also demonstrated to localize in neurones, whereas eEF1A1 is found in non-neuronal cells (Khalyfa *et al.*, 2001). Like its mRNA, eEF1A2 protein is present only in brain, heart and skeletal muscle. In neurones, eEF1A1 is the major isoform prior to postnatal day 7, but it is later replaced by eEF1A2, which is the only isoform present by postnatal day 14. The appearance of eEF1A2 protein during postdevelopmental period and the decline in eEF1A1 expression in brain, heart and muscle suggest that eEF1A1 is the embryonic form of peptide elongation factor, whereas eEF1A2 is the adult form (Khalyfa *et al.*, 2001).

The switch of expression between eEF1A1 and eEF1A2 has also been shown in toxin-induced skeletal muscle injury in rats (Khalyfa *et al.*, 1999). eEF1A1 is rapidly upregulated immediately after the Marcaine treatment, and corresponds with a decrease of eEF1A2 protein presence. However, this switch is reverted when regeneration-

associated proliferation ceases. An increased level of *Eef1a1* mRNA expression has been also observed in types 1 and 2 human diabetics as well as in nonobese diabetic mice (Reynet and Kahn, 2001). Recently, it is shown that the expression of eEF1A2 protein is activated upon myogenic differentiation (Ruest *et al.*, 2002). Differentiating myoblast cultures express eEF1A2 protein at a late stage of myotube differentiation. Upon serum deprivation-induced apoptosis, eEF1A2 protein disappears and is replaced by eEF1A1 in dying myotubes (Ruest *et al.*, 2002).

1.4.4 Functions of eEF1A2

Although eEF1A1 and eEF1A2 proteins share similar features such as molecular weight of about 50 kD, pI 9.76, transcript length 1.8-1.9 kb, and 92.4% primary amino acid sequence identity, the function of eEF1A2 is still elusive. Work in Xenopus and Drosophila has shown that the amino acid differences have not led to an important modification in function (Frydenberg *et al.*, 1991; Morales *et al.*, 1991). However, in order to understand the functions of eEF1A2, it is worth briefly reviewing the functions of eEF1A1. eEF1A1, which constitutes 1-3% of the total cytoplasmic content of the eukaryotic cell (Slobin, 1980), is a component of the valyl-tRNA synthase complex (Bec *et al.*, 1989), is associated with the mRNA ribonuclease protein complex, and is a participant in protein degradation (Merrick, 1992), including ubiquitin-dependent degradation of N^{α}-acetylated proteins (Gonen *et al.*, 1994). It has also been identified as an actin-binding protein (Yang *et al.*, 1990), functions in the reorganization of the cell cytoskeleton, and is a component of the spindle-organizing centre in mammalian cell (Marchesi and Ngo, 1993). An interaction between eEF1A1 and calmodulin (Kaur and Ruben, 1994) and between eEF1A1 and microtubule (Shiina *et al.*, 1994) have been described. Most cytoplasmic mRNA is anchored to either microtubules or actin filaments in eukaryotic cells, suggesting that the ability of eEF1A1 to alter the assembly and geometry of these polymers may be a crucial property of eEF1A1 in regulating peptide elongation (Condeelis, 1995). Moreover, eEF1A1 is known to be involved in embryogenesis (Krieg *et al.*, 1989), delayed cell senescence (Shepherd *et al.*, 1989), cell

proliferation (Sanders *et al.*, 1996) and oncogenic transformation (Tatsuka *et al.*, 1992). eEF1A1 is shown to be an overexpressed actin-binding protein in metastatic rat mammary adenocarcinoma (Edmonds *et al.*, 1996). eEF1A1 has been also shown to bind viral RNA and RNA polymerase (Blackwell and Brinton, 1997; Das *et al.*, 1998).

Because of the tissue-specific characteristics of eEF1A2, one cannot absolutely infer that it functions in the same as eEF1A1. And why two isoforms of eEF1A exist is still unclear. eEF1A2 acts as an important factor in protein synthesis as demonstrated by its activity in poly(U)-directed polyphenylalanine synthesis assay (Kahns *et al.*, 1998). eEF1A2:GDP complex may exchanges GDP foe GTP to repeat the cycle of peptide elongation during protein synthesis (Negrutskii and El'skaya, 1998). A comparison of the GTPase activity has been shown that eEF1A1 and eEF1A2 have indistinguishable activity in an in vitro translation system. However, the GDP dissociation rate constant is about 7 times higher for eEF1A1 than for eEF1A2, and eEF1A2 binds GDP more strongly than GTP whereas the opposite is true for eEF1A1 (Kahns *et al.*, 1998). eEF1A2 is a specific binding partner to the M4 muscarinic acetylcholine receptor (mAChR), and M4 mAChR acts as guanine exchange factor for eEF1A2 (McClatchy *et al.*, 2002). Differences in post-translational modification pattern might determine their differences in nucleotide preference. Two methylation sites in eEF1A1 (Lys55 and Lys165) are also modified in eEF1A2, but these two site are dimethylated in eEF1A1 whereas are trimethylated in eEF1A2 (Kahns *et al.*, 1998). These trimethylated sites in eEF1A2 may play a particular role in the synthesis of particular proteins in muscle.

Studies show that GTP inhibits binding of eEF1A1 to G-protein, whereas GDP does not have this effect (Dharmawardhane *et al.*, 1991). This may affect the ability to bind actin of eEF1A2 or at least in different manner from eEF1A1. Asparagine at position 197 in eEF1A1 is shown to influence nucleotide binding (Kahns *et al.*, 1998). In eEF1A2, this position is histidine. It seems likely that change of residue 197 could explain the different nucleotide dissociation rate of the two isoforms. Protein synthesis consumes a high proportion of cellular energy, and vast majority of this is used in peptide elongation. It would be advantageous for particular cells to reduce the rate of protein

synthesis in order to allow energy to be diverted to other processes, such as maintaining membrane potential in neurones or supporting contraction in heart and skeletal muscle. It could be possible that eEF1A2 uses less energy than eEF1A1 for the elongation process. Studies using the yeast two-hybrid system have demonstrated that eEF1A2, in contrast with eEF1A1, shows no or only a very weak affinity for the GEFs (Mansilla *et al.*, 2002). However, the N-terminal region of eEF1Bα, which is not present in the crystallographic structure, and subtle structural diversity caused by the amino acid difference, may be involved in the interaction between eEF1A2 and GEFs, (Andersen *et al.*, 2000; Mansilla *et al.*, 2002).

eEF1A2 is likely to be an important human oncogene (Lee, 2003). *EEF1A2* gene is amplified and its mRNA overexpressed in ~30% of primary human ovarian cancer (Anand *et al.*, 2002). Expression of wild-type eEF1A2 transforms rodent fibroblasts and increases their tumorigenicity in nude mice (Anand *et al.*, 2002). Amplification of *EEF1A2* and increased eEF1A2 mRNA and protein overexpression has also been reported in lungs and breast tumors (Wang *et al.*, 2004; Tomlinson *et al.*, 2005; Kulkarni *et al.*, 2006). In lung cancer, high expression of eEF1A2 correlates with increased Ki-67 expression and is associated with poor prognosis (Wang *et al.*, 2004). Furthermore, eEF1A2 may also have a role in metastatic development and it is overexpressed in metastatic rat mammary adenocarcinoma cell lines relative to non-metastatic controls (Pencil *et al.*, 1993; Edmonds *et al.*, 1996). Although these observations implicate eEF1A2 in oncogenesis, little is known about the molecular mechanisms by which eEF1A2 could enhance tumour development.

It has also been shown that the continuous expression of eEF1A2 resulting from adenoviral gene transfer protects differentiated myotubes from apoptosis, in which eEF1A1 replaces eEF1A2, by delaying their death, suggesting a protective function for eEF1A2 in skeletal muscle (Ruest *et al.*, 2002). This noncanonical function of the two proteins could probably explain the developmental switch of the two isoforms.

eEF1A has been determined by mass spectroscopy to be a possible binding partner for Akt2 and ectopic eEF1A2 expression has been shown to increase Akt (also known as protein kinase B, PKB) abundance (Lau *et al.*, 2006). Recently, eEF1A2 has been demonstrated to be a novel activator of Akt (Amiri *et al.*, 2006). Akt activation by eEF1A2 is dependent on PI3K. Furthermore, eEF1A2 induces filopodia production in rodent and human cell lines and enhances cell division and migration in an Akt- and PI3-K-dependent manner (Amiri *et al.*, 2006). This indicates an important role for eEF1A2 in controlling phophatidylinositol signalling, actin remodelling, and cell motility.

1.4.5 Subcellular Localization and Protein-Protein Interaction

1.4.5.1 Interaction of eEF1A and ZPR1

eEF1A is preferentially located in the cytoplasm of cells (Edmonds *et al.*, 1996; Minella *et al.*, 1996). eEF1A is reported to associated with the cytoskeleton through binding to actin, and furthermore to have a pronounced presence in the nucleus (Collings *et al.*, 1994; Janssen *et al.*, 1994; Barbarese et al., 1995; Billaut-Mulot *et al.*, 1996; Sanders *et al.*, 1996). Upon mitogenic stimulation, a fraction of the cytoplasmic eEF1A is shown to translocate into nucleus in complex with the zinc finger protein ZPR1 (Gangwani *et al.*, 1998). ZPR1 is located in the cytoplasm of quiescent mammalian cells, and redistribution of ZPR1 from the cytoplasm to the nucleus can be occurred in proliferating cells by treatment with mitogens, including epidermal growth factor (EGF) (Galcheva-Gargova *et al.*, 1996), suggesting that ZPR1 may function as a mitogenic signaling molecule. ZPR1 also binds to a group of tyrosine kinase receptor such as the EFG and platelet-derived growth factor receptors, but this binding is blocked after mitogenic stimulation (Galcheva-Gargova *et al.*, 1996). ZPR1 is about 98% cytoplasmic in serum-starved cells and is about 96% nuclear in EGF-treated cells, whereas eEF1A is not detected in the nucleus of serum-starved cells and 5% of the total eEF1A is detected in the nucleus after stimulation with EGF, indicating that both ZPR1 and eEF1A are

located in the nucleus of mitogen-treated cells (Gangwani *et al.*, 1998). The distribution of ZPR1 in the nucleus has been demonstrated to correspond to an accumulation within nucleoli (Galcheva-Gargova *et al.*, 1996), and this distribution is characterized by colocalization of ZPR1 with fibrillarin and RNA polymerase I (Galcheva-Gargova *et al.*, 1998). eEF1A can bind RNA and interact with RNA polymerase (Blackwell and Brinton, 1997; Das *et al.*, 1998). It is possible that the nucleolar complex of ZPR1 and eEF1A may functionally interact with RNA. Disruption of the binding of ZPR1 to eEF1A by mutational analysis results in an accumulation of cells in the G2/M phase of cell cycle and defective growth (Gangwani *et al.*, 1998).

Using monoclonal antibodies raised against ZPR1, ZPR1 was shown to localize in nuclear structures called gems and Cajal bodies (Gangwani *et al.*, 2001). Immunoprecipiation experiment with monoclonal antibody to ZPR1 from extracts of [^{35}S]methionine-labeled A431 cells and western blot analysis revealed a prominent 40 kDa band of SMN (Gangwani *et al.*, 2001). In addition, immunoprecipitations using anti-SMN monoclonal antibodies from [^{35}S]methionine-labeled HeLa cell cytoplasmic extract often pull down two unidentified bands of 60 and 50 kDa, which are similar to molecular weight of ZPR1 and eEF1A respectively (Charroux *et al.*, 2000). These evidences raise a question if ZPR1 and eEF1A could be part of the SMN complex.

1.4.5.2 Interaction of ZPR1 and SMN

Like ZPR1, SMN protein is present in the cytoplasm and in small subnuclear bodies, including gems (gemini of coiled bodies) and Cajal (coiled) bodies (Liu and Dreyfuss, 1996; Matera and Frey, 1998; Carvalho *et al.*, 1999). Immunolocalisation studies using anti-SMN monoclonal antibodies show several intense dots in HeLa cell nuclei, and these structures are Cajal bodies (Liu and Dreyfuss, 1996). Gems differ from Cajal bodies, in part, because of the absence of p80 coilin. In contrary, ZPR1 is not shown to colocalize with p80 coilin (Gangwani *et al.*, 1998). These SMN-containing subnuclear

bodies are not detected in some cell types, including cardiac muscle (Young *et al.*,2000). It has been reported that cytoplasmic SMN is involved in the biogenesis spliceosomal small nuclear proteins (snRNP) (Fischer *et al.*, 1997; Liu *et al.*, 1997) and that nuclear SMN may be involved in pre-mRNA splicing (Pellizzoni *et al.*, 1998). SMN has also been implicated in axonal transport in the spinal cord (Pagliardini *et al.*, 2000). Redistribution of SMN and ZPR1 from the cytoplasm to the nucleus is disrupted in cells from patients with SMA type I that have SMN1 mutation (Gangwani *et al.*, 2001). Decreased ZPR1 expression prevents SMN localization to nuclear bodies, suggesting that ZPR1 is required for SMN redistribution (Gangwani *et al.*, 2001). If eEF1A1 or eEF1A2 colocalises with ZPR1 or SMN, it would be interesting to study the role of eEF1A on ZPR1 or SMN localization.

1.5 Denervation and Muscles

1.5.1 An Overview

Denervation, injury, immobilization, bed rest, steroid therapy, sepsis, cancer, and aging are causes of muscle atrophy (Jagoe and Goldberg, 2001). The maintenance of muscle mass is controlled by a balance between protein synthesis and protein degradation. Denervation, immobilization, and unweighting in rats result in similar rate of loss in muscle mass, consistent with the idea that there are common mechanisms leading to atrophy (Bodine et al., 2001). Skeletal muscles in vertebrate derive from the paraxial mesoderm. In response to numerous inductions, muscle precursor cells (myoblasts) start expressing several transcriptional activators, which control the expression of muscle structural genes. A family of four proteins with such a regulation function has been identified, consisting of MyoD, myogenin (Edmondson and Olson, 1989; Wright *et al.*, 1989), myf5 (Braun *et al.*,1989)and myogenic regulatory factor (MRF) 4 (Rhodes and Konieczny, 1989), collectively referred to as the MyoD family (Buckingham, 1992). Myogenin and MyoD have been shown to be nuclear proteins (Tapscott *et al.*, 1988;

Brennan and Olson, 1990). This family belongs to a group of proteins containing a basic DNA-binding motif and a basic helix-loop-helix (bHLH) dimerization domain, including protooncogene c-myc (Stone *et al.*, 1987), the protein Twist involved in mesoderm formation (Thisse *et al.* ,1988), and the achaete-scute involved in neurogenesis (Villares and Cabrera, 1987). MyoD, myogenin, myf5 and MRF4 are expressed exclusively in skeletal muscle; there is no detectable expression in cardiac or smooth muscle. In addition to activating the expression of muscle-specific genes associated with terminal differentiation, members of the MyoD family can activate one another's expression and positively autoregulating their own expression in transfected cells (Thayer *et al.*, 1989; Edmondson *et al.*, 1992). Members of the MyoD family contain transcription activation domains in their amino and carboxyl termini that are important for efficient activation of muscle-specific transcription. The myogenic bHLH region functions in only certain cellular context. It plays a dual role in the control of muscle-specific transcription by mediating DNA binding and by conferring specificity to transcriptional activation (Davis *et al.*, 1990; Anthony-Cahill *et al.*, 1992). Fine mapping of the basic regions of MyoD and myogenin has revealed that two adjacent amino acid, alanine and threonine, which compose a so-called myogenic recognition motif, in the center of their DNA-binding domains confer muscle specificity to the basic region (Davis *et al.*, 1990; Brennan *et al.*, 1991).

All bHLH proteins recognize the nucleotide consensus sequence CANNTG, known as E-box, which is found in the control regions of most skeletal muscle-specific genes where it mediates muscle-specific transcription and trans-activation by myogenic HLH proteins (Lassar *et al.*, 1989; Emerson, 1990; Olson, 1990; Weintraub *et al.*, 1991). These E-boxes are surrounded by binding sites for other transcription factors that collaborate with the myogenic regulators to induce muscle transcription. The muscle creatine kinase gene, for example, is regulated by an enhancer that contains binding sites for myogenic HLH proteins, the muscle enhancer factor-2 (MEF-2), and the mesoderm-restricted homeodomain protein MHox (Cserjesi *et al.*, 1992). However, there are

muscle genes that are regulated by myogenic HLH proteins but which lack E-boxes. Activation of these types of genes is mediated by "intermediate" myogenic factors, which are themselves regulated by the MyoD family. Among these factors is MEF-2, a member of the MADS box family of transcription factors (Pollock and Treisman, 1991; Yu *et al.*, 1992). MEF-2 binds an A+T rich element found in the promoters and enhancers of numerous muscle-specific genes. MEF-2 transcripts are ubiquitous but accumulate preferentially in skeletal muscle, heart and brain, and detected only in skeletal and cardiac muscle nuclei, not in myoblast and nonmuscle cells (Yu et al., 1992). It has been reported to participate in the activation of genes specifically expressed in skeletal muscle, heart and neuronal tissues (Black and Olson, 1998; Krainc *et al.*, 1998). Therefore, MEF-2 may be a plausible candidate as a factor that activates the expression of eEF1A2.

MyoD and myf5 are expressed in proliferating myoblasts prior to initiation of differentiation, whereas myogenin does not become expressed at high levels until differentiation has been triggered by withdrawal of growth factors (Sassoon *et al.*, 1989). Myogenin is expressed during differentiation of all skeletal muscle cells, suggesting that the myogenin gene responses to a common myogenic regulatory pathway or is essential for skeletal muscle differentiation (Sassoon *et al.*, 1989). MyoD is important for inducing myoblast fusion. Transactivation experiments indicate that MRF4 differs from myogenin and MyoD in its ability to activate certain muscle specific genes (Yutzey *et al.*, 1990). MRF4 fails to activate transcription of the muscle creatine kinase, troponin-I, and myosin light chain-1/3 enhancers, whereas MyoD, myf5 and myogenin bind with equivalent affinities to the E-boxes of these genes.

1.5.2 Expression of Genes in Denervated Muscles

Responses of muscle to denervation can indicate that innervation modulates processes in the myofibre (Merlie *et al.*, 1984; Witzemann *et al.*, 1989). Innervation down-regulates a

subset of skeletal muscle synaptic proteins, such as nicotinic acetylcholine receptors (nAChRs) (Schuetze and Role, 1987), voltage-gated sodium channels, and adhesion molecules (Covault *et al.*, 1986), but does not modify the expression of other enzymes or structural proteins, such as creatine kinase, myosin light chain, and skeletal α–actin. nAChR genes, as well as other genes encoding for synaptic proteins, are initially expressed during myoblast differentiation but are later down-regulated by innervation. Myogenin and MyoD mRNA levels are down-regulated by innervation (Eftimie *et al.*, 1991). Denervation of adult muscle leads to a large accumulation of both transcripts. The changes in myogenin and MyoD mRNA levels during innervation, and after denervation, precede the changes of nAChR mRNA (Eftimie *et al.*, 1991).

The muscular chloride channel ClC-1 mRNA levels are shown to be down-regulated in denervated muscles (Sedehizade *et al.*, 1997). ClC-1 is essential for a normal excitability of mature muscle fibres (Klocke *et al.*, 1994), and not found in myotubes (Steinmeyer *et al.*, 1991). Its mRNA levels are upregulated during the first few weeks after birth. The functional destruction of the ClC-1 channel lead to the disease myotonia (Koch *et al.*, 1992).Whereas ClC-1 mRNA levels are lowered in mouse model of SMA, the α-subunit of nAchR (nAChRα), MyoD and myogenin mRNA levels are strongly elevated in muscle affected (Sedehizade *et al.*, 1997). Myogenin and MyoD are known to control the expression of the nAChRα gene by binding to and activating the enhancer region of the nAChRα gene (Piette *et al.*, 1990; Eftimie *et al.*, 1991). This might be the reason why there is the positive correlation between the expression of nAChRα, myogenin and MyoD mRNA.

1.5.3 Other Muscle-Specific Genes

There also are other muscle-specific genes that are developmentally regulated, and display isoform switching. Some of these are genes encoding contractile proteins, and others are genes encoding enzymes involved in energy metabolism. Myosin heavy chain,

a major component of contractile apparatus, has several developmentally regulated isoforms. An embryonic isoform is replaced with neonatal isoforms during development, and these are later replaced by fibre-type specific adult isoforms (Schiaffino *et al.*, 1989; LaFramboise *et al.*, 1991). The functional significance of these complex changes might lie in the different physiological needs of fetal, neonatal and adult muscles (Reiser *et al.*, 1988). Troponin T is another contractile protein that undergoes complex changes in isoform type during development (Wang *et al.*, 2001). Creatine kinase (Martinuzzi *et al.*, 1986; Schweighoffer *et al.*, 1986), aldolase A (Schweighoffer *et al.*, 1986), lactic dehydrogenase (Martinuzzi *et al.*, 1988), glycogen phosphorylase (Martinuzzi *et al.*, 1986; Schweighoffer *et al.*, 1986; Martinuzzi *et al.*, 1988), phosphoglycerate mutase (Martinuzzi *et al.*, 1988), and cytochrome c oxidase (COX) VIa (Taanman *et al.*, 1992) are examples of muscle enzymes that switch from their fetal, or ubiquitous, non-muscle isoforms to the correspondent muscle isoforms as development progresses.

1.5.4 Mitochondrial Translation and Tissue-Specific Mitochondrial Proteins

In addition to COX VIa, an alternative spliced variant of the voltage-dependent anion channel (VDAC, also called porin) isoform 3 is also specifically expressed to brain, heart and skeletal muscle in the mouse (Blachly-Dyson *et al.*, 1993; Sampson *et al.*, 1998). VDACs are functionally conserved proteins found in the outer mitochondrial membrane of all eukaryotes, and are the binding site for a few muscle enzymes, including creatine kinase. VDACs also conduct ATP. Oxidative phosphorylation (OXPHOS) disorders are generally multisystemic diseases that affect predominantly highly aerobic post-mitotic tissues, such as neurone and muscle (Smeitink *et al.*, 2001). Generation of ATP by OXPHOS of ADP requires the four complexes of the respiratory chains (complexes I-IV) and ATP synthase (complex V), all of which are located in the inner mitochondrial membrane. These five complexes consist of subunits that are encoded by both nuclear and mitochondrial genomes. The nuclear genomes encode most of the mitochondrial proteins, and control many mitochondrial functions, including

mitochondrial gene expression. In addition to coding for 13 structural proteins, mitochondrial DNA (mtDNA) also codes for rRNA genes and tRNA genes, which are required for mitochondrial translation (Grossman and Shoubridge, 1996). In human, complex IV is the only respiratory chain complex that contains muscle-specific, developmentally regulated subunits (Bonne *et al.*, 1993). Nuclear gene defects that impair mitochondrial translation have not been reported in patients with mitochondrial disorders. Except for the rRNAs and tRNAs encoded in mtDNA, all of the elements required for mitochondrial translation are encoded by nuclear genes. It is not known how either initiation of translation or selection of the initiation codon takes place in mammalian mitochondria.

1.5.5 Neuromuscular Junction and SMN

Using SMA animal models, it has been established that muscle atrophy precedes loss of motor neurones (Frugier *et al.*, 2000; Monani *et al.*, 2000), and the observed muscle phenotype was neurogenic in origin (Frugier *et al.*, 2000). It has been shown that SMN accumulates in growth-cone-like structure in neuronal cells during neuronal differentiation (Fan and Simard, 2002). The amount and subcellular localization of SMN vary during early mouse skeletal muscle development, and the cytoplasmic SMN peaks at postnatal day 6 just prior to the maturation of the NMJ (Fan and Simard, 2002), consistent with other reported indicating downregulation of SMN expression during myogenesis in vitro (Burlet *et al.*, 1998) and in comparisons of fetal and adult skeletal muscles (Williams *et al.*, 1999). During the first two weeks of postnatal life, diffuse staining and numerous small dot-like SMN particles were detected, as well as intense SMN staining in NMJ; however, after maturation, the intensity of cytoplasmic staining and number of dot-like SMN particles decreased significantly while remaining concentrated in the NMJ (Fan and Simard, 2002). These evidences suggest that the cytoplasmic SMN may possess a neuronal- and muscle-specific function. mRNAs and the structures needed for protein translation have been found in both neuronal dendrites

and axons (Job and Eberwine, 2001), suggesting that eEF1A may be functionally involved with SMN.

1.6 The wasted Mutant Mice and *Eef1a2* Gene

Mice with the autosomal recessive gene wasted (*wst*), the spontaneous mutation arising in the inbred mouse HRS/J variant at the Jackson laboratory in 1972, have been reported to develop neurological and immunological abnormalities (Shultz *et al.*, 1982). Wasted mice, bearing homozygous *wst/wst*, can be recognized at 20 days of age by tremor and uncoordinated body movements and then develop weight loss and progressive hindlimb paralysis, and die by the age of 28 days. Neuropathological examination reveals prominent vacuolar degeneration of anterior horn cells of the spinal cord and motor nuclei of the brainstem with the prominent accumulation of phosphorylated neurofilament heavy subunit (Lutsep and Rodriguez, 1989). Immunological involvement accompanied at the same time includes decreased numbers of circulating B and T lymphocytes, and progressive atrophy of spleen and thymus, which is the result of significant decline in cell numbers in these organs (Shultz *et al.*, 1982; Goldowitz *et al.*, 1985). Lymphoid cells from wasted mice aged more than 26 days have a defective response to radiation-induced DNA damage whereas fibroblasts have a normal DNA repair (Nordeen *et al.*, 1984; Inoue *et al.*, 1986; Tezuka *et al.*, 1986). These observed defects in DNA repair in wasted mice cells are not identical to those reported in cells from patients with ataxia-telangiectasia, the human autosomal recessive disorder characterized by immunodeficiency, ataxia, chromosomal instability, and hypersensitivity of lymphocytes to ionizing radiation, which is caused by defects in the ATM gene. Abnormally low levels of adenosine deaminase have been found in erythrocytes from the wasted mouse, suggesting that wasted mice are immunodeficient (Abbott *et al.*, 1986). In addition, compared with normal mice, wasted mice also show an increase in lymphocyte apoptosis (Potter *et al.*, 1998).

It has been shown that the wasted mutation is caused by a deletion spanning 15.8 kilobases that removes the promoter region and first exon, which is non-coding, in the 5' region of mouse *Eef1a2* gene on distal chromosome 2 (Chambers *et al.*, 1998). No evidence has been found of any other gene in this region. The deletion in this region completely abolishes the detectable expression of this gene in brain, heart and skeletal muscle. Expression of *Eef1a1* is normal but, like non-mutant mice, gradually declines in these tissues until is not detectable by postnatal day 25. Therefore, these tissues in wasted mice do not express both *Eef1a1* and *Eef1a2*, probably leading to a deficiency of protein synthesis in wasted mice, and development of neurological symptoms. However, roles of eEF1A2 in peptide elongation remain to be proved, although a high level of homology between these two proteins may suggest their similar functions. In the brain, eEF1A2 has been shown to colocalize with the M4 subtype of the muscarinic AchR (mAChR), and the intracellular third loop of M4 behaves as a GEF for eEF1A2 (McClatchy *et al.*, 2002), suggesting that eEF1A2 may play a role in the signaling of M4 mAchR in the brain, and the absence of eEF1A2 may cause motor symptoms of upper neurone degeneration via abnormal functioning of mAchR.

1.7 Project Aims

The overall aim of this project was to address the relative roles of eEF1A2 in muscle and neurone of wasted mice, which represent one of the few animal models for studying the pathogenesis of motor neurone diseases. There were three related aspects to this project. Firstly, to describe the characterization of neuromuscular abnormalities of wasted mice. Secondly, to study distribution and colocalisation of eEF1A2 and SMA. The last aim, which was the major, crucial, experiment was to construct a muscle-specific transgene and generate transgenic homozygous wasted mice that specifically express human eEF1A2 in skeletal muscle, but not in neurones, in order to evaluate the phenotype that results from loss of eEF1A2 in neurones but not muscle.

Chapter 2 Materials and Methods

2.1 Materials

2.1.1 Solutions and buffers

Unless otherwise indicated, solutions and buffers were prepared using either distilled or double distilled water, and were stored at room temperature. Cell culture media were supplied by Invitrogen.

2.1.2 Chemicals and reagents

Unless otherwise indicated, all laboratory chemicals for general use were obtained from either Sigma-Aldrich Ltd or Fisher Scientific Ltd.

2.1.3 Enzymes

Taq polymerase was supplied at a concentration of 5 U/μl by Invitrogen. High-fidelity *Tag* polymerase was purchased from Invitrogen. Restriction enzymes and DNA ligase were obtained either from New England Biolabs Applied Science or Roche. RNAase-A and DNase-I were supplied by Ambion.

2.1.4 Cell lines

Epicurican Coli JM109 competent cells were obtained from Stratagene.

2.1.5 Vectors

pcDNAT3.1(+)C-myc-His plasmid was purchased from Invitrogen. pHSA2000CAT plasmid was kindly provided by Edna Hardeman.

2.1.6 Antibiotics

All antibiotics were purchased from Sigma-Aldrich Ltd.

2.1.7 Markers

The 1 kb ladder DNA marker was obtained from Gibco BRL Life Technologies. The protein markers were obtained from Roche.

2.1.8 Mice

Non-transgenic and wasted mice were housed at the Biomedical Research Facility. Transgenic mice were housed at the Transgenic unit at the Western General Hospital. All mice were maintained in accordance with procedures outlined in the Home Office Animals (Scientific procedures) Act 1986. They were maintained on a 12-hourlight/12-hour dark cycle with access to food and water *ad libitum*. The diet was a standard chow diet.

2.1.9 General reagents, solution and buffer preparations

2.1.9.1 General solutions and buffers

Acrylamide	30% stock (19:1) 25% Acrylamide, 1.5% N, N'-methylenebisacrylamide
Acrylagelmide gel sample loading buffer	2x stock 98% deionized formamide, 10 mM EDTA pH 8.0, 0.025% xylene cyanol FF, 0.025% bromophenol blue
Agarose gel sample loading buffer	20 g Ficoll, 20 ml of 500 mM EDTA, in 100 ml dH_2O, Orange-G
10% Ammonium persulphate	10% weight: volume APS: dH_2O

	Stored aliquots at 4 °C
Betaine	5.5 M in dH_2O Stored aliquots at -20 °C
Bjerrum and Schafer-Neilson transfer buffer	5.82 g Tris, 2.93 g Glycine, 0.375 g SDS, 200 ml Methanol, dH_2O to 1 L
DNA extraction buffer	10 mM Tris HCl pH 7.0, 1 mM EDTA, 1% Sodium dodecyl sulphate (SDS), 0.3 M Sodium acetate pH 7.0
Deoxyribonucleoside triphospahtes	10 nM/µl of each dATP, dCTP, dGTP and dTTP in dH_2O, stored aliquots at -20 °C
Ethidium bromide	10 mg/ml in dH_2O Stored in darkness at room temperature
Laemnli running buffer	10x stock 30.8 g Tris, 144.2 g Glycine, 10 g SDS, dH_2O to 1 L
Microinjection buffer	10 mM Tris, 0.1 mM EDTA, pH 7.4 Autoclave and filter sterilize
Normal Ringer Solution	120 mM NaCl, 5 mM KCl, 2 $CaCl_2$, 1 mM $MgCl_2$, 0.4 NaH_2PO_4, 23.8 $NaHCO_3$, 5.6 Glucose

0.2 M Phosphate buffer, pH 7.6	13 ml of 0.2 M Sodium monobasic phosphate (NaH_2PO_4), 87 ml of 0.2 M Sodium dibasic phosphate (Na_2HPO_4) heptahydrate
Phenol: chloroform: isoamyl alcohol	25:24:1, Fluka (Sigma-Aldrich Ltd)
10x PCR buffer	10x stock 750 mM Tris HCl pH 9.0, 200 mM Ammonium sulphate, 0.1% weight: volume Tween
10% Sodium dodecyl sulphate	10% weight: volume SDS: dH_2O, pH 7.2 Heat to dissolve
Tail tip DNA extraction buffer	10 mM Tris pH 7.0, 1 mM EDTA, 1% SDS, 0.3 M sodium acetate pH 7.0
10x TAE	10x stock 0.4 M Tris HCL PH 8.0, 0.2 M Sodium acetate. 10 mM EDTA, 9 ml/L glacial acetic acid
20x TBE	20x stock 1.8 M Tris, 1.8 M Boric acid, 40 mM EDTA, pH 8.0
TE (Tris-EDTA)	10 mM Tris HCl pH 7.6, 1 mM EDTA pH 8.0

2.1.9.2 Growth media for bacterial cultures

Luria-Bertani (LB)-agar	15 g/L Bacto-agar, 10 g/L Bacto-tryptone, 5 g/L Bacto-yeast extract, 5 g/L NaCl, pH 7.0
Luria-Bertani (LB)-broth	10 g/L Bacto-tryptone, 5 g/L Bacto-yeast extract, 5 g/L NaCl, pH 7.0

2.1.9.3 Antibiotics

Ampicillin	stock 50 mg/ml in dH20 (50-100 µg/L in media)
Chloramphinicol	stock 34 mg/ml in dH_2O (20 µg/L in media)
Kanamycin	stock 10 mg/ml in dH_2O (10 µg/L in media)

2.1.9.4 Enzymes

Proteinase K	stock 50 mg/ml in dH_2O

2.1.10 General equipment

Unless otherwise indicated, centrifugation was performed on an eppendorf 5415 microfuge. The vortex used was a Jencons MS1 minishaker. Absorbance at 260 and 280 nm were read on a Pharmacia Biotech Ultrospec 3000 spectrophotometer. Mice were weight on a Soehnie, and their muscles were weighted on Sartorius BP150.

2.2 Methods

2.2.1 Standard DNA protocols

2.2.1.1 Extraction of genomic DNA from ear notches

Mice were ear notched at weaning (21 days old) for the purpose of identification and genotyping. Early ear notching was performed at 18-20 days old in the case that early phenotypes were to studied. There were two methods used.

2.2.1.1.1 Sodium hydroxide method

This is a quick method used for genotyping non-genetically modified mice. Mice were ear notched and the ear pieces were stored at -20 °C to avoid degradation of genomic DNA. DNA extraction was performed by boiling the ear notches in 0.6 ml of fresh 50 mM NaOH at 95 °C for 10 minutes. The tubes were vortexed and 50 µl of 1 M Tris-HCl pH 8.0 was added. The tubes were centrifuged at maximum speed for 6 minutes. The 0.3-ml supernatant was transferred to a new tube, and stored at -20 °C. 1 µl was used in the PCR.

2.2.1.1.2 Phenol: chloroform: isoamyl alcohol extraction

This method was used for genotyping transgenic mice and other mice that were housed in the Transgenic unit because it gave a cleaner result. Ear notches were incubated at 55 °C on a rocking tray overnight in 200 ml of digestion buffer containging 5 µl of Proteinase K (10 mg/ml). An equal volume of phenol: chloroform: isoamyl alcohol (25: 24: 1) was added to the DNA solution to be purified in a 1.5-ml microcentrifuge tube, and mixed gently for 5 minutes on a rocking platform. The tube was then microcentrifuged at for 10 minutes at 13,000 rpm at room temperature. The aqueous (top) phase containing DNA was removed using a 1000-µl pipetor and transferred to a new tube. The phenol: chloroform: isoamyl alcohol extraction steps were repeated until

a white precipitate was not present at the aqueous/organic interface. The DNA was then precipitated from the final aqueous phase by ethanol precipitation.

2.2.1.2 Small scale plasmid DNA preparation (miniprep, Sigma)

A single colony was inoculated into 5 ml of LB-broth containing 100 μg/ml ampicillin in a 50-ml tube, and was incubated with vigorous shaking at 225 rpm at 37 °C overnight. The cells were pelleted by centrifugation at 3000 rpm for 5 min. The cells were resuspended in 200 μl of the Resuspension solution containing RNase A. The resuspended cells were lyzed by adding 200 μl of the Lysis buffer. The cell debris was precipitated by adding 350 μl of the Neutralization/Binding buffer, and was centrifuged at more than 12,000 x g for 10 minutes. The clear lysate containing the plasmid DNA was bound to the column and centrifuged at more than 12,000 x g for 1 minute. Then, 100 μl of TE buffer was used to elute the plasmid DNA.

2.2.1.3 Large scale plasmid DNA preparation (maxiprep, Sigma)

A single colony was inoculated into LB-broth containing an appropriate antibiotic, and incubated with vigorous shaking at 225 rpm at 37 °C overnight. 150 ml of the overnight culture was pelleted by centrifugation at 5000 x g for 10 minutes. The cell pellets were resuspended in 12 ml of Resuspension/RNase A solution. 12 ml of Lysis solution was added and gently mixed by inversion. The lysis reaction was incubated at room temperature for 3-5 minutes. 12 ml of chilled Neutralization solution was added to the mixture and mixed immediately by gentle inversion. The chromosomal DNA, cell debris, proteins, lipids were allowed to precipitate for 5 minutes. The resulting lysate supernatant was filtered by attaching vacuum source to VacCap and vacuum was applied. 9 ml of Binding solution was then added to the filtered lysate. The filtered mixture was transferred to the prepared Binding column with vacuum on. The lysate was allowed to pass through. The column was then washed twice using Washing solution 1 and Washing solution 2 containing ethanol. The pellet was allowed to dye for 10 minutes. 3 ml of of dH_20 was used to elute the plasmid DNA.

2.2.1.4 Ethanol precipitation

The volume of the DNA sample was measured. The salt concentration was adjusted by adding 1/10 volume of sodium acetate, ph 5.2, (final concentration 0.3 M). After mixing well, 2 volume of ice-cold 100% ethanol (calculated after salt addition) were added and mixed well again. The DNA was then allowed to precipitate for 20-30 minutes on ice. The DNA was pelleted by centrifugation at 13,000 rpm for 15 minutes and the supernatant was decanted. The DNA was washed twice with 70% ethanol and allowed to air dry. The DNA was then resuspended in an appropriate volume (30-50 ul) of TE buffer.

2.2.1.5 Spectrophotometric quantification of DNA

DNA concentration and purity of a sample was calculated from the optical density (OD), which was determined by UV Spectrophotometry, e.g. DNA concentration (μg/ml) = ($OD_{260} - OD_{320}$) x 50 (DNA extinction coefficient) x dilution factor (i.e. 1000/20).

2.2.1.6 Restriction enzyme digestion

Restriction enzyme digestion was performed by incubating double-strand DNA molecules with an appropriate amount of restriction enzyme. In its respective buffer as recommended by the supplier, and at the optimal temperature for that specific enzyme. Typical digestions included a unit of enzyme per microgram of starting DNA, and one enzyme unit usually (depending on the supplier) is defined as the amount of enzyme needed to completely digest one microgram of double-stranded DNA in one hour at the appropriate temperature. The volume of the reaction depended on the amount and size of the DNA being digested. Larger DNAs were digested in larger total volumes (between 50-100 μl), as were greater amounts of DNA. These reactions usually are incubated for 1-3 hours, to insure complete digestion, at the optimal temperature for enzyme activity. If the DNA was to be used in a subsequent manipulation such as dephosphorylation or ligation, the enzyme was inactivated by heating at the recommended temperature for 10

minutes. An aliquot of the digestion should be assayed by agarose gel electrophoresis versus non-digested DNA and a size marker, if necessary. An aliquot of the digestion was assayed by agarose gel electrophoresis versus non-digested DNA and a size marker, if necessary prior to use in further procedures.

2.2.1.7 The polymerase chain reaction (PCR)

2.2.1.7.1 Primer design

The sequence of the gene of interest was searched on the NCBI and ENSMBL databases. The location of introns, coding region and any other points of interest such as polymorphism were studied. Oligonucleotide primers were designed using the Primer3. The criteria used to select primers included (1) primers with similar melting temperatures with 40-60% GC content, (2) size of PCR product between 150-500 bp, (3) primers 18-22 nucleotides, (4) GC at 3' end of primer, (5) no primer should contain more than 4 contiguous base pairs of homology to itself or counterpart and (6) the PCR product should have a predicted melting temperature (Tm) of 76-82 °C. Primers were placed on different exons so RNA-specific PCR is different in size from DNA contamination. Primers were purchased from either Invitrogen or Sigma, which were supplied as lyophilised products at a scale of synthesis of 50 nM.

2.2.1.7.2 PCR conditions

The amplification of DNA fragment using the PCR was performed in an MJ Gradient Cycler, by adding the reagents to either a 0.2 ml thin walled tube or a 48 well microtitre plate. Unless otherwise indicated, PCR was carried out in 1xPCR buffer, with 200 Um of dNTPs, 100 ug of each primer, 0.2 U of *Taq* polymerase, and template DNA, in a volume of 25 µl. The pipettes, tips, tubes, and reagents were sterile and kept separately from those used in other experiments. PCR reaction was set up in a designated room, where PCR products were prohibited. After an initial denaturation step of 95 °C for 3 minutes, the actual cycling steps consisted of 25-30 cycles of a denaturation step of 95 °C for 30 seconds, the appropriate annealing temperature (usually 55 °C) for 30 seconds,

and the extension step of 72 °C for 30 second, followed by the late extension step of 72 °C for 10 minutes. After PCR, aliquots of the mixture were loaded onto an agarose gel and electrophoresed to detect amplified products.

2.2.1.8 Agarose gel electrophoresis

Agarose gel electrophoresis was employed to check the progression of a restriction enzyme digestion, to quickly determine the yield and purity of a PCR reaction, and to size fractionate DNA molecules, which then could be eluted from the gel. Prior to gel casting, dried agarose is dissolved in buffer (0.5xTBE or 1xTAE buffer) by heating and the warm gel solution then was poured into a mold, which was fitted with a well-forming comb. The percentage of agarose in the gel varied. Although 0.8% agarose gels typically were used, in cases where the accurate size fractionation of DNA molecules smaller than 1 kb was required, a 1-2% agarose gel was prepared, depending on the expected size(s) of the fragment(s). Ethidium bromide was included in the gel matrix to enable fluorescent visualization of the DNA fragments under UV light. Agarose gels were submerged in electrophoresis buffer in a horizontal electrophoresis apparatus. The DNA samples were mixed with loading buffer and loaded into the sample wells. Electrophoresis usually was at 150 - 200 mA for 0.5-1 hour at room temperature, depending on the desired separation. When low-melting agarose was used for preparative agarose gels, electrophoresis was at 100-120 mA for 0.5-1 hour, again depending on the desired separation. Size markers were co-electrophoresed with DNA samples, when appropriate for fragment size determination. After electrophoresis, the gel was placed on a UV light box and an image of the fluorescent ethidium bromide-stained DNA separation pattern was taken using a digital imager.

2.2.1.9 Elution of DNA fragments from agarose gel

DNA fragments were eluted from low-melting temperature agarose 1x TAE gels using QIAquick gel extration kit (Qiagen). The band of interest was excised with a sterile razor blade, placed in a microcentrifuge tube, frozen at -70 °C, and then melted.

2.2.1.10 Purification of a PCR product for cloning

After an aliquot of the PCR mixture was analyzed on an agarose gel, the remainder of the reaction was purified by QIAquick PCR purification kit (Qiagen), which was used for purification of PCR products of 100 bp – 10 kb. After purification, amplified DNA fragments were used to ligate into a cloning vector.

2.2.1.11 Treatment of plasmid DNA for cloning

Vector and construct DNA were digested with restriction endonucleases, and purified from agarose gels (see 2.2.1.9). Removing 5' phosphates from the plasmid vector was not performed to prevent self-ligation of the vector because all of the vectors used and cut with two different restriction enzymes did not carried identical sticky ends.

2.2.1.12 Ligation of DNA

The enzyme used t ligate DNA fragments was T4 DNA ligase. Each reaction was performed in a 20 ul reaction containing 1x T4 DNA ligase buffer supplemented with ATP, 1 U of T4 DNA ligase, insert and vector DNA, and distilled water. A 3-fold molar excess of insert DNA: vector DNA was used for most cloning experiments. Ligations were performed at 16 °C or 4 °C overnight to facilitate sticky end ligation.

2.2.1.13 Transformation of competent *Escherichia coli*

For subcloning transformations, the host cells used were *E.coli* strain JM109 (Epicurean Coli) purchased from Stratagene, and stored at -80 °C. This *E.coli* strain is endonuclease (*end*A) deficient, greatly improving the quality of miniprep DNA, and is recombinant (*rec*A) deficient, improving insert stability. The cells were thawed on ice for 10 minutes. A 100 µl aliquot was used for one transformation, which was performed in a 14-ml Falcon tube. 3 µl of 20 µl ligation reaction were added, mixed with the cells, and incubated on ice for 30 minutes. The cells were then heat-pulsed at 42 °C for 45 seconds,

and returned to ice for another 2 minutes. 900 µl of pre-warmed LB media (with no antibiotics) were added and mixed with the cells. The samples were then incubated at 37 °C on rotor-shaker at 225-250 rpm for 45 minutes to recover the cells. After incubation, aliquots of 100 ul were plated on LB-agar plates (pre-warmed at room temperature) with an appropriate selective antibiotic, and incubated overnight at 37 °C.

2.2.1.14 Colony screening

Autoclaved toothpicks were used to pick single colonies for PCR. A colony was first suspended in a small amount of dH_2O (typically 5 µl), and subsequently streated on a fresh LB-agar plate. The suspended colony was incubated at 95 °C for 3 minutes, and 1 ul was subsequently used for PCR.

2.2.1.15 Sequencing of DNA

Automated dye-terminator cycle-sequencing, which is a chain termination method, was used to sequence plasmid DNA and PCR products. Plasmid DNA was ready for direct sequencing once it had been extracted and appropriately diluted. PCR products, however, first had to be cleaned (see 2.2.1.10). The primer was a primer used in PCR, and each primer was used in a separate reaction. The DNA was sequenced in both directions. The sequencing reactions were set up in 0.5 ml PCR tubes and contained BigDye (which contains Taq DNA polymerase, standard dNTPs, and labeled ddNTPs; ABgene), one primer, DNA template, and deionised water to a total volume of 10 ul. The sequencing process was carried out in an MJ Gradient Cycler, and comprised one cycle of 96 °C for 1 minute, followed by 24 cycles of 96 °C for 30 seconds, 50 °C for 15 seconds, and 64 °C for 4 minutes. After the completion of the thermocycler steps, the labeled sequencing products were run on polyacrylamide gels and sequenced on the ABI 3100 Automated Capillary DNA Sequencer (Applied Biosystem) at the MRC facility unit, Western General Hospital. The sequences were then analysed using the Bioedit software.

2.2.2 Reverse transcription – PCR (RT-PCR)

2.2.2.1 Isolation of total RNA from mouse tissues

The tissues of interest were removed from mice using sterile, RNase-free instruments. The tissues were then flash frozen by immersion in liquid nitrogen and stored in cryovials in liquid nitrogen prior to RNA extraction. The RNA samples were processed simultaneously to reduce the variability among the different RNA samples. Total RNA was isolated using TRIzol™ reagent. The 50-mg frozen tissue was homogenized in 1.0 ml of TRIzol. 200 µl of chloroform for each 1.0 ml of TRIzol used were added. The samples were vigorously shaked for 15 seconds and incubated for 3 minutes at room temperature. The homogenate was then at 12,000 rpm for 15 minutes at 4 °C. The colourless, upper aqueous phase containing the RNA was removed and transferred to a clean microcentrifuge tube and 500 µl of isopropanolol per 1 ml of the TRIzol used were added and mixed well. The RNA was allowed to precipitate at room temperature for 15 minutes, and then centrifuged at 12,000 rpm for 15 minutes at 4 °C. The supernatant was discarded and the RNA pellets were washed twice using 1 ml of 75% ethanol. The samples were vortexed after addition of each ethanol wash and centrifuged at 7,500 rpm for 3 minutes at 4 °C. The last drop of ethanol was removed and the RNA pellets were allowed to dry for approximately 10 minutes at room temperature. After drying, the RNA pellets were resuspended in 1 µl of DEPC-treated ddH_2O per 1 mg of tissue sample, vortex mixed, placed on ice for 10 minutes, heated at 65 °C for 10 minutes and placed on ice before storage. The total RNA was stored at -70 °C.

2.2.2.2 Isolation of total RNA from HeLa cells

The PARIS™ kit (Ambion) was used to extract RNA from HeLa cells. The procedure was done at room temperature as recommended by the manufacturer. The RNA was eluted in 50 µl of Elution Solution, and stored at -70 °C. Prior to using the RNA in RT-PCR, trace of DNA contamination was removed by treating the RNA with DNase.

2.2.2.3 Treatment of RNA for RT-PCR

The RNA was treated with recombinant DNase I (Ambion) to remove trace to moderate amounts of contaminating DNA prior to using it in RT-PCR. 0.1 volume of 10x DNase I buffer and 1 µl of DNase I were added to the RNA in 50 µl reaction. The sample was then incubated at 37 °C for 20-30 minutes. 1 volume of DNase Inactivation Reagent was added and the sample was incubated for 2 minutes at room temperature with occasional mixing. The sample was centrifuged at 13,000 rpm for 1.5 minutes at 4 °C. The supernatant containing treated RNA was transferred to a new tube.

2.2.2.4 Quantification of total RNA

RNA concentration and purity of a sample was determined by UV Spectrophotometry, e.g. RNA concentration (µg/ml) = (OD_{260} – OD_{320}) x 40 (RNA extinction coefficient) x dilution factor (i.e. 500/10).

2.2.2.5 cDNA synthesis

First-strand complementary DNA was reversed transcribed from total RNA using RETROSCRIPT kit (Ambion) according to the manufacturer's instructtions. The Moloney-Murine Leukemia Virus (M-MLV) Reverse Transcriptase was chosen for its higher stability and lower intrinsic RNase H activity, compared to AMV Reverse Transcriptase. The traditional two-step RT-PCR was performed. 3 µg total RNA was mixed with 2 µl of random decamers and nuclease-free water to a volume of 12 µl. The sample was mixed, spinned, and heated at 85 °C for 3 minutes. The sample was then placed on ice. To the sample were added 2 µl of 10x RT buffer, 4 µl of dNTPs mix, 1 µl of RNase inhibitor, 1 µl of M-MLV reverse transcriptase, and nuclease-free water to a total volume of 20 µl. The sample was mixed gently and incubated at 42 °C for 1 hour. The sample was then incubated at 92 °C for 10 minutes to inactivate the reverse transcriptase. The cDNA was stored at -20 °C or was proceeded to the PCR (see 2.2.1.7.2).

2.2.3 Real-time RT-PCR

2.2.3.1 Sample preparation

Muscles dissected from mice were flash frozen by immersion in liquid nitrogen and stored in cryovials in liquid nitrogen prior to RNA extraction. Total RNA extraction was performed using the PARIS kit (Ambion) according to the manufacturer's instructions. The total RNA was eluted with 50 µl RNase-free elution solution by centrifugation, and DNase treated (see 2.2.2.3). Isolated total RNA integrity was verified by an average optical density (OD) OD_{260}/OD_{280} nm absorbance ratio. 2 µg total RNA was reverse transcribed with M-MLV reverse transcriptase in a volume of 20 µl, using random decamers. Therefore, the concentration of 100 ng cDNA (reverse transcribed total RNA) per µl was achieved. All reagents used for reverse transcription were obtained from the RETROSCRIPT kit (Ambion). Finally, cDNA was diluted 1:2 with nuclease-free water prior to using in real-time PCR.

2.2.3.2 Selection of primers for real-time RT-PCR

Primers were selected to bind specifically to mouse cDNA using Universal ProbeLibray software (Roche Applied Science). The sequences of primers were shown in the respective chapters. Primers were generated commercially by Invitrogen.

2.2.3.3 Optimisation of real-time PCR

Conditions of real-time PCRs were optimized in a MJ Gradient cycler with regard to Taq polymerase, forward and reverse primers, and various annealing temperatures (55-65 °C). RT-PCR amplication products were separated on a 4% agarose gel electrophoresis. Optimised conditions were transferred on the real-time PCR protocols.

2.2.3.4 Real-time PCR

Real-time PCR mixture was prepared in a volume of 12.5 µl, containing 1x iQ SYBR Green Supermix (Biorad; 2x stock solution containing 100 mM KCl, 40 mM Tris-HCl

pH 8.4, 0.4 mM of each dNTP, iTag DNA polymerase 50 units/ml, 6 mM $MgCl_2$, SYBR Green I, 20 nM fluoresein, and stabilizers), 100 µg of forward and reverse primers, and nuclease-free water (Ambion). 50 ng Cdna was used as PCR template. The reactions were performed in a 0.2-ml 98-well plate in the MyiQ cycler (Biorad). Each assay was performed in triplets. The cycling conditions comprised 10 minutes of template denaturation step at 95 °C, followed by 40 cycles of denaturation at 94 °C for 15 seconds and primer annealing/extension step at the gene-specific primer temperature for 30 seconds. After the amplification and quantification programme, melting curve programme was peformed at 60-95 °C with a heating rate of 0.1 °C per second. The threshold cycle (Ct) for each transcript was defined as the point at which the fluorescence rose appreciably above the background fluorescence, and determined by MyiQ software (BioRad).

2.2.4 Cell culture

HeLa cells were maintained in Dulbecco's modified Eagle's medium (DMEM, GIBCO BRL) containing 4,500 mg/L D-glucose and 2 mM L-glutamine supplemented with 10% heat-inactivated fetal bovine serum (FBS), 0.1 mM non-essential amino acids (NEAA) , 100 U/ml penicillin, and 100 U/ml streptomycin, at 37 °C with 5% CO_2.

2.2.5 Transfection

Transient transfection was performed in HeLa cells using Lipofectamine 2000 Reagent (Life Technologies). Cells were transfected with pcDNA3.1(+)C-hEEF1A2-myc which was purified with GenElute Plasmid Miniprep kit (Sigma). The day before transfection, the cells were trypsinised, counted, and plated in 24-well plates in 0.5 ml of DMEM containing 10% FBS and without antibiotics at 8×10^4 cells per well so that they were 90-95% confluent on the day of transfection. For each well of cells to be transfected, 0.8 µg of DNA was diluted into 50 µl of OPTI-MEM I Reduced Serum Medium without serum. 1.5 µl of Lipofectamine 2000 Reagent was diluted into 50 µl OPTI-MEM I Medium and incubated for 5 minutes at room temperature. The diluted DNA and the

diluted Lipofectamine 200 Reagent were combined and incubated at room temperature for 20 minutes to allow DNA-Lipofectamine 2000 Reagent complexes to form. Growth medium was then removed from cells, and 0.5 ml of medium without serum was added to each well, followed by adding of 100 µl of DNA-Lipofectamine 2000 Reagent complexes directly to each well and mixing gently. The cells were incubated at 37 °C with 5% CO_2 for 4-5 hours. 0.5 ml of DMEM with 20% FBS was added for a final concentration of 10% FBS. The cells were incubated at 37 °C until 24 hours post-transfection or until they were ready to assay for transgene expression.

2.2.6 Western blot analysis

2.2.6.1 Protein extraction

Tissues of interest were dissected from mice and immediately flash frozen by immersion in liquid nitrogen, and stored at -70C. Tissues were homogenized in cold RIPA buffer (150 mM NaCl, 10 mM Tris-HCl pH 7.2, 0.1% w/v SDS, 1.0% Triton X-100, 1% w/v deoxycholate, and 5 mM EDTA) supplemented with 1x Complete Antiprotease Cocktail (Roche). Samples were centrifuged at 14,000 rpm at 4 °C for 5 minutes. Supernatants were transferred to a new tube, quantified, and stored at -20 °C for further analysis.

2.2.6.2 Protein quantification

The Bradford protein assay was used to measure protein concentration, using the Bradford DC Protein Assay detection kit (Biorad) according to the manufacturer's instructions. 25 µl of Reagent A and 200 µl of Reagent B were mixed with 5 µl of protein sample, and incubated at room temperature for 5 minutes. The absorbance was measured at 595 nm using an EL312e Microplate Bio-Kinetics Reader (Bio-Technologies Instruments). A standard curve was constructed by plotting absorbance obtained from a range of bovine serum albumin (BSA) dilutions between 0-1.4 mg/ml, and was used as a reference for determining the concentration of proteins.

2.2.6.3 Sodium dodecyl sulphate-polyacrylamide gel electrophoresis (SDS-PAGE)

30-50 μg of protein from each sample was mixed with an equal volume of 2x Laemnli sample buffer containing 2% w/v sodium dodecyl sulphate, boiled 100 °C for 2 minutes, and separated by SDS-PAGE on 12.5% acrylamide gel with 4.2% stacking gel. The Broad Range Prestained ladders (BioRad) were used as markers. Gels were run using a Bio-Rad Protean III at 150 V and 20 mA for approximately 2 hours in Laemnli running buffer, and subsequently electroeluted onto a polyvinylidene difluoride (PVDF) Hybond-P membrane (Amersham Pharmacia Biotech) in Bjerrum and Schafer-Neilson transfer buffer, using a BioRad Trans-Blot SD transfer apparatus at 20 V and 150 mA for a minigel for 25-30 minutes.

2.2.6.4 Immunoblotting

After protein transfer, the blotting membrane was incubated overnight at 4 °C in blocking buffer containing 5% w/v fat-free powdered milk and 0.1% v/v Tween 20 in phosphate-bufferred saline (PBS). Membranes were rinsed with PBS and incubated in the blocking buffer with the primary antibody (Table 2-1) for 1-2 hours at room temperature. The membranes were then washed three times with PBS containing 0.1% v/v Tween 20, and bound antibodies were detected using an appropriate horseradish peroxidase (HRP)-conjugated secondary antibody for 1 hour at room temperature. The membranes were washed three times with PBS with 0.1% v/v Tween 20 and proteins were visualized using an enhanced chemiluminescence (ECL or ECL plus) Western blotting detection kit (Amersham Pharmacia Biotech). The membranes were exposed to a MACO-X-RAY HS90 medical film and the film was developed using a Hyper Processor (Amersham Life Science).

Table 2-1 Antibodies used for immunoblotting

Antibody	Dilution	Source
eEF1A2	1:500	Sheep polyclonal (Newbery, 2003)
Akt	1:100	Rabbit polyclonal (Abcam)
Phospho-Akt	1:100	Rabbit monoclonal (Abcam)
β-actin	1:1000	Rabbit polyclonal (Sigma)
β-tubulin	1:1000	Rabbit polyclonal (Abcam)

2.2.6.5 Data analysis of Western blots

Western blots were quantified using an enhanced chemiluminescent ECL or ECL Plus (Amersham Pharmacia Biotech), a Hyper Processor machine (Amersham Life Science), and Image J software. Band intensities were calculated, and background was subtracted.

2.2.7 Histological studies

2.2.7.1 Muscle preparations

Triceps and quadriceps were dissected from each mouse, and snap frozen in isopentane cooled in liquid nitrogen prior to storage at -70 °C. 12-micron sections were cut mid-belly in a cryostat and were attached to a glass slide prior to staining with haematoxylin and eosin.

2.2.7.2 Microdissection of muscles

For neuromuscular junction studies, hindlimb and abdominal muscles were removed from each mouse and were immersed in Normal Ringer Solution (NRS) supplemented with O_2 for 10 minutes prior to microdissecton. The muscle samples were pinned onto silica dishes filled with NRS, and examined under a dual-lens stereo microscope. Under the microscope, the major blood vessels and associated fascia were carefully removed. Transverse abdominis (TA) and lumbrical muscle were then dissected to be a thin layer, and ready for immunocytochemistry.

2.2.7.3 Haematoxylin and eosin staining

Sections were immersed in the filtered Harris Haematoxylin for 1 minute, and rinsed with tap water until the water was clear. The sections were incubated in eosin stain for 1-2 minutes, rinsed with tap water, and dehydrated in ascending alcohol solutions of 50%, 70%, 80%, 95% for 2 times, and 100% for 2 times, followed by clearing with xylene for 3-4 times. The glass slides were mounted in an organic mounting medium, pertex (CellPath).

2.2.7.4 Succinic dehydrogenase (SDH) staining

Snap frozen section was incubated in the incubation medium (10 ml of 0.2 M Phosphate Buffer, 270 mg Sodium Succinate, and 10 mg Nitro Blue Tetrazolium) for 60 minutes at 37 °C. The coverslips were then washed with three exchanges of dH_2O. Nitro Blue Tetrazolium was removed with three exchanges of the acetone solution in increasing then decreasing concentration of 30, 60, and 90% acetone in dH_2O. 90% acetone was left covering the sections until a faint purplish cloud is seen over the section. The sections were washed several times with dH_2O and then mounted with a mounting medium.

2.2.7.5 Measurement of the muscle fibre numbers and cross-sectional areas

All fibres in each haematoxylin-stained section were counted, and the cross-sectional areas of all fibres were measured using the Image J software.

2.2.8 Immunofluorescence analysis

2.2.8.1 Immunostaining of neuromuscular junctions

Lumbrical and TA preparations for immunocytochemistry were fixed in 0.1 M PBS containing 4% w/v paraformaldehyde for 30-40 minutes before labeling acetylcholine

receptors by incubating in a-bungarotoxin (BTX) conjugated to 5 mg/ml tetramethyl-rhodamine isothiocyanate (TRITC-a-bungarotoxin, Molecular Probes) for 20 minutes. Muscles were blocked in 4% BSA and 0.5% Triton X in 0.1 M PBS for 30 minutes, and incubated in a 1:200 dilution of primary antibodies directed against 165 kDa neurofilament proteins (2H3, Developmental Studies Hybridoma Bank) and a 1:200 dilution of the synaptic vesicle protein SV2 (Developmental Studies Hybridoma Bank) overnight. Muscles were then blocked in blocking solution for 30 minutes and incubated in a 1:200 dilution of sheep anti-mouse antibody conjugated to the fluorescent label FITC (Diagnostics Scotland). Muscles were whole-mounted in Vectashield (Burlingame) on slides for subsequent imaging.

2.2.8.2 Immunofluorescence in HeLa cells

HeLa cells were cultured on glass coverslips, rinsed with PBS, and then fixed in cooled methanol at for 10 minutes at -20 °C. The cells were then permeabilized with cooled acetone for 1 minute at -20 °C. The coverslips were blocked with 3% bovine serum albumin in PBS with 0.5% Tween-20 (PBS-T) for 30 minutes at room temperature, and then incubated with primary antibodies for 1 hour at room temperature. Double labelling for myc-tagged eEF1A2 and SMN was carried out by sequential incubations (1 hour) with a monoclonal mouse anti-Myc antibody (Invitrogen) and FITC-conjugated anti-mouse IgG antibody (Vector Laboratories), and then goat anti-SMN antibody (Abcam) and Texas-Red-conjugated anti-goat secondary antibody (Vector Laboratories). Antibodies were diluted in PBS to appropriate dilution: 1:5000 for anti-Myc antibody; 1:500 for anti-SMN antibody; 1:500 for secondary antibodies. Cells were rinsed once and washed with PBS-T three times (5 minutes) between each antibody incubation. The coverslips were mounted on slides using Vectashield with DAPI (4', 6-diamidio-2-phenylindole; Vector Laboratories), and examined by immunofluoresence microscope using conventional microscope Axioskop2 MOT (Carl Zeiss).

2.2.9 Production of transgenic mice

2.2.9.1 Preparation of DNA constructs for microinjection

The transgene fragment was excised from pUC19 plasmid containing a transgene by restriction endonuclease digestion. The transgene fragment was separated on a 0.8% low-melting agarose gel in 1x TAE gel, and the band was visualised under UV light and removed with a sterile scalpel. The transgene fragment was electroeluted overnight from the gel slice using the Elutrap® Electroelution System (Schleicher & Schuell BioScience), and eluted in TE buffer. From this step, in order to minimize dust contamination in the further DNA preparation, non-filtered tips were used, and all tips, eppendorfs, and gloves were rinsed with sterile dH_2O. The DNA was concentrated by ethanol precipitation. The concentration of the DNA construct was determined by running an aliquote on a mini agarose gel against known DNA standard. The DNA was then diluted to 2 ng/µl in injection buffer, and stored at -20 °C for subsequent microinjection.

2.2.9.2 Collection of fertilized oocytes

The mouse strain used to generate transgenic mice was C56BL/6J x CBA. Female donor mice, aged of 4-8 weeks, were injected intraperitoneally with 10 IU of pregnant mare serum gonadotrophin (PMSG, Intervet) three days prior to embryo collection and microinjection. A day prior to microinjection, the donor mice were injected intraperitoneally with 10 IU of human chorionic gonadotrophin (hCG, Intervet). In the evening on the same day, each donor mouse was set up to mate with one proven stud male, aged of 8 weeks – 8 months. On the morning of the day of microinjection the females were examined for the presence of a copulation plug in the vagina. To collect the fertilized oocytes, mice were sacrificed by cervical dislocation. The mice were positioned on their back and the abdomen was swabbed with 70% ethanol. A horizontal incision was made in the mid-abdomen, and the ski was pulled off the abdomen. The peritoneum was opened and the oviducts were removed and placed in a depression slide with M2 medium. The oocytes were dissected out under a stereo-microscope, transferred

to M2 medium containing 400 mg/ml of hyaluronidase, and incubated for less than 3 minutes. The embryos were transferred into M2 medium with a transfer pipette and washed for another three to four times in M2 medium. The embryos were then incubated in M16 medium at 37 °C in 5% CO_2 until ready for microinjection.

Donor mice were prepared by technicians at the Transgenic unit, and collection of oocytes was performed by Dr. Brendan Doe.

2.2.9.3 Microinjection

Ten to twenty oocytes were suspended in a drop of M2 medium on a depression slide and the slide was palced onto the microscope stage. 1-2 µl of DNA was transferred using an Eppendorf microloader pipette into the needle holder. Microinjection was performed under an inverse stereo microscope (Zeiss Axiovert 100). The embryo which had visible pronuclear were held in position that the male pronucleus (a bigger one containing a single nucleolus) was in the equatorial plane of the oocyte by gently suction with a holding pipette. The injection needle (Femtotips, Eppendorf) was slowly inserted into the pronucleus. The drawn out injection pipette was then gently pushed through the zona and into the nucleus whereby the DNA was injected by gently pushing the pedal of the micromanipulator (Narishige M151). The injection needle was pulled out as soon as the pronucleus was swollen noticeably. The fertilized oocytes which survived micromanipulation were transferred to the oviduct of pseudopregnant recipients.

Microinjection procedure was performed by Dr. Brendan Doe.

2.2.9.4 Embryo transfer

The recipient females at the age of about 8 weeks to 6 months were mated with vasectomised males the evening before the transfer. The next morning the females were examined for the presence of a copulation plug. The females which were positive for the plug were used for the embryo transfer. The recipients were anaesthetised by

intraperitoneal injection with a mixture of 0.9 µl of a 100 mg/ml ketamine HCl solution and 0.1 µl of a 2% xylazine HCl solution. The side of the lower part of the back was shaved and swabbed with 70% ethanol, and a small transverse incision was made with dissecting scissors to expose the ovary, oviduct, and uterus. The mouse was then placed on the stage of stereo-microscope, and the opening of the oviduct (infundibulum) was located. The embryos contained in a transfer pipette were injected into the infundibulum. The fat pad, ovary, oviduct and uterus were then picked up and pushed back inside the body wall, which was subsequently closed with one or two stitches. The skin was then closed with wound clips. Mice were kept warm until the effects of the anaesthesia had worn off and monitored to ensure that there were no post-operative complications.

2.2.9.5 Identification of progeny mice for transgene integration

All offspring were examined for integration of the transgene into genomic DNA at weaning (3 weeks of age) by PCR of genomic DNA isolated from ear punches. Genomic DNA was isolated using phenol: chloroform: isoamyl alcohol method (see 2.2.1.1.2). Mice that had not incorporated the transgene were sacrificed by cervical dislocation.

2.2.10 Bioinformatics

BioEdit Sequence Alignment Editor: http://www.mbio.ncsu.edu/BioEdit/bioedit.html
Electronic PCR: http://www.ncbi.nlm.nih.gov/sutils/e-pcr/
Ensembl Genome Browser: http://www.ensembl.org/index.html
ExPaSy Proteomics Server: http://www.expasy.org/
Image J software: http://rsb.info.nih.gov/ij/
Mouse Genome Informatics (MGI): http://www.informatics.jax.org/
Primer 3 Input: http://frodo.wi.mit.edu/cgi-bin/primer3/primer3_www.cgi
Sanger Blast Search Service: http://www.sanger.ac.uk/DataSearch/blast.shtml
Sequence alignment program for DNA or proteins: http://www.ebi.ac.uk/clustalw/
Universal Probe Library: https://www.roche-applied-science.com/sis/rtpcr/upl/adc.jsp
VEGA Genome Browser: http://vega.sanger.ac.uk/index.html

Chapter 3 Characterization of Wasted Mice

3.1 Introduction

The autosomal recessive wasted mutation gives rise to a set of features that include progressive muscle wasting, weight loss, progressive paralysis, degeneration of anterior horn cells of spinal cord, with abnormalities of motor nuclei in the brainstem, decreased numbers of circulating lymphocytes, and early death of the *wst/wst* homozygotes by approximately 28 days. The *Eef1a2* gene was found to partially deleted in mice with the wst mutation (Chambers *et al.*, 1998). Expression of eEF1A2 is tissue-specific, and limited to the terminally differentiated cells of the brain, heart, and skeletal muscle. In skeletal muscle in wild-type mice, eEF1A1 and eEF1A2 are reciprocally expressed. eEF1A1 is expressed in early postnatal stages and diminished by postnatal day 25, whereas eEF1A2 is not detectable at early stages but is strongly expressed at day 25. A natural decline in eEF1A1 and loss of eEF1A2 from the *wst* mutation mean there is no translation elongation factor 1a in the wasted mouse, giving rise to a hypothesis that loss of eEF1A2 may be a cause of muscle wasting in wasted mice.

3.1.1 Causes of muscle atrophy

Skeletal muscle atrophy that occurs in muscles of animals is a result of denervation, immobilization, aging, starvation, and a number of disease states. Regardless of the initiating event, skeletal muscle atrophy is characterized by a decreased in protein content, fibre diameter, force production, and fatigue resistance. The different types of conditions producing atrophy imply different types of molecular triggers and signaling pathways for muscle wasting. Denervation, damage, or disease processes may reverse the pattern of gene expression typical for the healthy mature muscle fibre. On the other hand, the expression of some genes is relatively independent of the stage of maturation and innervation of the muscle fibre (Pette and Vrbova, 1985; Eftimie *et al.*, 1991). The myogenic factors (MYFs), a class of transcription factors, play a role in the early steps

of determination and differentiation as well as maintenance of the differentiated state. In mature muscle, the MYFs, myogenin and MyoD are dramatically down-regulated compared to levels in early developmental stages of muscle.

Loss of eEF1A2, however, occurs in wasted mice. To date, there is no evidence whether muscle wasting in wasted mice is neurogenic or myopathic in origin. To address this question, I conducted experiments to investigate the primary causes of muscle wasting in wasted mice.

3.1.2 Muscle atrophy and Akt protein

Two recent studies have expanded knowledge about the mechanisms involved in the development of skeletal muscle atrophy. These reports (Sandri *et al.*, 2004; Stitt *et al.*, 2004), have provided direct evidence for a role of Akt1 signaling as a modulator of the expression of two important genes involved in the progression of muscle atrophy, the E3 ubiquitin ligases atrogin-1 or Muscle Atrophy F box (MAFbx) and the Muscle Ring Finger-1 (MuRF-1), and their regulation by a family of transcription factors termed Fork-head box O (FOXO). Exciting new evidence demonstrates that the expression of atrogin-1 (MAFbx) and MuRF-1 is controlled by a signaling network that comprises FOXOs and their regulation by Akt1. These new findings are important not only from the atrophy standpoint, but also from the integration of cellular regulatory networks perspective as they created a scenario in which a key molecule that is positively involved in cellular growth via protein synthesis when in its active state, also negatively regulates the opposite process (protein degradation). Such interactions suggest that the dynamic regulation of skeletal muscle mass is not simply a balance between protein synthesis and degradation but is a rather finely coordinated process. These findings have also established a key role of PI3-K signaling growth factor/cytokine-mediated cell survival, with Akt functioning as a direct link to the apoptotic machinery. Active Akt directly phosphorylates pro-apoptotic BAD, resulting in its association with the 14-3-3 protein and consequent de-activation. The subsequent release of anti-apoptotic Bcl-2 and

Bcl-x_L results in a shift away from programmed cell death towards cell survival (Datta *et al.*, 1997).

Skeletal muscle atrophy is a devastating condition seen in many catabolic diseases such as cancer, sepsis, and denervation as well as in neuromuscular disorders such as ALS (Lynch, 2001). Recent studies in mice and rats have shown a dramatic upregulation in MAFbx and MuRF-1 in conditions causing muscle atrophy including denervation, and have suggested that the transcriptional regulation of MAFbx and MuRF-1 is controlled by an Akt/Forkhead (FKHR)-dependent signaling pathway (Gomes *et al.*, 2001; Lee *et al.*, 2004). In ALS patients, as seen in the ALS mouse model, skeletal muscle atrophy is associated with an increase in MAFbx and a decrease in active Akt (Léger *et al.*, 2006). Whether or not the observations in other rodent models of human skeletal muscle are similar to those observed in ALS patients and ALS transgenic mice requires investigation.

While perturbations in normal signaling could reflect impairment within the muscle, increases in protein content or activity could instead reflect a compensatory mechanism to regulate the loss of muscle mass associated with denervation. In addition, these changes could indicate an upregulation of anti-apoptotic pathways within the muscle, thereby promoting not only cell survival within the tissue itself, but potentially targeting the damaged motor neuron as well.

A recent study has shown that eEF1A is a potential binding partner of Akt2 (Lau *et al.*, 2006). It is possible that muscle atrophy in wasted mice may lead to activation of Akt and its downstream proteins such as mTOR, resulting in promoting of protein synthesis in order to compensate for ongoing muscle atrophy. The aim of this chapter was to determine whether Akt, a downstream peptide of the PI3-K pathway, showed elevations in protein expression and/or phosphorylation within progressively denervated skeletal muscle in wasted mice.

3.2 Results

3.2.1 Motor function in wasted mice

As loss of eEF1A2 might contribute to motor neuron degeneration, I examined wasted mice aged from 20 day postnatal, when their motor function was still normal and no disease symptoms were yet observed. I scored motor function in the hind limbs using a rating scale (modified from Lambrecht *et al.*, 2003) of 5 (normal function) to 0 (absence of movement) as shown in the table 3-1.

Table 3-1 Neurological rating scale

Score	Motor function
5	Normal function
4	Hind limbs are stretched but remain rigid when the mouse is lifted by its tail, normal walking
3	No stretching of hind limbs when lifted by tail, normal walking
2	Rigid hind limbs when lifted by tail, ataxic or knuckling walking
1	Rigid hind limbs when lifted by tail, hind limb movement but unable to walk
0	Rigid limbs when lifted by tail, total absence of movement

3.2.1.1 Progressive paralysis after weaning in wasted mice

Wild-type mice showed normal motor function in the hind limbs for the entire duration of the analysis, as shown in table 3-2. In contrast, all six wasted mice showed signs of paralysis beginning at weaning (score 4 ± 0) and progressed to severe paralysis with an absence of movement (score 0.33 ± 0.58, $P < 0.005$) at age of 27 days and died by 28 days postnatal. Ataxic walking was observed in wasted mice from age of 23 days ($P < 0.005$). Figure 3-1 shows the neurological outcome and neurological score of wasted mice compared to those of age-matched wild-type mice.

Table 3-2 Neurological rating scores of hind limbs of wasted mice and wild-type controls.

	D20	**D21**	**D22**	**D23**	**D24**	**D25**	**D26**	**D27**
Control 1	5	5	5	5	5	5	5	5
Control 2	5	5	5	5	5	5	5	5
Control 3	4	5	5	5	5	5	5	5
Control 4	4	5	5	5	5	5	5	5
Control 5	5	5	5	5	5	5	5	5
Control 6	5	5	5	5	5	5	5	5
Mean	4.67	5.00	5.00	5.00	5.00	5.00	5.00	5.00
S.D.	0.52	0	0	0	0	0	0	0
wst/wst 1	5	4	3	3	3	2	2	1
wst/wst 2	4	4	3	3	2	2	1	0
wst/wst 3	4	4	4	2	2	2	2	0
wst/wst 4	4	4	4	3	2	2	2	0
wst/wst 5	5	4	3	3	3	2	1	1
wst/wst 6	4	4	3	2	2	2	2	0
Mean	4.33	4.00	3.33	2.67	2.33	2.00	1.67	0.33
S.D.	0.52	0	0.52	0.52	0.52	0	0.52	0.52
P value vs. controls *	0.31	←		< 0.005		→		

* Mann-Whitney test.

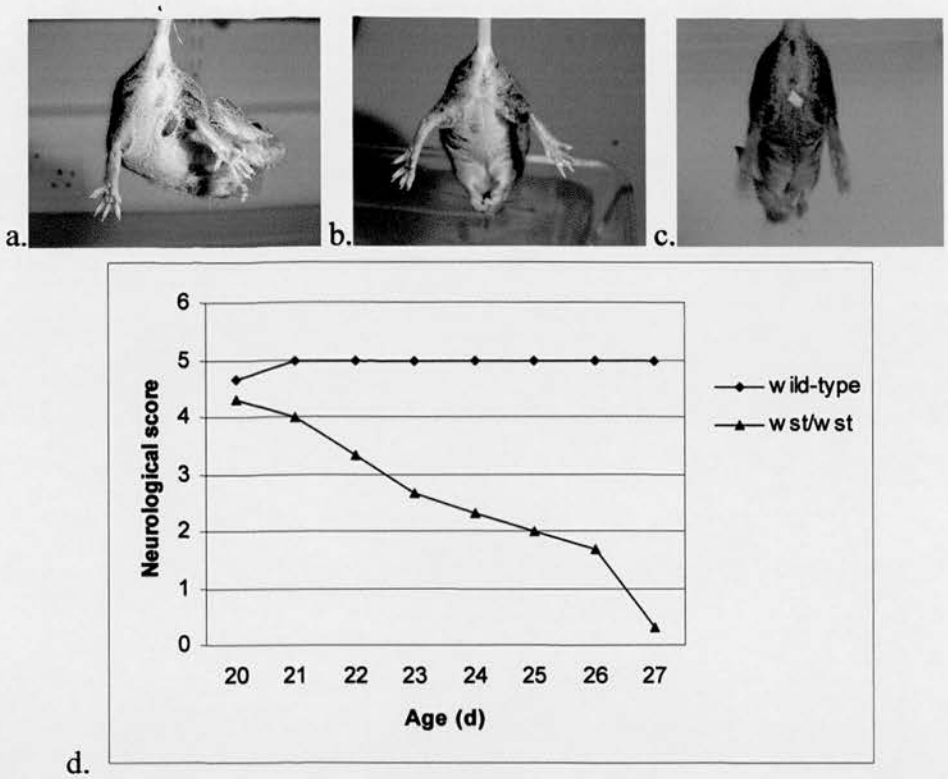

Figure 3-1 Neurological score. (a) 24-day-old wild-type mouse with score 5. (b) 21-day-old wasted mouse with score 4. (c) 24-day-old wasted mouse with score 3. (d) Means of neurological scores in wasted mice compared to those of age-matched wild-type mice.

3.2.2 Muscle pathology in wasted mice

Mice were culled by cervical dislocation and muscle tissue was separated from bone and immediately frozen in liquid nitrogen. Segments of muscle from wild-type and wasted mice were snap frozen in ice-cooled isopentane and 12-um sections were cut in a cryostat before staining.

3.2.2.1 Decrease in the cross-sectional area of fibres in wasted muscle

The average fibre area in the quadriceps muscle of wild-type and wasted mice was calculated by counting 200-1,000 fibres in the transverse section of muscles from three 25-day mice for each genotype, and dividing the total area of the counted fibres by fibre number. Fibre atrophy in the wasted muscles was documented by the overall decrease in the cross-sectional area of fibres (Figure 3-2a). The muscle fibre area in wasted mice was $176 \pm 7\ \mu m^2$, whereas the muscle fibre area in wild-type controls was $249 \pm 17\ \mu m^2$ ($P < 0.005$). To underline this finding, analysis of fibre size differences showed a significant decrease in total fibres per field in the muscles of 25 day-old wasted mice as shown in table 3-3 ($P < 0.0001$), and a significant smaller fibre diametre in wasted muscles (16.9 ± 0.9 um in wasted muscles, 20.6 ± 1.1 um in wild-type muscles, $P < 0.0001$), as shown in figure 3-2b.

Table 3-3 Overall fibre atrophy in wasted mice documented by an increase in total fibre number per field (40x), $P < 0.0001$.

Muscle Fibre Analysis	Wild Type	Wasted
Average Total fibres/Field	84	120
Minimum diameter (μm)	18.3	15.7
Maximum diameter (μm)	22.5	19.1

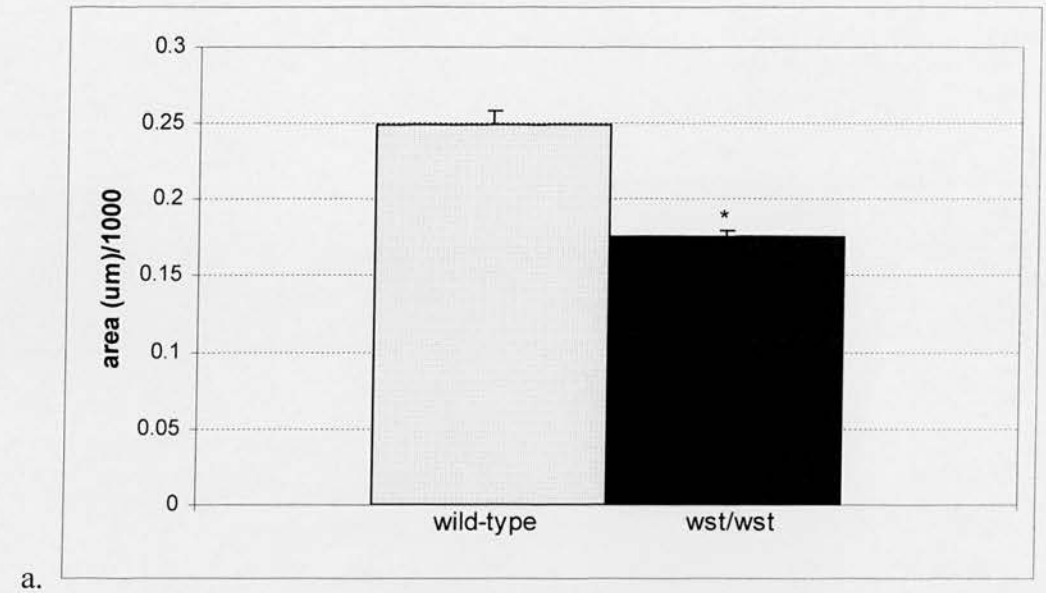

a.

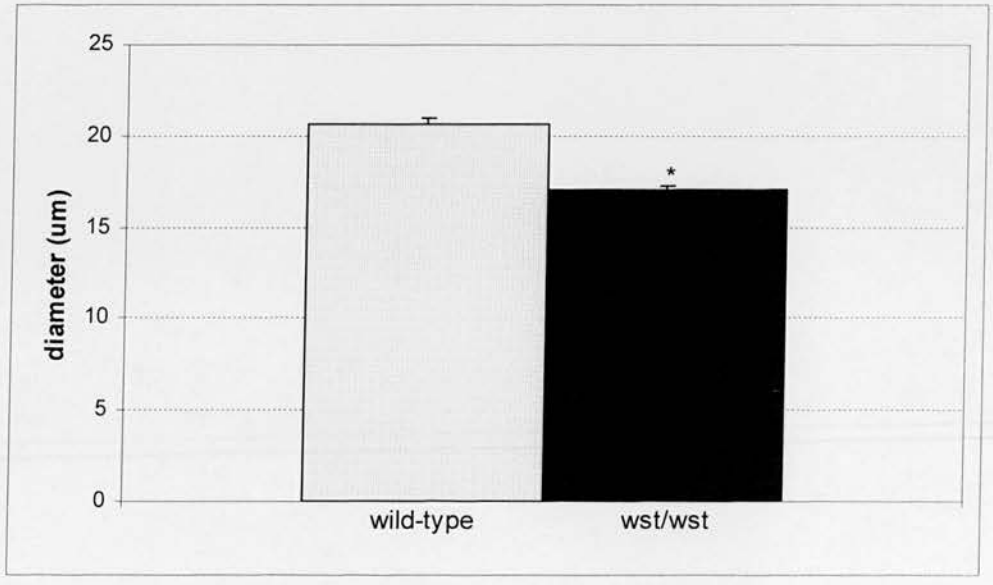

b.

Figure 3-2 Analysis of fibre size differences. (a) Average fibre area in quadriceps of wild-type and wasted mice (* $P < 0.005$). (b) Average fibre diameter in quadriceps of wild-type and wasted mice (* $P < 0.0001$).

3.2.2.2 Muscle atrophy in wasted mice has features of neurogenic atrophy

Hematoxylin and eosin-stained cross-sections of triceps and quadriceps from three wasted and wild-type 25 day-old mice were analysed. In addition to the overall decrease in the cross-sectional area of fibres in wasted mice, I found that some pathologic processes were found in the muscle. The muscle fibres of wild-type mice were of relatively uniform size and shape, with nuclei located in the periphery of the cells (Figure 3-3a). In contrast, the muscles of wasted mice showed small angular fibres and pyknotic nuclear clumps, which are a characteristic feature of neurogenic atrophy (Figure 3-3b-d). The small angular fibres were often basophilic in H&E stains. Multiple small groups of atrophic fibres were also demonstrated. The findings of atrophic groups of angular fibres suggested that the process was in the early stage of denervation.

Wasted muscle pathology showed a range of severity. Pyknotic nuclear clumps were clumps of myonuclei, which are an end product of denervation atrophy. The contractile apparatus of the remainder of myofibres largely disappeared. The finding of pyknotic nuclear clumps in muscles of wasted mice suggests that denervation exists without reinnervation. These pathologic findings were demonstrated in both upper limb and lower limb muscles.

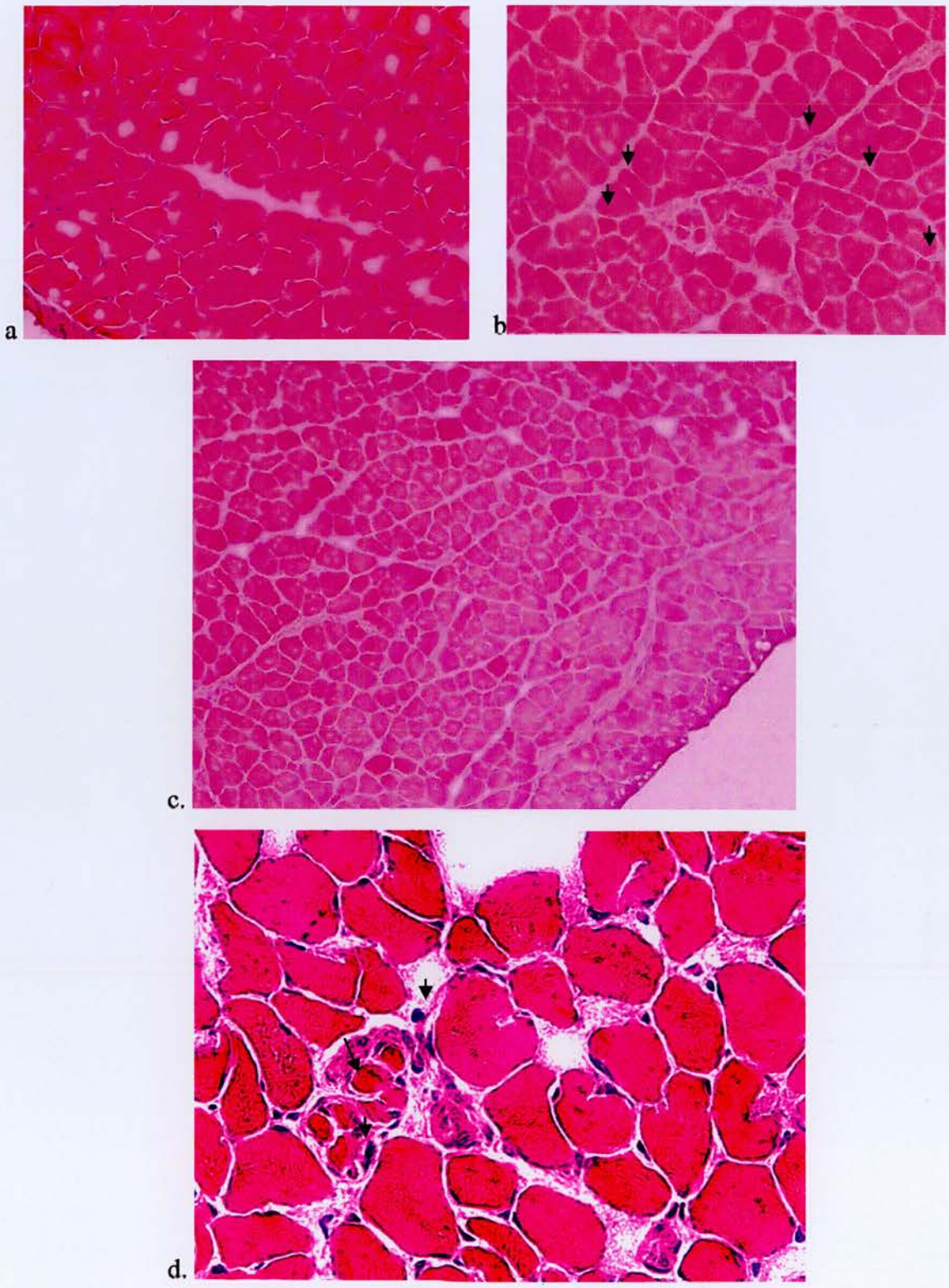
a
b
c.
d.

Figure 3-3 Hematoxylin and eosin-stained cross-sections of muscles of 25-day-old mice. (a) Quadriceps of wild-type mouse (40x). (b, 40x and c, 20x) Quadriceps of wasted mouse, showing angulated atrophic fibres (arrowheads). (d) Triceps of wasted mouse (60x), showing severe fibre atrophy with prominent pyknotic nuclei (arrowheads). Some fibres show severe loss of contractile apparatus (arrows).

3.2.2.3 Regenerating muscle fibres were found in muscle of wasted mice

Hematoxylin and eosin-stained cross-sections of quadriceps from 25 day-old wasted mice occasionally showed centralized nuclei as shown in figure 3-4, whereas they were not found in wild-type muscle. Although this finding was variable, it is worth mentioning because centralized nuclei are typical of regenerating muscle fibres, which might have been thought not to happen in muscle of wasted mice.

3.2.2.4 Muscle from wasted mice showed an increase in mitochondrial staining

Succinate dehydrogenase (SDH) staining of quadriceps from 25 day-old wasted and age-matched wild-type mice was used to study mitochondrial dysfunction. SDH stain is the most sensitive and specific stain for mitochondrial proliferation in muscle fibres. Increased SDH staining of muscle fibres indicates abnormality in mitochondrial function. I found that muscle fibres from wasted mice stain darkly for SDH compared with muscle from wild-type mice, as shown in figure 3-5. Increased SDH staining could be found in regenerating muscle fibres. This finding helps support the above finding of centralized nuclei in wasted muscle fibres and suggests that there is a regenerative potential in wasted muscle, although mitochondrial disease could not be excluded.

a.

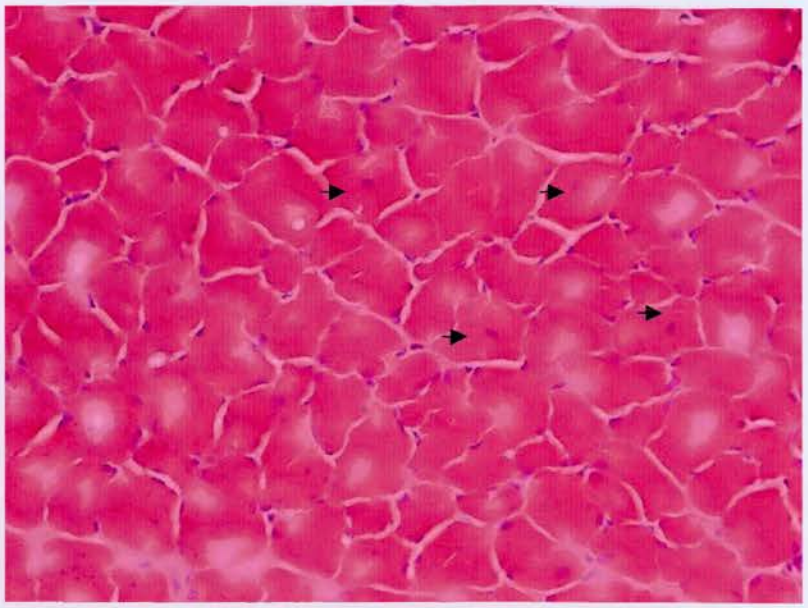

b.

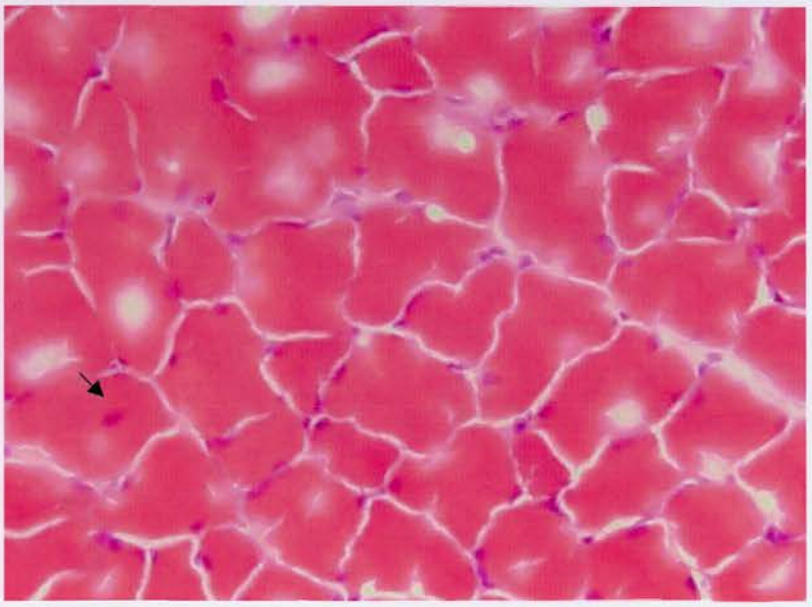

Figure 3-4 Hematoxylin and eosin-stained cross section of quadriceps of two 25-day-old mice, (a) 40x and (b) 60x, showing centralized nuclei typical of regenerating muscle fibres (arrows).

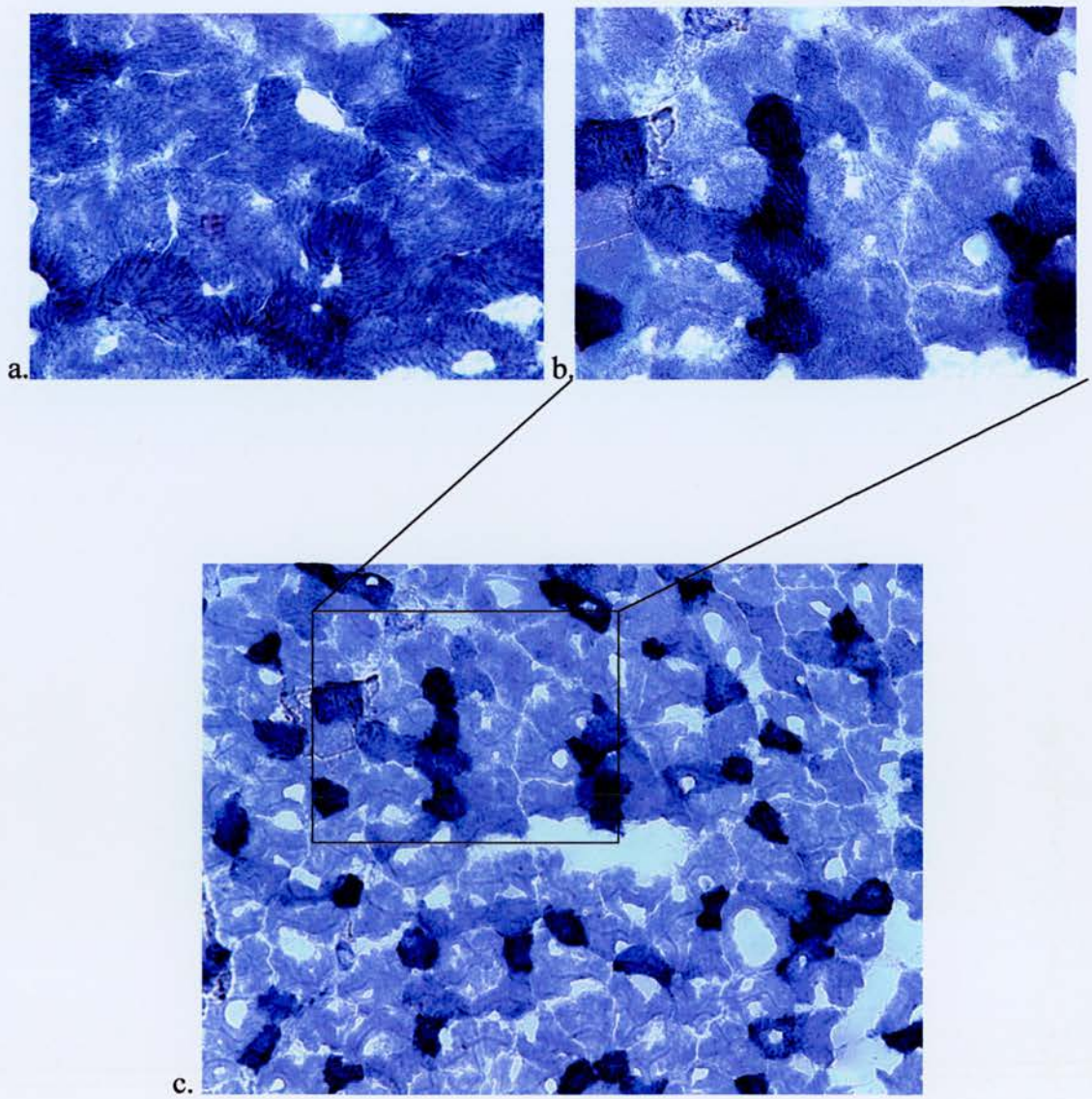

Figure 3-5 Succinyl dehydrogenase-stained cross sections of quadriceps of 25-day-old mice. (a) Wild-type mouse. (b and c) Wasted mouse, showing an increase in SDH staining.

3.2.3 Abnormalities of neuromuscular junctions in wasted mice

To determine whether the degenerative process involves terminal axons, labeling of NMJ of skeletal muscles, including transverse abdominis (TA) and lumbricals, was performed. Muscles from wild-type and wasted mice were microdissected and fixed in 4% paraformaldyhyde in PBS before labeling postsynaptic acetylcholine receptors with α-bungarotoxin (BTX) conjugated to tetramethylrhodamine isothiocyanate (TRITC-α-bungarotoxin). Muscles were then incubated overnight in primary antibody raised against 165-kDa isoform of neurofilament proteins and the synaptic vesicle protein SV2 and visualized with sheep anti-mouse FITC-conjugated secondary antibodies. Neuromuscular junctions were imaged using a laser scanning confocal microscope.

Microdissection and immunostaining were performed by myself and Dr. Thomas Gillingwater.

3.2.3.1 Progressive retraction of motor nerve terminals in wasted mice associated with muscle denervation

Immunocytochemical staining of neurofilament middle subunit (NF-M), SV2, and TRITC-α-BTX labeling of NMJs of TA and lumbricals in 23 and 25 day-old wild-type mice showed normal NMJs characterized by being plaques with branched structures (pretzel-shaped) in which presynaptic and postsynaptic specializations are closely associated (Figure 3-6a). By contrast, a lack of overlying terminal axons was observed in some synaptic areas of wasted mice, which further indicated the presence of a muscle denervation process, as shown in figure 3-6b and 3-6c. In addition to vacant motor endplates, other synaptic areas displayed striking abnormalities, including reduction of branched subneural apparatus, changes of terminal axons or both (Figure 3-6d). Sometimes the terminal axon collaterals were very thin and terminated in a "retraction bulb" swelling (Figure 3-6d). Evidence of progressive muscle denervation was observed in the TA muscles of wasted mice as young as 17 days old.

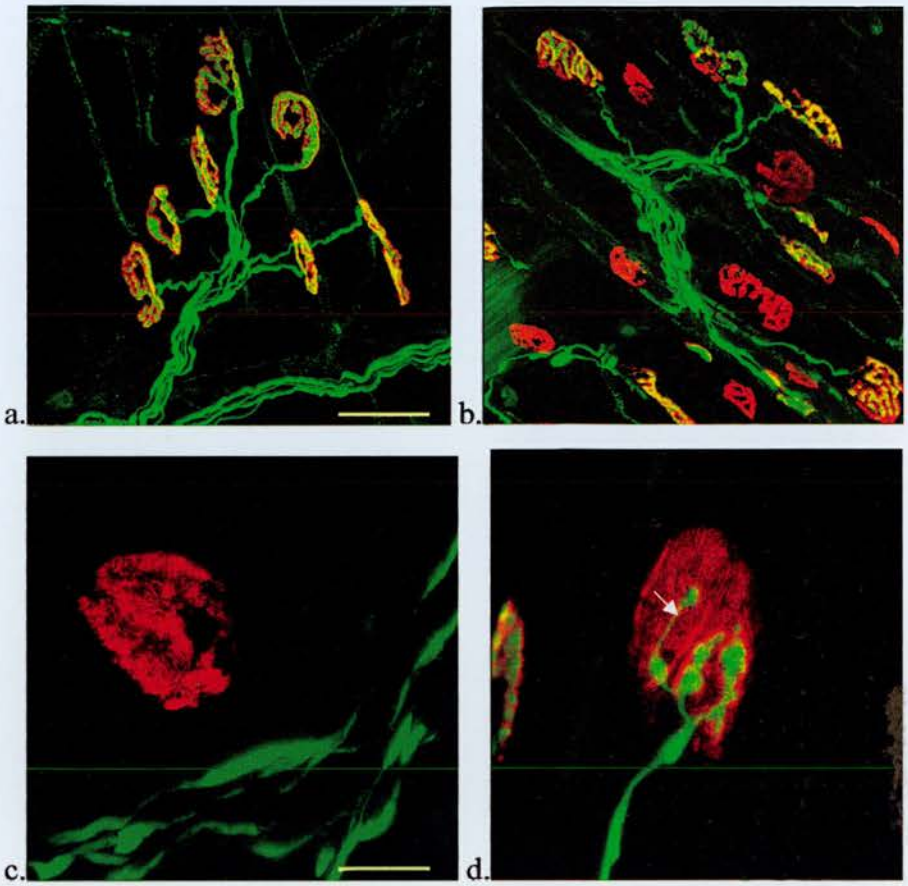

Figure 3-6 Denervated motor endplates and changes of terminal axons. Immunostaining of neuromuscular junctions on preparations of TA muscles with antibodies against neurofilament/SV2 (green) and counterstaining with TRITC-α-BTX (red). (a) 25-day-old control. (b and c) 23-day-old wasted mouse, showing a lack of overlying terminal axons. (d) 23-day-old wasted mouse, showing reduction of branched subneural apparatus. The arrow indicates a thin axon terminating in a "retraction bulb". Scale bar = 100 μm (a, b), = 20 μm (c,d).

3.2.3.2 Accumulation of neurofilaments in synaptic terminals of neuromuscular junctions in wasted mice

Synaptic terminals filled with NF-M were present in wasted mice but not in the controls of the same age (Figure 3-7). An accumulation of NF-M in wasted mice suggested that an aberrant cytoskeletal organization of terminal motor axons occurred in wasted mice. Surprisingly, no axonal sprouting was detectable in NMJs examined, despite the presence of denervated NMJ intermixed with accumulation of NF-M in synaptic terminals. These results indicate an abnormal organization of synaptic terminals associated with a defect of axonal regeneration in wasted mice.

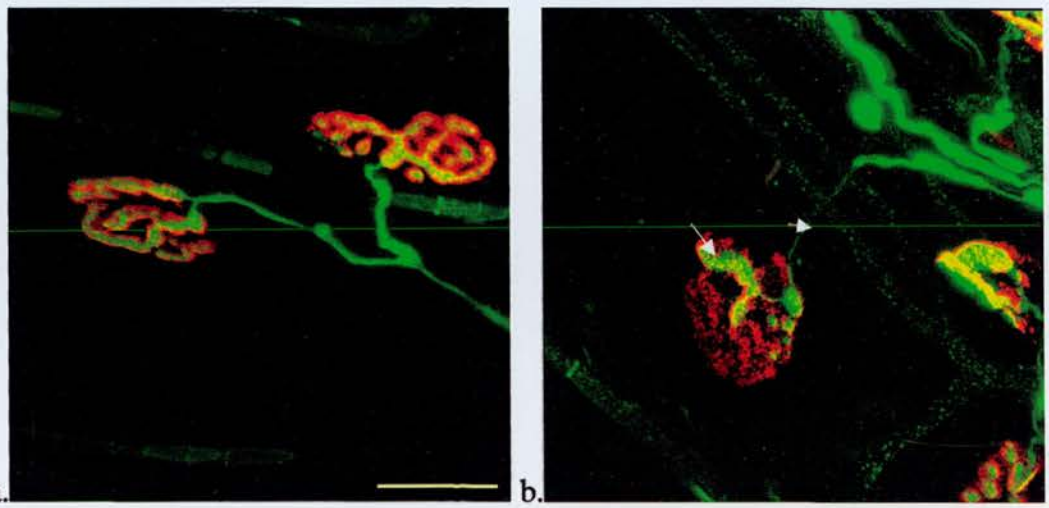

Figure 3-7 Accumulation of neurofilaments in terminal axons of wasted mice. (a) 23-day-old TA of a control mouse. (b) 23-day-old TA of a wasted mouse, revealing terminal axons filled with neurofilaments (arrow). The arrowhead indicates thinning of a distal axon. Scale bar = 20 μm.

3.2.4 Expression of nerve-regulated genes in muscle of wasted mice

Neurodegenerative diseases are less clear-cut with regard to molecular causes and physiological effects. Genes have been assigned to some forms of familial amyotrophic lateral sclerosis and spinal muscular atrophy. However, the ubiquitous expression of these genes does not give a hint as to why the nervous system is preferentially affected.

This part of my thesis deals with wasted mice that could represent an animal model for human motor neuron diseases. I studied genes for the α1 subunit of acetylcholine receptor (AchRα1), for the myogenic factor myogenin, and for the muscular chloride channel ClC-1, the expression of which in normal skeletal muscles is developmentally regulated and nerve-dependent.

Gene expression was evaluated by real-time quantitative RT-PCR using SYBR green 1 kit on total RNA extracted from the muscle quadriceps of 25 and 28 day-old wasted and wild-type mice. As the conventional use of a single gene for normalization leads to relatively large errors (Vandesompele *et al.*, 2002), the measures herein were normalized to RNA levels of two reference genes, β-actin (a structure-related gene) and GAPDH (a metabolism-related gene). Primer sequences are presented in Table 3-4.

3.2.4.1 Confirmation of primer specificity

The specificity of real-time PCR products was documented with 4% high resolution agarose gel electrophoresis and resulted in a single product with the desired length. In addition a melting curve analysis was performed at temperatures from 55 to 95 °C with a heating rate of 0.1 °C per second and a continuous fluorescence measurement, which resulted in single specific melting temperature as follows: AchRα1, 82.5 C; myogenin, 89.2 °C; ClC-1, 83.5 °C; β-actin, 85.5 °C; and GAPDH, 85.1 °C. No primer-dimers were generated during the 40 real-time PCR amplification cycles. Figure 3-8 show the results of melt curve analysis.

Table 3-4 Real-time RT-PCR Primers

Gene name	Orientation	Nucleotide sequence (from 5' to 3')	Size of the amplicon (bp)
AchRα1	Forward	ACCTGGACCTATGACGGCTCT	67
	Reverse	AGTTACTCAGGTCGGGCTGGT	
Myogenin	Forward	CTACAGGCCTTGCTCAGCTC	200
	Reverse	AGATTGTGGGCGTCTGTAGG	
ClC-1	Forward	CTGCATTTGGAAGGCTGGTAGGAG	161
	Reverse	AATGACGGCTGTGGAGACTGTGTG	
β-actin	Forward	CCCTGTATGCCTCTGGTCGT	103
	Reverse	ATGGCGTGAGGGAGAGCAT	
GAPDH	Forward	TGAAGCAGGCATCTGAGGG	102
	Reverse	CGAAGGTGGAAGAGTGGGAG	

3.2.4.2 Real-time PCR amplification efficiencies and linearity

To ensure comparability between the five (three target genes and two reference genes) real-time PCR assays, I determined the PCR efficiency of each individual assay by measuring serial dilutions of 100 ng cDNA from a wild-type muscle sample in triplicate. Only Ct values less than 40 were used for calculation of the PCR efficiency from the given slope in MyiCycler software according to the equation: PCR efficiency (E) = $(10^{[-1/slope]} - 1) \times 100$. Figure 3-9 shows some examples of the real-time PCR efficiencies, in which Ct cycles versus cDNA (reverse transcripted total RNA) concentration input (n = 3) were plotted to calculate the slope. All investigated transcripts showed high real-time PCR efficiency of more than 98%, with high linearity (Pearson correlation coefficient $r \geq 0.95$).

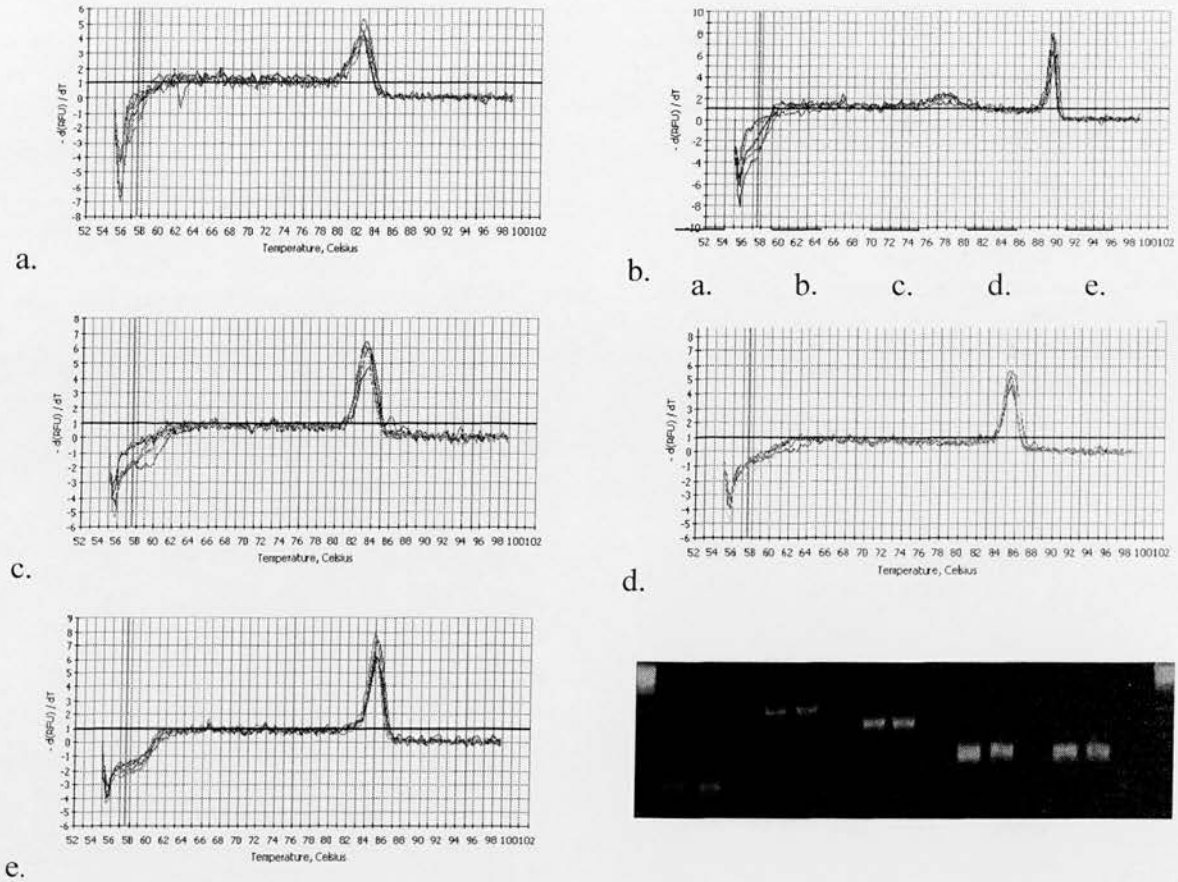

Figure 3-8 Melting curve analysis and high-resolution gel electrophoresis resulting in single product specific melting temperature for AchRα1 (a), myogenin (b), ClC-1 (c), β-actin (d), and GAPDH (e). The plots displayed the negative first derivative of the fluorescence (-dF/dT) against temperature

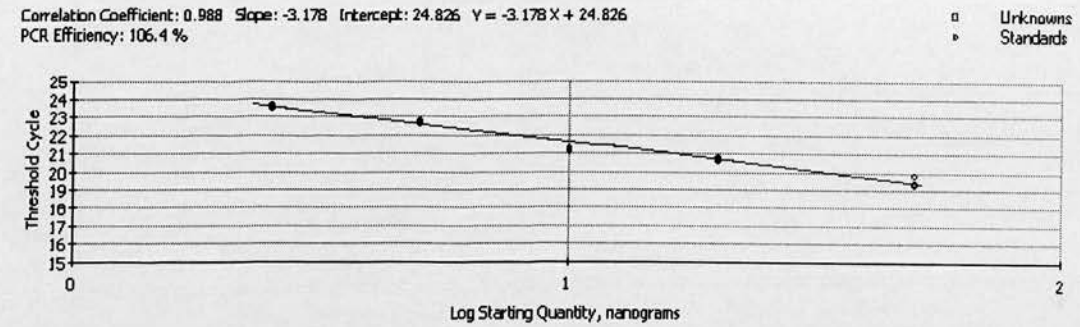

a

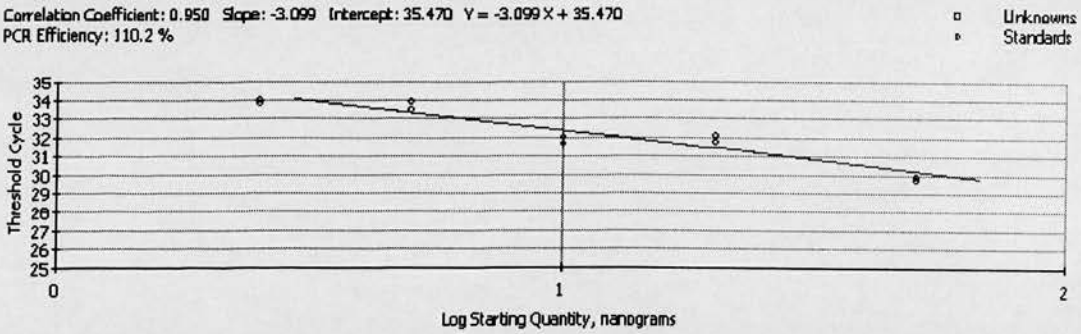

b

Figure 3-9 Determination of real-time PCR efficiencies of reference gene, GAPDH (a), and target gene, AchRα1 (b).

3.2.4.3 Intra-assay variation

To confirm the accuracy and reproducibility of real-time PCR, the intra-assay precision was determined in three repeats within one MyiCycler run. The calculation of test precision was based on the Ct variation and the Ct mean value. The table 3-5 shows intra-assay variation was less than 1.5% for all assays.

Table 3-5 Intra-assay variation of real-time RT-PCR

		Mean (n = 3)	Ct variation (%)
AchRα1	control	32.067	0.14
	sample	31.467	0.26
Myogenin	control	30.133	0.32
	sample	30.533	0.32
ClC-1	control	28.100	0.28
	sample	30.667	0.09
β-actin	control	26.933	0.97
	sample	27.133	1.16
GAPDH	control	23.067	1.42
	sample	22.500	0.48

3.2.4.4 Expression of the genes encoding AchRα1 and Myogenin in wasted mice

The expression of many muscle-specific genes is dependent on development and innervation. In mature muscle, myogenin is drastically down-regulated compared to the level in early developmental stages of muscle. In the same way, much lower concentrations of mRNAs for α1 subunits of AchR are found in healthy mature muscle than in myotubes. Denervation may reverse the pattern of gene expression. The principal patterns of genes expression typical for denervated muscle were confirmed for the wild-type mouse (Klocke *et al.*, 1994). For the gene expression analysis in wasted mice, I selected β-actin as a reference gene because its expression is relatively independent of

the state of maturation and innervation of the muscle fibres (Eftimie *et al.*, 1991; Pette D and Vrbovà G, 1985), and used GAPDH, a common housekeeping gene, as a second reference gene to support the results.

3.2.4.4.1 Wasted mice showed an upregulation of AchRα1 and myogenin genes

As the above studies suggested that muscle atrophy in wasted mice might be a result of denervation, to provide further support for these findings I investigated the expression of denervation-sensitive genes, AchRα1 and myogenin, in hindlimb muscle, quadriceps, from asymptomatic (20 days old) and symptomatic (25 days old) wasted mice, and age-matched wild-type controls (n = 3 for each group). Figure 3-10 shows that the transcripts of AchRα1 in quadriceps of 25 day-old mice are significantly upregulated 4.33-fold above the levels in wild-type mice (P = 0.0159). Interestingly, the upregulation of AchRα1 was also detected in wasted mice at age of 20 days old when no motor abnormalities were found, and the levels of expression were 32-fold higher than RNA from muscles of wild-type mice (P = 0.0004).

In a similar fashion, the expression of myogenin in 25 day-old wasted mice was elevated 10-fold higher than in wild-type mice (P = 0.0013), as shown in figure 3-10. In 20 day-old mice, the levels of myogenin expression were 2.35-fold higher than RNA from quadriceps of wild-type mice (P = 0.0091). When normalized to the levels of GAPDH expression, the levels of AchRα1 and myogenin followed the same pattern as that of β-actin gene (Figure 3-11). The positive correlation between AchRα1 and myogenin may reflect a mechanistic relationship as myogenin is a transcription factor which is known to control the expression of the AchRα1 gene (Eftimie *et al.*, 1991; Piette *et al.*,1990).

3.2.4.4.2 Downregulation of ClC-1 genes in wasted mice

The muscular chloride channel ClC-1 is another denervation-sensitive gene. In contrast to AchRα1 and myogenin, ClC-1, which regulates excitability, is only found in mature skeletal muscle, not in myotubes, and is downregulated upon denervation. Whereas levels of gene expression for AchRα1 and myogenin were elevated in wasted mice, those for ClC-1 were lowered. Normalized to the expression levels of β-actin, those of ClC-1 in wasted mice were 5- and 2.63-fold lower than in wild-type mice at age of 25 ($P = 0.001$) and 20 ($P = 0.0234$) days old, respectively (Figure 3-10). Similar patterns were demonstrated when normalized to the expression levels of GAPDH, as shown in figure 3-11.

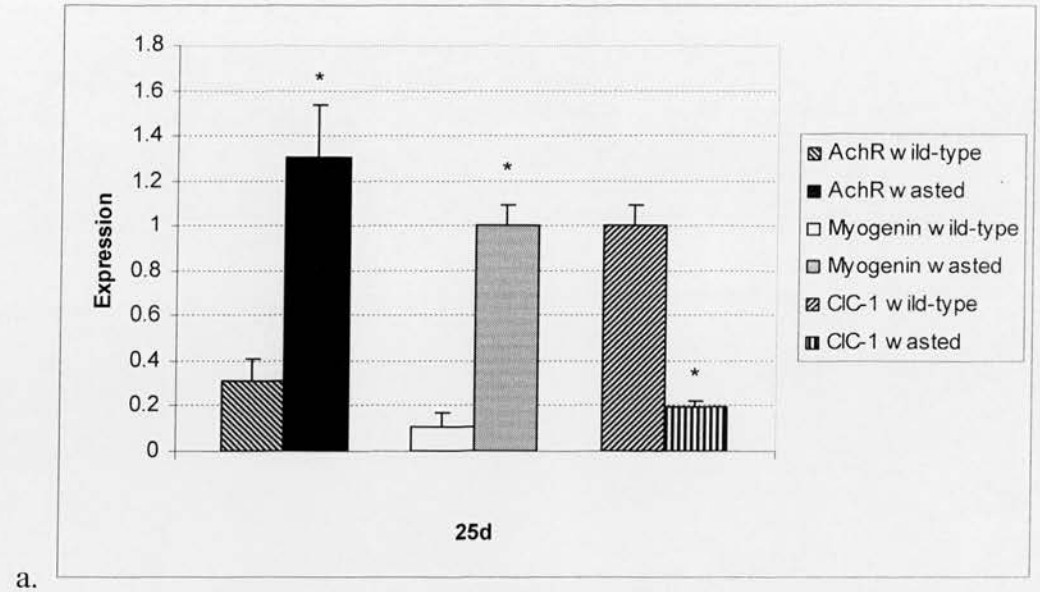

a.

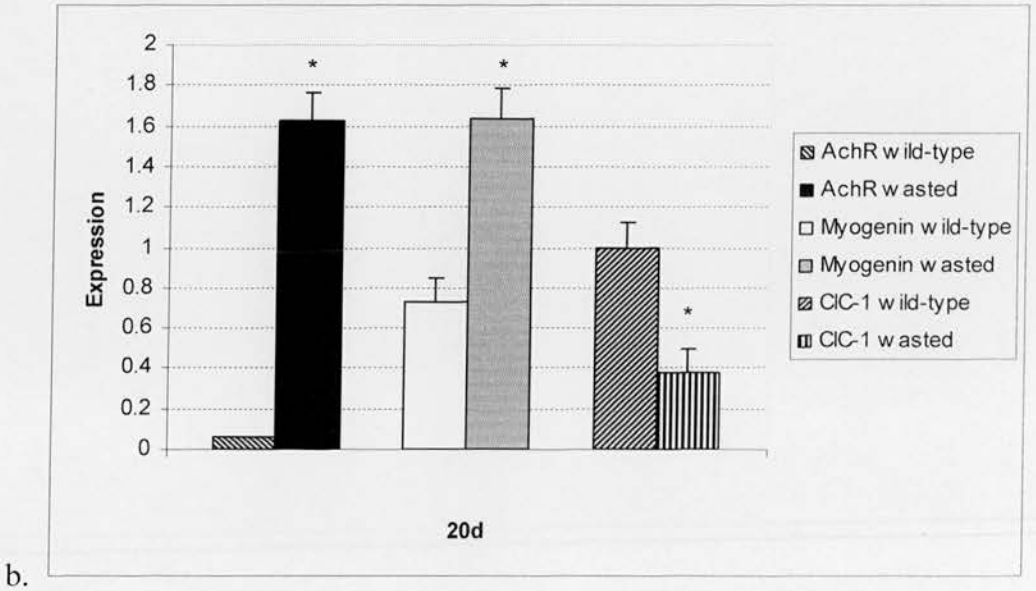

b.

Figure 3-10 Expression levels of AchRα1, myogenin, and ClC-1 genes in quadriceps of 25-day-old (a) and 20-day-old (b) wasted mice, normalized to those of β-actin. Asterisks denote statistical significance for comparisons (Unpaired *t*-tests).

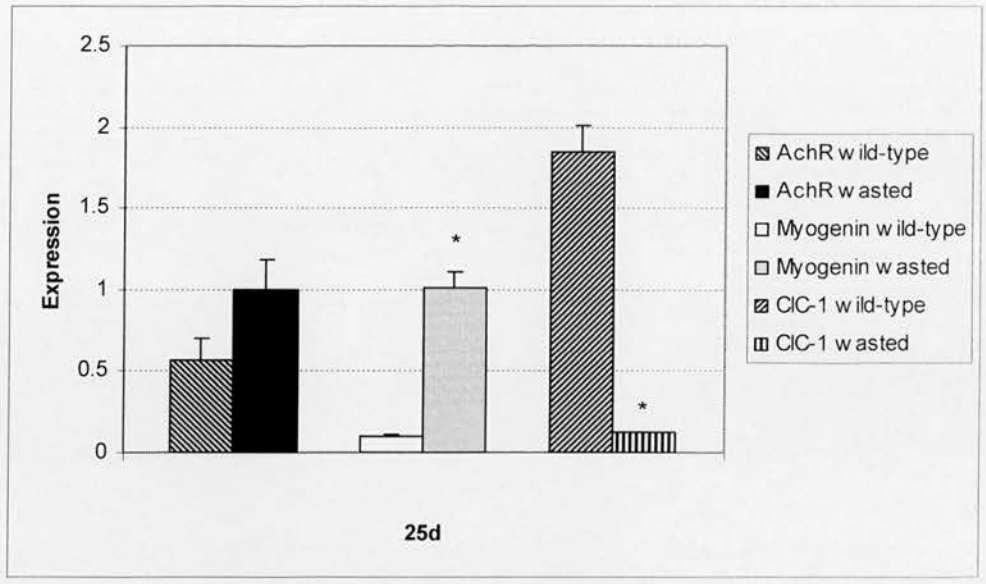

a.

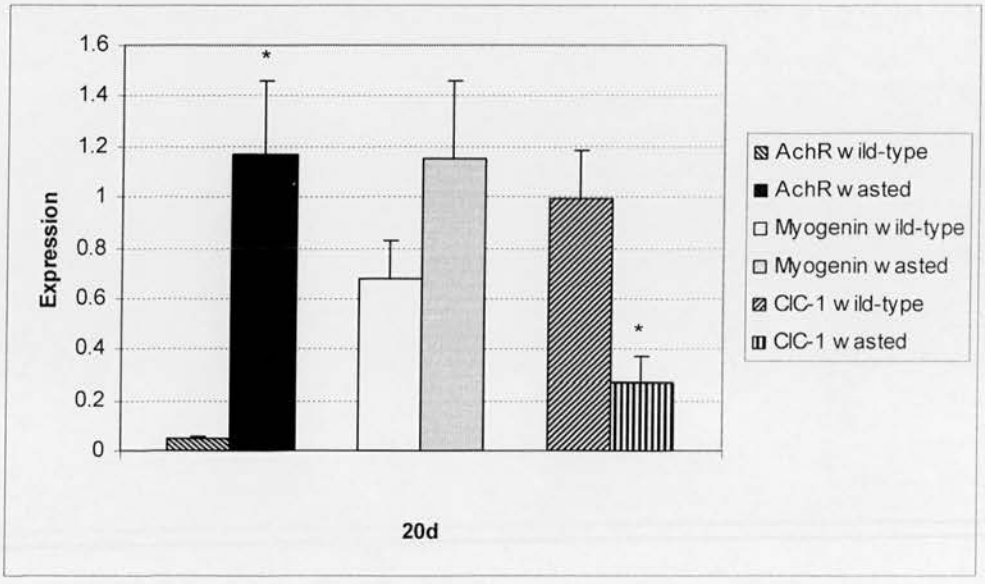

b.

Figure 3-11 Expression levels of AchRα1, myogenin, and ClC-1 genes in quadriceps of 25-day-old (a) and 20-day-old (b) wasted mice, normalized to those of GAPDH. Asterisks denote statistical significance for comparisons (Unpaired *t*-tests).

3.2.5 Skeletal muscle atrophy in wasted mice reveals an increase in Akt protein

3.2.5.1 Western analysis of protein

Wasted and wild-type mice were culled at 25 days old, when rigidity and ataxic walking are prominent. Figure 3-12 demonstrate the Western blot images and graph values of the levels of Akt expression for each animal. All of the wasted samples show an elevation of Akt protein to varying degrees, compared to those of age-matched wild-type mice. The same findings were seen for the expression of Akt-P, as shown in figure 3-13.

At the age of 25 days old, levels of Akt in wasted mice (0.497 ± 0.105) were significantly different from their age-matched controls (0.147 ± 0.053), with $P < 0.05$ (Figure 3-14). Levels of Akt-P expression in 25-day-old wasted mice were 0.386 ± 0.052, compared with those of wild-type controls of 0.054 ± 0.006, with $P < 0.005$ (Figure 3-14).

a.

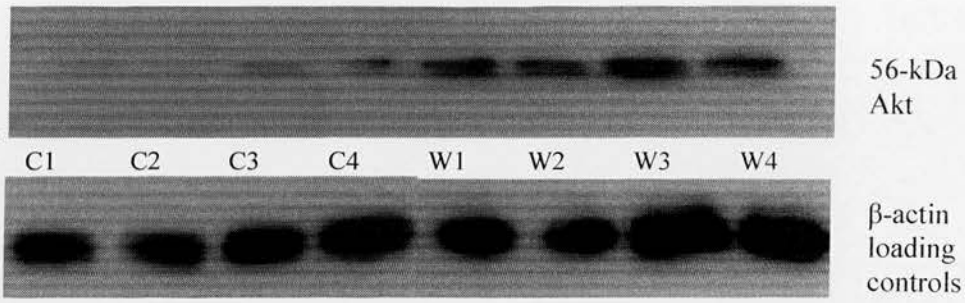

b.

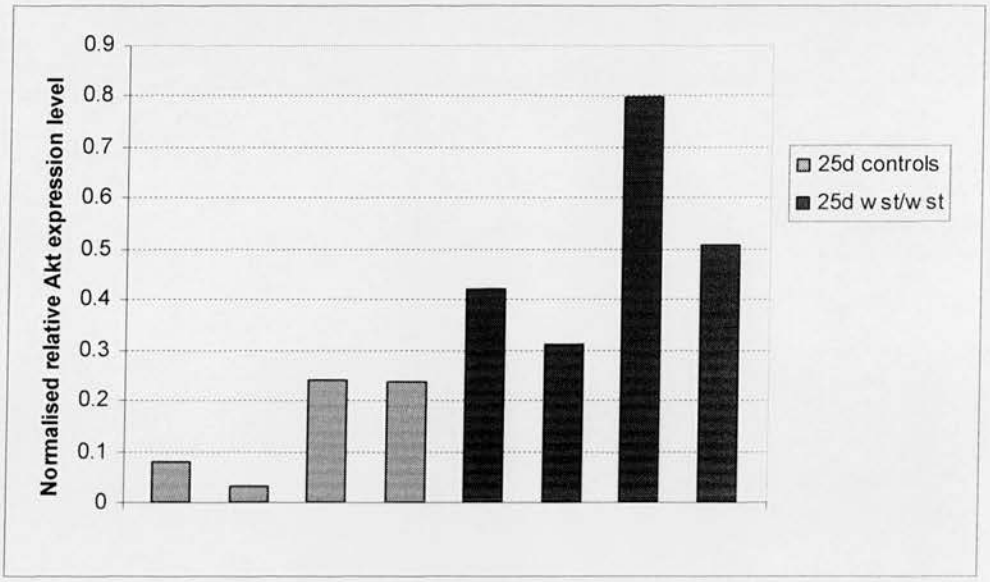

Figure 3-12 Akt protein expression levels in 25-day-old wasted mice. Western blot images (a) and graph values (b) are of four age-matched wild-type littermates (C1-C4) and wasted mice (W1-W4).

a.

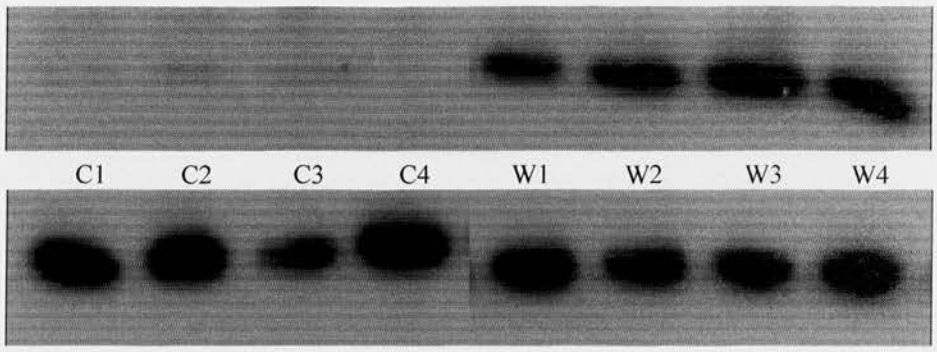

56-kDa Akt-P

β-actin loading controls

b.

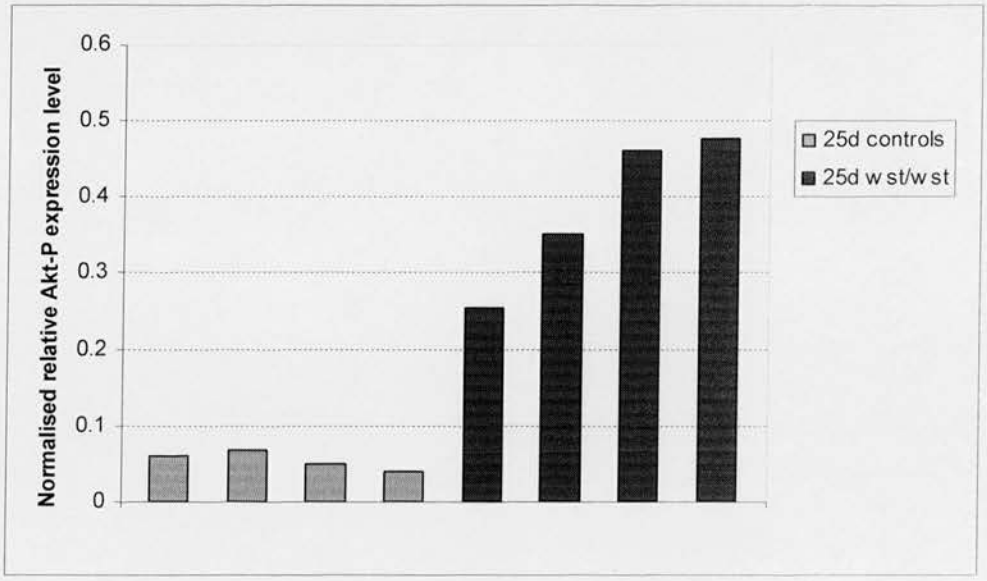

Figure 3-13 Akt-P protein expression levels in 25-day-old wasted mice. Western blot images (a) and graph values (b) are of four age-matched wild-type littermates (C1-C4) and wasted mice (W1-W4).

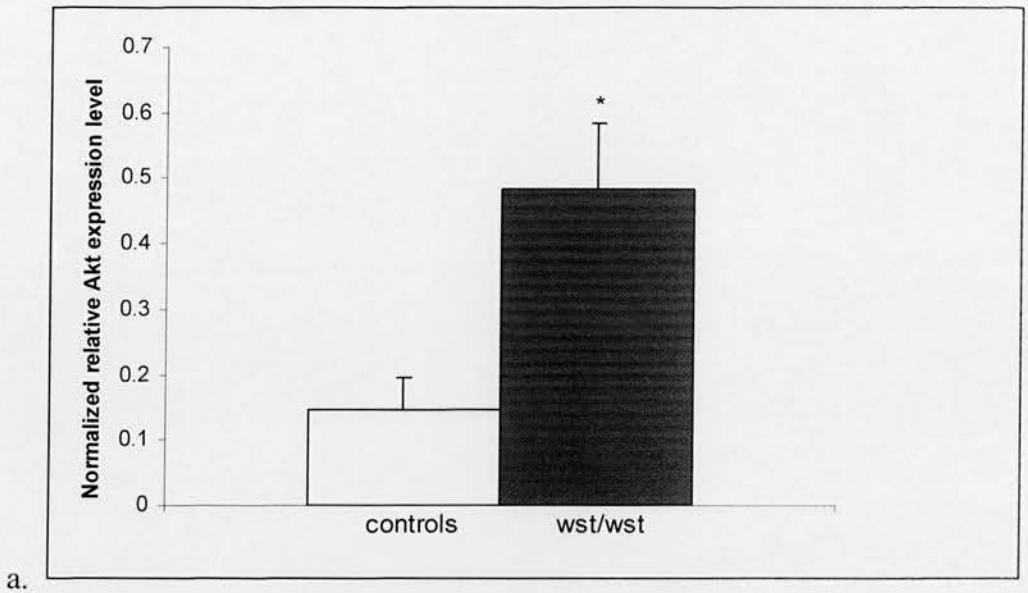

a.

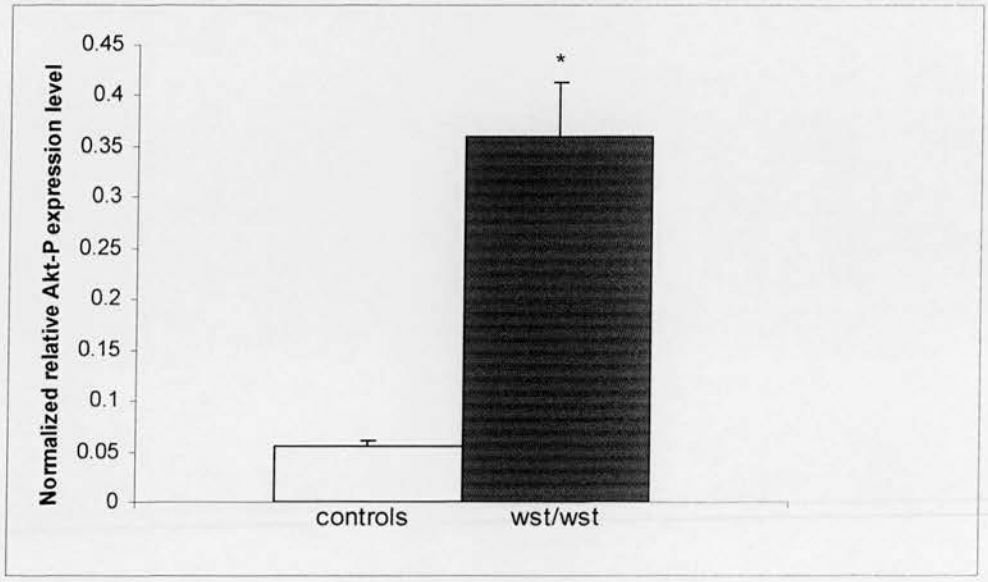

b.

Figure 3-14 Expression levels of Akt (a) and Akt-P (b) in 25-day-old wasted mice. Values are presented as means $\pm$ S.E.M (n = 4 per group). Asterisks denote $P < 0.05$ (a), and $P < 0.005$ (Unpaired *t*-test).

3.3 Discussion

3.3.1 Causes of muscle atrophy in wasted mice

The causes of muscle atrophy and how the loss of eEF1A2 in wasted mice leads to muscle atrophy have not been identified. I have demonstrated here and found several clues of evidence that suggest that muscle atrophy in wasted mice is neurogenic in origin. It has been previously shown that the loss of eEF1A2 in muscle of wasted mice leads to a disproportionate decline in muscle mass as wasted mice deteriorate (Newbery *et al.*, 2005). That this change was due to fibre atrophy in the wasted muscles was documented here by the overall decreased in the cross-sectional area of fibres and in the decreased diameter.

The finding of angulated atrophic fibres in muscle of wasted mice suggests the early stage of denervation. If a motor unit that was originally innervated by a type 1 nerve loses its innervation, a number of isolated atrophic fibres will be initially scattered about a small region of the muscle. Pyknotic nuclear clumps that are found in the same muscles that present angulated fibres suggests the degenerative process is ongoing, even that some fibres were getting into the late stage of fibre denervation. In human, these findings of neurogenic changes can occur in disorders that affect motor neurons, including anterior horn cells (eg. motor neuron disease), motor neuropathy, peripheral neuropathy, and disorders that affect intramuscular nerve twigs. In wasted mice, these findings are consistent with the previous publications that showed vacuolation in anterior horn cells (Lutsep and Rodrigeuz, 1989; Newbery *et al.*, 2005). Grouped atrophic muscle fibres characteristic of muscle denevation were also found in a transgenic mouse model of SMA (Frugier etal., 2000) and ALS (Gurney *et al.*, 1994; Ripps *et al.*, 1995; Wong *et al.*, 1995; Bruijn *et al.*, 1997).

The examination of wasted mice occasionally revealed centralized nuclei typical of regenerating muscle fibres. Although they can be found in myopathy, the number of

centralized or internal nuclei in such a condition would be marked. The increased SDH staining in wasted muscle demonstrated here may give another supporting clue for regenerating fibres in wasted muscle. Mitochondrial proliferation is one of the striking responses observed in skeletal muscle exposed to a variety of physiological conditions (Freyssenet *et al.*, 1996; Hood *et al.*, 2000). It has been demonstrated that skeletal muscle regeneration is accompanied by a dramatic stimulation of mitochondrial biogenesis concomitant with the onset of muscle differentiation (Duguez *et al.*, 2002). The signals involved in the stimulation of mitochondrial biogenesis during muscle regeneration remain to be determined, but they most likely result form the combinatorial interplay of different molecular events. For example, it has been shown in transgenic mice expressing a locally acting isoform of insulin-like growth factor-1 (mIgf-1) that is expressed in skeletal muscle that mIgf-1 may act as a survival factor by prolonging the regenerative potential of younger muscle (Musarò *et al.*, 2001). Skeletal muscle atrophy occurs as a result of a variety of conditions such as aging, denervation, immobilization and starvation. Regardless of the initiating event, muscle atrophy is characterized by a decrease in protein content, fibre diameter, force production, and fatigue resistance. It is interesting that wasted mice in which loss of eEF1A2, a protein involved in translation step of protein synthesis is found, and in which eEF1A1 is undetectable after 21 days of age, may still have the potential to regenerate muscle fibres. The response of skeletal muscle to denervation is complex. On the one hand, as also seen here in wasted mice, individual muscle fibres undergo significant atrophy, and there is considerable disassembly of the contractile apparatus, along with significant myonuclear loss. On the other hand, there is a considerable increase in the satellite cell population within days of denervation (Hanzliková *et al.*, 1975; McGeachie and Allbrook *et al.*, 1978; Ontell, 1974; Viguiè *et al.*, 1997) as well as the formation of new muscle fibres (Borisov *et al.*, 2001; Dedkov *et al.*, 2001). In denervated muscle in rat, levels of eEF1A1 protein remain very low for the first 10 days after denervation (Khalyfa *et al.*, 2003). During this period, the satellite cell population associated with the denervated muscle fibres roughly doubles (Snow, 1983), and the muscle fibres themselves begin to show signs of atrophy. By 30 days after denervation, the level of eEF1A1 protein (normally expressed at very

low levels at this age) have shown a significant increase. However, this observation in rat cannot be applied to wasted mice in which the expression of eEF1A1 protein progressively declines in atrophic muscle, although it is still detectable at low levels at 28 days old (Khalyfa *et al.*, 2001). Even though it is expressed at low levels after weaning, the activity of eEF1A1 protein in muscle of symptomatic wasted mice may account for protein synthesis in such regenerating muscle fibres.

To determine whether the degenerative process also involved motor axons, labeling of NMJ of skeletal muscles was performed. A lack of terminal axons was observed in some synaptic areas of wasted mice studied, which further indicates the presence of a muscle denervation process. Moreover, terminal axons were filled with NF-M as determined by immunolabeling. Synaptic terminals filled with NF were already present in 17-day-old wasted mice but not in controls, indicating that this change occurs early in the development of wasted phenotype. Surprisingly, no axonal sprouting was detectable, despite the presence of denervated NMJ intermixed with NMJ showing terminal axons filled with NF. These results indicate an abnormal organization of synaptic terminals associated with a defect of axonal regeneration in wasted mice. These findings in wasted mice are similar to those in *Smn* mutant mice, a mouse model of spinal muscular atrophy (SMA) (Cifuentes-Diaz et al., 2002), but different from those found in SOD^{G34A} transgenic mice, a mouse model of ALS characterized by motor neuron degeneration (Gurney et al., 1994). No terminal axon filled with NF and numerous axonal sprouts were observed in the ALS model, indicating that NMJ changes are not only specific to *Smn* mutant mice, but also in wasted mice. The accumulation of NF in terminal axons in wasted and *Smn* mutant mice may have common pathogenic processes. Whether the accumulation of NF is a primary effect of the loss of eEF1A2 or SMN function or a secondary event via an unidentified pathway remains to be investigated. Cytoskeletal components play a major role in axonal growth and plasticity. Abnormalities of accumulation of NF in terminal axons of wasted mice may contribute to the defects in terminal axon growth and plasticity, as suggested by the retraction of motor nerve terminals and the defect in axonal sprouting. The resulting aberrant cytoskeletal

organization at the NMJ of wasted mice may contribute to the loss of motor neuron function. Moreover, the relatively marked degenerative changes in terminal axons contrast with the mild abnormalities in anterior horns of spinal cord during the early stage of wasted phenotype, as shown by the presence of gliosis without reduction of motor cell bodies in 19 day-old wasted mice (Newbery *et al.*, 2005), suggesting that degeneration of motor neuron cell bodies may result from a dying-back axonopathy starting from terminal axons.

To further support the consistency of my results, the levels of gene expression of nerve-regulated genes were studied in quadriceps of wasted mice. I show here that the neuromuscular disease in wasted mice leads to drastic upregulation of the genes for AchRα1 and for the myogenic factor myogenin. The disease also leads to mild to moderate reduction of the muscular chloride channel ClC-1 transcripts. Myogenin is a transcription factor that is shown to control the expression of the AchRα gene (Eftimie *et al.*, 1991; Gunning *et al.*, 1983), and, like other myogenic factors, is itself regulated by electrical activity. In normal muscle fibres, the effect of membrane depolarization is mediated by Ca^{2+} fluxes and the activation of protein kinase Cα (PKCα). Activated PKCα phosphorylates and thereby inactivates myogenin, thus suppressing transcription of the AchRα gene (Huang *et al.*, 1994; Huang *et al.*, 1993; Huang and Schmidt, 1994; Huang *et al.*, 1992). As mRNA levels for myogenin and AchRα are higher both in immature and in denervated muscle fibres than in innervated adult muscle fibres, they indicate either regeneration or physiologic denervation. The same gene regulation holds for the downregulation of the expression of ClC-1 in wasted mice. ClC-1 mediates the Cl^- conductance of the plasma membrane. Not only does ClC-1 control the excitability of adult muscle, but its own expression is dependent on actual muscle activity (Klocke *et al.*, 1994). Thus, it supports the findings in muscle pathology and in changes of gene expression in wasted mice that there is concomitant ongoing denervation and muscle fibre regeneration during the degenerative process.

3.3.2 Muscle atrophy in wasted mice and Akt protein

The severe and progressive muscle wasting resulting from ongoing denervation is a key clinical feature of motor neuron diseases. Perturbations have been seen in the PI3-K pathway in neural tissue of both human and murine models of ALS (Wagey *et al.*, 1998, Hu *et al.*, 2003a, Hu *et al.*, 2003b), yet very few studies have examined biochemical and molecular changes occurring within the muscle. I therefore chose to examine skeletal muscle from wasted mice, a potential murine model of progressive denervation, to determine if Akt and its phosphorylated protein, a key downstream peptide of PI3-K pathway, were affected in the diseased muscle.

As hypothesized, a significant upregulation of Akt was found in the skeletal muscle of wasted mice. At the severe symptom period and at end-stage, levels of both Akt protein and its phosphorylated form were significantly higher in wasted mice than values observed in age-matched wild-type controls. PI3-K signaling has been shown to be involved in multiple cellular functions, including muscle growth and cell survival. It is possible that these changes in Akt may reflect an attempt by the muscle to target downstream effectors responsible for these functions.

Together with the immunohistochemistry studies in NMJs of wasted mice in chapter three, that showed a progressive muscle denervation, the observed increases in Akt and phosphorylated Akt appear in conjunction with increases in denervation, suggesting that the muscle may be upregulating Akt in response to continual denervation, and the rise in Akt may contribute to maintenance of muscle mass until the point where excessive denervation and resultant myofibre death overpower its function.

The elevation in phosphorylated Akt implies that factors upstream in the signaling may be altered as well. Significant increases in PI3-K activity have been found in short-term denervated rat hind limb (Bertelli *et al.*, 2003). Various trophic factors have also been shown to be elevated in muscle in a number of models of denervation. An upregulation

of local growth factors such as IGF-1, resultant from the progressive denervation, could be responsible for triggering the PI3-K signaling cascade, thereby targeting Akt. However, Bertelli and colleagues (Bertelli et al., 2003) found that phosphorylated Akt levels were reduced in the denervated muscle when compared to control tissue, even with increased PI3-K activities. Other experiments also revealed decreased Akt protein and phosphorylation content in denervated rat hind limb, versus sham-operated controls (Wilkes and Bonen, 2000). In human, skeletal muscle atrophy in ALS has been revealed to show a reduction in Akt activity (Léger *et al.*, 2006). These results appear to contradict my current findings, but differences could exist due to different models of denervation. For example, some studies examined changes in rat skeletal muscle at only 3 minutes (Wilkes and Bonen, 2000) and 4 hours (Bertelli *et al.*, 2003) after acute denervation via removal of a portion of sciatic nerve. At such immediate time points, it is possible that the findings could represent a temporal sequence. PI3-K activity appears to have been stimulated directly upon denervation (Bertelli *et al.*, 2003), but a 4 hour window may not allow enough time to observe commensurate results downstream at Akt.

Alternatively, in wasted mice, myofibre denervation is an ongoing process which could result in continual signaling to upregulate PI3-K and downstream targets such as Akt. As more fibres become denervated with disease progression, an increased release of trophic factors could occur, resulting in increased PI3-K activity and gradual elevations in downstream Akt and phosphorylated Akt, as the findings in wasted mice suggest.

Apoptosis has been shown to be a component of denervation-induced atrophy (Allen *et al.*, 1997, Schoser *et al.*, 2001) and Akt has been shown to phosphorylate proteins involved in both apoptotic and atrophic signaling pathways, such as caspase 9 or FOXO (Toker, 2000, Sandri *et al.*, 2004, Stitt *et al.*, 2004). Phosphorylation of these proteins results in their de-activation, thereby contributing to the suppression of both programmed cell death and catabolic pathways simultaneously.

Levels of Akt and its phosphorylated protein in wasted mice could also be elevated in an attempt to regulate muscle mass, as the role of Akt in protein synthesis has also been substantially documented. Different Akt content and activity has been found to exist between individual muscle cells, and during muscle regeneration, endogenous Akt phosphorylation and activity were upregulated only in innervated, not denervated fibres (Pallefaccina *et al.*, 2002). If so, the findings of moderate to high Akt intensity in my current study may represent a small number of innervated fibres remaining within a localized cluster of denervated areas. This could represent an upregulation of processes in an attempt to regulate losses within specific motor units, targeting not only denervated but remaining innervated fibres as well.

Maintenance of muscle mass requires a balance between hypertrophic and atrophic pathways. While Akt has been previously been shown to activate protein synthetic pathways, recent evidence suggests a role for Akt in the suppression of atrophy through FOXO. Studies have recently demonstrated that inhibition of FOXO factors via Akt-mediated phosphorylation results in a downregulation of MAFbx and MuRF-1 (Sandri *et al.*, 2004, Stitt *et al.*, 2004) with subsequent suppression of atrophic protein degradation (Sacheck *et al.*, 2004).

It is unclear whether an increase in Akt and its phosphorylated proteins in skeletal muscle of wasted mice are operating to target imperative biological processes, or if they are instead only a result of the disease state of the muscle. Further studies will aid in the further understanding of the role of Akt in progressively denervated muscle, potentially via identification of relevant downstream targets.

Chapter 4 Transfection of HeLa cells to study redistribution and colocalisation of eEF1A2 and SMN: Analysis by Quantitative Immunocolocalisation

4.1 Introduction

The eEF1A protein is one of the most abundant proteins in mammalian cells and plays a pivotal role in protein synthesis. eEF1A is present mainly in the cytoplasm of cells, but a small proportion of eef1a molecules has been previously identified in the nucleus (Colling *et al.*, 1994, Janssen *et al.*, 1994, Barberse *et al.*, 1995, Billaut-Mulot *et al.*, 1996, Sandres *et al.*, 1996). It has been reported that ZPR1 binds to eef1a in human A431 epidermal carcinoma cells (Gangwani *et al.*, 1998). ZPR1 is located in the cytoplasm of quiescent mammalian cells. Treatment with mitogens, including EGF, causes the redistribution of ZPR1 from the cytoplasm to the nucleus (Galcheva-Gargova, *et al.*, 1996). EGF stimulation of A431 cells also triggers the formation of ZPR1/eEF1A complexes and the the translocation of both ZPR1 and eEF1A from the cytoplasm to the nucleus. There are two isoforms of eEF1A, eEF1A1 and a highly homologous (92%) isoform, eEF1A2. The function of eEF1A in the nucleus has not been identified. The redistribution of eEF1A in proliferating cells suggest that this protein, either eEF1A1 or eEF1A2 isoform, may be involved in a signaling pathway that communicates mitogenic signals from the cytoplasm to the nucleus.

Although a few report reports described a nuclear localization for eEF1A, some studies have been unable to show shuttling or nuclear localization of eEF1A (Calado *et al.*, 2002, Bohnsack *et al.*, 2002). It has been demonstrated that eEF1A interacts with exportin-5 (Exp-5) and Exp-5 mediates nuclear export of eEF1A, causing eEF1A to be strictly excluded from nuclei.

The nuclear localization of eEF1A isoforms and involvement of eEF1A in the nuclear processes remain to be established. Studies have shown that both eEF1A isoforms are expressed in neurons (Lee *et al.*, 1995, Lee *et al.*, 1993) and in pheochromocytoma cells (PC12) (Petroulakis and Wang, 2002). In PC12 cells, a preferential synthesis of eEF1A1 over eEF1A2 has been demonstrated upon nerve growth factor (NGF) stimulation. As the absence of eEF1A2 is implicated in neurodegeneration in the mouse mutant, *wasted*, it would be interesting to investigate the redistribution of eEF1A2 in cells in the starved condition and upon mitogenic stimulation.

In addition to the interaction of ZPR1 and eEF1A, studies have shown that SMN co-immunoprecipitates with ZPR1. Immunoprecipitation of SMN and ZPR1 was drastically reduced when cells were grown in the absence of serum and was restored upon serum refeeding (Gangwani *et al.*, 1998). One hallmark of spinal muscular atrophy is the failure of SMN to localize within the nuclear bodies (Gangwani *et al.*, 2001). It is not known whether eEF1A2 is in the same ZPR1-SMN pathway, or whether or not the entire complex is translocated into the nucleus together. I therefore conducted transfection experiments and studied colocalization of eEF1A2 and SMN using quantitative immunocolocalization.

4.2 Results

4.2.1 Construction of epitope-tagged hEEF1A2 expression plasmid

The strategy for this study was to clone a human eEF1A2 cDNA amplified by PCR from the I.M.A.G.E cDNA clone into the expression vector pcDNA3.1(+)C-myc-His, following by transfection and immunofluoresecnce analysis.

4.2.1.1 PCR amplification of the human eEF1A2 cDNA from pOTB7-hEEF1A2

PCR primers (Table 4-1) were designed to amplify the human eEF1A2 full-length cDNA from the I.M.A.G.E clone, pOTB7-hEEF1A2. The *Hind*III restrtiction site was introduced into the 5' end of the forward primer and the *Xho*I restriction site was introduced to the 5' end of the reverse primer in order to subclone the insert into the *Hind*III and *Xho*I sites of the vector.

Table 4-1 Primers for amplification of the full-length human eEF1A2 cDNA. The underlines indicate *Hind*III and *Xho*I sites for the forward and reverse primers, respectively.

Primer name	Primer sequence (5' to 3')
hEF12c_forward	CGC GCA AGC TTA ATG GGC AAG GAG AAG ACC CAC ATC
hEF12c_reverse	GGC GTT CTC GAG CG CTC TTC TTC TCC ACG TTC TTG

Double strand cDNAs of 1,357 bps were synthesized by PCR at 94 °C for 2 minutes for a pre-heat step, followed by 94 °C for 1 minute, 55 °C for 45 minutes, and 72 °C for 1 minute for 34 cycles. The resulting PCR products were visualized on an agarose gel and purified. The PCR products were then digested with *Hind*III and *Xho*I, and gel purified before subcloning into the *Hind*III/*Xho*I site of pcDNA3.1(+)C plasmid.

4.2.1.2 Preparation of the expression vector pcDNA3.1(+)C-myc-His

The 5,500-bp expression vector pcDNA3.1(+)C, which contains the Myc epitope, was digested with *Hind*III and *Xho*I restriction enzymes. As these two restriction sites were close together, the vector was dephosphorylated with shrimp alkaline phosphatase to decrease the non-recombinant background caused by incomplete digestion with one of the enzymes, which was undetectable by gel analysis. Following digestion and dephosphorylation, the vector was gel-purified prior to insert ligation to reduce residual nicked and supercoiled plasmid.

4.2.1.3 Cloning of the full-length human eEF1A2 cDNA into the vector pcDNA3.1(+)C-myc-His

The 1,357-bp full-length human eEF1A2 cDNA was cloned into the *Hind*III/*Xho*I sites of pcDNA3.1(+)C-myc-His plasmid at a 3:1 or 5:1 insert to vector ratio at room temperature with an overnight incubation. Transformation was performed in the E.coli strain JM109 as described in 2.2.1.13. Selection for transformation was accomplished by plating on medium containing ampicillin.

4.2.1.4 Screening and analysis of the transformants

After cloning, transformed E.coli colonies were screened by colony PCR, using insert-specific promers, and restriction digestion analysis to identify the desired construct. Table 4-2 shows the sequences of the primers used for colony PCR, and figure 4-1 shows the images of right PCR products obtained from colony PCR, and of the result of restriction digestion with *Hind*III and *Xho*I restriction enzymes, confirming the success of cloning. Figure 4-2 shows the map of the pcDNA3.1(+)C-hEEF1A2-myc, which was ready for transfection.

Table 4-2 Human eEF1A-2 cDNA-specific primers for colony screening

Primer name	Primer sequence (5' to 3')	Size of the amplicon (bp)
hEF12sc_forward	TCA TCG GCC ACG TGG ACT CC	311
hEF12sc_reverse	CGA TCA GCA CTG CGC AGT CC	

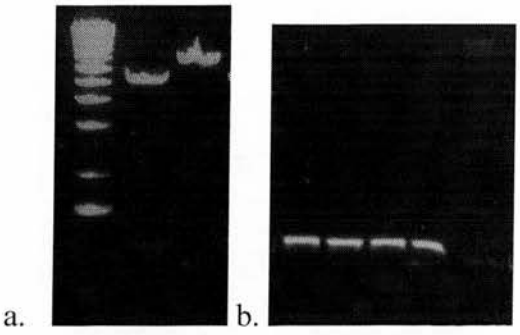

a. b.

Figure 4-1 Images of gel elecrophoresis showing the right product of restriction digestion analysis (a), and of colony screening (b).

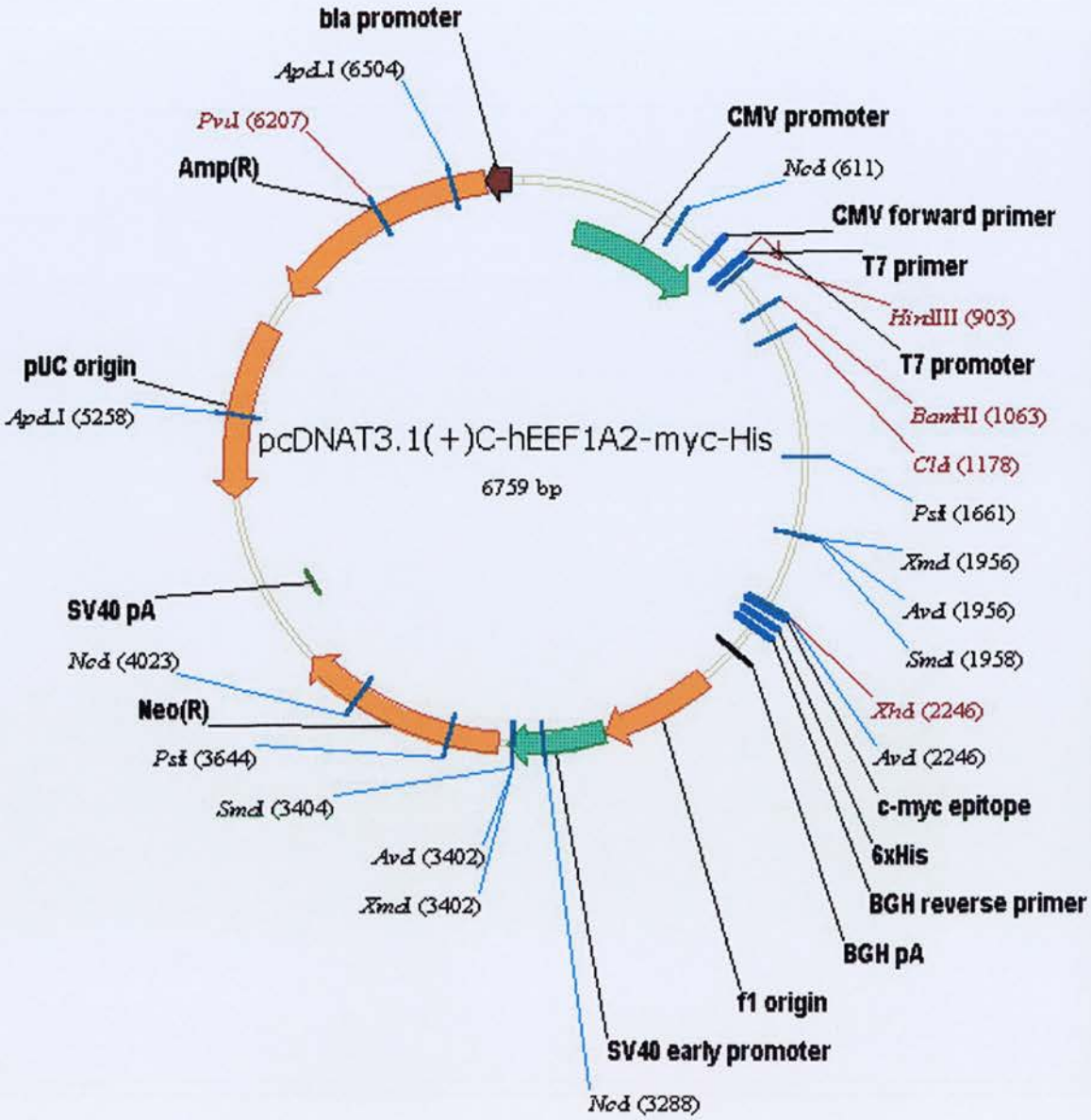

Figure 4-2 Map of the pcDNA3.1(+)C-hEEF1A2-myc. The full-length human eEF1A2 cDNA is located between the *Hind*III and *Xho*I sites.

4.2.1.5 Sequencing of the pcDNA3.1(+)C-hEEF1A2-myc

The pcDNA3.1(+)C-hEEF1A2-myc was partially sequenced across the insert to ensure that no mutation was introduced in the PCR process of insert preparation. The T7 promoter/priming site and BGH reverse priming site located in the pcDNA3.1(+)C-myc-His were simply chosed for primer designing, as shown in table 4-3.

Table 4-3 Sequencing primers for the pcDNA3.1(+)C-hEEF1A2-myc

Primer name	Primer sequence (5' to 3')
T7 promoter/priming_forward	TAA TAC GAC TCA CTA TAG GG
BGH priming_reverse	TAG AAG GCA CAG TCG AGG

The sequenced result was aligned to the reference human eEF1A2 cDNA sequence, NM_001958, and demonstrated 100% identity, as shown in figure 4-3.

```
CLUSTAL W (1.83) multiple sequence alignment

RefSeq          ------------------------------------------ATGGGCAAGGAGAA 14
seq             TAATACGACTCACTATAGGGAGACCCAAGCTGGCTAGTTAAGCTTAATGGGCAAGGAGAA 60
                                                           **************

RefSeq          GACCCACATCAACATCGTGGTCATCGGCCACGTGGACTCCGGAAAGTCCACCACCACGGG 74
seq             GACCCACATCAACATCGTGGTCATCGGCCACGTGGACTCCGGAAAGTCCACCACCACGGG 120
                ************************************************************

RefSeq          CCACCTCATCTACAAATGCGGAGGTATTGACAAAAGGACCATTGAGAAGTTCGAGAAGGA 134
seq             CCACCTCATCTACAAATGCGGAGGTATTGACAAAAGGACCATTGAGAAGTTCGAGAAGGA 180
                ************************************************************

RefSeq          GGCGGCTGAGATGGGGAAGGGATCCTTCAAGTATGCCTGGGTGCTGGACAAGCTGAAGGC 194
seq             GGCGGCTGAGATGGGGAAGGGATCCTTCAAGTATGCCTGGGTGCTGGACAAGCTGAAGGC 240
                ************************************************************

RefSeq          GGAGCGTGAGCGCGGCATCACCATCGACATCTCCCTCTGGAAGTTCGAGACCACCAAGTA 254
seq             GGAGCGTGAGCGCGGCATCACCATCGACATCTCCCTCTGGAAGTTCGAGACCACCAAGTA 300
                ************************************************************

RefSeq          CTACATCACCATCATCGATGCCCCCGGCCACCGCGACTTCATCAAGAACATGATCACGGG 314
seq             CTACATCACCATCATCGATGCCCCCGGCCACCGCGACTTCATCAAGAACATGATCACGGG 360
                ************************************************************

RefSeq          TACATCCCAGGCGGACTGCGCAGTGCTGATCGTGGCGGCGGGCGTGGGCGAGTTCGAGGC 374
seq             TACATCCCAGGCGGACTGCGCAGTGCTGATCGTGGCGGCGGGCGTGGGCGAGTTCGAGGC 420
                ************************************************************

RefSeq          GGGCATCTCCAAGAATGGGCAGACGCGGGAGCATGCCCTGCTGGCCTACACGCTGGGTGT 434
seq             GGGCATCTCCAAGAATGGGCAGACGCGGGAGCATGCCCTGCTGGCCTACACGCTGGGTGT 480
                ************************************************************

RefSeq          GAAGCAGCTCATCGTGGGCGTGAACAAAATGGACTCCACAGAGCCGGCCTACAGCGAGAA 494
seq             GAAGCAGCTCATCGTGGGCGTGAACAAAATGGACTCCACAGAGCCGGCCTACAGCGAGAA 540
                ************************************************************

RefSeq          GCGCTACGACGAGATCGTCAAGGAAGTCAGCGCCTACATCAAGAAGATCGGCTACAACCC 554
seq             GCGCTACGACGAGATCGTCAAGGAAGTCAGCGCCTACATCAAGAAGATCGGCTACAACCC 600
                ************************************************************

RefSeq          GGCCACCGTGCCCTTTGTGCCCATCTCCGGCTGGCACGGTGACAACATGCTGGAGCCCTC 614
seq             GGCCACCGTGCCCTTTGTGCCCATCTCCGGCTGGCACGGTGACAACATGCTGGAGCCCTC 660
                ************************************************************

RefSeq          CCCCAACATGCCGTGGTTCAAGGGCTGGAAGGTGGAGCGTAAGGAGGGCAACGCAAGCGG 674
seq             CCCCAACATGCCGTGGTTCAAGGGCTGGAAGGTGGAGCGTAAGGAGGGCAACGCAAGCGG 720
                ************************************************************

RefSeq          CGTGTCCCTGCTGGAGGCCCTGGACACCATCCTGCCCCCCACGCGCCCCACGGACAAGCC 734
seq             CGTGTCCCTGCTGGAGGCCCTGGACACCATCCTGCCCCCCACGCGCCCCACGGACAAGCC 780
                ************************************************************

RefSeq          CCTGCGCCTGCCGCTGCAGGACGTGTACAAGATTGGCGGCATTGGCACGGTGCCCGTGGG 794
seq             CCTGCGCCTGCCGCTGCAGGACGTGTACAAGATTGGCGGCATTGGCACGGTGCCCGTGGG 840
                ************************************************************

RefSeq          CCGGGTGGAGACCGGCATCCTGCGGCCGGGCATGGTGGTGACCTTTGCGCCAGTGAACAT 854
seq             CCGGGTGGAGACCGGCATCCTGCGGCCGGGCATGGTGGTGACCTTTGCGCCAGTGAACAT 900
                ************************************************************
RefSeq          CACCACTGAGGTGAAGTCAGTGGAGATGCACCACGAGGCTCTGAGCGAAGCTCTGCCCGG 914
seq             CACCACTGAGGTGAAGTCAGTGGAGATGCACCACGAGGCTCTGAGCGAAGCTCTGCCCGG 960
                ************************************************************

RefSeq          CGACAACGTCGGCTTCAATGTGAAGAACGTGTCGGTGAAGGACATCCGGCGGGGCAACGT 974
seq             CGACAACGTCGGCTTCAATGTGAAGAACGTGTCGGTGAAGGACATCCGGCGGGGCAACGT 1020
                ************************************************************
```

Figure 4-3 Alignment of the partially sequenced pcDNA3.1(+)C-hEEF1A2-myc to the reference sequence of human eEF1A2 cDNA, NM_001958.

4.2.2 Transient transfection of HeLa cells and calculation of transfection effieciency

HeLa cell culture and transient transfection were performed as described in 2.2.4 and 2.2.5. To determine the best ratio of the pcDNA3.1(+)C-hEEF1A2-myc plasmid to Lipofectamine 2000 reagent so as to achieve the highest transfection efficiency, the ratio of the plasmid to the transfection reagent was set as shown in table 4-4.

Table 4-4 Ratio of the pcDNA3.1(+)C-hEEF1A2-myc plasmid to Lipofectamine 2000 reagent for transfection

Amount of plasmid (μg)	Amount of transfection reagent (μl) for each ratio		
	1:1	1:2	1:3
0.8	0.8	1.6	2.4
1.0	1.0	2.0	3.0
1.2	1.2	2.4	3.6
1.6	1.6	3.2	4.8

For calculation of transfection efficiency, regions were chosen in the middle of each slide quarter. Micrographs of these areas were taken at 20x magnification, and the images were recorded for further analysis using ImageJ software. eEF1A2-myc-expressing cells were counted in each of the areas and then all DAPI-stained nuclei were counted within the same areas. The relative percentage of eEF1A2-myc-expressing cells per 20x area was determined by dividing the number of the eEF1A2-myc-positive cells by the total number of DAPI-stained nuclei times 100. The average percentage of transfected cells was then calculated using the data from each area of the slides, as shown in figure 4-4. Although there was no statistically significant difference, compared with the manufacturer's recommended ratio of 1:2 ($P = 0.5$), the 1:3 ratio of 0.8-ug

plasmid provides a potential to gave the highest transfection efficiency at 19.5 $\pm$ 4.1% (mean $\pm$ SEM), and this ratio was used for further transfection experiment.

a.

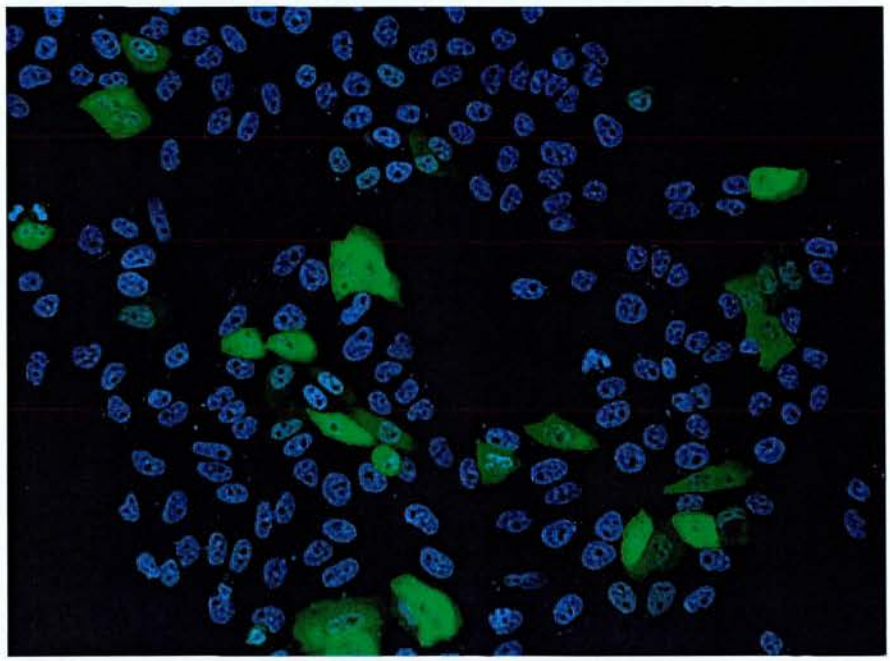

b.

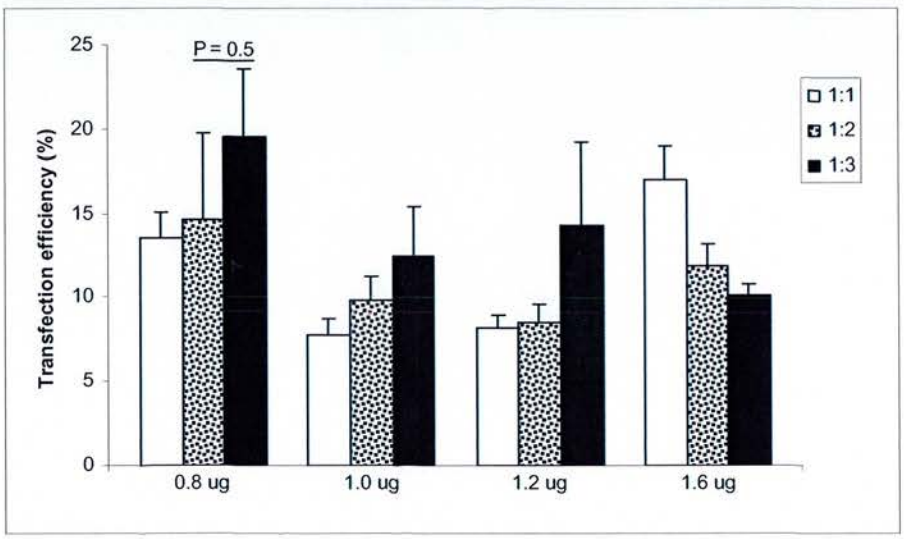

Figure 4-4 Transfection efficiency. (a) A representative image of transfection at the ratio 1: 3 of plasmid (0.8 µg) to transfection reagent. (b) Graph comparing transfection efficiency for each ratio of each amount of the plasmid.

4.2.3 Immunofluorescence analysis

HeLa cells grown at 37 °C in DMEM with 10% calf serum (control) were incubated in serum-free medium for 24 hours (starved), and then treated with either 10% calf serum for 12 hours or 100-nM epidermal growth factor (EGF) for 15 minutes at 37 °C. The cells were examined by conventional immunofluorescence microscopy using a mouse monoclonal antibody to the c-Myc epitope. DNA was stained with DAPI. No fluorescent signal was detected when the cells were incubated with primary or secondary antibody only.

4.2.3.1 Cytoplasmic localisation of eEF1A2 in control and starved HeLa cells

As described in previous studies, eEF1A is an abundant protein that is present mainly in the cytoplasm of the cells (Edmonds *et al.*, 1996). By transfecting the HeLa cells with the plasmid pcDNA3.1(+)C-hEEF1A2-myc and using a specific antibody against the c-Myc epitope, I found that eEF1A2 (green), an isoform of eEF1A, is mainly located in the cytoplasm of the cells, as shown in figure 4-5. In serum-starved cells, eEF1A2 was still confined in the cytoplasm, as shown in figure 4-6.

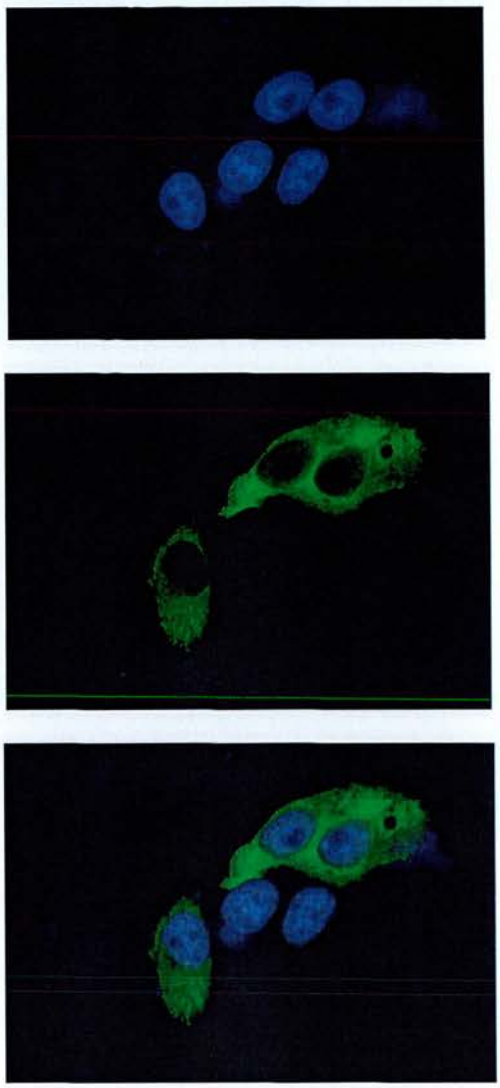

Figure 4-5 Cytoplasmic localization of eEF1A2 in the cytoplasm of HeLa cells grown in the presence of serum. Fluorescein (green) and DAPI (blue) represent eEF1A2 and DNA, respectively.

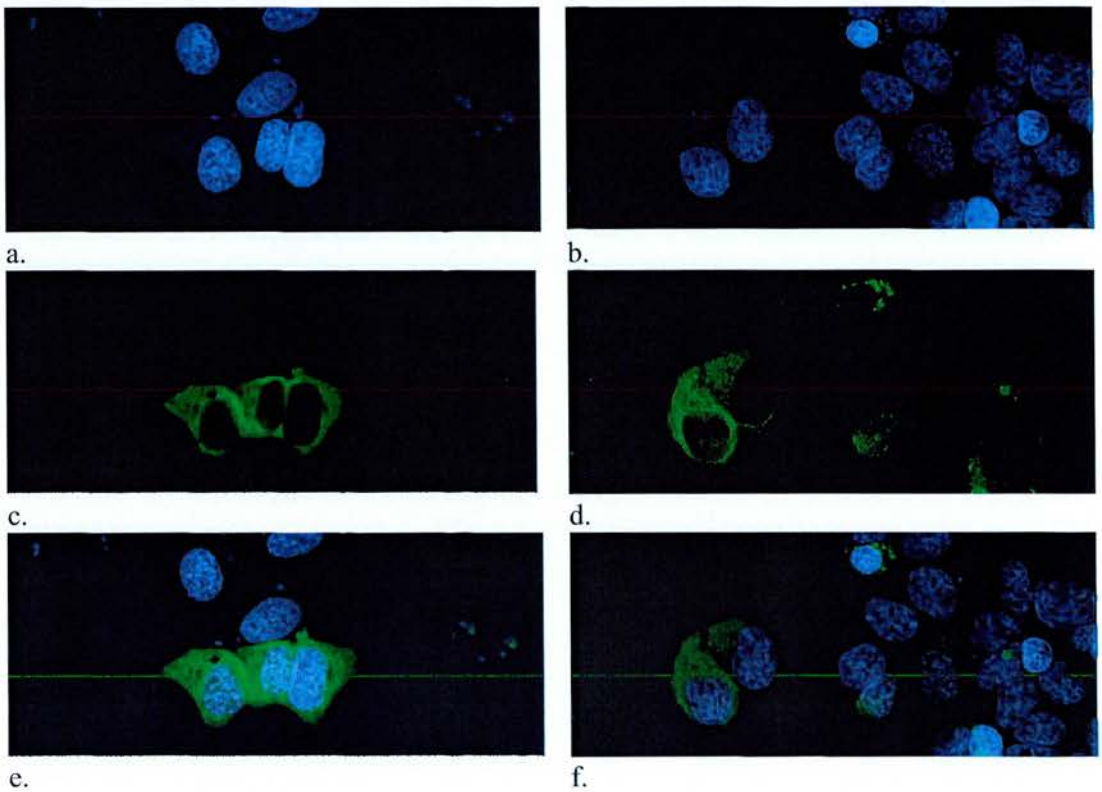

Figure 4-6 Cytoplasmic localization of eEF1A2 in 24-hour serum-starved HeLa cells. Images on the left and right panels were taken from different transfection slides. Fluorescein (green) and DAPI (blue) represent eEF1A2 and DNA, respectively.

4.2.3.2 Redistribution of eEF1A2 to the nucleus in serum-treated and mitogen-activated HeLa cells

While eEF1A2 was not detected in the nucleus of serum-starved cells, I compared eEF1A2 localization in serum-treated (Figure 4-7) and EGF-activated cells (Figure 4-8). Diffuse cytoplasmic staining was detected for both serum-treated and EGF-activated cells. Upon treatment with serum or EGF, a fraction of the eEF1A2 molecules was observed to redistribute from the cytoplasm to the nucleus. The punctate distribution of eEF1A2 in the nucleus may suggest that this isoform of eEF1A accumulate within nucleoli of the mitogen-treated cells.

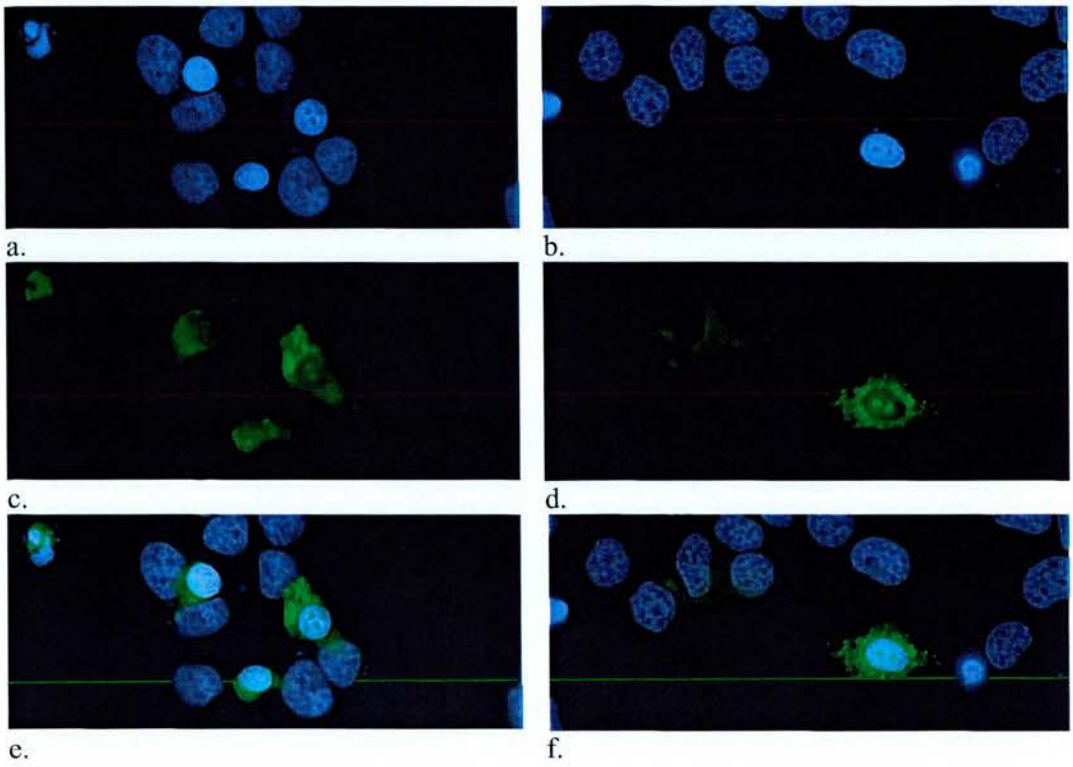

Figure 4-7 Redistribution of eEF1A2 from the cytoplasm to the nucleus in serum-treated HeLa cells. Images on the left and right panels were taken from different transfection slides. Fluorescein (green) and DAPI (blue) represent eEF1A2 and DNA, respectively.

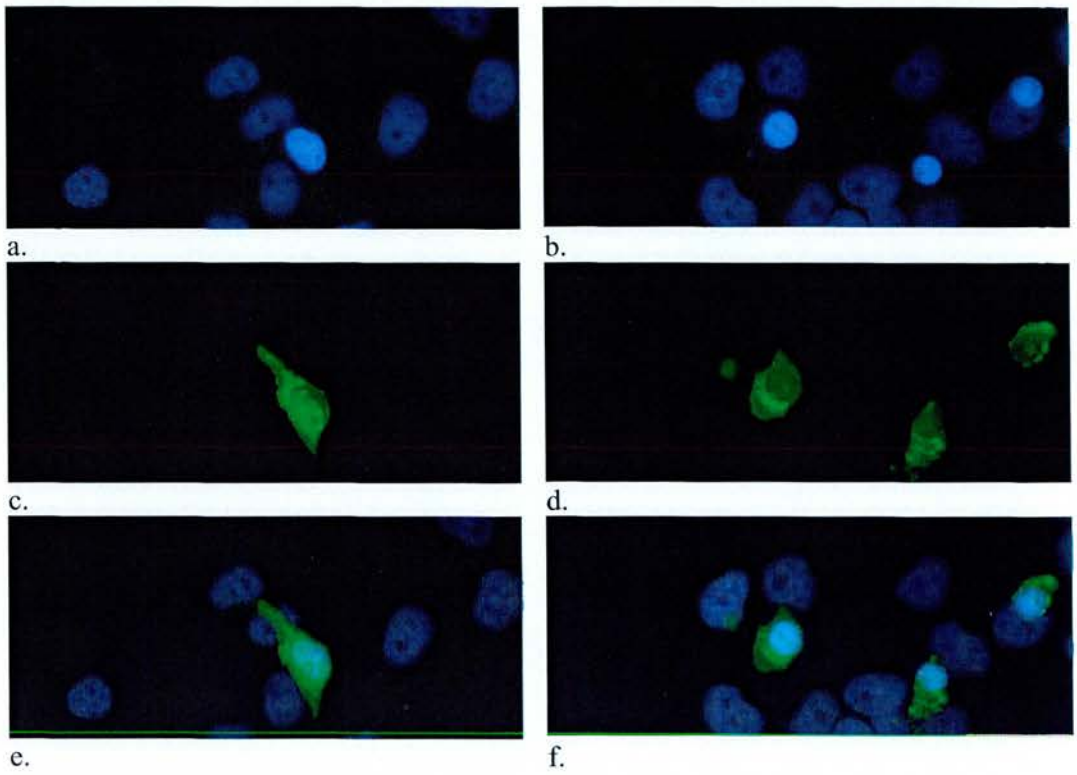

Figure 4-8 Redistribution of eEF1A2 from the cytoplasm to the nucleus in EGF-treated HeLa cells. Images on the left and right panels were taken from different transfection slides. Fluorescein (green) and DAPI (blue) represent eEF1A2 and DNA, respectively.

4.2.4 Quantitative Immunocolocalisation

Immunocolocalisation of eEF1A2 with SMN in HeLa cells was studied by using double-labelling immunostaining and a new quantitative test of colocalisation by intensity correlation analysis (ICA). Double-labelling of myc-tagged eEF1A2 and SMN was carried out by sequential incubation with a monoclonal mouse anti-Myc antibody and FITC-conjugated anti-mouse IgG secondary antibody, and then goat anti-SMN antibody and Texas-red-conjugated anti-goat secondary antibody. As conventional colocalisation is based on a dye-overlay method, this technique only provides an indication of coexistence of two proteins in the same regions. It does not address whether the intensity of staining for the two proteins varies in synchrony, as would be expected if they are components of the same complex. A limitation of the dye-overlap method is that when one protein target is distributed across most of the cell, a second protein will be identified as colocalised even when its distribution is totally random with respect to the first. I used a newly developed method to test for protein colocalisation by staining intensity correlation analysis (Li *et al.*, 2004). The ICA imaging was performed according to the standard method as described by Li *et al.* (2004). HeLa cells were imaged on a Zeiss Axioskop upright fluorescence microscope. All comparisons were made from pairs of single deconvolved image. The Image-J plug-in software was used to do the ICA analysis. Interpretation of the ICA analysis is based on an ICA plot and an intensity correlation quotient (ICQ). The ICA plot is a scatterplot of normalized dye A versus dye B staining intensities, which provides clues to their staining relationship by representing as the product of the differences from the mean (PDM), i.e. for each pixel. The PDM value is calculated by (dye A intensity – mean dye A intensity) x (dye B intensity – mean dye B intensity). The ICQ, a statistically testable quotient, is generated by subtraction 0.5 from the PDM value (to distribure the quotients to the -0.5 to +0.5 range), and used to provide an overall index of whether the staining intensities are associated in a random, a dependent or a segregated manner. With random staining ICQ = ~0; dependent staining $0 < ICQ \leq +0.5$, and for segregated staining $0 > ICQ \geq -0.5$. If myc-tagged eEF1A2 and SMN were parts of the same complex then their staining

intensities should vary in synchrony, whereas if they were on different complexes of structures they would exhibit asynchronous staining, termed dependent and segregated staining, respectively.

4.2.4.1 eEF1A2 associates with SMN in the cytoplasm

I have previously demonstrated that myc-tagged eEF1A2 is widely distributed in the cytoplasm of HeLa cells, both in normal and serum-starved conditions. To determine colocalisation of eEF1A2 with SMN, a visual inspection of the fluorescence staining pairs suggested colocalisation of the proteins in the cytoplasm (Figure 4-9). I used the ICA method to test a staining relationship between myc-tagged eEF1A2 and SMN. As shown in figure 4-10, the products of difference from mean (PDM) plots were highly skewed toward positive values (Figure 4-10, centre and right panels), consistent with a dependent staining pattern. Furthermore, the calculated ICQ values, as shown in figure 4-11, were consistently positive and significant ($+0.185 \pm 0.03$; $P = 0.0034$; $n = 5$), indicating that the intensities in two images, green and red, varied in synchrony (i.e. they were dependent). The ICQ is based on the non- parametric sign-test analysis of the PDM values and is equal to the ratio of the number of positive PDM values to the total number of pixel values. Therefore, in any image where the intensities vary together, the PDM will be positive. This analysis provided compelling evidence that staining for myc-tagged eEF1A2 varied in synchrony with that for SMN, consistent with the formation of a complex with the cytoplasm of HeLa cells.

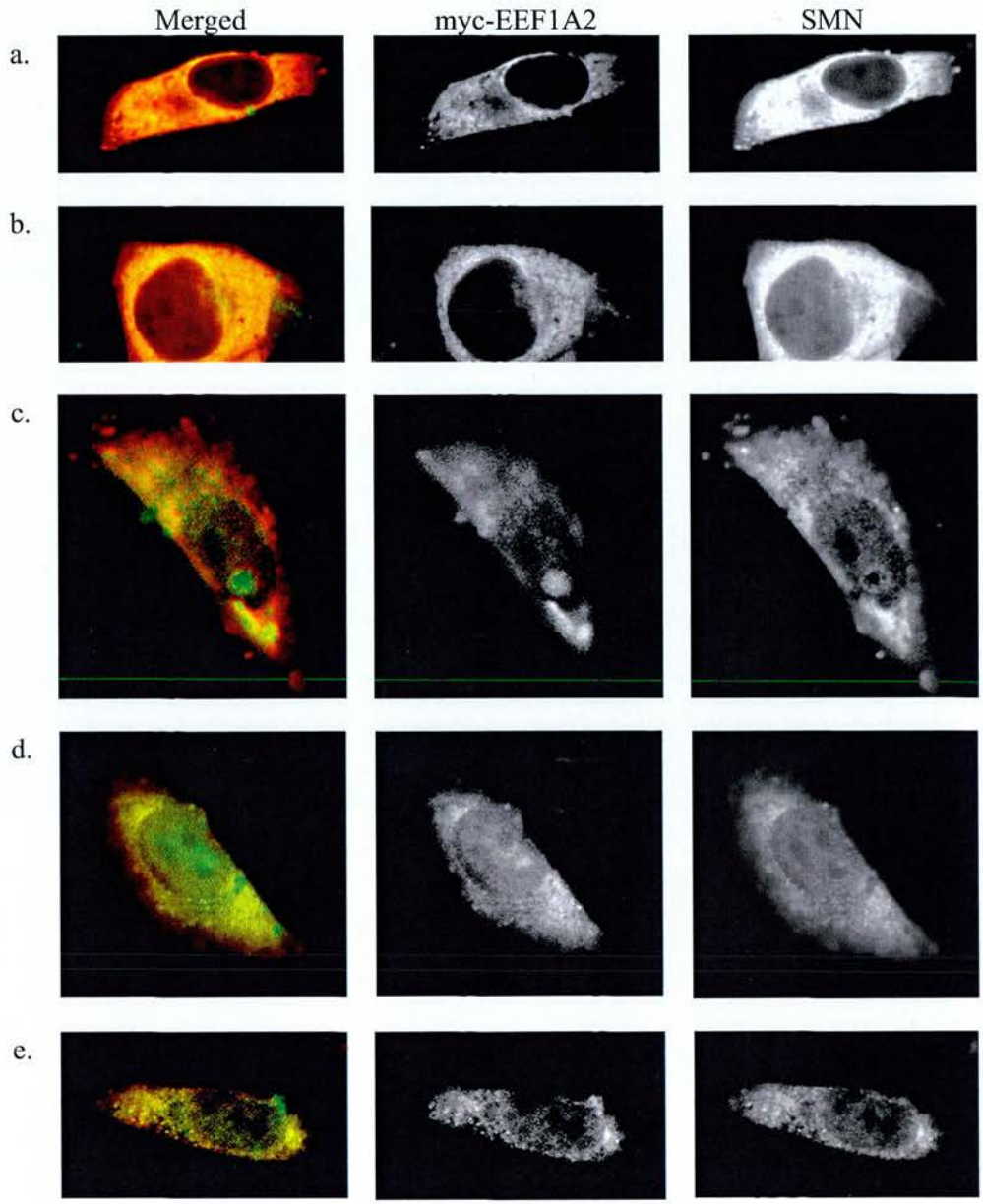

Figure 4-9 HeLa cells stained with anti-myc antibody and anti-SMN antibody. The left panels show merged images of each analysed cell, using intensity correlation analysis. The centre and right panels show gray-scale images after background subtraction and threshold adjustment for intensity correlation analysis.

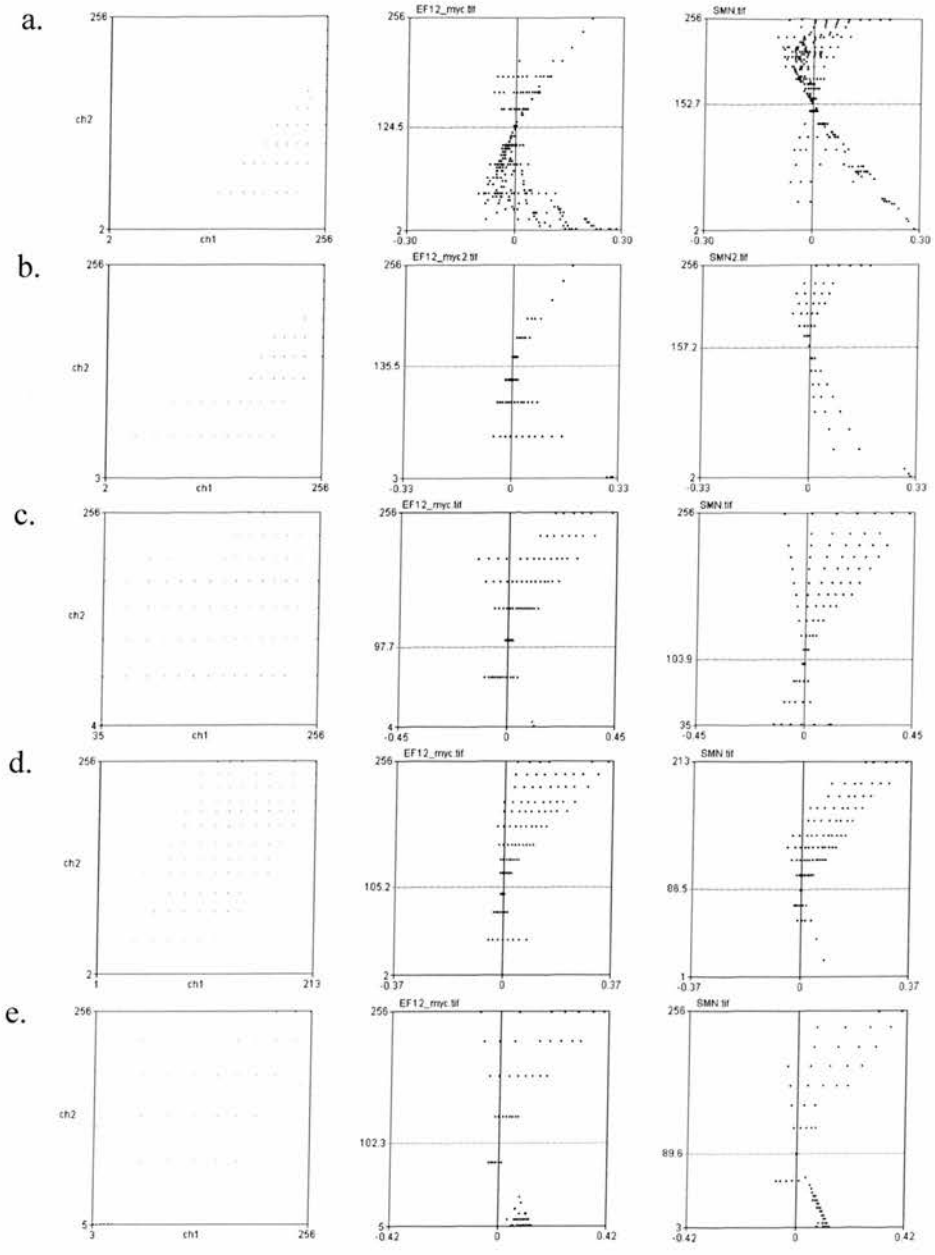

Figure 4-10 Intensity correlation analysis. Each row (a-e) represents the ICA plots of the cells, a-e, in figure 4-9. For the centre and right panels, the y-axis is the PDM (products of differences from mean) values, and the x-axis is the green (eEF1A2) or red (SMN) intensity. The left panel shows the frequency scatter plots of eEF1A-2 intensity (y-axis) versus SMN intensity (x-axis). The ICQ = +0.097, +0.152, +0.183, +0.222, and +0.271 for a, b, c, d, and e, respectively.

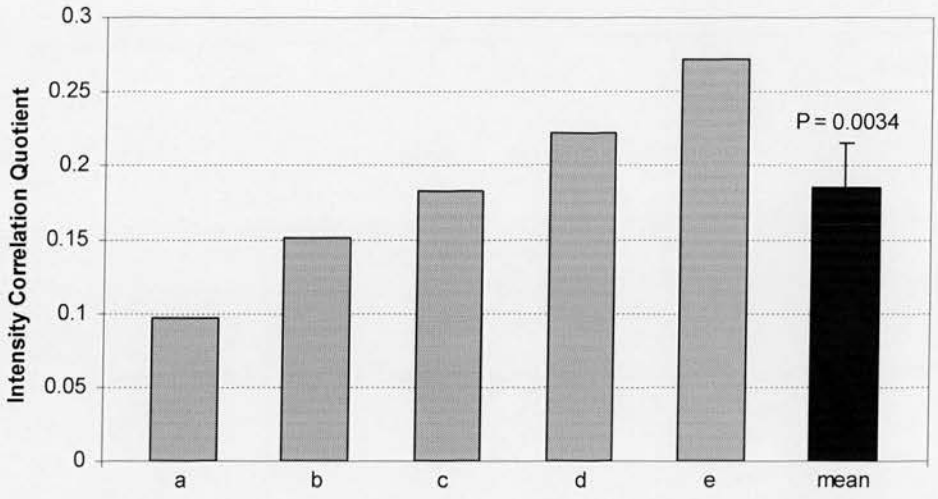

Figure 4-11 Graphs representing quantitative immunocolocalisation, showing the intensity correlation quotient, analysed by the ICA method, of the cells a-e in figure 4-9 and 4-10. The mean ICQ equals +0.185 $\pm$ 0.03 (mean $\pm$ SEM, Student's *t* test).

4.2.4.2 eEF1A2 and SMN in the nucleus of serum-treated HeLa cells

In an attempt to determine whether the eEF1A2 colocalised with SMN in the nucleus of serum-treated or EGF-activated cells, only some cells were seen both myc-tagged eEF1A2 and SMN in the same nuclei. The representative analyses were shown in figure 4-12. The average ICQ for colocalisation in the serum-treated cells was +0.112. This was inconsistent. Although in some treated cells there was evidence of a dependent relation between eEF1A2 and SMN (Figure 4-12a and b; ICQ = +0.271), some cells showed a random relation (Figure 6-12d and e; ICQ = -0.047). In the nucleus of treated cells, a poor staining intensity relation was observed, as shown in figure 4-12c and f. No high pixel intensity of myc-tagged eEF1A2 was seen at both low and high SMN staining intensities. This could be a limitation of the ICQ method, e.g. perhaps an inability to resolve colocalisation in components of small organelles.

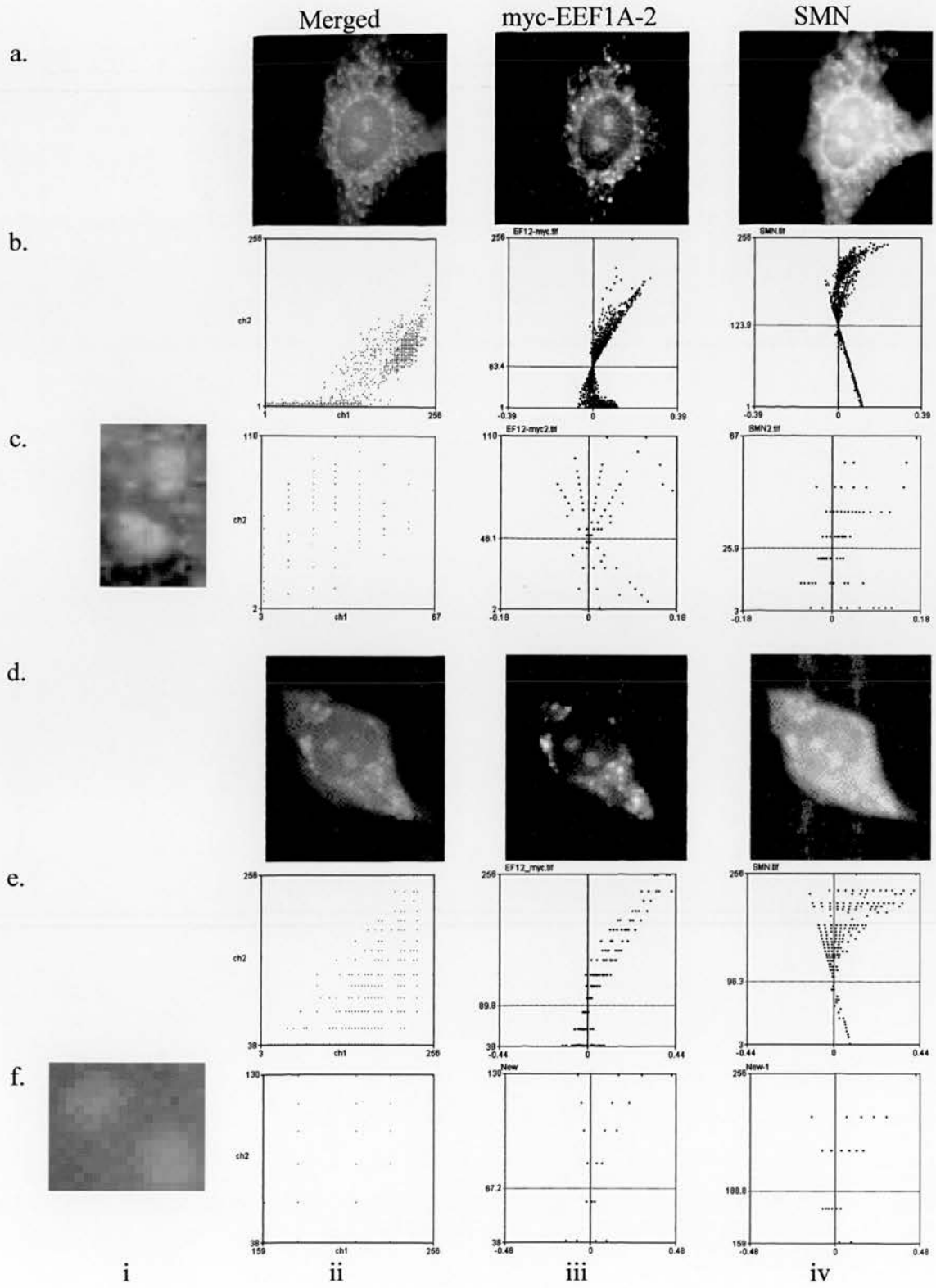
Merged
myc-EEF1A-2
SMN
a.
b.
c.
d.
e.
f.
i
ii
iii
iv

Figure 4-12 Intensity correlation analysis of representative immunostaining images of two serum-treated HeLa cells stained with anti-myc antibody and anti-SMN antibody. The iii and iv panels of the row a and d show gray-scale images after background subtraction and threshold adjustment. The i panel of the row a and d shows merged images of each analysed cells. For the iii and iv panels of the row b, c, e and f, the y-axis is the PDM (products of differences from mean) values, and the x-axis is the green (eEF1A2) or red (SMN) intensity. The ii panel shows the frequency scatterplots of eEF1A-2 intensity (y-axis) versus SMN intensity (x-axis). The rows (b) and (e) represent the ICA plots of the whole cell areas. The ICQ values of the row (b) equal +0.271, and of (e) equals -0.047. The rows (c) and (f) represent images of the intranuclear areas (the i panel) and the ICA plots of the intranuclear areas (the ii-iv panels) of the cells in (a) and (d), respectively. Note the diffuse pixel intensities in (c) and (f).

4.3 Discussion

The eEF1A2 protein is preferentially located in the cytoplasm of cells. I demonstrated that a fraction of eEF1A2 redistributes to the nucleus after treatment with serum and a mitogen, EGF. Immunoflurescence analysis revealed that the nuclear eEF1A2 exhibited a punctuate appearance. This finding was consistent with previous studies that described the nuclear localization of the eEF1A protein family (Billaut-Mulot *et al.*, 1996, Sanders *et al.*, 1996, Gangwani *et al.*, 1998). However, some studies were unable to demonstrate nuclear localization of eEF1A (Bohnsack *et al*,. 2002, Calado *et al.*, 2002). Exp5 is shown to be a functional nuclear export receptor for eEF1A. It is a tRNA binding protein, and this complex actively suppresses nuclear translation by promoting nuclear export of eEF1A. The reason for these opposite findings might be differences in cell culture condition. In Calado *et al* (2005), HeLa cells were grown in steady-state in the presence of 10% calf serum, whereas in other studies including my experiment, the cells were stressed by serum starvation prior to refeeding with serum or stimulating with mitogens. It is possible that redistribution of eEF1A2 to the nuclei of stressed cells was stimulated by serum or mitogens to compensate intranuclear translation or other processes of tRNA processing. It has also been claimed recently that a significant proportion (10-15%) of cellular protein synthesis takes place in the nucleus, and occasionally reports of nuclear pools for some translation factors were proposed to support that claim (Iborra *et al.*, 2001).

Like eEF1A2, SMN is present in both the cytoplasm and the nucleus, where it accumulates in punctate structures including gem and Cajal bodies (Liu and Dreyfuss, 1996; Matera and Frey, 1998; Young *et al.*, 2000). By using double-labeling immunostaining and a quantitative analysis of staining dependency, I found that eEF1A2 and SMN exhibited a moderately strong staining intensity correlation (Figure 4-10). This indicates that eEF1A2 and SMN vary in synchrony and suggests that a proportion of cytoplasmic eEF1A2 colocalizes with SMN. SMN has been demonstrated to interact with ZPR1 and the SMN/ZPR1 complex redistributes to and colocalizes to subnuclear

structures (Gangwani *et al.*, 2001). It has been postulated that upon EGF stimulation, ZPR1 binds to eEF1A and SMN in the cytoplasm and redistributes to the nucleus (Matera and Hebert, 2001). Immunoprecipitations with anti-SMN antibodies has been shown to pull down two unidentified bands with mobilities very similar to those of ZPR1 and eEF1A (Charroux *et al.*, 2000). Based on quantitative immunocolocalization as described above, it is possible that eEF1A2 could be part of the so-called SMN complex.

I next examined the association of eEF1A2 with SMN in the nucleus of serum-treated cells. Unfortunately, there were no satisfactory ICA results to determine their relation. This is possible that a fraction of cytoplasmic eEF1A2 that is translocated into the nucleus is small, and only a tiny proportion of this fraction may colocalize with SMN, or that interaction between eEF1A2 and SMN in the nucleus exists only in a particular stage of the cell cycle.

Chapter 5 Construction and Characterization of muscle-specific human *EEF1A2* transgene

The aims of this study are to construct transgenic mice expressing muscle-specific human eEF1A2 and to determine the phenotype that results from loss of eEF1A2 in neurons.

5.1 Construction of muscle-specific human *EEF1A2* transgene

5.1.1 Introduction

Homozygous *wst/wst* mice develop severe muscle wasting and degeneration of motor neurons, beginning at 3 weeks after birth and die by age of 28 days. In humans, muscle wasting is a common and clinically important outcome of several neurological disorders, which include diseases of the central nervous system such as motor neuron disease (MND) and spinal muscular atrophy (SMA), and of muscle itself such as Duchenne muscular dystrophy. A deletion in the promoter and first exon of the *Eef1a2* gene, resulting in the absence of *Eef1a2* mRNA, was identified in wasted mice (Chambers *et al.*, 1998). Unlike eEF1A1, eEF1A2 is specifically-expressed in neuron, heart, and skeletal muscle, which are largely composed of long lived terminally differentiated cells. Using an immunoflurorescene study, our publication has demonstrated very thin motor axon collaterals terminating in a retraction bulb swelling, and abnormal motor end plate occupancies (Newbery *et al.* 2005).

A human EEF1A2-containing P1-derived artificial chromosome (PAC) has previously been constructed by Dawn Loh (Loh, 2003) and was used to generate transgenic mice. The human EEF1A2 PAC was found to correct the wasted phenotype since the body

weights of transgenic wasted mice were similar to their wild-type littermates. This was also reflected in the correction of spleen and thymus atrophy in the transgenic wasted mice. In addition, none of the transgenic wasted mice showed any sign of tremor or paralysis, and lethality was also rescued.

Herein, I constructed a muscle-specific human *EEF1A2* transgene in order to produce transgenic wasted mice specifically expressing human eEF1A2 in muscle, and to evaluate the phenotype to see whether loss of eEF1A2 in neuron and heart but presence in muscle lead to muscle wasting and other neuromuscular abnormalities.

5.1.2 Strategy

In order to evaluate the phenotype that results from tissue-specific expression of eEF1A2 in muscles but not neuron, transgenic mice carrying a human *EEF1A2* gene that was driven by the muscle-specific promoter were generated.

Human *EEF1A2* gene has been mapped to chromosome 20q13.3 (Lund *et al.*, 1996). The coding regions of the human *EEF1A1* and *EEF1A2* are very similar, whereas the level of similarity in the 5'UTRs, 3'UTRs, introns, and upstream promoter regions is very low (Knudsen *et al.*, 1993). To avoid the isolation of genomic DNA from either *EEF1A1* or pseudogenes, the pUC19-EEF1A2 plasmid, constructed by Julia Boyd in our group by subcloning the human *EEF1A2* gene from the PAC-EEF1A2, made by Dawn Loh, into pUC19 was used to isolate the human *EEF1A2* gene. The gene coding for the human eEF1A2 has been isolated and sequenced, and the structure and the activity of its promoter has been characterized (Bischoff *et al.*, 2000). The human *EEF1A2* spans approximately 10 kb and consists of eight exons. The transcription initiation site is located at the position 1780-2030, immediately upstream of the first exon, and the predominant transcription initiation site is localized to an adenine nucleotide 166 bp upstream to the initiator codon or AUG. The core promoter region sufficient to drive

transcription ranges from the position -16 to +92. These regions were removed and replaced with the muscle-specific promoter.

Transgenic mice were produced containing the full-length coding region of human *EEF1A2* gene driven by the human skeletal muscle actin (HSA) promoter. The efficacy of the HSA promoter to drive gene expression was first characterized by Brennan and Hardeman, who reported the advantages of this promoter to be its tissue specificity, developmentally correct expression, level of expression, and the fact that α-skeletal actin gene is expressed naturally in all types of skeletal muscle (Brennan and Hardeman, 1993). This promoter has been used previously to successively generate transgenic mice with muscle-specific expression (Crawford *et al.*, 2000; Spencer *et al.*, 2002; Spencer and Mellgren, 2002; Kent *et al.*, 2004). Reports of transgenic studies using the quail troponin I gene, the rat MLC1/3f gene, the mouse muscle creatine kinase gene, the rat myosin light chain 2 gene, and the a-myosin heavy chain gene have looked at the ability of gene promoter to direct striated muscle-specific, and in some cases developmentally correct, expression. The level of expression achieved by these transgenes has not been quantified in the context of the normal expression of the endogenous gene. In contrast, the -2000 to +239 region of the *HSA* gene is a highly tissue-specific promoter known to be capable of directing expression of up to 53% of the endogenous gene in adult skeletal muscle. Additionally, it has the advantage over other isoforms of the contractile protein multigene families that a-skeletal actin is expressed in all skeletal muscle types. During development, α-cardiac actin is the predominant isoform of sarcomeric α-actin in mice, and it is only post-partum that there is a switch to α-skeletal actin (Gunning *et al.*, 1987; Brennan and Hardeman, 1993). Thus, by using the α-skeletal actin promoter, any possibilities that embryonic expression of *EEF1A2* might interfere with development was minimized. The promoter and the first exon of the *HSA* gene (from -2000 to +239, relative to the transcription initiation site) were isolated from pHSA2000CAT plasmid (kindly provided by Edna Hardeman).

5.1.3 Results

5.1.3.1 Isolation and preparation of human α-skeletal actin promoter

Three parameters of regulation of the human α-skeletal actin, which include level of expression, tissue specificity, and developmental regulation, are mediated by sequences within the region -2000 to +239 of the promoter (Brennan and Hardeman, 1993). These three aspects of the regulation are located in the pHSA200CAT plasmid that, as shown in figure 5-1, was used for isolating the promoter for this project. The 2, 372-bp fragment used for constructing the transgene was isolated by PCR. PCR was chosed as a method to isolate the fragment instead of restriction endonuclease digestion because of a limitation of restriction sites in the pUC19-EEF1A2 that was used to isolate the sequence.

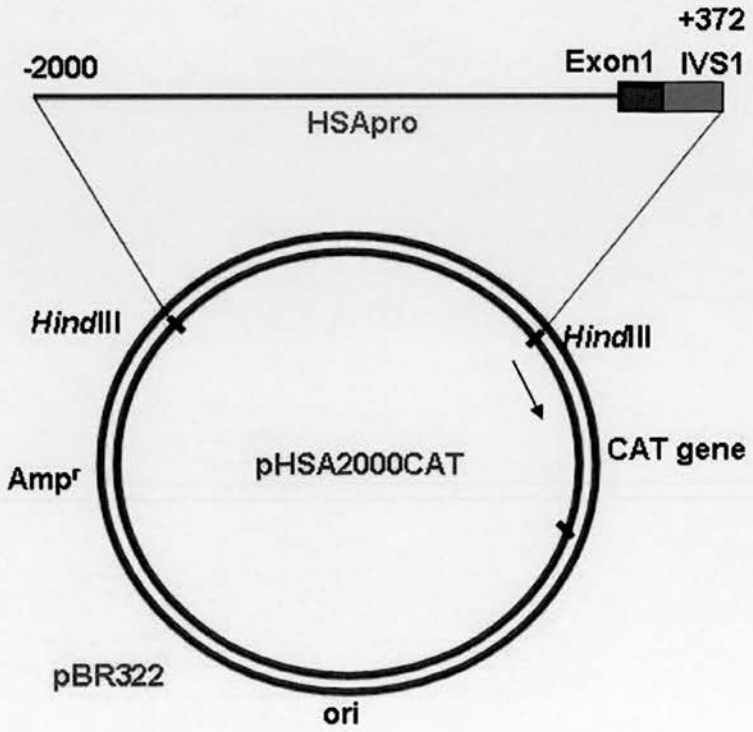

Figure 5-1 pHSA2000CAT plasmid

In the pHSA200CAT plasmid, a 2,372-bp fragment starting at a *Hind*III site 2,000 bp upstream from the site of transcription initiation contains the first exon and 271 bp of the

first intron and ends at the *Hind*III site. PCR primers were designed to generate *Hind*III and *Age*I sites at the 5' and 3' terminus of the fragment, respectively (Table 5-1).

Table 5-1 Primers for HSA insert amplification. *Hind*III and *Age*I restriction sites are indicated in bold for the forward and reverse primers, respectively.

Primer name	Orientation	Nucleotide sequence (from 5' to 3')
HSAins	Forward	CGC GC**A AGC TT**T CTG TAA GGA AAG GT
	Reverse	GGC GTT **ACC GGT** AAA GCG CGT GTG GCT

To reduce the risk of the potential for introducing mutations when using PCR for insert preparation, I used enzymes with high fidelity obtained from Expand High Fidelity PCR system (Roche). The System contains Taq DNA polymerase and Tgo DNA polymerase with proofreading activity. The 5'-3' polymerase activity of Taq DNA polymerase and the 3'-5' exonuclease or proofreading activity of Tgo DNA polymerase provided improved results, compared to Taq DNA polymerase without Tgo DNA polymerase. The PCR condition and cycling are shown in chapter 2, Materials and Methods.

By using this protocol, a single band of the correct size was visualized on agarose gel electrophoresis. The PCR products were purified from primers, nucleotides, polymerase, and salts using QIAquick PCR Purification kit prior to restriction digestion with *Hind*III and *Age*I. The human a-skeletal actin promoter inserts derived from PCR were prepared for cloning by restriction digestion with *Hind*III and *Age*I, followed by gel purification.

5.1.3.2 Isolation and preparation of the vector containing human *EEF1A2*

The 21,543-bp pUC19 plasmid (Figure 5-2) carrying human *EEF1A2* and its promoter was used to prepare the vector for subsequent cloning. Originally, the 18,891-bp human

EEF1A2 gene and its promoter were cloned into the *Hind*III and *Kpn*I sites of the plasmid pUC19. After analysis of restriction sites of this plasmid, the AgeI site was a unique site that was located at the position 102-bp upstream to the second exon. Thus, the 7,751-bp fragment containing the promoter of human *EEF1A2* was removed from this plasmid by restriction digestion using the enzyme *Hind*III and *Age*I. The 13,783-bp pUC19 carrying human *EEF1A2* gene without the promoter was separated from the promoter after restriction digestion by gel electrophoresis, and purified by gel purification prior to ligation and transformation.

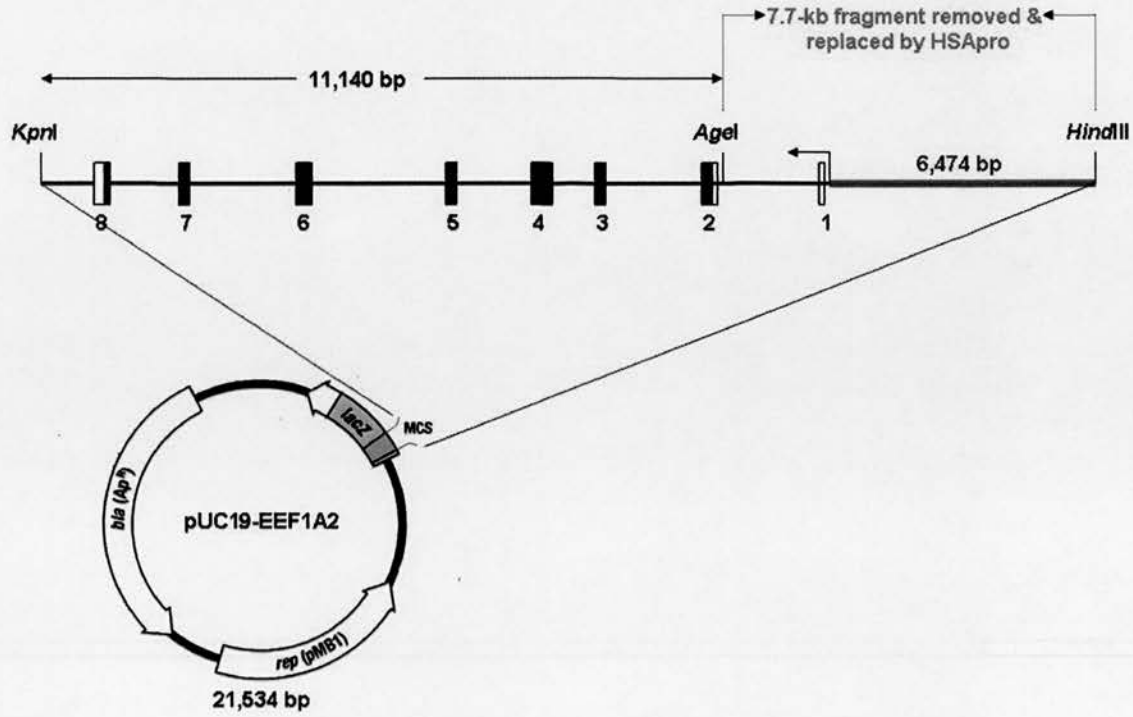

Figure 5-2 Diagram of the pUC19-EEF1A2 used for preparation of the vector for subsequent cloning

When recovering DNA from the gel slice, 10 mM Tris-HCl, pH 8.5 was used an elution buffer instead of water or TE because DNA might degrade in absence of a buffering agent when using water, and EDTA in TE might inhibit subsequent enzyme reactions,

which might be a cause of unsuccessful transformation that occurred sometimes in this experiment.

5.1.3.3 Cloning of the human α-skeletal actin promoter into the pUC19-EEF1A2 vector

The 2.3-kb fragment of the human α-skeletal actin promoter was ligated to the *Hind*III-*Age*I sites of the 13.7-kb pUC19-EEF1A2 vector, upstream to the human *EEF1A2* sequence. Several ligation conditions were preformed in order to give successful transformation. The condition that gave a desired result was performing incubation at 4-6 °C overnight.

5.1.3.4 Screening and analysis of the construct

Transformed *E.coli* colonies were screened for inserts by direct colony PCR using HSA-specific primers, as shown in Table 5-2. The PCR condition and cycling are shown in chapter 2, Materials and Methods.

Table 5-2 Primers for direct colony PCR screening.

Primer name	Orientation	Nucleotide sequence (from 5' to 3')	Size of the amplicon (bp)
HSApro	Forward	GAT GAC TAC AAG GTG GAC TG	277
	Reverse	ACT ATG TGT GTC CCT CTC CT	

Large scale preparations of the pUC19-HSA-EEF1A2 plasmid were prepared from the positive colonies. The construct was sequenced to screen for mutations, and restriction-digested to screen for the intact integrity of the transgene and to ensure the presence of intact restriction sites for subsequent isolation. Sequencing of the construct was performed on the whole sequences of the human α-skeletal actin promoter, using

primers presented in table 5-3. Figure 5-3 shows where the primer sequences are on the construct. For the human *EEF1A2* gene, sequencing was performed on the coding sequences from the exon 2 to the exon 8, and the polyadenylation site and signal sequences, using primers shown in table 5-4. Both forward and reverse strands of the transgene construct were sequenced.

Table 5-3 Primers for PCR sequencing of HSA region of the pUC19-HSA-EEF1A2. Four nucleotide sequences for both forward and reverse primers were designed to span around 800 bps for accurate sequencing.

Primer name	Orientation	Nucleotide sequence (from 5' to 3')
seqHSA	F1	ATG CTT CCG GCT CGT AT
	F2	ATG TCC CTG AGT TCA TC
	F3	AGT GCG TCC TAC AGG AG
	F4	GAG ACA CTC CAT ATA CG
seqHSA	R1	GGA TGT GCT TAA GTG CT
	R2	GTT CCC CTC CTG TAG GA
	R3	CGT ATA TGG AGT GTC TC
	R4	ACC ACG ATG TTG ATG TG

5'
cggaagagcgcccaatacgcaaaccgcctctccccgcgcgttggccgattcattaatgcagctggcacgac
aggtttcccgactggaaagcgggcagtgagcgcaacgcaattaatgtgagttagctcactcattaggcacc
ccaggctttacactttatgcttccggctcgtatgttgtgtggaattgtgagcg
F1
gataacaatttcacacaggaaacagctatgaccatgattacgccaagctt (End of pUC19 sequence)

(Start of *HSA* sequence)
tctgtaaggaaaggtaagagttgaactgagcaagagttttgaaaaatagtgacaatcccattctcctttgg
aatgcgcacaaatattgaggtatccagtgaacggcagcaaatttcctaccttcaaggcccaaatgtaagct
agtccccttacgttacatgcagctcatttgctaagtggtttttttctagtatctccactactcgctgacac
aggaggacacaggatgttaaaaaggaaatacagttctgtcaattattcacttactctccaaaatacttgga
agaactaaatatggaaccataggagactttatcctcaccgcatagtccctatactagtcaaactccttatt
ttttaattgatcatttttaggaaggtagcattttattcactagaacatttttgttaatacttgtttatttt
tgggatgaactgccatgatgtgggctacagaggagggtcgcatatgcttccatccccctttagagaatcc
acacctgtcccagttgctgggttccactaccaaaagtgaattgcaactattttaggagcacttaagcacat
R1
ccgaaaaatgagtgattctgttctggcccacaccacatcactgatgtacccccttaaagcatgtccctgag
ttcatcacaga F2
agactgctcctcctgtgccctccacaaggttagaactgtccttgtcttagggaaaaaggagagagagagag
agagagagagagagagagagagagagagagagagagagggacaggcaccaactgggtaacctctgctgacc
cccactctactttaccataagtagctccaaatccttctagaaaatctgaaaggcatagccccatatatcag
tgatataaatagaacctgcagcaggctctggtaaatgatgactacaaggtggactgggaggcagcccggcc
ttggcaggcatcatcctctaaatataaagatgagtttgttcagcctttgcagaaggaaaaactgccaccca
tcctagagtgccgcgtccttgtccccccacccccctccaatttattgggaggaaggaccagctaagcctcat
ctaggaagagcccctcacccatctccacctccactccaggtctagccagtcctgggttgtgacccttgtct
ttcagccccaggagagggacacacatagtgccaccaaagaggctgggggagggcctcagcccaccaaaacc
tggggccagtgcgtcctacaggaggggaaccctcacccctcaatccctttaggagacccaagggcgctgc
gcgtccctgag F3 R2
gcggacagctccgtgtgctcaggctttgcgcctgacaggcctatccccgggagcccccgcgcctcctcccc
ggcgctccgccctcgcctcccccccgccagttgtctatcctgcgacagctgcgcgccctccggccgccggtg
gccctctgtgcggtgggggaaggggtcgacgtggctcagcttttggattcagggagctcgggggtgggaa
gagagaaatggagttccaggggcgtaaaggagagggagttcgccttccttcccttcctgagactcaggagt
gactgcttctccaatcctcccaagcccaccactccacacgactccctcttcccggtagtcgcaagtgggag
tttggggatctgagcaaagaacccgaagaggagttgaaatattggaagtcagcagtcaggcaccttcccga
gcgcccagggcgctcagagtggacatggttggggaggcctttgggacaggtgcggttcccggagcgcaggc
gcacacatgcacccaccggcgaacgcggtgaccctcgccccaccccatcccctccggcgggcaactgggtc
gggtcaggaggggcaaacccgctagggagacactccatatacggcccggcccgcgttacctgggaccgggc
caacccgctcc F4 and R3
ttctttggtcaacgcagggacccgggcgggggcccaggccgcgaaccggccgagggaggggctctagtg
cccaacacccaaatatggctcgagaagggcagcgacattcctgcggggtggcgcggagggaatgcccgcgg
gctatataaaacctgagcagagggacaagcGGCCACCGCAGCGGACAGCGCCAAGTGAAGCCTCGCTTCCC
CTCCGCGGCGACCAGGGCCCGAGCCGAGAGTAGCAGTTGTAGCTACCCGCCCAGgtagggcaggagttggg
aggggacaggggacagggcactaccgaggggaacctgaaggactccggggcagaacccagtcggttcacc
tggtcagccccaggcctgcgccctgagcgctgtgcctcgtctccggagccacacgcgcttt (End of
HSA sequence)

(Start of *EEF1A2* sequence)
accggtctccccaccaccactggccccacagaatcactgcagccccctcgccctgagccagagcaccccg
ggtcccgccagcccctcacactcccagcaaaatgggcaaggagaagacccacatcaacatcgtggtcatcg
R4
gccacgtggactccggaaagtccaccac 3'

Figure 5-3 Locations of the primers for HSA sequencing. Forward primers are in bold, and reverse primers are underlined.

Table 5-4 Primers for PCR sequencing of the coding sequences, exon 2 to exon 8, of the pUC19-HSA-EEF1A2. The primer segE8 were designed to cover the polyadenylation site in addition to exon 8.

Primer name	Orientation	Nucleotide sequence (from 5' to 3')
seqE2	F	GAG ACA CTC CAT ATA CG
	R	GAG ATG CCA AGC CTG GCC AC
seqE3	F	CTG TAA CAA GCA GCT CGC AC
	R	GAG CCA GAC TGG GTG AGG G
seqE4	F	GGA GAG GCC TGG AAG TGA G
	R	GTG CCA CCT GCC GGT GCC TCG
seqE5	F	AGC AGT ACT CCT GGA AGC A
	R	AGA GAT TGG AGA CAG CCC
seqE6	F	CTT TGT TGG TTT CCA GGC TC
	R	GAC AGT CCT GCT GCT GTC C
seqE7	F	CCT CCA GTC AGC ACT CCG G
	R	CTG CCA TGC TCT GGG CCA AGC
seqE8	F	CGT GTT CCG AGG ACA TTC C
	R	CAG GGA GTG AAG GAT GCT G

There were no mutations found in any of the regions sequenced. The results of sequencing are given in Appendix 1. Figure 5-4 shows the schematic diagram of pUC19-HSA-EEF1A2.

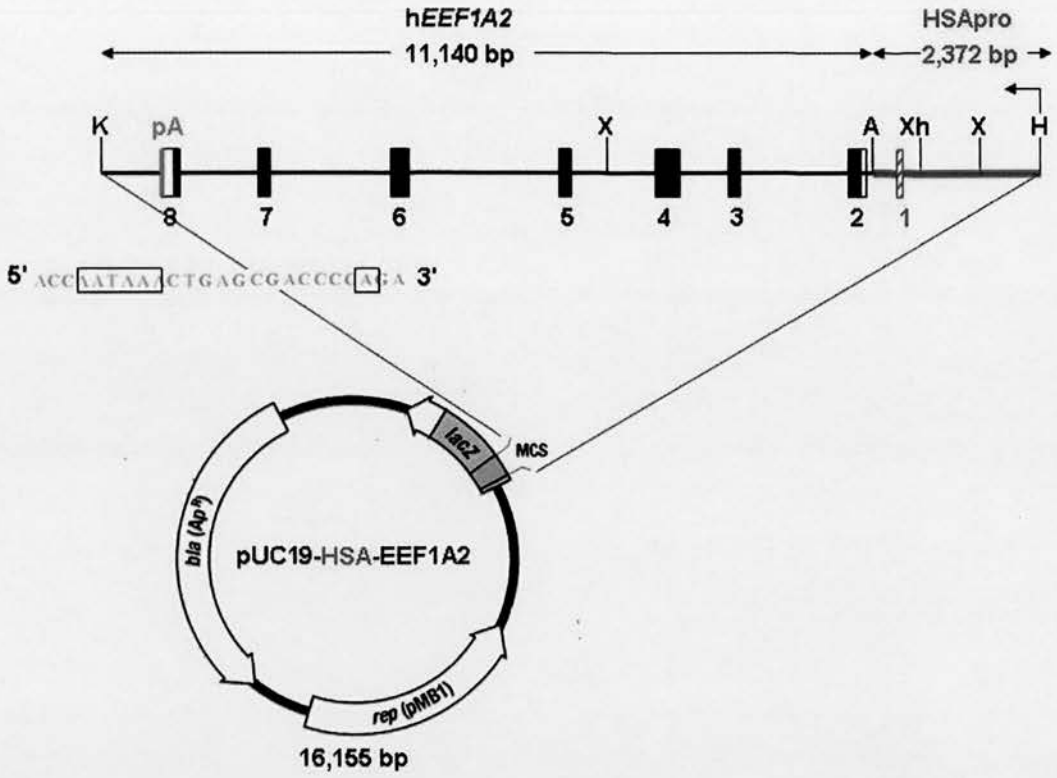

Figure 5-4 Diagram of pUC19-HSA-EEF1A2. The 13,512-bp *Hind*III-*Kpn*I fragment includes the 2,372-bp *Hind*III-*Age*I fragment of HSA promoter and the 11,140-bp *Age*I-*Kpn*I fragment of human *EEF1A2*. pA (in red) denotes the polyadenylation site and signal sequence, shown as a nucleotide sequence in the diagram. Restriction sites represented by H, *Hind*III; X, *Xba*I; XH, *Xho*I; A, *Age*I; K, *Kpn*I.

For restriction mapping, the unique restriction endonucleases, *Hind*III, *KpnI*, *Xho*I, *Xba*I, and *Age*I, were located only in the transgene sequences, and used for restriction digestion. The result of restriction digestion showed that, as shown in figure 5-5, the integrity of the transgene was intact.

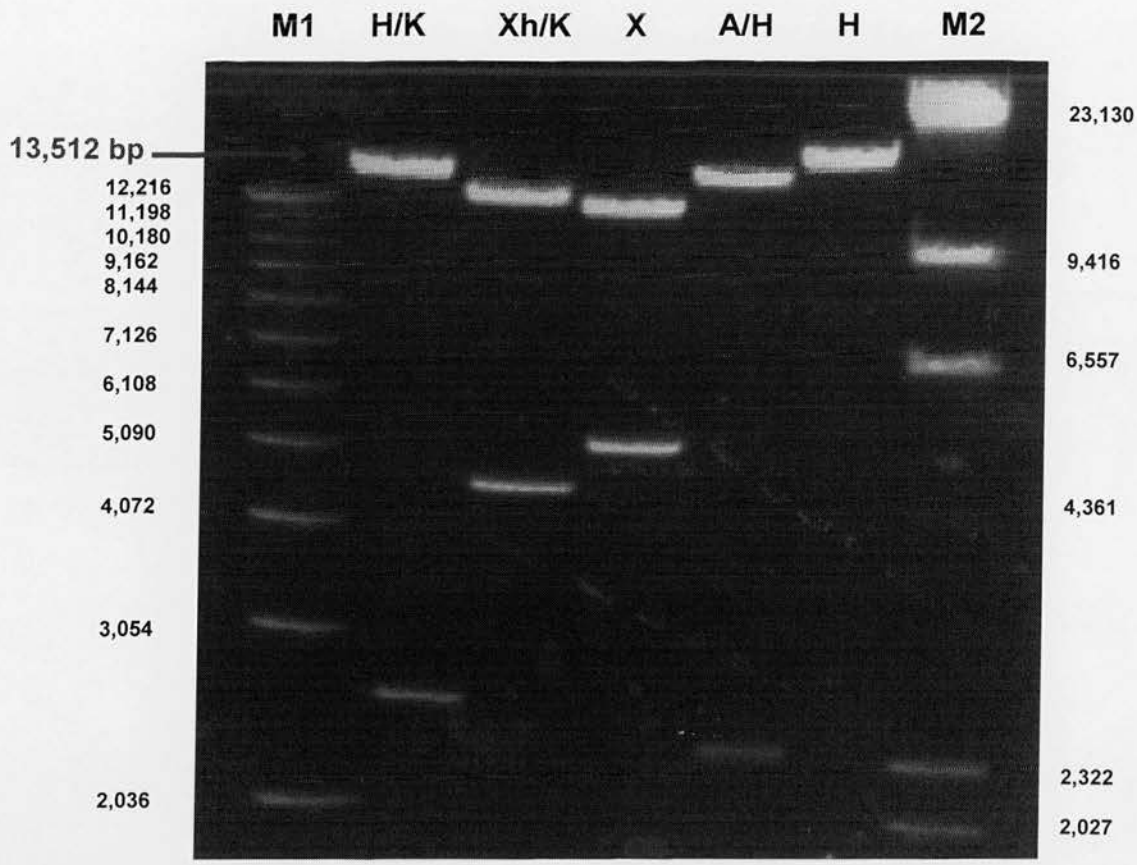

Figure 5-5 Photograph of restriction mapping. pUC19-HSA-EEF1A2 was digested with the restriction enzymes represented by H, *Hind*III; K, *Kpn*I; Xh, *Xho*I; X, *Xba*I; A, *Age*I. The 13,512-bp HSA-EEF1A2 transgene was yielded by H/K digestion. Digestions with other restriction enzymes also gave the right-size products. Two markers, M1 and M2, were used to determine the size of products. Predicted digestion-product sizes: H/K, 13,512 and 2,643 bp; Xh/k, 11,467 and 4,688 bp; X, 10,866 and 5,289 bp; A/H, 13,783 and 2,372; H, 16,155 bp.

5.2 Generation of transgenic mice

5.2.1 Preparation of DNA construct for microinjection

The 16,155-bp pUC19-HSA-EEF1A2 plasmid was digested with *Hind*III and *Kpn*I to isolate a 13,512-bp fragment that included the HSA promoter, the *EEF1A2* gene from exon 2 to exon 8 including their introns, and the polyadenylation site and signal sequences. The 13,512-bp transgene was separated by 0.8% agarose gel electrophosis. The band of the transgene was cut from the gel and further purified by electroelution using Elutrap Starter kit (Schleicher & Schvell). The fragment was then concentrated by ethanol precipitation. The concentration of the purified transgene was measured using an UV spectrophotometer. The transgene was then diluted to a concentration of 2 ng/ul with injection buffer, and its concentration was confirmed by comparing with *Hind*III-digested λ phage on an agarose gel. The male pronucleus of fertilized C57BL/6J embryos was microinjected by Brendon Doe. The embryos were then transferred into the oviduct of the pseudo-pregnant mice to complete their gestation.

5.2.2 Analysis of progeny mice for transgene integration

A total of 38 offspring were obtained. Of these, one died. The offspring were screened for the presence of the transgene by PCR analysis of genomic DNA isolated from ear clips at three weeks of age using the phenol: chloroform: isoamyl alcohol method. The primers were designed to detect the sequence of the HSA-EEF1A2 junctions, as shown in figure 5-6. In addition, the second PCR was used to identify the exon 5 of human *EEF1A2* gene in order to confirm the presence of transgene in case the HSA-EEF1A2 junction region could not be easily amplified, as shown in Table 5-5.

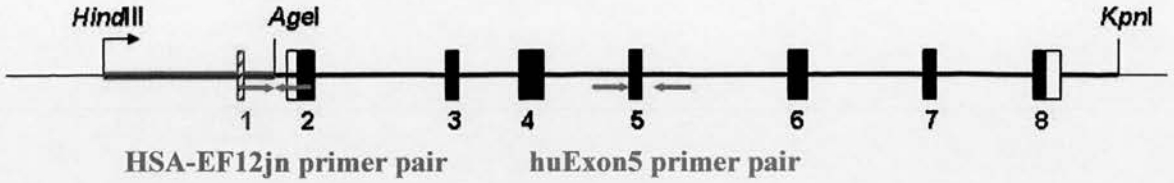

Figure 5-6 Diagram of the HSA-EEF1A2 constructs used as transgenes showing sites in designing screening primers.

A third assay that detected an endogenous mouse beta-globin gene was designed in order to demonstrate that the DNA preparations were amenable to PCR (Table 5-5). Mice were tested with both assays so that no transgenic founder was mistakenly discarded because ear clip DNA was not suitable for PCR.

Table 5-5 Primers used for screening HSA-EEF1A2 transgenic mice

Primer name	Orientation	Nucleotide sequence (from 5' to 3')	Size of the amplicon (bp)
HSA-EF12jn	F	GCC GAG AGT AGC AGT TGT A	313
	R	GAT GTT GAT GTG GGT CTT C	
huExon5	F	AGC AGT ACT CCT GGA AGC A	344
	R	AGA GAT TGG AGA CAG CCC	
Beta-Globin	F	CCA ATC TGC TCA CAC AGG ATA GAG AGG GCA GG	494
	R	CCT TGA GGC TGT CCA AGT GAT TCA GGC CAT CG	

Two founders (5.4%), one male and one female, were positive for the transgene. Mice that had not incorporated the transgene were culled by cervical dislocation.

5.2.3 Production and maintenance of transgenic lines

Typically, transgenic founders are bred to mice of defined genetic background such as C57BL/6. Due to a limitation of time for this project, the two transgenic founders were bred to heterozygous wasted (*wst*/+) mice in order to produce a sufficient amount of male and female heterozygous mice carrying the transgene (tg/+ *wst*/+) for further breeding. The transgenic offspring were maintained as hemizygotes.

5.2.4 Production of homozygous wasted mice carrying the HSA-EEF1A2 transgene

To generate homozygous wasted offspring carrying the HSA-EEF1A2 transgene (+/tg *wst*/*wst*), heterozygous wasted mice carrying the HSA-EEF1A2 transgene (tg/+ *wst*/+) were bred with non-transgenic heterozygous wasted mice (+/+ *wst*/+), as shown in figure 5-7. The expected genotypes are shown in figure 5-8. The frequency of wasted homozygotes carrying the HSA-EEF1A2 transgene that were produced would be at 1 in 8. Of two transgenic founder mice, the female one did not yield any transgenic progeny after the five litters were screened.

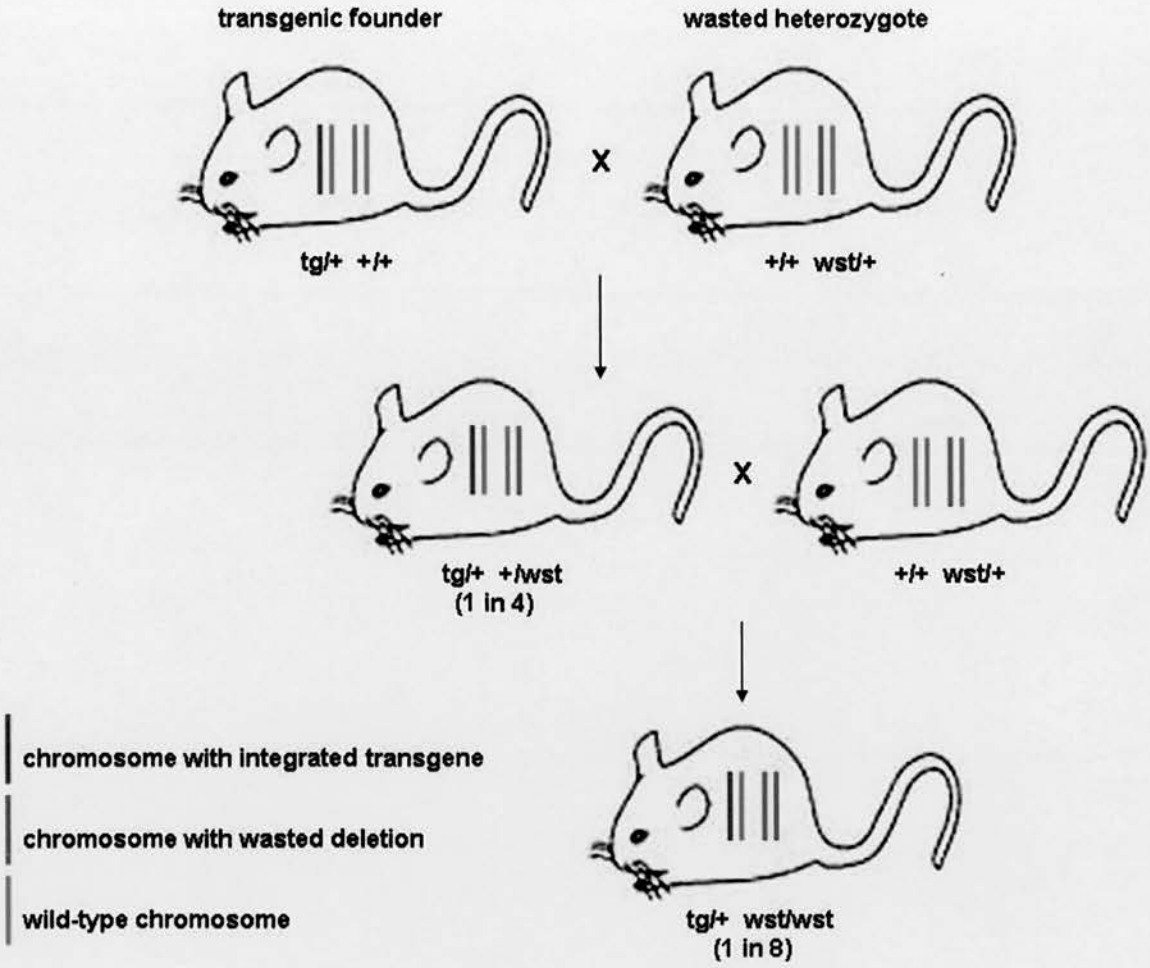

Figure 5-7 Breeding scheme for production of homozygous wasted mice carrying the HSA-EEF1A2 transgene.

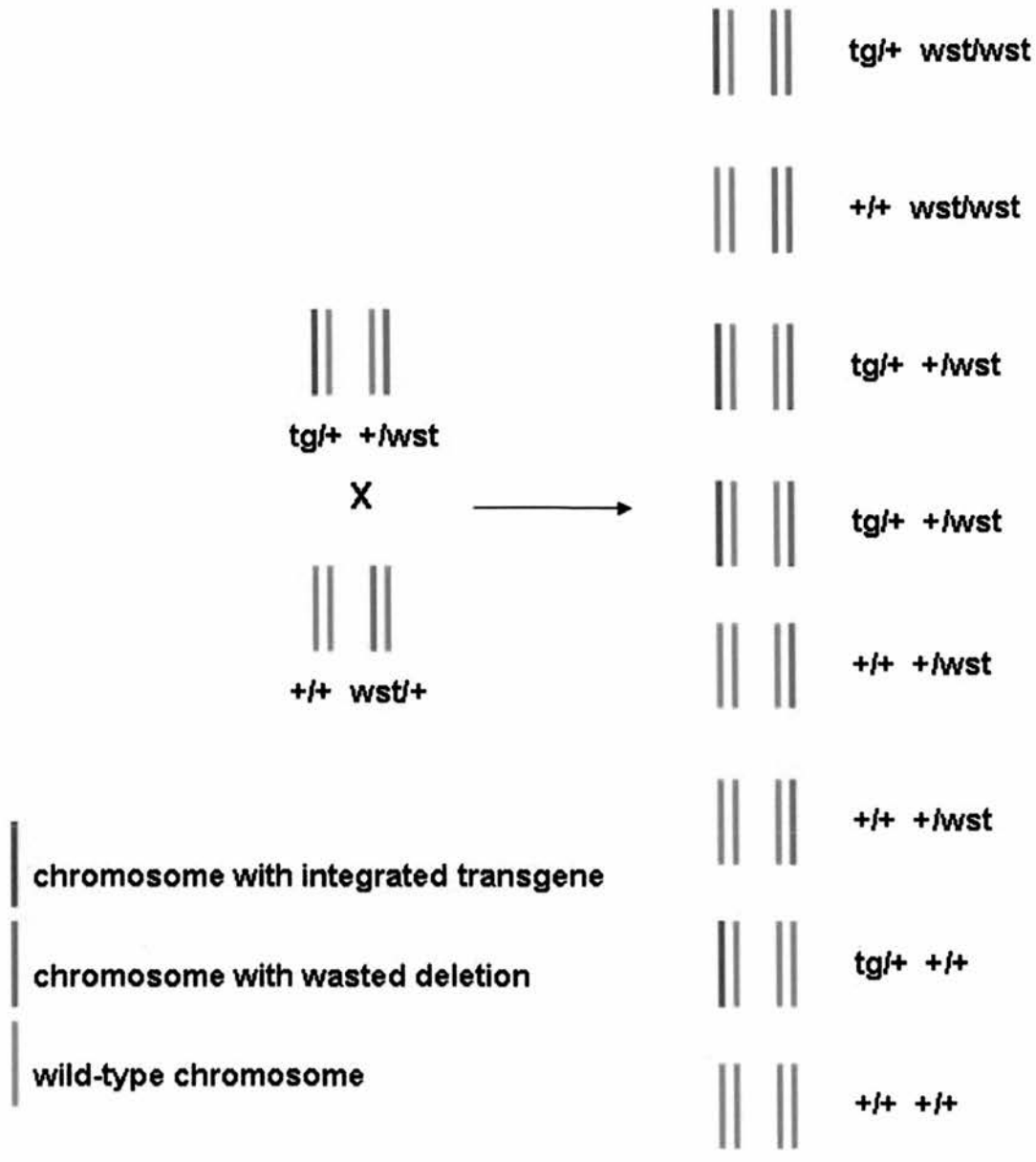

Figure 5-8 Diagram showing possible outcome from mating a transgenic wasted heterozygote with a non-transgenic wasted heterozygote.

5.2.5 Identification of transgenic HSA-EEF1A2 wasted mice

The offspring from these matings were genotyped at the time of weaning using three sets of primers which included the HSA-EEF1A2-junction primers, the wasted allele (wstspan)-specific primers, and the wild-type allele (P2)-specific primers. The P2 primers were designed to detect a portion of the wasted deletion sequence. The wstspan primers were employed to detect the *wst* deletion. The forward or 'split' primer of the wstspan primers was designed with 18 nucleotides from just outside the 5' end of the wst deletion, and 6 nucleotides from just outside the 3' end of the *wst* deletion as illustrated by figure 5-9. Using the P2 and wstspan primers helped distinguish wasted homozygotes from heterozygotes. Positive amplification of both P2 and wstspan PCR products indicates DNA is isolated from the heterozygotes. The absence of P2 product and the presence of wstspan product indicate wasted homozygotes.

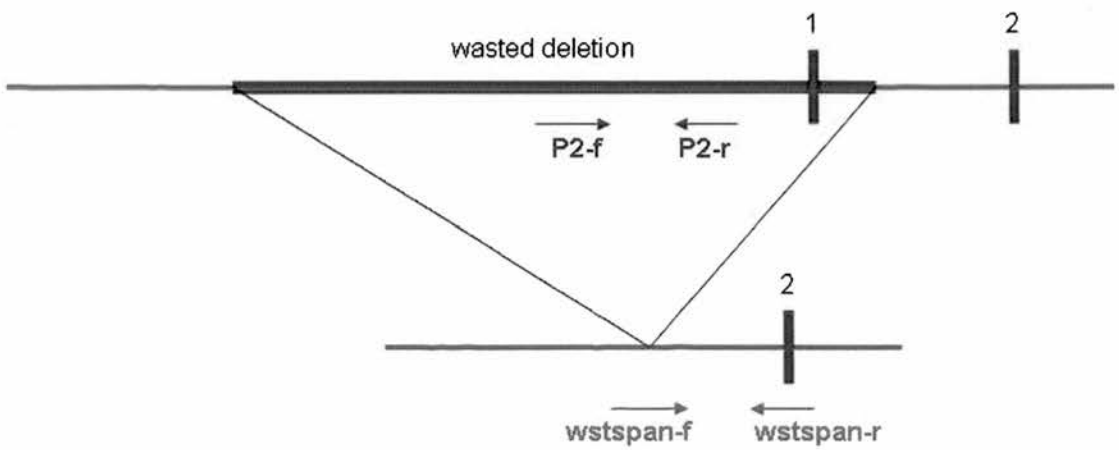

Figure 5-9 Diagram showing the strategy for designing the primers for genotyping wasted mice.

5.2.6 Protein expression and tissue specificity of the HSA-EEF1A2 transgenic wasted mice

Western blots were used to screen and confirm expression of the transgene in tissues of transgenic HSA-EEF1A2 homozygous wasted mice using an antibody against the eEF1A2 protein (Figure 5-10). The human eEF1A2 protein was found to be expressed in skeletal muscle of transgenic wasted mice, as shown in figure 5-10a – 5-10f, although its expression in cardiac muscle was also found in some transgenic wasted mice (Figure 5-10d and 5-10e). However, these findings was consistent with Dr. Hardeman's studies (Brennan and Hardeman, 1993), which used the HSA promoter to drive muscle-specific expression of a transgene and showed muscle-specific expression of the transgene together with its expression in cardiac muscle in some transgenic mouse lines. Some transgenic wasted mice produced in my study showed expression of eEF1A2 in stomach and eyes in addition to its expression in heart, as shown in figure 5-10f. This expression pattern could be a result of random integration of the transgene, in which franking sequences might contain regulatory elements of nearby genes that acted on the promoter of the transgene as an enhancer, which could lead to ectopic expression of the transgene. However, as eEF1A2 was not found to be expressed in the nervous system but was present in muscle, the pattern of expression in heart, stomach, or eyes was considered not to affect the studies of muscle denervation.

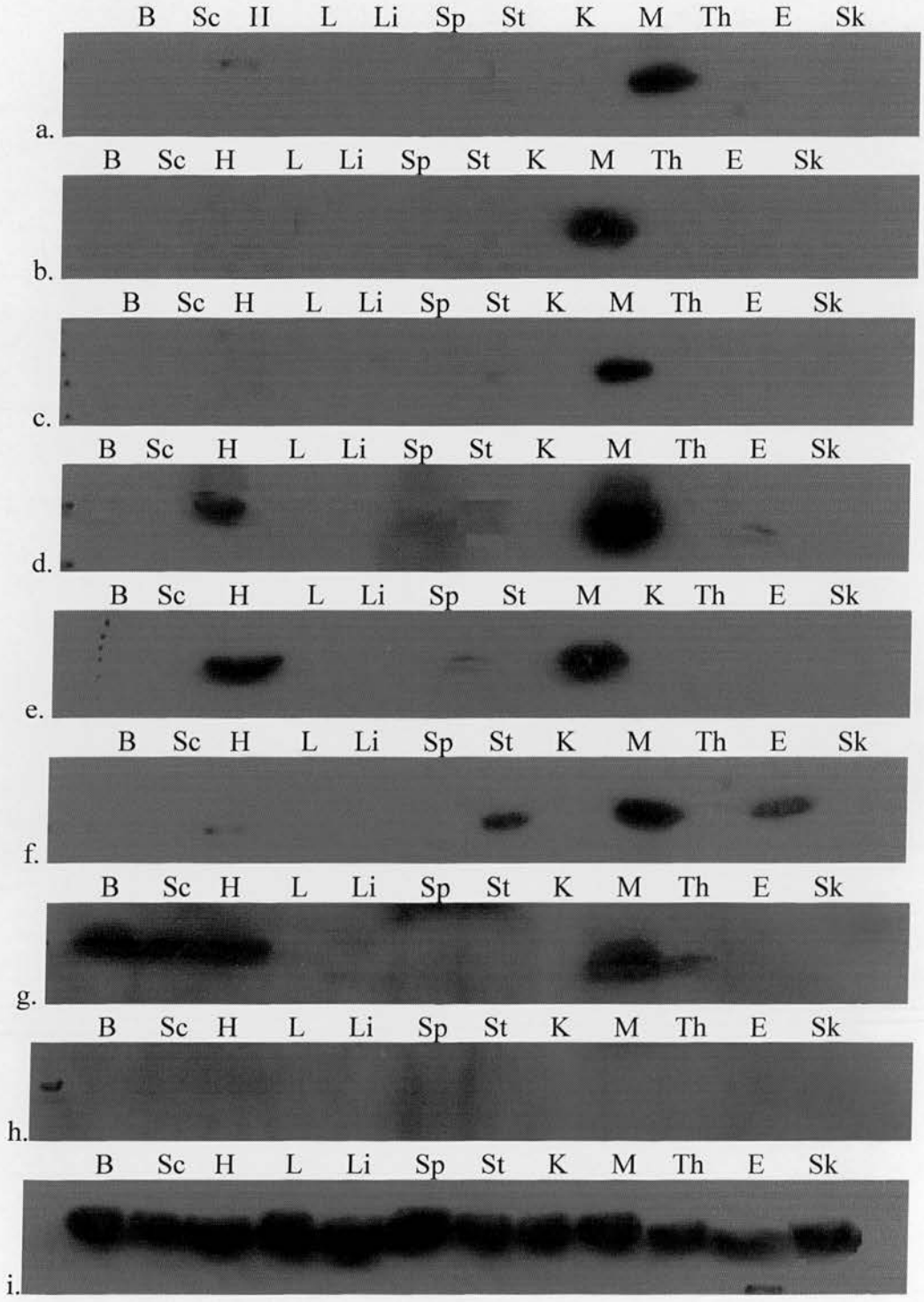

Figure 5-10 Expression of eEF1A2 in transgenic wasted and non-transgenic wild-type tissues. (a) – (f) Tissues from transgenic wasted mice. (d) and (e) Tissues for female. (g) Tissues from a non-trasngenic wild-type mouse. (h) Tissues from a non-transgenic

wasted mouse. (i) Photograph representing loading control. eEF1A2 is not detected in brain and spinal cord of transgenic mice. Tissues: B, brain; Sc, spinal cord; H, heart; L, lung; Li, liver; Sp, spleen; St, stomach; K, kidney; M, skeletal muscle; Th, thymus; E, eye; Sk, skin.

In transgenic heterozygous wasted mice (tg/+ *wst*/+), expression of eEF1A2 was significantly higher than the expression in non-transgenic heterozygous wasted littermates (+/+ *wst*/+), with P value equals 0.0085, as shown in figure 5-11.

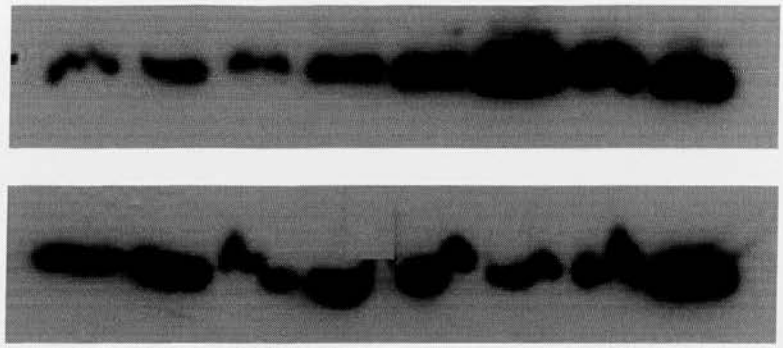

a.

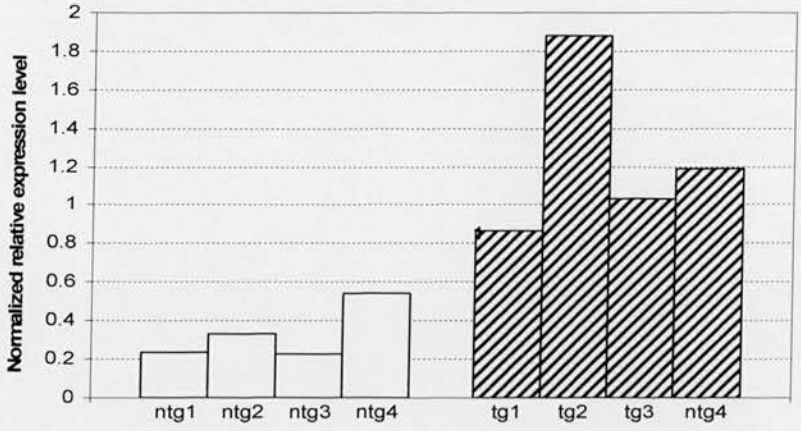

b.

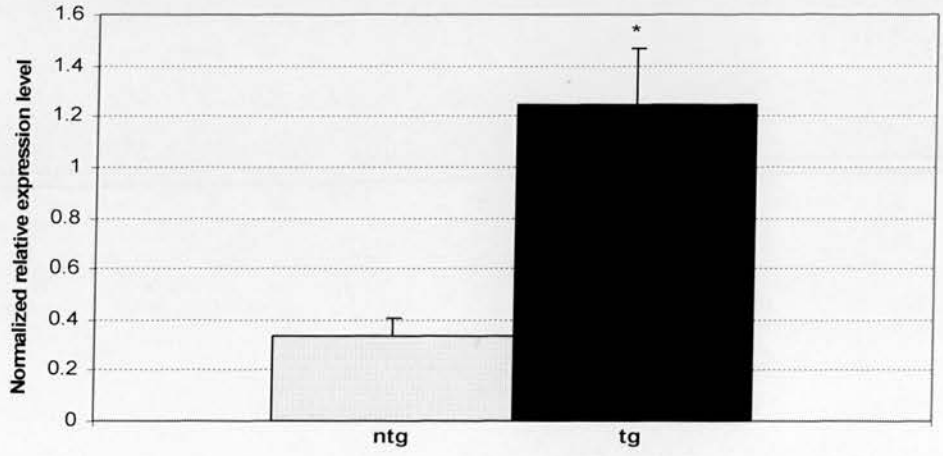

c.

Figure 5-11 Comparison of eEF1A2 expression in muscle from non-transgenic and transgenic heterozygous wasted littermates. (a) Western analysis for eEF1A2 in

muscle samples. (b) Relative expression level for each muscle sample. (c) Average of relative expression from 4 muscle samples for each genotype. Asterisk denotes P = 0.0085 (Unpaired *t*-tests).

5.3 Analysis of transgenic HSA-EEF1A2 homozygous wasted mice

5.3.1 Comprehensive phenotype assessment of sensorimotor functions

Muscle and lower motor neurone function of the transgenic homozygous wasted mice were assessed and compared with those of controls and non-transgenic wasted mice by using modified SHIRPA (**S**mithKline **H**arwell/**I**mperial College/**R**oyal Hospital/**P**henotype **A**ssessment) primary screen of neurologic function (Rogers et al., 1997; Hatcher et al., 2001). A wide array of tests enhances capability of defining deficient and spared functions. The SHIRPA primary screen consists of quantitative and semi-quantitative observations of reflexes and basic sensorimotor functions as well as body weight and size. In my study, the tests for assessment of muscle and sensorimotor functions were used, although some of the results could be used to interpret other aspects of neurologic function such as spinocerebellar and sensory functions. However, assessment of autonomic function and neuropsychiatric functions were not included in this study. Transgenic homozygous 25-day-old wasted mice (n = 6) were assessed and compared to age-matched non-transgenic wasted mice (n = 6) and wild-type controls (n = 6). For a quantitative measure, group comparisons were assessed by the unpaired student *t*-test.

As presented in table 5-6, HSA-EEF1A2 transgenic wasted mice were distinguishable from non-transgenic wild-type controls on certain aspects of the primary screen. The mean body weight of transgenic wasted mice was lower than that of controls ($P < 0.0001$), and their body length was shorter than that of controls ($P < 0.0005$; Table 5-6 and Figure 5-12). The HSA-EEF1A2 transgenic group showed significant abnormalities in every array of the tests except the tail-lifting test, with $P < 0.0001$ for gait, and body tremor, $P < 0.001$ for spontaneous activity and contact righting reflex, $P < 0.005$ for grip

strength and wire manoeuvre, and $P < 0.05$ for righting reflex. These abnormalities indicated an impairment of lower motor neurone and spinocerebellar functions, including muscle.

Non-transgenic wasted mice differed from controls on the same aspects as those of transgenic wasted mice, including body weight and length, with the same ranges of statistic significances, except for grip strength and wire manoeuvre, in which those of non-transgenic wasted mice showed a greater significance than those of transgenic wasted mice. However, there was no statistic significance in any aspect of the tests between transgenic and non-transgenic wasted mice ($P > 0.1$). These results meant that with regard to sensorimotor function tests used in this study as well as body weight and length, HSA-EEF1A2 transgenic wasted mice were indistinguishable from non-transgenic spontaneous mutant wasted mice.

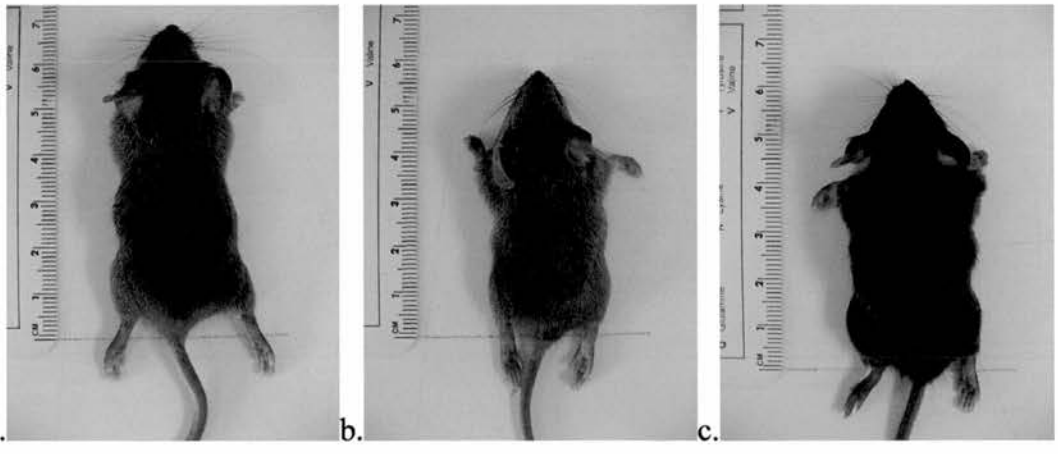

Figure 5-12 Length comparisons of a non-transgenic wild-type control (a), a HSA-EEF1A2 transgenic wasted mouse (b), and a non-transgenic wasted mouse (c).

Table 5-6 Mean ± S.E.M. values from the modified SHIRPA primary screen of HSA-EEF1A2 transgenic wasted mice, non-transgenic wasted mice and non-transgenic controls

Tests	Controls	Non-tg, wst/wst	Tg, wst/wst
Viewing jar			
Body position	3.0 ± 0	3.0 ± 0	3.0 ± 0
Spontaneous activity	2.0 ± 0	1.2 ± 0.2 [a]	1.2 ± 0.2 [a]
Respiratory rate	2.0 ± 0	2.0 ± 0	2.0 ± 0
Body tremor	0.0 ± 0	2.0 ± 0 [a]	2.0 ± 0 [a]
Open-field			
Gait	0.0 ± 0	1.0 ± 0 [a]	1.0 ± 0 [a]
Tail-lifting			
Trunk curl	1.0 ± 0	1.0 ± 0	1.0 ± 0
Limb grasping	1.0 ± 0	1.0 ± 0	1.0 ± 0
Visual placing	3.0 ± 0	2.8 ± 0.2	2.8 ± 0.2
Horizontal grid			
Grip strength	2.2 ± 0.2	1.0 ± 0 [a]	1.2 ± 0.2 [b]
Body tone	1.0 ± 0	1.0 ± 0	1.0 ± 0
Horizontal wire			
Wire manoeuvre	0.2 ± 0.2	1.2 ± 0.2 [b]	1.2 ± 0.2 [b]
Righting reflex	0.0 ± 0	0.8 ± 0.2 [a]	0.7 ± 0.2 [c]
Tube			
Contact righting reflex	1.0 ± 0	0.0 ± 0 [a]	0.2 ± 0.2 [a]
Body measures			
Weight (g)	12.1 ± 0.2	7.7 ± 0.2 [a]	7.7 ± 0.5 [a]
Length (cm)	7.1 ± 0.1	6.0 ± 0.1 [a]	6.0 ± 0.1 [a]

[a] $P < 0.001$ vs. controls (unpaired t-test).

[b] $P < 0.005$ vs. controls (unpaired t-test).

[c] $P < 0.05$ vs. controls (unpaired t-test).

5.3.2 Progressive paralysis in HSA-EEF1A2 transgenic wasted mice

Motor function in the hind limbs of HSA-EEF1A2 transgenic wasted mice was scored using the neurological rating scale as previously presented in chapter 3, table 3-1. The scores were compared to those of non-transgenic wasted mice and wild-type controls. The number of mice for each group was varied with age, as shown in table 5-7. However, there were six animals in each group at the beginning of the evaluation. The groups were compared with the unpaired *t*-test.

Two of HSA-EEF1A2 transgenic wasted mice were allowed to live until they got the neurological score of zero at the age of 30 days, and then were culled. As presented in table 5-7 and figure 5-13, the transgenic group showed signs of paralysis beginning at weaning (score 4 ± 0), and progressed to severe paralysis with an absence of movement (score 0.5 ± 0.58, $P < 0.009$, $n = 4$) at the age of 29 days. Of these, two died, and the other two were culled at the age of 30 days with the score of zero. The trend of progression of paralysis observed in the transgenic group was similar to that of non-transgenic wasted mice when compared to the controls. When compared the neurological scores of the transgenic wasted mice to those of non-transgenic wasted group, no statistically significant difference was observed at any age of the mice, as shown in table 5-7. Although the transgenic group seemed to live 1-2 days longer than the non-transgenic wasted mice, the number of animals was too small to make this conclusion. Ataxic walking was observed to occur 1 day later in the HSA-EEF1A2 transgenic wasted mice, at 24 days old (score 2.83 ± 0.41) than the non-transgenic wasted group, at 23 day olds (score 2.83 ± 0.41).

Table 5-7 Neurological rating scores of hind limbs of HSA-EEF1A2 trasngenic wasted mice, non-transgenic wasted mice, and wild-type controls.

	D20	**D21**	**D22**	**D23**	**D24**	**D25**	**D26**	**D27**	**D28**	**D29**	**D30**
Control 1	5	5	5	5	5	5	5	5	5	5	5
Control 2	5	5	5	5	5	5	5	5	5	5	5
Control 3	4	5	5	5	5	5	5	5	5	5	5
Control 4	5	5	5	5	5	5	5	5	5	5	5
Control 5	4	5	5	5	5	5	5	5	5	5	5
Control 6	5	5	5	5	5	5	5	5	5	5	5
Mean	4.67	5.00	5.00	5.00	5.00	5.00	5.00	5.00	5.00	5.00	5.00
S.D.	0.52	0	0	0	0	0	0	0	0	0	0
Ntg-wst 1	5	4	3	3	3	2	2	1	1		
Ntg-wst 2	4	4	3	3	2	2	1	0	0		
Ntg-wst 3	4	4	4	3	2	2	1	1	0		
Ntg-wst 4	5	4	3	3	3	2	2	1	1		
Ntg-wst 5	4	4	3	3	2	2	1	0	0		
Ntg-wst 6	4	4	4	2	2	2					
Mean	4.33	4.00	3.33	2.83	2.33	2.00	1.40	0.60	0.40	-	-
S.D.	0.52	0	0.52	0.41	0.52	0	0.55	0.55	0.55	-	-
P value vs. controls*	0.31	←		< 0.005		→	←	< 0.009	→		
Tg-wst 1	5	4	3	3	3	2	2	1	1	1	0
Tg-wst 2	5	4	3	3	3	2	2	2	1	1	0
Tg-wst 3	4	4	3	3	3	2	2	1	1	0	
Tg-wst 4	4	4	3	3	3	2	2	1	1	0	
Tg-wst 5	4	4	4	3	2	2	1	1	0		
Tg-wst 6	5	4	3	3	3	2					
Mean	4.50	4.00	3.17	3.00	2.83	2.00	1.80	1.20	0.80	0.50	0
S.D.	0.55	0	0.41	0	0.41	0	0.45	0.45	0.45	0.58	0
P value vs. controls*	0.64	←		< 0.005		→	←	< 0.009	→		
P value vs. ntg-wst*	0.64	0.90	0.59	0.90	0.11	0.90	0.27	0.12	0.27	-	-

* Mann-Whitney test.

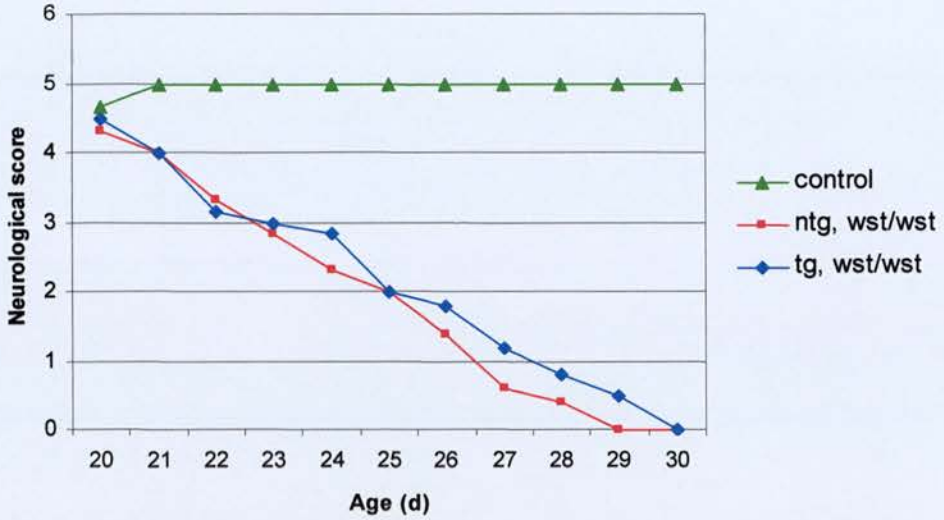

Figure 5-13 Mean of the neurological scores in hind limbs of HSA-EEF1A2 transgenic wasted mice compared to those of non-transgenic wasted mice and wild-type controls.

5.3.3 A decline in body weight and muscle mass

Spontaneous mutant homozygous wasted mice have been shown to begin to lose weight at about 21 days of age, with a significant decline to less than their normal littermates by 23 days (Tezuka *et al.*, 1986). Recently, the decline in body weight of wasted mice has been demonstrated to occur along with a disproportionate decline in muscle, in which the mean muscle:body weight ratio in wasted mice was 1.49 compared with 4.44 in heterozygous mice by day 27 (Newbery *et al.*, 2005). In my study, I compared total body weights of HSA-EEF1A2 transgenic homozygous wasted mice, which expressed eEF1A2 specifically in skeletal muscle, with those of non-transgenic wasted mice and normal littermates so as to investigate whether expression of eEF1A2 in muscle affected body weight of wasted mice.

HSA-EEF1A2 transgenic wasted mice showed a gradual incline in body weight to their peaks of 8.57 $\pm$ 0.98 grams at day 20, then began to progressively decline to less than

body weights of non-transgenic normal littermates with a statistically significant difference at day 21 (8.00 $\pm$ 0.08, $P < 0.05$), as shown in figure 5-14 and table 5-8. At day 25, the average weight of transgenic wasted mice was 7.50 $\pm$ 1.38 grams, whereas that of non-transgenic normal littermates was 12.8 $\pm$ 0.92 grams ($P < 0.0001$). Non-transgenic homozygous wasted mice showed a decline in their body weights compared with those of controls similar to HSA-EEF1A2 transgenic wasted mice. Their weights also reached a peak of 8.50 $\pm$ 0.53 grams at day 20, then began to decline. However, the statistical significance, compared to controls, was observed at 1 day (day 22) later than that of transgenic wasted mice (P vs. controls < 0.05). There was no significantly statistic difference observed in body weight measurements at any age of animals between transgenic and non-transgenic wasted mice

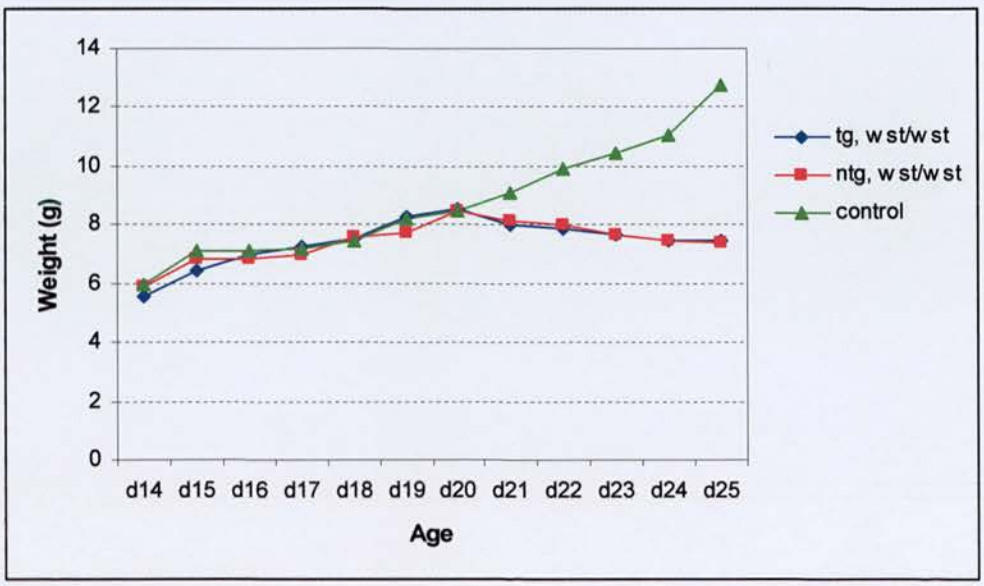

Figure 5-14 Body weights of HSA-EEF1A2 transgenic wasted mice, non-transgenic wasted mice, and controls

Table 5-8 Body weights of HSA-EEF1A2 transgenic wasted mice, non-transgenic wasted mice, and non-transgenic controls

	D14	D15	D16	D17	D18	D19	D20	D21	D22	D23	D24	D25
Body weight (g) ± S.D.												
Controls	6.00 ± 0.47	7.13 ± 0.35	7.13 ± 0.64	7.20 ± 0.93	7.50 ± 0.53	8.20 ± 0.63	8.50 ± 0.71	9.10 ± 0.74	9.9 ± 0.74	10.5 ± 0.97	11.08 ± 1.86	12.8 ± 0.92
Non-tg, wst/wst	5.88 ± 0.64	6.88 ± 0.83	6.88 ± 0.64	7.00 ± 0.79	7.63 ± 0.74	7.75 ± 1.13	8.50 ± 0.53	8.14 ± 1.35	8.00 ± 1.11	7.71 ± 0.95	7.50 ± 0.55	7.38 ± 0.72
Tg, wst/wst	5.57 ± 0.53	6.43 ± 0.79	7.00 ± 0.82	7.29 ± 1.11	7.57 ± 1.13	8.29 ± 1.38	8.57 ± 0.98	8.00 ± 0.08	7.86 ± 0.90	7.67 ± 1.21	7.50 ± 1.05	7.50 ± 1.38
P value *												
Tg, wst/wst vs. controls	0.101	0.0413	0.7451	0.8545	0.8629	0.8644	0.8629	0.011	0.0001	0.0001	0.0008	< 0.0001
Tg, wst/wst vs. non-tg, wst/wst	0.3416	0.3079	0.7451	0.6272	0.9411	0.5364	0.8606	0.8142	0.4435	0.9381	1.0000	0.8580
Non-tg, wst/wst vs. controls	0.6395	0.4483	0.4483	0.5962	0.6819	0.4491	1.0000	0.0775	0.0260	< 0.0001	0.0005	< 0.0001

* Unpaired *t*-test.

Muscle:body wet weight ratio was further analyzed. Quadriceps muscles from aged-matched HSA-EEF1A2 transgenic wasted mice, non-transgenic wasted mice, and normal littermates were weighed at 20 to 29 days of age. As shown in table 5-9 and figure 5-15, both transgenic and non-transgenic wasted mice showed a disproportionate decline in muscle mass as they deteriorated. At the age of 24-25 days onwards, their muscle:body weight ratios were significantly lower than those of normal mice ($P < 0.05$). By day 29, the average muscle:body weight ratio in transgenic wasted mice was 1.73 ± 0.45 compared with 3.70 ± 0.14 in normal controls ($P < 0.02$), whereas the ratio in non-transgenic wasted mice was 1.57 ± 0 (P vs. controls < 0.005). There was no significantly statistic difference in muscle:body weight ratio between the transgenic wasted mice and non-transgenic wasted group at any age of animals. The size of the spleen of the transgenic wasted mice was also observed and was similar to that of non-transgenic wasted mice, as shown in Appendix 2.

Table 5-9 Mean ± S.D. and P values of muscle:body wet weight ratios of HSA-EEF1A2 transgenic wasted mice compared with non-transgenic wasted mice and controls.

	D20-D-21	D24-D25	D28-D29
Muscle:Body weight ratio (x 10^3) ± S.D.			
Controls	3.44 ± 0.06	3.88 ± 0.25	3.70 ± 0.14
Non-tg, *wst/wst*	2.76 ± 0.91	1.85 ± 0.59	1.57 ± 0
Tg, *wst/wst*	3.20 ± 0.28	1.41 ± 0.02	1.73 ± 0.45
P value *			
Tg, *wst/wst* vs. controls	0.3574	0.0051	0.0106
Tg, *wst/wst* vs. non-tg, *wst/wst*	0.5778	0.4098	0.6640
Non-tg, *wst/wst* vs. controls	0.3989	0.0465	0.0022

* Unpaired *t*-test

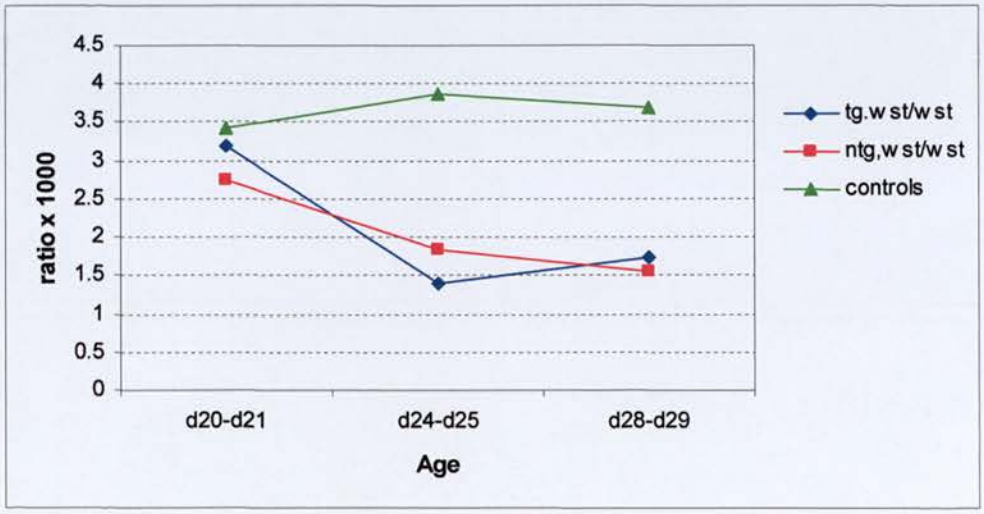

Figure 5-15 Muscle:body wet weight ratios of HSA-EEF1A2 transgenic wasted mice compared with non-transgenic wasted mice and controls.

5.3.4 Muscle pathology in HSA-EEF1A2 transgenic wasted mice

5.3.4.1 Analysis of fibre size differences

Quadriceps muscles were taken from three 28-day-old HSA-EEF1A2 transgenic wasted mice, non-transgenic wasted mice and non-transgenic wild-type controls. 200-700 fibres in the transverse sections from each group were analysed. Data (means $\pm$ S.E.M) were compared between groups by the unpaired *t*-test. Fibre analysis showed a significant smaller fibre diameter in transgenic wasted mice compared with the controls (15.5 $\pm$ 0.2 um in transgenic group, 20.8 $\pm$ 0.3 um in control group, $P < 0.0001$), as shown in table 5-10 and figure 5-16. When compared the transgenic wasted mice with the non-transgenic wasted group (15.5 $\pm$ 0.2 um) there was no statistical significance between the groups.

Table 5-10 Minimum and maximum diameters of muscle fibres

Muscle Fibre Analysis	Tg, wst/wst	Ntg, wst/wst	Wild Type
Minimum diameter (um)	14.3	13.5	18.5
Maximum diameter (um)	16.1	16.5	22.4

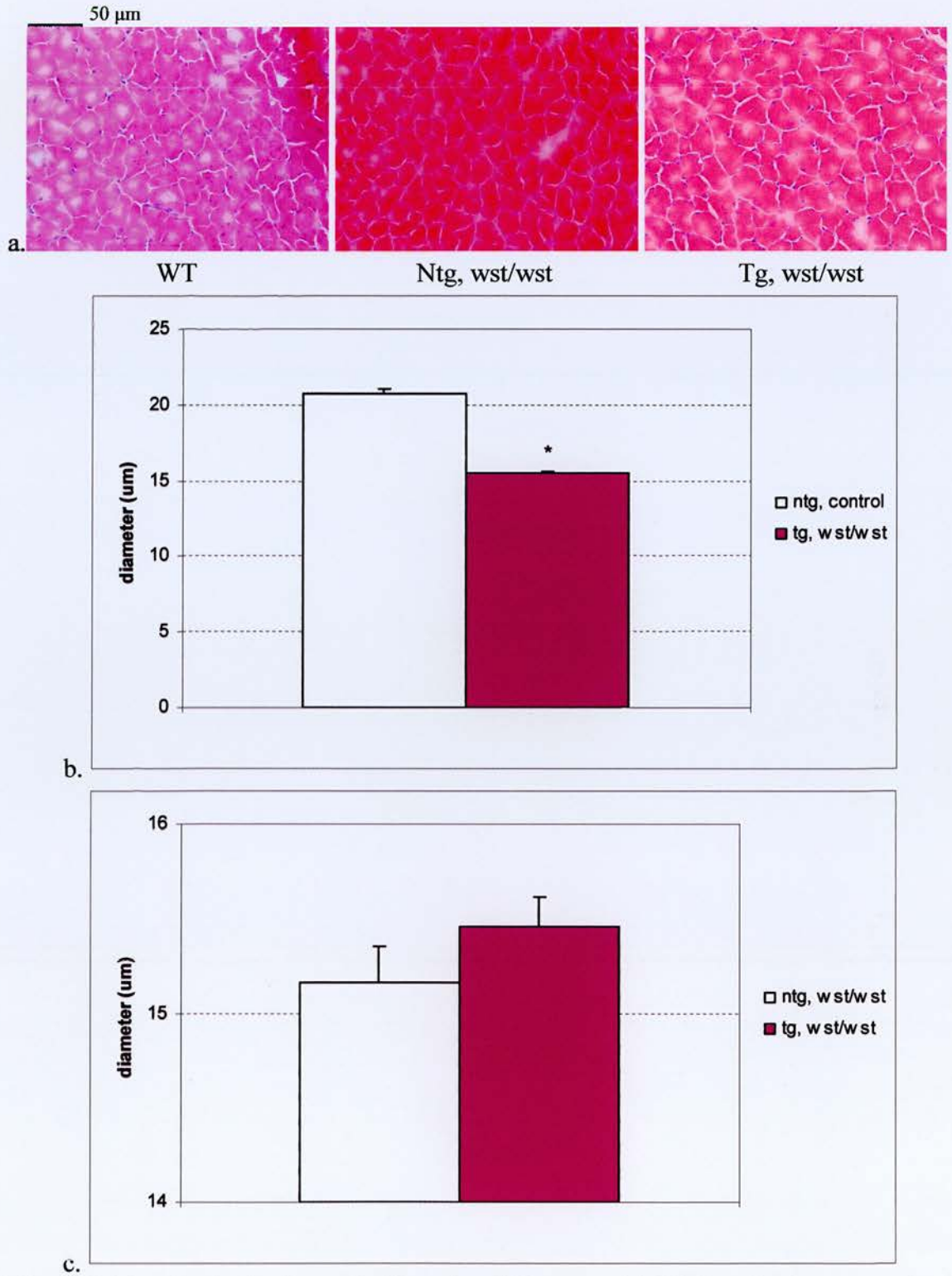

Figure 5-16 Analysis of muscle fibre size differences. (a) H&E-stained cross-sections. (b and c) Comparisons between groups of mice. Asterisk denotes $P < 0.0001$.

5.3.4.2 Muscle in HSA-EEF1A2 transgenic wasted mice shows features of neurogenic atrophy

Hematoxylin and eosin-stained cross-sections of quadriceps from three 28 day-old HSA-EEF1A2 transgenic wasted mice were analysed. Multiple small groups of atrophic fibres were demonstrated in addition to small angular fibres (Figure 5-17). These findings suggested that the pathologic process was in the early stage of denervation, like those previously demonstrated in muscle of spontaneous mutant wasted mice (see 3.2.2.2). A range of severity in muscle pathology was found. Pyknotic nuclear clumps, an end product of denervation atrophy, were also found in several areas of severely atrophic fibres, which suggested that denervation existed without reinnervation. The findings of these pathologic processes are the same as those found in spontaneous mutant wasted mice (Figure 3-3), suggesting that neurologic atrophy in wasted mice might be a result of the loss of eEF1A2 in nerve fibres that supply the muscle rather than of the loss of eEF1A2 in muscle itself.

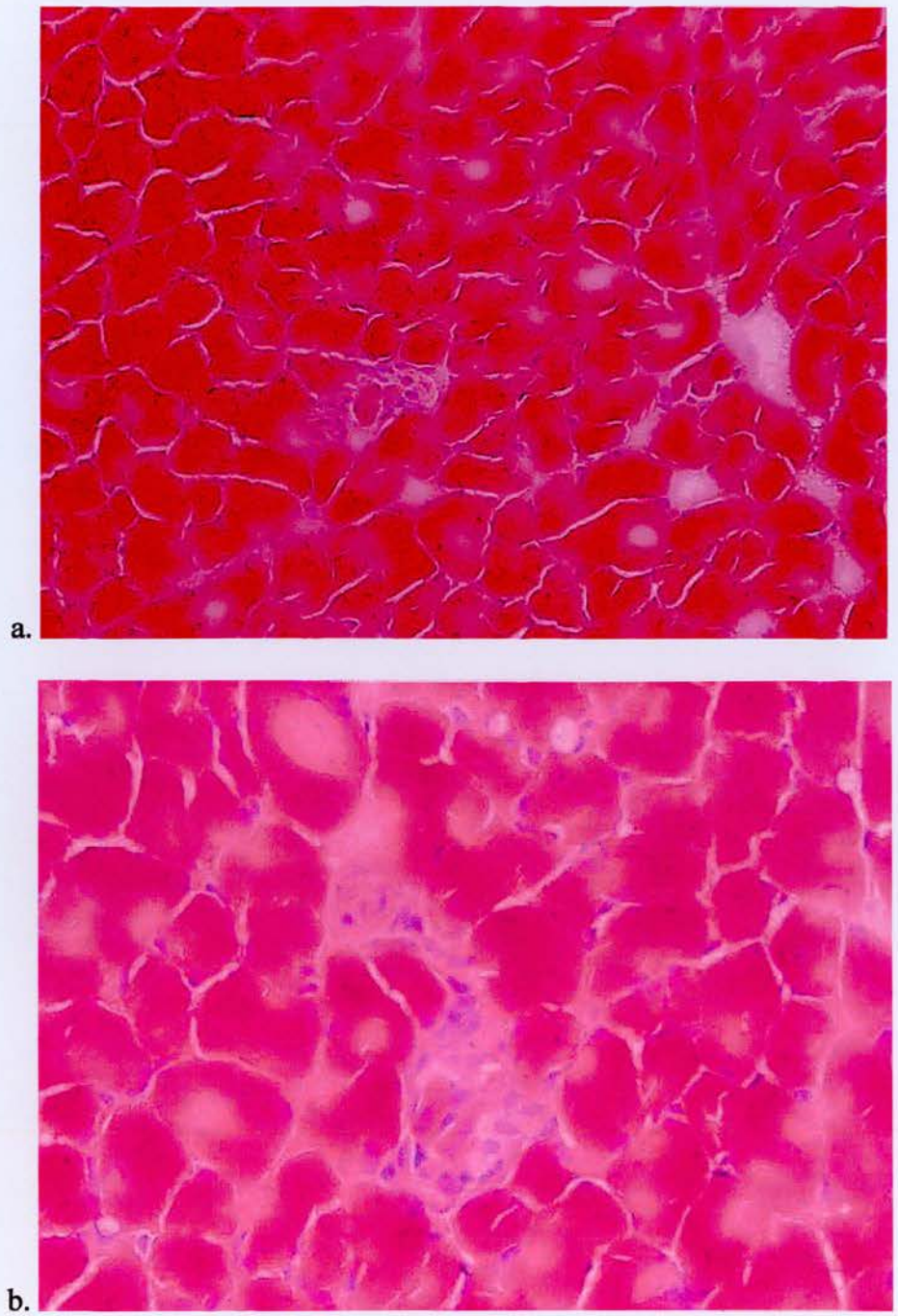

Figure 5-17 Hematoxylin and eosin-stained cross-sections of muscles of 28-day-old HSA-EEF1A2 transgenic wasted mice, showing grouped atrophic fibres with severe loss of contractile apparatus and prominent pyknotic nuclei. (a) 20x magnification. (b) 60x magnification.

5.3.4.3 Evidence of regenerating muscle fibres is found in muscle of HSA-EEF1A2 transgenic wasted mice

Centralized nuclei have previously been found in muscles from 25-day-old wasted mice, as described in 3.2.2.3. Herein, they were also demonstrated in muscles from 25-day-old HSA-EEF1A2 transgenic wasted mice (Figure 5-18), suggesting that the regenerating process of muscle fibres is taking place during the ongoing process of muscle denervation.

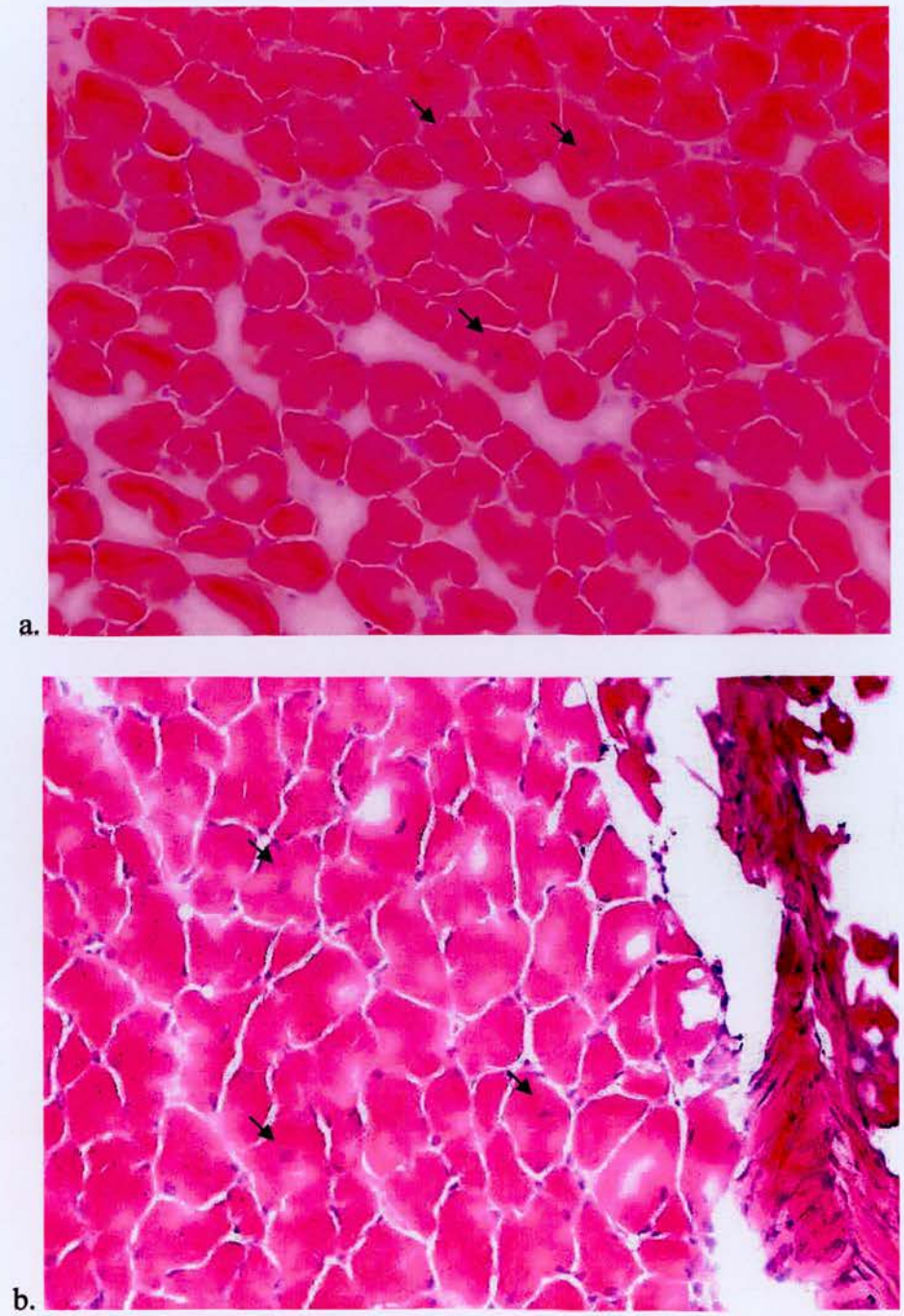

Figure 5-18 Hematoxylin and eosin-stained cross sections of quadriceps of two 25-day-old HAS-EEF1A2 transgenic wasted mice (a and b, 40x), showing centralized nuclei typical of regenerating muscle fibres (arrows).

5.3.5 Expression of nerve-regulated genes in muscle of HSA-EEF1A2 transgenic wasted mice

As previously shown in 3.2.4, muscle of homozygous wasted mice showed upregulation of AchRα1 and myogenin, and downregulation of ClC-1, which is a typical pattern found in atrophic muscle resulting from denervation. In order to confirm that muscle atrophy in wasted mice is a consequence of denervation, I studied patterns of these denervation-sensitive genes in muscle of HSA-EEF1A2 transgenic wasted mice, in which there is no eEF1A2 protein expressed in nerves but only in muscles, the hypothesis being that the lack of eEFA2 in nervous system, but not in muscle, is a leading cause of muscle atrophy in wasted mice.

5.3.5.1 HSA-EEF1A2 transgenic wasted mice showed an upregulation of AchRα1 and myogenin, and downregulation of ClC-1

Hindlimb muscles, quadriceps, were taken from 29-day-old HSA-EEF1A2 transgenic wasted mice, non-transgenic wasted, and wild-type littermates (n = 3 for each group). Student's unpaired *t*-test was used to compare data (mean ± S.E.M) between groups. Figure 5-19 shows the levels of expression of AchRα1, myogenin, and ClC-1 genes, which are normalized to those of β-actin. As expected, the transcripts of AchRα1 in muscle of transgenic mice were a significantly upregulated 8.59-fold above the levels in wild-type mice ($P < 0.0005$). In a similar fashion, the expression of myogenin were elevated 21.83-fold higher than in wild-type mice ($0 < 0.005$). Interestingly, the levels of expression of AchRα1 and myogenin in HSA-EEF1A2 transgenic wasted mice (8.85 ± 0.65 for AchRα1; 21.83 ± 2.46 for myogenin) were higher than those in non-transgenic wasted group (5.88 ± 1.23 for AchRα1; 1.33 ± 0.36 for myogenin), when normalized to the levels in wild-type controls. The difference is significant in the expression of myogenin, where P is less than 0.005 (transgenic vs. non-transgenic).

When normalized to the levels of GAPDH expression, the levels of AchRα1 and myogenin followed the same patterns as that of β-actin gene, as shown in figure 4-18. When compared between the transgenic and non-transgenic groups with normalization to the levels of GAPDH expression in wild-type controls, the HSA-EEF1A2 transgenic wasted mice showed a higher expression of AchRα1 (22.33 $\pm$ 1.88 in transgenic; 9.12 $\pm$ 1.88 in non-transgenic; $P < 0.01$) and myogenin (25.57 $\pm$ 5.83 in transgenic; 6.03 $\pm$ 1.99 in non-transgenic; $P < 0.05$).

For the expression of ClC-1 gene, which is downregulated upon denervation, the levels of its expression were lowered in muscle of the HSA-EEF1A2 transgenic wasted mice, compared to those of wild-type controls. Normalized to the expression of β-actin, those of ClC-1 in the transgenic wasted mice were 6.67-fold lower than in wild-type mice ($P < 0.05$), as shown in figure 4-17. Similar patterns were demonstrated when normalized to the expression levels of GAPDH (Figure 5-20). However, unlike the expression of AchRα1 and myogenin, there was no significant difference of ClC-1 expression between the transgenic and non-transgenic wasted mice (0.13 $\pm$ 0.8 vs. 0.39 $\pm$ 0.06 when normalized to β-actin expression; 0.25 $\pm$ 0.07 vs. 0.61 $\pm$ 0.09 when normalized to GAPDH expression).

Values (mean $\pm$ S.E.M) of the levels of expression of AchRα1, myogenin, and ClC-1 are given in table 5-11.

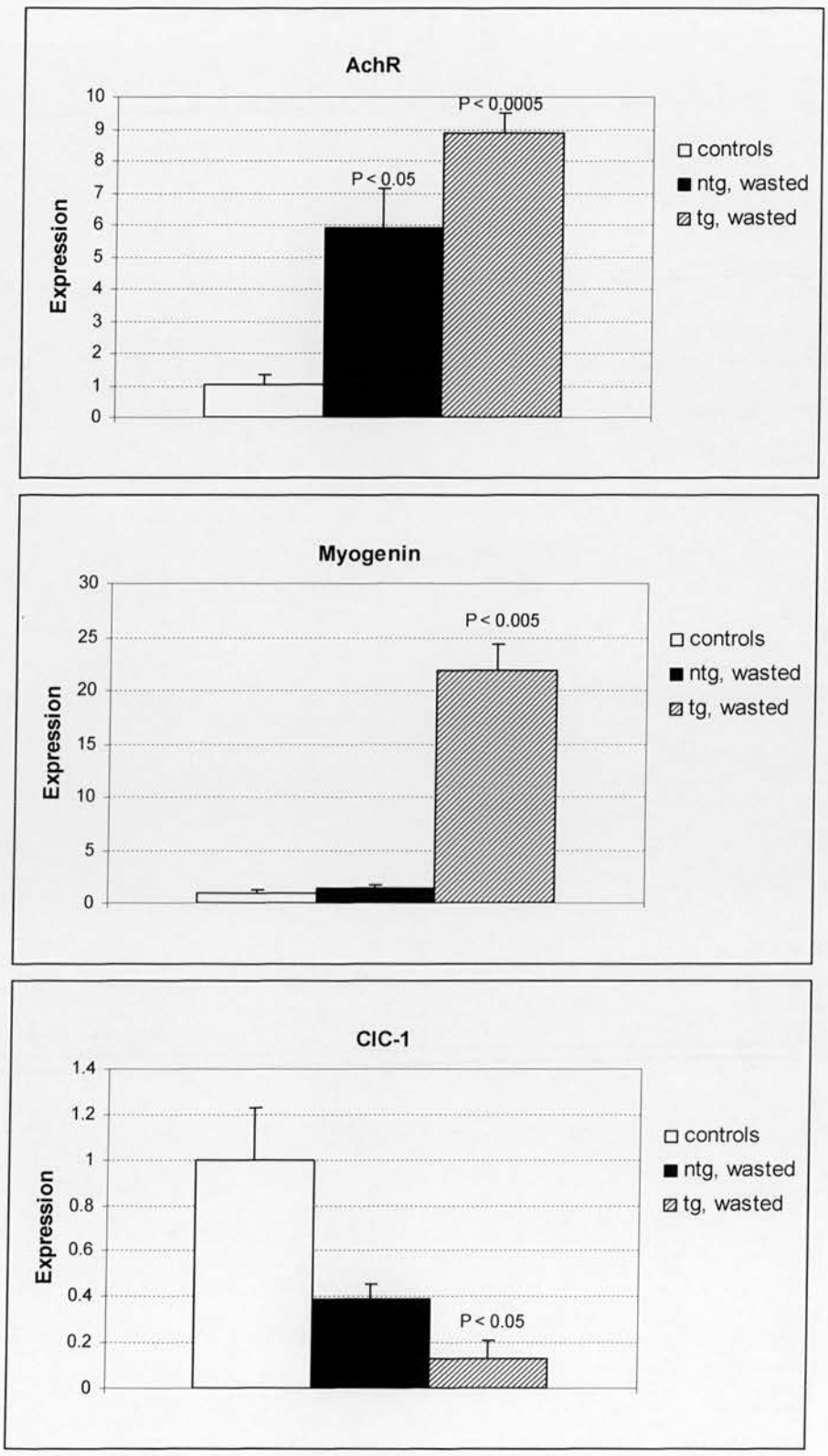

Figure 5-19 Expression levels normalized to those of β-actin

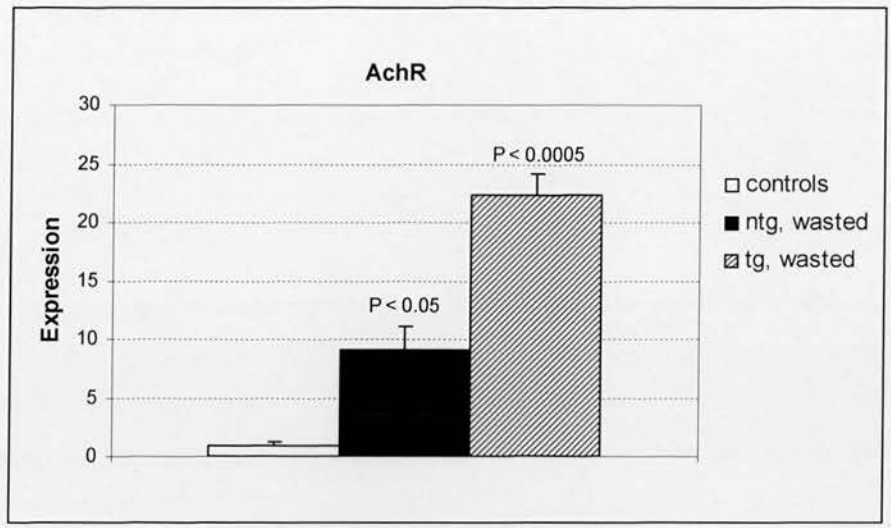

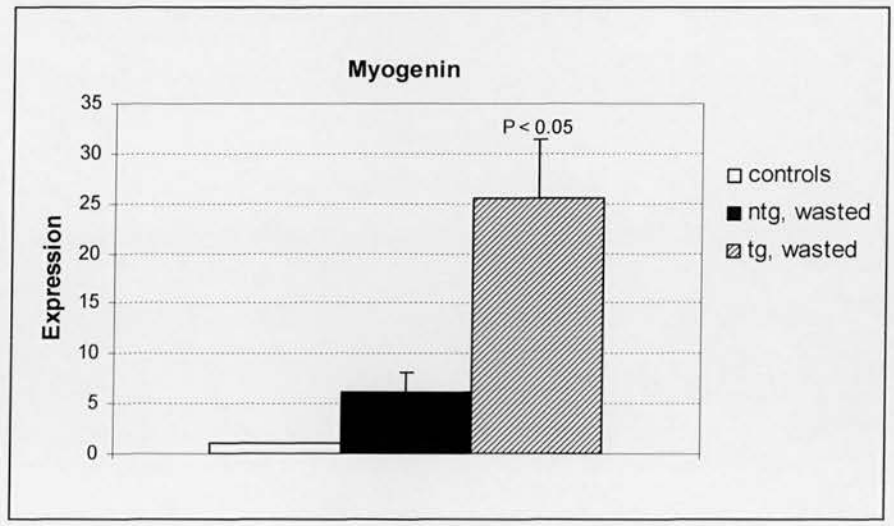

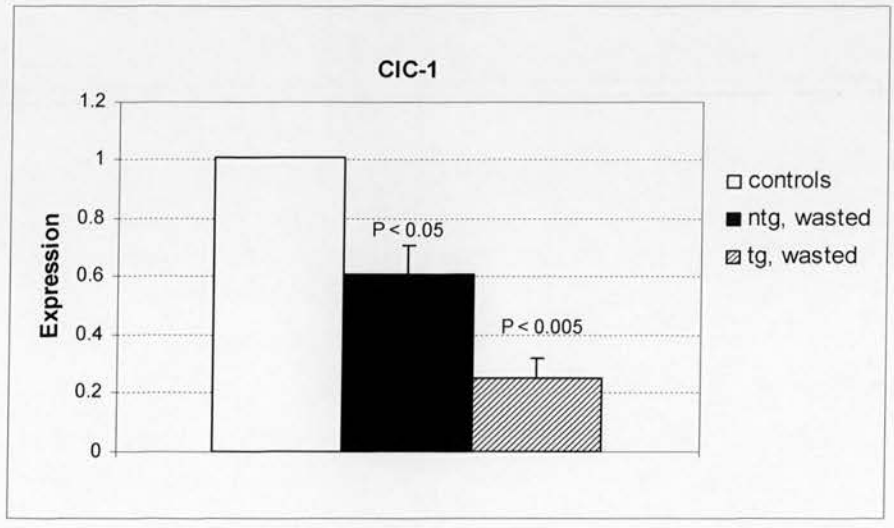

Figure 5-20 Expression levels normalized to those of GAPDH

Table 5-11 Mean ± S.E.M of the levels of expression of AchRα1, myogenin, and ClC-1 in muscle of 29-day-old transgenic wasted, non-transgenic wasted, and wild-type controls.

Mice (n = 3)	Normalized to β-actin			Normalized to GAPDH		
	AchRα1	Myogenin	ClC-1	AchRα1	Myogenin	ClC-1
Controls (+/+ +/+)	1.03 ± 0.32	1.00 ± 0.23	1.00 ± 0.23	1.00 ± 0.29	1.00 ± 0.12	1.01 ± 0.10
Non-tg, wasted (+/+ wst/wst)	5.88 ± 1.23 (P < 0.05)	1.33 ± 0.36	0.39 ± 0.06	9.12 ± 1.88 (P < 0.05)	6.03 ± 1.99	0.61 ± 0.09 (P < 0.05)
Tg, wasted (tg/+ wst/wst)	8.85 ± 0.65 (P < 0.005)	21.83 ± 2.46 (P < 0.005)	0.13 ± 0.08 (P < 0.05)	22.30 ± 1.88 (P < 0.0005)	25.57 ± 5.83 (P < 0.05)	0.25 ± 0.07 (P < 0.005)

(Unpaired *t*-test)

5.3.5.2 EEF1A2 promotes expression of AchRα1 and myogenin in denervated muscle

As the expression of AchRα1 and myogenin in the HSA-EEF1A2 transgenic wasted mice were significantly higher than those in non-transgenic wasted group, it would be interested to figure out that whether these high levels of expression were a direct effect of a high level of eEF1A2 protein in the HSA-EEF1A2 transgenic wasted mice with no regard to denervation. To address this question, the levels of expression of AchRα1 and myogenin were compared between transgenic non-wasted (tg/+ *wst*/+) and transgenic wasted (tg/+ *wst*/*wst*), including non-transgenic wild-type mice as controls. Quadriceps from six 25-day-old mice for each groups were taken for real-time RT-PCR.

The expression of AchRα1 mRNA in muscle of HSA-EEF1A2 transgenic wasted mice (11.82 ± 1.63) was significantly higher than in muscle of transgenic non-wasted (1.92 + 0.48) and controls groups (2.27 ± 0.70), with P = 0.005 (Figure 5-21). For myogenin mRNA expression, the transgenic wasted mice also showed significantly higher expression (10.59 ± 1.58) than the transgenic non-wasted (1.00 ± 0.24) and controls (1.90 ± 0.52), with P < 0.0005, as shown in figure 5-22. No differences in the expression of AchRα1 and myogenin mRNAs between transgenic non-wasted mice and wild-type controls were found. For ClC-1 mRNA expression, as expected, there was no difference in the expression between the transgenic non-wasted mice and controls, but its

expression was lowered in the transgenic wasted group (Figure 5-23). Similar patterns were demonstrated when normalized to the levels of GAPDH mRNA expression, as shown in figure 5-24.

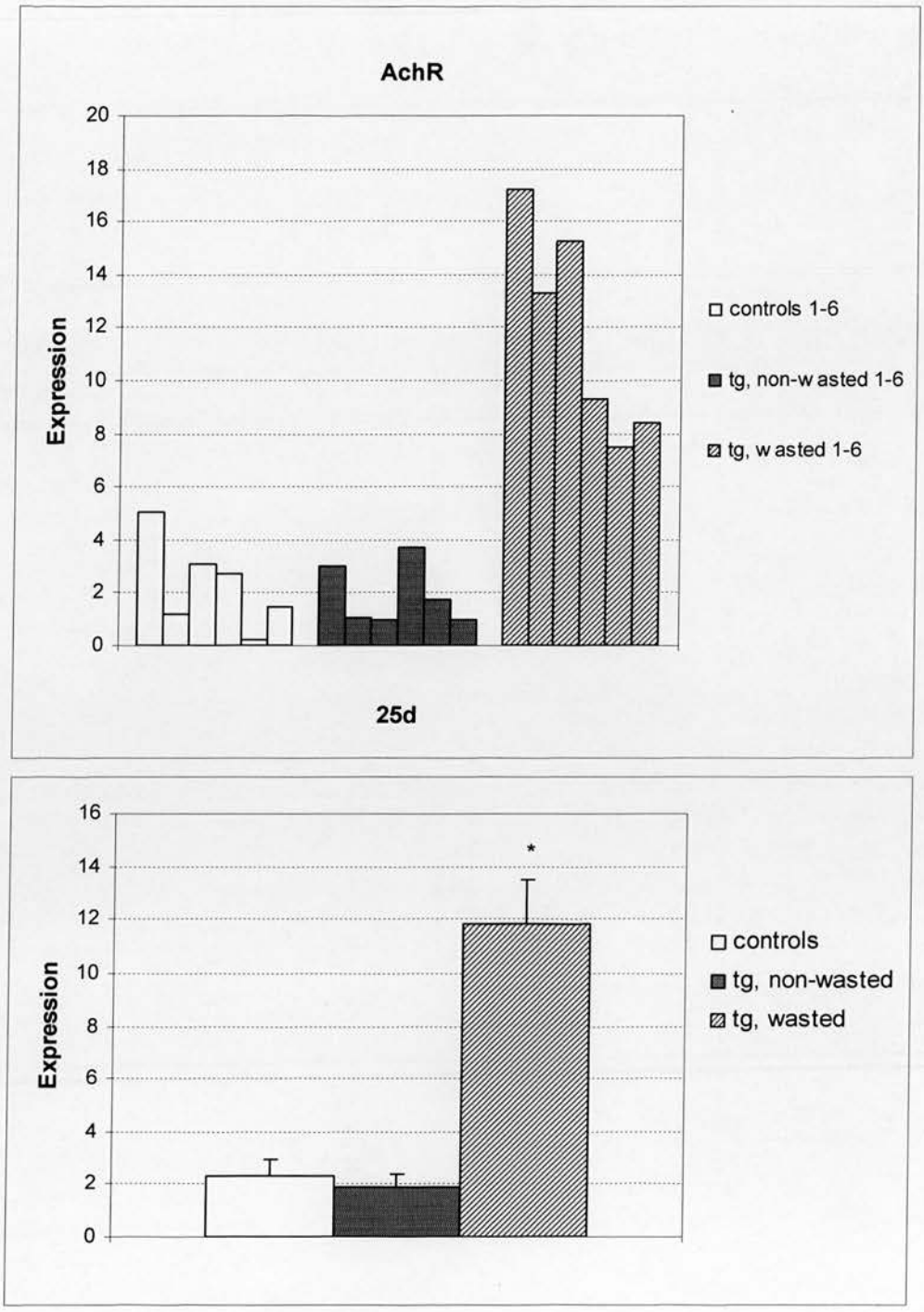

Figure 5-21 Expression of AchRα1 mRNA in quadriceps of 25-day-old mice (n = 6 for each group), normalized to those of β-actin. Asterisk denotes P = 0.005.

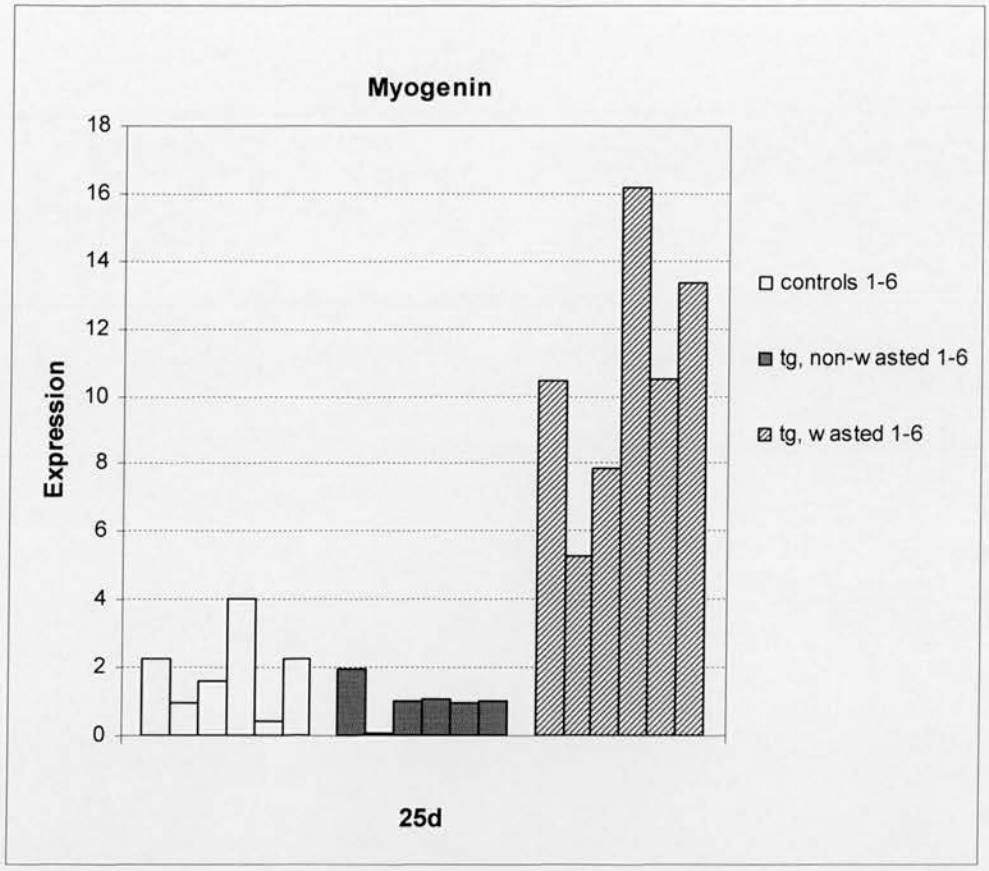

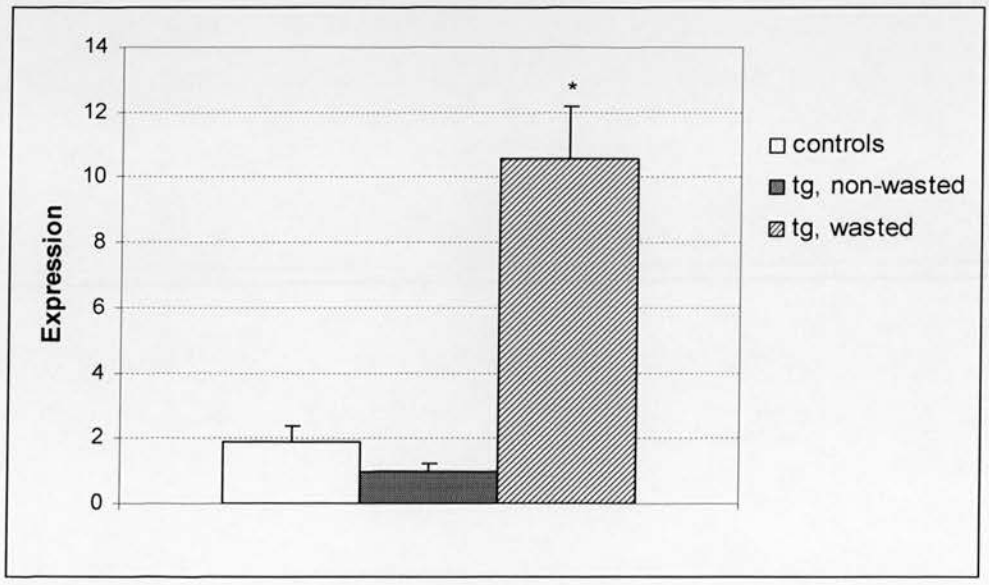

Figure 5-22 Expression of myogenin mRNA in quadriceps of 25-day-old mice (n = 6 for each group), normalized to those of β-actin. Asterisk denotes $P < 0.0005$.

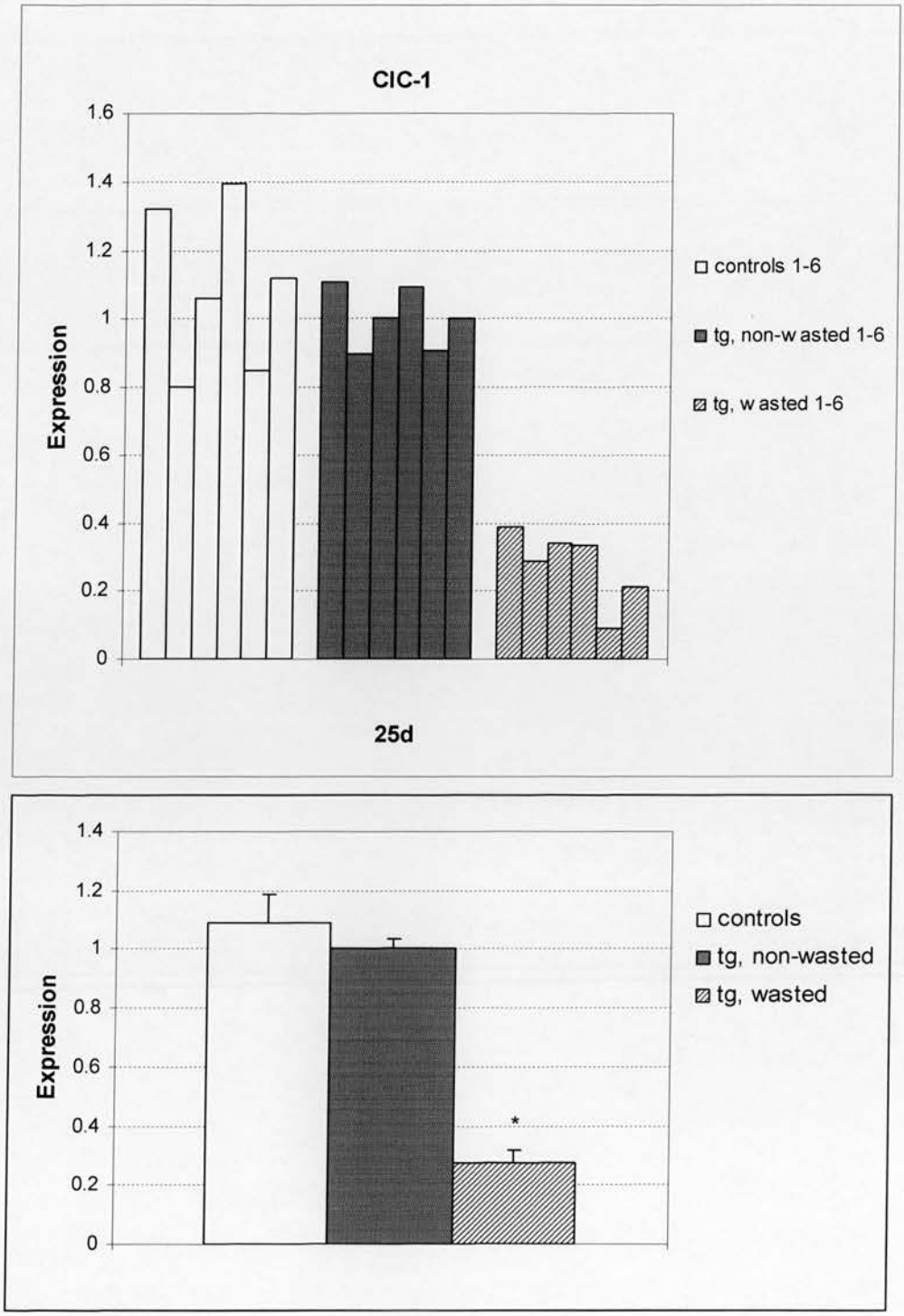

Figure 5-23 Expression of ClC-1 mRNA in quadriceps of 25-day-old mice (n = 6 for each group), normalized to those of β-actin. Asterisk denotes $P < 0.0001$.

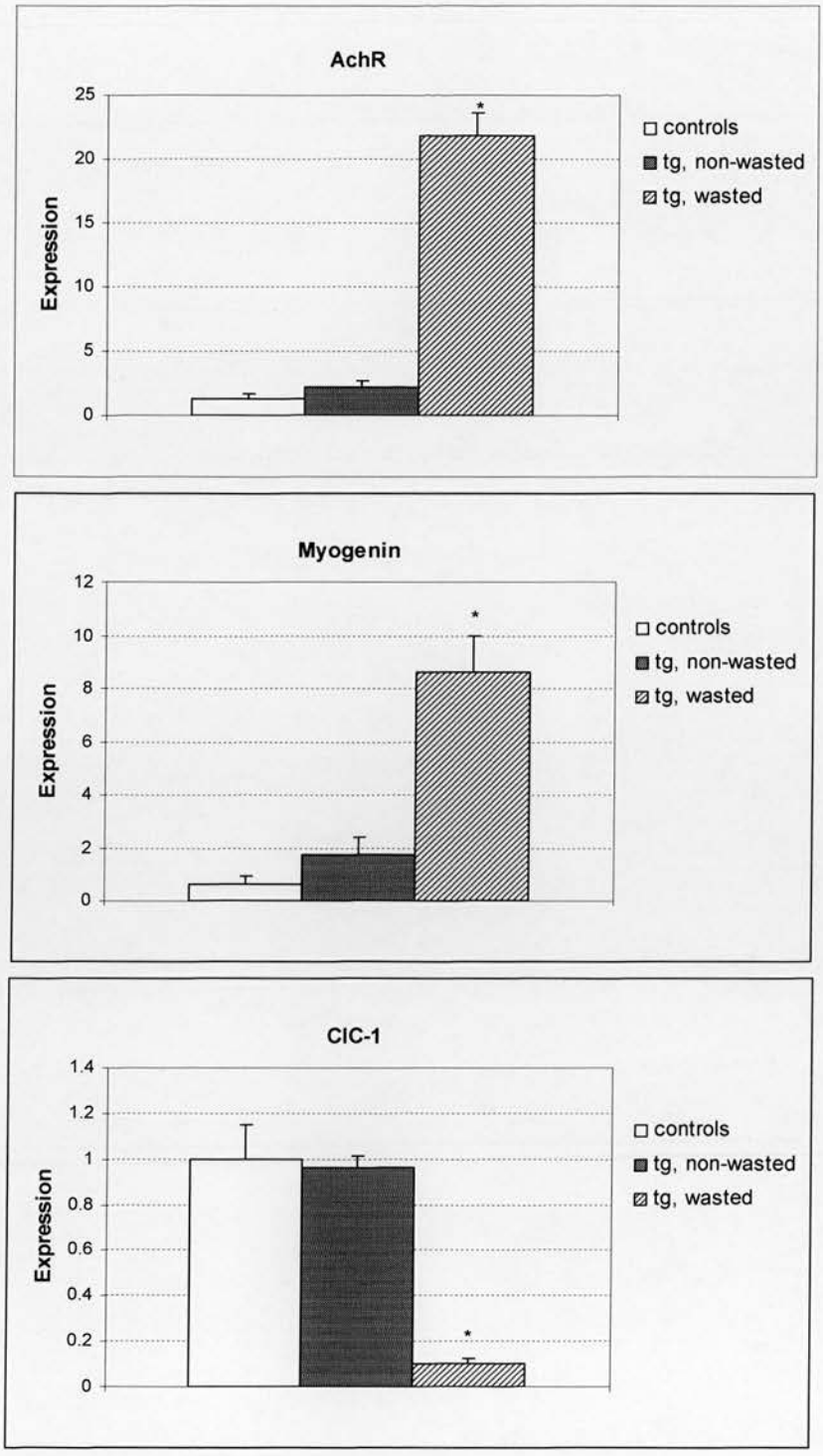

Figure 5-24 Expression of AchRα1, myogenin, and ClC-1 mRNAs in quadriceps of 25-day-old mice (n = 6 for each group), normalized to those of GAPDH. Asterisks denote $P < 0.0001$ for AchR1, $P = 0.0001$ for myogenin, and $P < 0.005$ for ClC-1.

In a similar fashion, 29-day-old transgenic wasted mice showed a high level of AchRα1 and myogenin expression, whereas there was no difference in the expression between the transgenic non-wasted and controls (n = 3 for each group), as presented in figure 5-25 and 5-26. These findings, including from 5.3.5.1, indicate that muscle denervation leads to an increased expression of AchRα1 and myogenin in wasted mice, whether they are HSA-EFF1A2 transgenic or spontaneous mutant, but their levels of expression are remarkedly increased if the animals also express a high level of the eEF1A2 protein in muscle.

Values (mean ± S.E.M) of the levels of expression of AchRα1, myogenin, and ClC-1 are given in table 5-12.

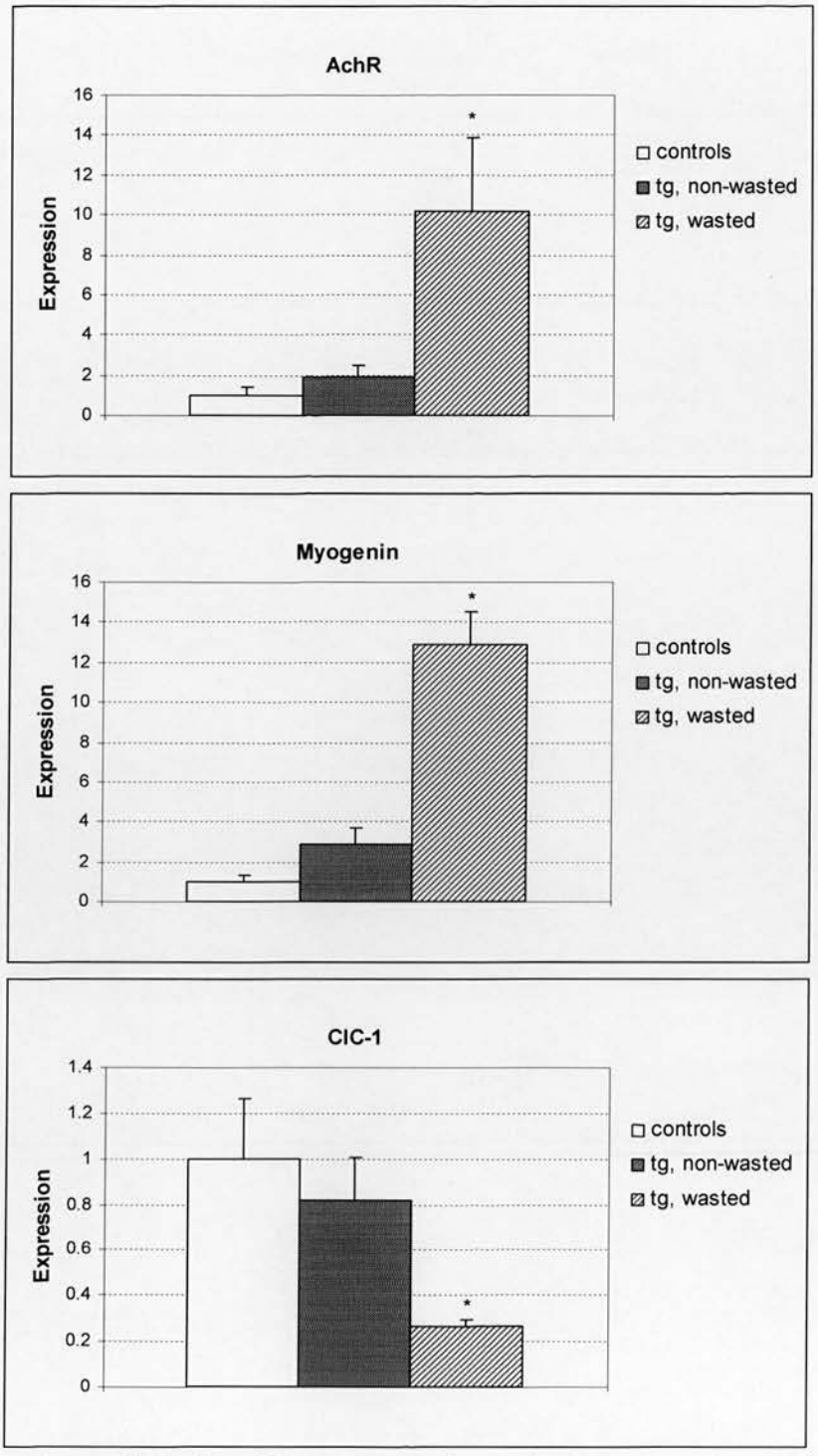

Figure 5-25 Expression of AchRα1, myogenin, and ClC-1 genes in quadriceps of 29-day-old mice (n = 3 for each group), normalized to those of β-actin. Asterisks denote $P < 0.05$ for AchRα1, $P < 0.005$ for myogenin, and $P < 0.05$ for ClC-1.

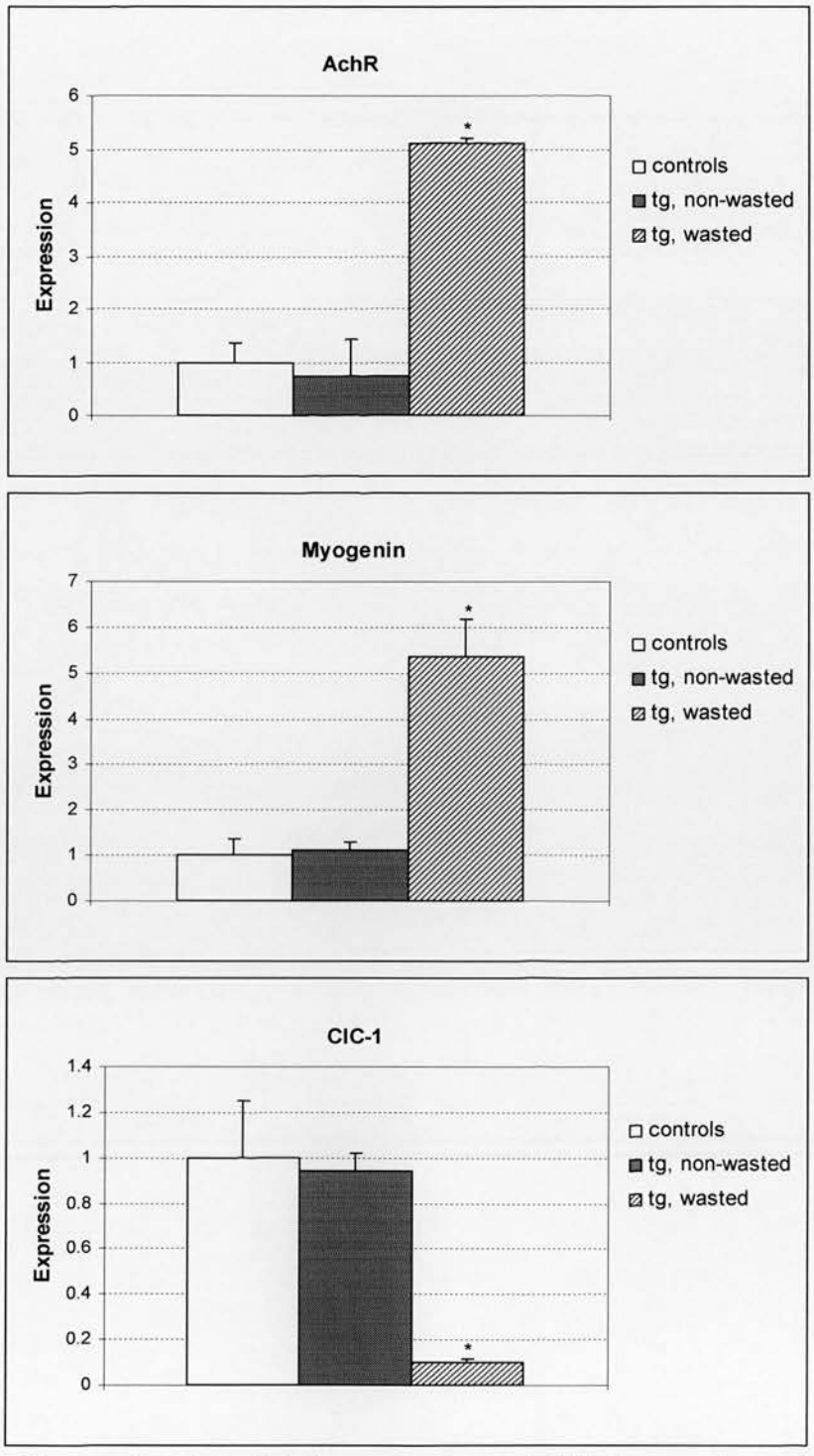

Figure 5-26 Expression of AchRα1, myogenin, and ClC-1 genes in quadriceps of 29-day-old mice (n = 3 for each group), normalized to those of GAPDH. Asterisks denote $P < 0.01$ for AchRα1, $P < 0.01$ for myogenin, and $P < 0.05$ for ClC-1.

Table 5-12 Mean ± S.E.M of the levels of expression of AchRα1, myogenin, and ClC-1 in muscle of 29-day-old transgenic wasted, transgenic non-wasted, and wild-type controls.

Mice (n = 3)	Normalized to β-actin			Normalized to GAPDH		
	AchRα1	Myogenin	ClC-1	AchRα1	Myogenin	ClC-1
Controls (+/+ +/+)	1.00 ± 0.36	1.00 ± 0.33	1.00 ± 0.26	1.00 ± 0.35	1.00 ± 0.37	1.00 ± 0.25
Tg, non-wasted (tg/+ +/+)	1.90 ± 0.54	2.90 ± 0.82	0.82 ± 0.19	0.74 ± 0.67	1.13 ± 0.16	0.94 ± 0.08
Tg, wasted (tg/+ wst/wst)	10.15 ± 3.73 ($P < 0.05$)	12.88 ± 1.64 ($P < 0.005$)	0.26 ± 0.03 ($P < 0.05$)	5.11 ± 1.20 ($P < 0.01$)	5.34 ± 0.85 ($P < 0.01$)	0.10 ± 0.02 ($P < 0.05$)

(Unpaired *t*-test)

5.4 Discussion

Data of the transgenic study presented here is unfortunately somewhat preliminary due to time constraints in experiments relating to the generation of transgenic progeny. In some instances the number of transgenic lines generated for the HSA-EEF1A2 construct and the number of progeny analysed may be not sufficient enough to make firm conclusions. However, data presented here gives useful and interesting knowledge or information regarding the role of eEF1A2 in motor neurons and muscles of wasted mice.

5.4.1 Production of transgenic progeny

Of two transgenic founder mice, one male and one female, the female one did not yield any transgenic progeny after the five litters were screened. Analysis of some of the offspring indicated that there possibly were more than one separate transgene integration event, and transgenes were transmitted independently, as eEF1A2 protein was also detected in eyes and stomach. However, this pattern of expression did not affect my study on muscle denervation because eEF1A2 protein was not expressed in all HAS-EEF1A2 transgenic homozygous wasted mice used in the study.

5.4.2 Characterization of HSA-EEF1A2 transgenic wasted mice

5.4.2.1 Primary screen

The screening battery was designed by modification of the SHIRPA primary screen. Only the tests for assessment of muscle and sensorimotor functions were used. Despite its simplicity, correct interpretation of the measurements depends on what is considered normal for the controls being examined. Systematic SHIRPA primary screens have not been carried out on heterozygous and homozygous wasted mice. In the present study, non-transgenic wild-type animals were used as normal controls and non-transgenic homozygous wasted mice were used as wasted controls. HSA-EEF1A2 transgenic wasted mice were distinguishable from non-transgenic normal controls on several

sensorimotor measures of the primary screen, in addition to physical differences. However, the transgenic group was unable to distinguish from the non-transgenic wasted mice. Balance and coordination, which are a category in the SHIRPA secondary screen, have been examined in spontaneously mutant-wasted mice, using a rotorod (Newbery *et al.*, 2005). Taken together with my present study, it might be possible to conclude that muscle, lower motor neurone, and spinocerebellar functions are the main systems involved in motor and behavioural abnormalities in wasted mice. As some tests can be used for evaluation of other nervous systems, such as righting reflex, it would be interested to examine wasted mice in other aspects of the SHIRPA primary screen. Correlations should also be undertaken, when more mice are produced enough, in the experimental group between body weight and length, on one hand, and other variables, on the other, by using the Pearson product-moment correlation test.

5.4.2.2 Evidence of denervation atrophy

Spontaneous mutant-wasted mice lack the eEF1A2 protein in neurones, heart, and muscle, and exhibit muscle atrophy on ageing. The results from Chapter 3 indicate that denervation is a cause of atrophy. Here, I generated and examined HSA-EEF1A2 transgenic homozygous wasted mice, and the results showed that muscle pathology and regulation of denervation-sensitive genes are the same as those found in spontaneous wasted mice. These findings suggest that the loss of eEF1A2 in motor neurone, but not in muscle, is a leading cause of muscle wasting. Compensation of eEF1A2 for the complete loss of eEF1A1 in muscle by 21 days of wasted mice could not rescue these pathologic processes. Muscle of the HSA-EEF1A2 transgenic wasted mice occasionally contained centralized nuclei typical of regenerating muscle fibres. The extent of centralized nuclei cannot be studied easily under light microscope of H&E sections. Fibres with centralized nuclei have been shown to induce expression of the myosin heavy chain (MyHC) neonatal isoform, a hallmark of regenerating myofibres, in insulin-like growth factor-1 transgenic model (Musarò *et al.*, 2001). To further analysis of muscle regeneration in transgenic or non-transgenic wasted mice,

immunohistochemistry using MyHC or proliferation cell nuclear antigen (PCNA) antibodies is needed.

The high level of expression of AchRα1 and myogenin in muscle of HSA-EEF1A2 transgenic wasted mice compared with non-transgenic wasted group is an interesting finding, although the results in Figure 5-19 and 5-20 do not show an increase in myogenin expression in the non-transgenic wasted group, like those found in wasted mice in Chapter 3 (Figure 3-10 and 3-11). This could be explained by an internal error of the experiment such as pipetting error because the levels of AchRα1 and myogenin have been shown to express in the similar patterns, and myogenin itself is a transcription activator for AchRα1. The high level of expression of AchRα1 and myogenin in muscle of HSA-EEF1A2 transgenic wasted mice could be an effect of the increased level of expression of EEF1A2 as their levels of expression in transgenic non-wasted mice (Figure 5-21 to 5-26) are not increased. The response of skeletal muscle to denervation is complex. At the molecular level, the reaction of skeletal muscle to denervation embodies many cellular processes. On the one hand, individual muscle fibres undergo significant atrophy along, and there is considerable disassembly of the contractile apparatus, along with significant myonuclear loss. On the other hand, there is a considerable increase in the satellite cell population within days of denervation, as well as formation of new muscle fibres in long-term denervated muscle (Borisov *et al.*, 2001; Dedkov *et al.*, 2001; Snow 1983; Viguie *et al.*, 1997). Denervation also leads to apparently paradoxical patterns of genes expression, in which genes or proteins that normally function only during the prenatal period are expressed (Adam *et al.*, 1995; Voytik *et al.*, 1993). A high level of expression of eEF1A2 in transgenic wasted mice may play a role in the upstream regulation of other genes or proteins, at least for AchRα1 and myogenin.

Chapter 6 General Discussion

There are many mouse models of MND, each with their own advantages and disadvantages. Wasted mice represent one of the few model systems for which the basic molecular defect has been identified. There are three related aspects to this project, all aimed at addressing the relative roles of eEF1A2 in muscle and neurons. Firstly, to describe the characterization of neuromuscular abnormalities of spontaneous mutant wasted mice, and evaluate whether muscle atrophy in wasted mice is a consequence of denervation or intrinsic muscle diseases. Secondly, to study distribution and colocalisation between eEF1A2 and SMN in mammalian cells. The last aspect, which is the major and crucial experiment, is to generate transgenic homozygous wasted mice that specifically express human eEF1A2 in muscle, in order to evaluate the phenotype that results from loss of eEF1A2 in neurons but not muscle.

6.1 Neuromuscular abnormalities in wasted mice

Wasted mice exhibit severe muscle wasting and degeneration of motor neurons, beginning at 21 days after birth and die by the age of 28 days. The principal finding of this study is that muscle of wasted mice shows evidence of neurogenic atrophy (denervation), characterized by the presence of multiple small groups of small angular fibres and pyknotic nuclear clumps. Muscle pathology shows a range of severity. The finding of atrophic groups of angulated fibres suggests that the process is in the early stage of chronic denervation. The finding of pyknotic nuclear clumps, which is an end product of denervation atrophy, indicates that denervation exists without reinnervation. Numerous small regions of grouped angular atrophic muscle fibres have also been demonstrated in patients with ALS (Fischer *et al.*, 2004), and mouse models of ALS (Gurney *et al.*, 1994; Ripps *et al.*, 1995; Wong *et al.*, 1995; Bruijin *et al.*, 1997). By contrast, although small groups of atrophic fibres can be found in muscle of patients with SMA (Adams and Victor, 1993) and a transgenic mouse model of SMA (Frugier *et*

al., 2000), the small muscle fibres are often rounded, and large hypertrophied muscle fibres are usually found. In addition, pyknotic nuclear clumps are not present in SMA.

At the level of neuromuscular junctions, I report here the lack of terminal axons observed in synaptic areas of muscle from wasted mice, which is consistent with the muscle denervation process. Examination of wasted NMJ also shows striking abnormalities of terminal axons filled with NF, with reduction of branched structures of the subneural apparatus. Moreover, no axonal sprouting is detectable. These results indicate an abnormal organization of synaptic terminals associated with a defect of axonal regeneration. These abnormalities are similar to those found in *Smn* mutant mice, but contrast with SOD^{G93A} transgenic mice (Cifuentes-Diaz *et al.*, 2002), indicating that NMJ changes in wasted and *Smn* mutant mice may be caused by a common axonal degenerative process. Previous studies have demonstrated accumulation of NF in perikaryons of SOD^{G93A} (Gurney *et al.*, 1994), *Smn* (Cifuentes-Diaz *et al.*, 2002), and wasted mice (Lutsep and Rodriguez, 1989; Newbery *et al.*, 2005). These data indicate that NF accumulation observed in these mutants results from distrinct pathways. Whether the accumulation of NF is a primary effect of the loss of eEF1A2 or SMN function, or a secondary event via an unidentified pathway remains to be investigated.

NF are normally not present in synaptic terminals, and it is thought that NF are degraded by a calcium-activated protease to prevent the accumulation of NF in terminal axons (Schlaepfer, 1974; Schlaepfer and Micko, 1978). As cytoskeletal components play a major role in axonal growth and plasticity (Tanaka and Sabry, 1995), abnormal accumulation of NF in terminal axons of wasted and *Smn* mutant mice may contribute to the defect in terminal axonal growth and plasticity, as suggested by the paucity of terminal arborization, the reduction of branched structures of the subneural apparatus, and the defect in axonal sprouting. The resulting aberrant cytoskeletal organization at the NMJ of wasted mice may contribute to the loss of motor neurone function. The finding of accumulation of NF in terminal axons, presented in this thesis, and in neuronal cell bodies in spinal cord of wasted (Lutsep and Rodriguez, 1989; Newbery *et al.*, 2005) and

Smn mutant mice (Cifuentes-Diaz *et al.*, 2002) with normal or mild reduction in motor neurone cell bodies suggest that degeneration of motor neurons may result from a dying-back axonopathy starting from terminal axons.

Several mouse models of MND such as SOD^{G93A} (Fischer *et al.*, 2004), *pmn* (progressive motor neuropathy) and *mnd* (motoneuron degeneration) have been characterized as "dying-back" neuropathies (Fischer *et al.*, 2000). However, neuronal and axonal degeneration are not necessarily linked, and in some situations, may occur by separate and independent mechanisms (Coleman and Perry 2002; Finn *et al.*, 2000; Deckwerth and Johnson 1994). Wasted mice should represent a valuable model for elucidating the pathway linking these phenomena.

6.2 Regenerating muscle fibres in muscle of wasted mice

Examination of H&E-stained muscle sections of wasted mice also gives an interesting finding. Muscle of wasted mice occasionally contains centralized myonuclei, which are absent from wild-type muscle. Centralized nuclei are typical of regenerating muscle fibres, which might have been thought not to happen in muscle of wasted mice that express neither isoform of eEF1A. In an absence of immunochemical data, one needs to look at the tissue composition and known changes in denervated muscle to try to infer reasons for possible mechanisms. Skeletal muscle contains a complex array of cell types. Among its principal components are multi-nucleated muscle fibers and muscle satellite cells, which are cells located in close association with muscle fibers and containing precursors capable of giving rise to new muscle fibers. Concurrently, new myotubes have been shown to begin to form in association with both intact atrophying and degenerating muscle fibres (Dedkov *et al.*, 2001). The newly forming myotubes have the characteristics of embryonic muscle fibres, which during normal development contain high levels of eEF1A1. The activity of eEF1A1 protein in muscle of symptomatic wasted mice may contribute to protein synthesis in regenerating muscle fibres. This

hypothesis is partly supported by the expression of eEF1A1 at low levels in 28-day-old wasted mice (Khalyfa *et al.*, 2001) It is also possible that upregulation of myogenin that is expressed in both immature and denervated muscle fibres, which I have demonstrated in this thesis, plays a role in regeneration of muscle fibres in wasted mice.

Myogenesis requires energy production for the execution of a number of regulatory and biogenesis events. I have found an increase in SDH staining in muscle of wasted mice, giving another supporting clue for regenerating muscle fibres. It has been shown that skeletal muscle regeneration is accomplished by a marked stimulation of mitochondrial biogenesis concomitant with the onset of muscle cell differentiation (Duguez *et al.*, 2002). However, as SDH stain is the most sensitive and specific stain for mitochondrial proliferation, increased SDH staining may indicate mitochondrial dysfunction. Mitochondrial dysfunction has been reported to occur in skeletal muscle of ALS patients (Dupuis *et al.*, 2003) and SOD^{G93A} transgenic mice (Leclerc *et al.*, 2001), in addition to central nervous system. It is thus necessary to determine mitochondrial abnormalities, both morphologically and functionally, in muscle of wasted mice prior to make a confirmed conclusion regarding its role in regenerating muscle fibres.

6.3 Expression of nerve-regulated genes in muscles of wasted mice

To support the findings in muscle and NMJ of wasted mice that suggest muscle atrophy is neurogenic, I have investigated expression of nerve-regulated genes in muscle of wasted mice, and demonstrated that the patterns of gene expression are characteristic for the type of denervation. These results are similar to the studies in some mouse models for human spinal muscular atrophies, including the mutant "wobbler" (*wr*), "muscle deficient" (*mdf*), and *pmn* (Sedehizade *et al.*, 1997). The positive correlation between the expression of nicotinic AchRα1 and that of myogenin reflects a mechanistic relation. Studies suggest that the dependence of the expression of AchRα1 on the activity pattern

of muscle is mediated by the myogenic transcription factors MyoD and/or myogenin. A tight correlation between the time course of the expression of the AchRα1 and that of MyoD and myogenin after muscle denervation and during muscle maturation has been found in that the changes of MyoD/myogenin expression preceded that of AchRα1 (Eftimate *et al.*, 1991; Piette *et al.*, 1990). The amount of AchR on the muscle cell surface changes during myogenesis and upon muscle innervation and denervation. During embryogenesis, AchRs appear throughout the muscle cell surface. In mature, innervated muscle, AchR is found in very dense clusters localized to the NMJ. Denervation of muscle results in a renewed synthesis of AchRs, which again appear throughout the surface of the muscle fibre (Evans *et al.*, 1987).

The expression of ClC-1 is also developmentally regulated. There is very little ClC-1 mRNA in myotubes, ClC-1 mRNA levels are steeply upregulated during the first few weeks after birth (Steinmeyer *et al.*, 1991, Wischmeyer *et al.*, 1993). The chloride channel ClC-1 controls the excitability of adult muscle but its own expression is dependent on actual muscle activity. This regulation is probably mediated, at least in part, by myogenic factors (Klocke *et al.*, 1994). ClC-1 mRNA is reduced upon denervation (Lorkovic and Tomanek 1977; Klocke *et al.*, 1994).

It has been shown that myogenin and MyoD bind to and activate the enhancer region of the AchRα gene (Piette *et al.*, 1990). The E (CANNTG) boxes, the *cis* elements that bind myogenic factors, are also found in the 5' regulatory region of the mouse *Clc-1* gene. E boxes, consensus binding sites for muscle-specific transcription factors of the MyoD/myogenin family, are found in many muscle specific genes.

I show here that a chronic denervation in wasted mice leads to changes in denervation-sensitive gene expression. The drastic upregulation of AchRα1 and myogenin could be used as a sensitive indicator of the pathological state of muscle. As mRNA levels of MyoD, myogenin, and AchRα are higher both in immature and in denervated muscle fibres than in innervated adult muscle fibres, they indicate either regeneration or

physiological denervation. The same holds for the down-regulation of ClC-1 mRNAs. These findings also support the evidence of regenerating muscle fibres in ongoing atrophying muscle of wasted mice, as described above.

6.4 A potential role of Akt in muscle of wasted mice

The molecular mechanisms of muscle atrophy in human are poorly understood. A recent study showed that at the protein level ALS patients had a 68% lower content of the active phosphorylated Akt protein, and SOD^{G93A} transgenic mice also had a reduction in the active Akt protein content (Léger *et al.*, 2006). These findings contrast with the data I have found in muscle of wasted mice. Muscle of wasted mice shows a significant increase in Akt and phosphorylated Akt proteins as demonstrated by western blot analysis. There are several signaling proteins that can act as upstream regulators of translational mechanisms that have been associated with the decreased protein synthesis rate caused by muscle atrophy. The protein kinase Akt has been shown to have growth-promoting effects in muscle, and it is a known upstream activator of protein synthesis (Rommel *et al.*, 2001; Takahashi *et al.*, 2002). Proteins downstream of Akt that are involved in regulating protein synthesis are mTOR and p70S6 kinase (Nader *et al.*, 2002). One report has shown that overexpression of Akt attenuates denervation-induced atrophy in rodents by 70% (Bodine *et al.*, 2001). Muscle unloading is also associated with a decrease in both mTOR (Reynolds *et al.*, 2002) and p70S6 kinase phosphorylation (Bodine *et al.*, 2001; Hornberger et al., 2001), which is consistent with the decreased translation rate. Upon stimulation by hormones or growth factors, Akt phosphorylates target molecules that have been implicated in glucose metabolism, proliferation, and cell survival (Lawlor and Alessi 2001; Whiteman *et al.*, 2002). A recent study has shown that eEF1A is a potential binding partner in a protein complex with Akt2 (Lau *et al.*, 2006). Three isoforms of Akt have been characterized in mammals, with Akt2 being expressed particularly in insulin responsive tissues, including fat, muscle, and liver (Altomare *et al.*, 1995). The interaction of Akt2 and

eEF1A may have implications in cytoskeletal regulation. A role eEF1A in regulation of cytoskeletal dynamics, directing protein synthesis to sites of cell activity, has been postulated (Liu *et al.*, 2002). Association of Akt with eEF1A may be important in directing it to particular regions of the cell. Elevations in Akt in muscle of wasted mice, which lack both eEF1A1 and eEF1A2, may reflect compensatory changes occurring in muscle in response to denervation, potentially in an attempt to maintain muscle mass and protein synthesis or alternately, promote cell survival. Figure 6-1 shows an Akt signalling network during hypertrophy and atrophy.

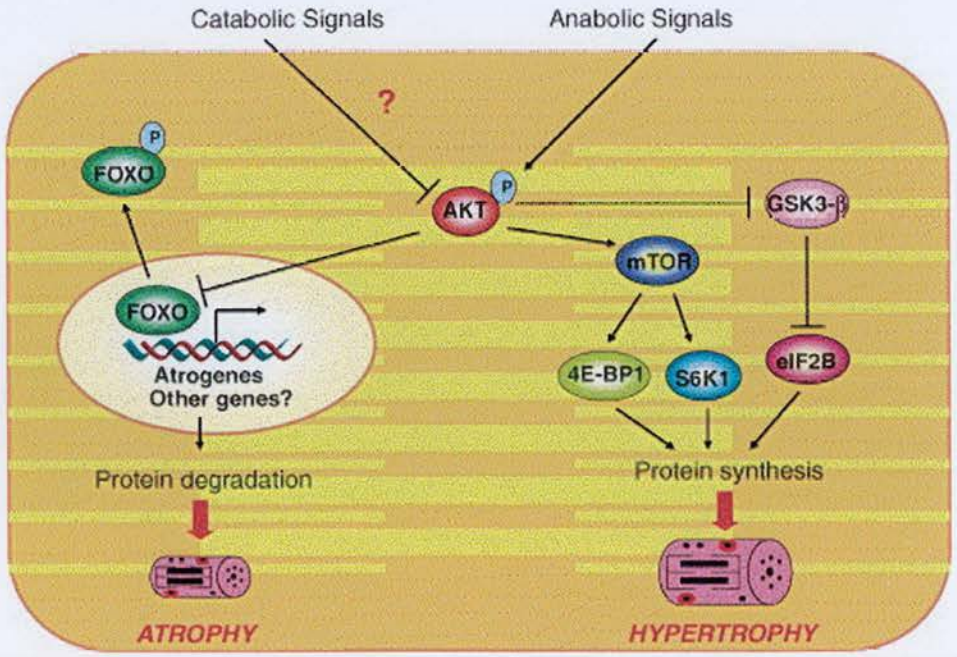

Figure 6-1 Akt signalling network during hypertrophy and atrophy. Akt lies at the centre of a network in which its activation regulates the protein synthetic machinery and its inactivation allows the expression of possibly atrophy-associated genes (→ activation, —| inhibition). Reproduced from Nader (2005).

To address whether an increase in Akt and its phosphorylation proteins in skeletal muscle of wasted mice are operating to target imperative biological processes, further studies on relevant downstream targets will aid in an understanding of the role of Akt in progressively denervated muscle. These can be done by studying changes in PI3-K, mTOR, p70S6 kinase, or BAD. Additional support for the role of Akt and its downstream targets has been carried out in Sprague-Dawley rats and C57BL/6 mice, showing that genetic activation of the Akt/mTOR pathway is sufficient to cause hypertrophy and prevent atrophy *in vivo*, whereas genetic blockade of this pathway blocks hypertrophy *in vivo* (Bodine *et al.*, 2001). Recently, eEF1A2 has been shown to activate Akt in a PI3-K-dependent fashion (Amiri *et al.*, 2006).

6.5 Distribution of eEF1A2 and its colocalisation with SMN in HeLa cells

The eEF1A protein is mainly present in the cytoplasm of cells. Nuclear localization of eEF1A has been identified in some studies (Colling *et al.*, 1994; Janssen *et al.*, 1994; Barberse *et al.*, 1995; Billaut-Mulot *et al.*, 1996; Sandres *et al.*, 1996). However, two recent reports have been unable to show nuclear localization of eEF1A (Calado *et al.*, 2002; Bohnsack *et al.*, 2002). The reasons for these opposite findings might be differences in cell culture conditions. In this thesis, I have demonstrated that upon serum or EGF stimulation, a small proportion of eEF1A2 molecules redistribute from cytoplasm to the nucleus of previously serum-starved HeLa cells. Intranuclear eEF1A2 may be involved in nuclear translation. This finding supports the earlier study (Iborra *et al.*, 2001) that has demonstrated 10-15% of cellular protein synthesis occur in the nucleus.

There is some indirect evidence implying that eEF1A may be part of the so-called SMN complex (Gangwani *et al.*, 1998; Gangwani *et al.*, 2001; Charroux *et al.*, 2000). Similarity in NMJ abnormalities between wasted and *Smn* mutant mice has been shown

in this thesis, suggesting that there might be a pathogenic process in common. One hallmark of SMA is the failure of SMN to localize within the nuclear bodies (Gangwani *et al.*, 2001). By using a transfection study and quantitative immunocolocalisation, the result in this thesis suggests that a proportion of cytoplasmic eEF1A2 colocalises with SMN. This finding supports the result of immunoprecipitation with anti-SMN antibodies that often pull down a 50-kD band similar to that of eEF1A (Charroux *et al.*, 2000).

The ICA-ICQ costaining analysis is a key element of this study. It was used for the first time to study colocalization of syntaxin 1, $G\alpha_o$, and N-type calcium channel complex at a presynaptic nerve terminal (Li *et al.*, 2004). This technique is distinguished from the usual dye-overlap method by its focus on the variations in protein concentrations across the cell and not simply their locations. Perhaps the worst limitation of the dye-overlap method is that when one protein target is distributed across most, or all, of the cell, a second protein will be identified as colocalised even when its distribution is totally random with respect to the first. The ICA method avoids this mistake because if a randomly distributed protein overlaps with a broadly staining one, it will not be reported as associated because it does not vary in synchrony. The ICQ in this method serves as a statistically testable, single-value assessment of the relationship between the stained protein pairs. The ICA-ICQ analysis represents a powerful complement to standard immunoprecipitation (IP) tests for analysis of protein complexes (Li *et al.*, 2004). The strength of the IP approach lies in identifying proteins bound in high-affinity complexes. However, it has disadvantages in missing any low-affinity associations because of the necessary washing steps, and in the requirement for solubilization of the tissue, which effectively eliminates virtually all clues not only to the location of the complex within the cell, but even from which cell or tissue type the complex originates. ICA-ICQ analysis, on the other hand, has advantages in identifying potential low-affinity protein complexes and in retaining information on the cellular and subcellular location. Its limitation is an inability to resolve colocalisation of two proteins that are components of a small organelle, which might be a cause of the poor staining intensity relation that is found when analyzing colocalisation of myc-tagged eEF1A2 and SMN in the nucleus.

6.6 Wasted mice expressing human eEF1A2 in skeletal muscle

Here, I report the creation of a transgenic mouse model, by the expression of human eEF1A2 under transcriptional control of the human α-skeletal actin promoter, that has the potential to be used as a model for studying pathogenesis of motor neurone degeneration, or even motor neuropathy, all of which resulting in denervation of muscle. The HSA promoter was chosen since it is transcribed specifically in skeletal muscle (Muscat and Kedes, 1987). The promoter is well characterized and the 2.2-kb fragment used contains all necessary elements for selective expression in skeletal muscle (Brennan and Hardeman, 1993). During development, α-cardiac actin is the predominant isoform of sarcomeric α-actin (Grunning *et al.*, 1987), and it is only post-partum that there is a switch to α-skeletal actin (Brennan and Hardeman, 1993). Thus, by using the HSA promoter, any possibility that embryonic expression of eEF1A2 might interfere with development was minimized.

Investigations of the HSA-EEF1A2 transgenic homozygous wasted mice support the hypothesis that loss of eEF1A2 in neurons, but not in muscle, of wasted mice leads to development of muscle atrophy. Although the primary screen I used to assess mouse phenotype is not the full screening battery, but only covers the sensorimotor category, it gives enough information to determine abnormalities and distinguish the transgenic mice from non-transgenic wild-type controls. The results can also be used as a useful body of data by which one can reproducibly assess the effect of a genetic manipulation or strain variation. Evaluation at the younger age will give some more useful information that might be used to follow-up the mice and distinguish between groups. In this thesis, transgenic mice, non-transgenic wasted controls, and non-transgenic wild-type controls were assessed at 25 days, and the results shows that the transgenic wasted mice are indistinguishable from the non-transgenic wasted group. An additional method for assessment of motor function was used. This method has been used to assess motor function in the hind limbs of *SOD1*^{G93A} *Vegfa* transgenic mice (Lambrechts *et al.*, 2003).

The neurological scores show no significant differences between the transgenic and non-transgenic wasted mice, suggesting that the presence of eEF1A2 in muscle of wasted mice does not modify the deteriorated motor function. Because of the limited availability of wasted mice carrying the transgene, I could not analyze whether there is difference in survival rate between the transgenic and spontaneous wasted mice.

The presence of the transgene results in high expression of human eEF1A2 protein in skeletal muscle of transgenic wasted mice. Although the efficacy of HSA promoter to drive gene expression was confirmed (Brenna and Hardeman, 1993), this does not guarantee that the expressed protein is functional. One possibility that the HSA-EEF1A2 transgenic wasted mice have no phenotypic differences, both physically and histologically, is that the expressed eEF1A2 protein in muscle is non-functional. It is difficult to verify whether the expressed eEF1A2 protein is functional since the methods have not yet been well developed. The easiest, but indirect and time-consuming, method is to perform primary muscle cell culture and study the protective role of eEF1A2 against caspase-3-mediated apoptosis (Ruest *et al.*, 2002). eEF1A2 was shown to protect cultured differentiated myotubes from apoptosis by delaying their death, which suggests a prosurvival function for eEF1A2 in skeletal muscle. Its protective function is the first noncanonical function associated with the protein. However, this method has not yet been carried out *in vivo*. It will also be interesting to study *in vivo* the expression and effect of eEF1A2 in skeletal muscle during aging and determine whether the loss of eEF1A2 may expedite the age-dependent myofibre decline in skeletal muscle. However, the findings of high levels of the expression and no mutation found from the sequencing results suggest that the expressed eEF1A2 protein should be functional.

As in spontaneous wasted mice, muscle pathology of transgenic wasted mice shows abnormalities compatible with denervation, which include grouped small angular muscle fibres in the background of generalized small fibres. However, it cannot be clearly stated whether these findings are more like those found in ALS or SMA, as grouped muscle fibre atrophy and small angular atrophic fibres can be found in both diseases. The

grouped atrophic pattern found in wasted mice is rather scattered and not as marked as that found in ALS and SMA. Hypertrophic muscle fibres, which can be found in SMA, are not observed in wasted mice. Internal nuclei found in wasted mice are found in some cases of SMA, however, in SMA this finding is more prominent. Increased internal nuclei is also a typical finding in muscle diseases, however, most of the fibres are large. It should be noted that in normal human skeletal muscle, as many as 3% of the myofibres can have internal nuclei (Carpenter and Karpati., 2001; Eagel and Franzini-Armstrong, 1994).

Transgenic wasted mice also show a physical feature, like that found in spontaneous wasted animals, to which the term "tremor" is assigned. In neurological terminology, tremor is a rhythmic oscillatory, non-purposeful movement of a body part produced by regular or sequential contractions of opposing muscles. Its pathogenesis is believed to result from dysfunction of basal ganglia. However, pathological abnormalities in basal ganglia of wasted mice have not been identified. Intention tremor observed at the neck of wasted mice may result from dysfunction of the cerebellar pathway. Body tremor in wasted mice, however, could be referred to the term "fasciculation", or physiologically, "fibrillation". Fibrillation activity, the spontaneous incoordinate activity of muscle, is often found in denervated muscle. This can be easily confirmed by electromyography (EMG). In human, it is one of the most classic and easily detectable signs of muscle denervation (Midrio 2006). Fasciculation or fibrillation is a characteristic clinical feature of ALS. Its presence indicates active denervation. Recently, based on the results obtained with *in vitro* myogenesis, it was proposed that fibrillation is related to the autocrine activation of AchRs in muscle membrane (Bandi *et al.*, 2005).

Upregulation of AchRα1 and myogenin, and downregulation of ClC-1 mRNAs are also demonstrated in HSA-EEF1A2 transgenic wasted mice, like those found in non-transgenic wasted mice. These patterns of gene expression are compatible with denervation. It is widely accepted that nicotinic AchRs play an important role during myogenesis. Increased expression of AchRα1 not only supports the presence of muscle

denervation in wasted mice, it probably also supports the findings of centralized nuclei and increased SDH staining, suggesting that muscle regeneration takes place in ongoing denervated muscle in wasted mice.

The major aim of this thesis is to study the role of eEF1A2 in pathogenesis of motor neurone disease in wasted mice. I have reported here that the loss of eEF1A2 in neurones, but not in muscle, leads to denervation of muscle in wasted mice, suggesting a specific role in neurons. Although eEF1A1 and eEF1A2 proteins share similar features such as molecular weight of about 50 kD, transcript length 1.8-1.9 kb, and 92.4% amino acid sequence similarity (Knudsen *et al.*, 1993), the function of eEF1A2 is still elusive, and why two isoforms exist has never been understood. In light of the results obtained with this thesis, eEF1A2 might have some unidentified, but specific roles in regulation of survival of motor neurone. It has been shown in skeletal muscle that eEF1A2 has a prosurvival function against caspase-3-mediated apoptosis (Ruest *et al.*, 2002). Caspase-1 and caspase-3 have been shown to be activated in motor neurone death in SOD1 mutant mice (Pasinelli *et al.*, 2000). It is possible that eEF1A2 also plays a protective role in neurone via the caspase pathway.

6.7 Future work

6.7.1 Characterization of wasted mice

I have reported here some characterization of wasted mice, mainly on muscle pathology, neuromuscular abnormalities, and patterns of gene expression in muscle. The findings point to the cause of muscle atrophy as denervation, or more specifically, degeneration of motor axons. From a clinical point of view, it would be more useful if more studies could be conducted to narrow down whether wasted mice could be a model for which forms of human motor neurone degeneration, and even to confirm the results presented in this thesis. ATPase staining can be used to investigate fibre type grouping. Finding of

fibre type grouping indicates chronic denervation with reinnervation or collateral sprouting. It is also helpful in identifying primary myopathy that may exist in muscle of wasted mice as eEF1A2 is known to be specifically expressed in muscle. Increased SDH staining as found in wasted mice may indicate mitochondrial diseases, in addition to regenerating muscle fibres. Other staining used for studying mitochondrial disorders such as cytochrome oxidase and NADH-TR staining would be useful since altered mitochondrial function has recently been found in skeletal muscle in ALS patients (Echaniz-Laguna *et al.*, 2006).

I have demonstrated in HeLa cell transfection assays that eEF1A2 partially colocalizes with SMN in the cytoplasm. Skeletal muscle has been reported as another tissue targeted by the *Smn* defect, leading to destabilization the sarcolemma as determined by marked reduction of dystrophin expression and upregulation of utrophin (Cifuentes-Diaz *et al.*, 2001). Both proteins represent key components of skeletal muscle fibres linking the F-actin cytoskeleton to the extracellular matrix. Therefore, an *Smn* defect directed to either neurons or skeletal muscle cell leads to destabilization of cytoskeletal components or interacting proteins in targeted tissues. eEF1A1, but not eEF1A2, is known to interact with actin and microtubules, which are components of the cytoskeleton (Liu *et al.*, 2002; Shiina *et al.*, 1994; Yang *et al.*, 1990). It is possible that in skeletal muscle cells, eEF1A2 and SMN may interact via an unidentified pathway. It will be interesting to investigate expression of dystrophin and utrophin, using immunostaining and western blot analysis, in muscle of wasted mice and normal controls. The results will give additional information on the role of eEF1A2.

I have shown here that muscle of wasted mice show an increase in Akt and phosphorylated Akt proteins. eEF1A contains a minimal Akt2 phosphorylation motif RXRXXT (residues 67-72) and is therefore a potential Akt2 substrate. Loss of eEF1A2 in wasted mice thus may induce upregulation of Akt. It is possible that eEF1A interacts with Akt2 through a complex with β-tubulin (Lau *et al.*, 2006). However, whether Akt2 interacts directly with eEF1A or β-tubulin remains a question to be addressed.

6.7.2 eEF1A2 and its roles in motor neurons and muscle

Cell death pathways differ in several mouse models with motor neurone degeneration. The analysis of gene expression alterations in motor neurons provides one means of studying their specific vulnerability. With the development in technology for isolating individual cells using laser capture microdissection, it has been possible to analyze molecular changes in one particular cell type such as muscle cell or neuronal cell. Furthermore, gene expression profiling of mRNA from these cells has become possible by the use of microarray and quantitative real-time RT-PCR. The combined use of these technologies in investigating muscle cell or neuronal cells of spontaneous wasted mice, HSA-EEF1A2 transgenic wasted mice, and control animals could be a further tool to investigate specific cell death in particular cell types, that link to a role of eEF1A2.

A prosurvival function for eEF1A2 has been demonstrated in skeletal muscle (Ruest *et al.*, 2002). A switch between two peptide eEF1A isoforms has been shown in cultured differentiated myotubes (Ruest *et al.*, 2002), as well as in tissue during development (Khalyfa *et al.*, 2001). This switch from eEF1A1 to eEF1A2 may confer to the long lived, terminally differentiated myotubes a translation elongation factor, which also prevents accidental cell death from occurring. It will be interesting to see whether this protective function of eEF1A2 behaves in neurons in the manner that is similar to its behaviour in skeletal muscle.

To study the relative roles of eEF1A2 in muscle and neurons, I have already generated transgenic mice specifically expressing eEF1A2 in muscle. Although I have found that the presence of eEF1A2 in muscle, but not in neurons, does not modify phenotypes of wasted mice, the roles of eEF1A2 in muscle have not yet been studied. In order to evaluate the phenotype that results from loss of eEF1A2 in muscle, but not in neurons, generating transgenic wasted mice which specifically express eEF1A2 in neurons will be another useful mouse model. The transgenic mice can be produced by using neuron-

specific promoter such as rat neuron-specific enolase (NSE) promoter to drive expression of eEF1A2 in neurons.

References

Abbott, C M, *et al.* (1986). Deficiency of adenosine deaminase in the wasted mouse. *Proceedings of the National Academy of Sciences* **83**: 693-695.

Abbott, C M and Proud, C G (2004). Translation factors: in sickness and in health. *Trends in Biochemical Sciences* **29**: 25-31.

Adams, L, *et al.* (1995). Adaptation of nicotinic acetylcholine receptor, myogenin, and MRF4 gene expression to long-term muscle denervation. *The Journal of Cell Biology* **131**: 1341-1349.

Adams, R D and Victor, M (1993). Principles of Neurology. 5th Edition. McGraw-Hill Inc, New York, NY

Al-Chalabi, A, *et al.* (1998). Recessive amyotrophic lateral sclerosis families with the D90A SOD1 mutation share a common founder: evidence for a linked protective factor. *Human Molecular Genetics* **7**: 2045-2050.

Al-Chalabi, A, *et al.* (1999). Deletions of the heavy neurofilament subunit tail in amyotrophic lateral sclerosis. *Human Molecular Genetics* **8**: 157-164.

Al-Chalabi, A, *et al.* (1996). Association of apolipoprotein E epsilon 4 allele with bulbar-onset motor neuron disease. *Lancet* **347**: 159-160.

Allen, D L, *et al.* (1997). Apoptosis: a mechanism contributing to remodeling of skeletal muscle in response to hindlimb unweighting. *American Journal of Physiology* **273**: C579-C587.

Al-Maghrebi, M, Cojocel, C and Thompson M S (2005). Regulation of elongation factor-1 expression by vitamin E in diabetic rat kidneys. *Molecular and Cellular Biochemistry* **273**: 177-183.

Altomare, D A, *et al.* (1995). Cloning chromosomal localization and expression analysis of the mouse Akt2 oncogene. *Oncogene* **11**: 55-60.

Amiri, A, *et al.* (2006). eEF1A2 activates Akt and stimulates Akt-dependent actin remodeling, invasion and migration. *Oncogene* Nov 20; [Epub ahead of print]

Anand, N, *et al.* (2002). Protein elongation factor EEF1A2 is a putative oncogene in ovarian cancer. *Nature Genetics* **31**: 301-305.

Andersen, G R, *et al.* (2000). Structural basis for nucleotide exchange and competition with tRNA in the yeast elongation factor complex eEF1A:eEF1Balpha. *Molecular Cell* **6**: 1261-1266.

Andersen, P M, *et al.* (1997). Phenotypic heterogeneity in motor neuron disease patients with CuZn-superoxide dismutase mutations in Scandinavia. *Brain* **120**: 1723-1737.

Ann, D K, *et al.* (1991). Isolation and characterization of the rat chromosomal gene for a polypeptide (pS1) antigenically related to statin. *The Journal of Biological Chemistry* **266**: 10429-10437.

Anthony-Cahill, S J, *et al.* (1992). Molecular characterization of helix-loop-helix peptides. *Science* **255**: 979-983.

Aoki, M, *et al.* (1998). Mutations in the glutamate transporter EAAT2 gene do not cause abnormal EAAT2 transcripts in amyotrophic lateral sclerosis. *Annals of Neurology* **43**: 645-653.

Azzouz, M, *et al.* (2000). Prevention of mutant SOD1 motoneuron degeneration by copper chelators in vitro. *Journal of Neurobiology* **42**: 49-55.

Bandi, E, *et al.* (2005). Autocrine activation of nicotinic acetylcholine receptor contributes Ca^{2+} spikes in mouse myotubes during myogenesis. *Journal of Physiology* **568**: 171-180.

Barbarese, E, *et al.* (1995). Protein translation components are colocalized in granules in oligodendrocytes. *Journal of Cell Sciences* **108**: 2781-2790.

Beal, M F (2000). Energetics in the pathogenesis of neurodegenerative diseases. *Trends in Neuroscience* **23**: 298-304.

Beal, M F, *et al.* (1997). Increased 3-nitrotyrosine in both sporadic and familial amyotrophic lateral sclerosis. *Annals of Neurology* **42**: 644-654.

Beaulieu, J M and Julien, J P (2003). Peripherin-mediated death of motor neurons rescued by overexpression of neurofilament NF-H proteins. *Journal of Neurochemistry* **85**: 248-256.

Beaulieu, J M, Nguyen, M D and Julien, J P (1999a). Late onset death of motor neurons in mice overexpressing wild-type peripherin. *Journal of Cell Biology* **147**: 531-544.

Beaulieu, J M, *et al.* (1999b). Interactions between peripherin and neurofilaments in cultured cells: disruption of peripherin assembly by the NF-M and NF-H subunits. *Biochemistry and Cell Biology* **77**: 41-45.

Bec, G, *et al.* (1989). Valyl-tRNA synthetase from rabbit liver. I. Purification as a heterotypic complex in association with elongation factor 1. *The Journal of Biological Chemistry* **264**: 21131-21137.

Bertelli, D F, *et al.* (2003). Reversal of denervation-induced insulin resistance by SHIP2 protein synthesis blockade. *American Journal of Physiology, Endocrinology, and Metabolism* **284**: E679-687.

Bertrandy, S, *et al.* (1999). The RNA-binding properties of SMN: deletion analysis of the zebrafish orthologue defines domains conserved in evolution. *Human Molecular Genetics* **8**: 775-782.

Billaut-Mulot, O, *et al.* (1996). Trypanosoma cruzi elongation factor 1-alpha: nuclear localization in parasites undergoing apoptosis. *Gene* **174**: 19-26.

Bischoff, C, *et al.* (2000). The human elongation factor 1 A-2 gene (EEF1A2): complete sequence and characterization of gene structure and promoter activity. *Genomics* **68**: 63-70.

Blachly-Dyson, E, *et al.* (1993). Cloning and functional expression in yeast of two human isoforms of the outer mitochondrial membrane channel, the voltage-dependent anion channel. *The Journal of Biological Chemistry* **268**: 1835-1841.

Black, B L and Olson, E N (1998). Transcriptional control of muscle development by myocyte enhancer factor-2 (MEF2) proteins. *Annual Review of Cell and Developmental Biology* **14**: 167-196.

Blackwell, J L and Brinton, M A (1997). Translation elongation factor-1 alpha interacts with the 3' stem-loop region of West Nile virus genomic RNA. *Journal of Virology* **71**: 6433-6444.

Bodine, S C, *et al.* (2001). Identification of ubiquitin ligases required for skeletal muscle atrophy. *Science* **294**: 1704-1708.

Bodine, S C, *et al.* (2001). Akt/mTOR pathway is a crucial regulator of skeletal muscle atrophy and can prevent muscle strophy in ivvo. *Nature Cell Biology* **3**: 1014-1019.

Bohnsack, M T, *et al.* (2002). Exp5 exports eEF1A via tRNA from nuclei and synthesizes with other transport pathways to confine translation to the cytoplasm. *The EMBO Journal* **21**: 6202-6215.

Bonne, G, *et al.* (1993). Expression of human cytochrome c oxidase subunits during fetal development. *European Journal of Biochemistry* **217**: 1099-1107.

Borthwick, G M, *et al.* (1999). Mitochondrial enzyme activity in amyotrophic lateral sclerosis: implications for the role of mitochondria in neuronal cell death. *Annals of Neurology* **46**: 787-790.

Borisov, A B, Dedkov, E I and Carlson, B M (2001). Interrelations of myogenic response, progressive atrophy of muscle fibers and cell death in denervated skeletal muscle. *Anatomical Records* **264**: 203-218.

Brahe, C (2000). Copies of the survival motor neuron gene in spinal muscular atrophy: the more, the better. *Neuromuscular Disorders* **10**: 274-275.

Brands, J H, *et al.* (1986). The primary structure of the alpha subunit of human elongation factor 1. Structural aspects of guanine-nucleotide-binding sites. *European Journal of Biochemistry* **155**: 167-171.

Braun, T, *et al.* (1989). A novel human muscle factor related to but distinct from MyoD1 induces myogenic conversion in 10T1/2 fibroblasts. *EMBO Journal* **8**: 701-709.

Brennan, K J and Hardeman, E C (1993). Quantitative analysis of the human α-skeletal actin gene in transgenic mice. *Journal of Biological Chemistry* **268**: 719-725.

Brennan, T J, *et al.* (1991). Mutagenesis of the myogenin basic region identifies an ancient protein motif critical for activation of myogenesis. *Proceedings of the National Academy of Sciences* **88**: 5675-5679.

Brennan, T J and Olson, E N (1990). Myogenin resides in the nucleus and acquires high affinity for a conserved enhancer element on heterodimerization. *Genes and Development* **4**: 582-595.

Bristol, L A and Rothstein, J D (1996). Glutamate transporter gene expression in amyotrophic lateral sclerosis motor cortex. *Annals of Neurology* **39**: 676-679.

Bruijn, L I, *et al.* (1997). ALS-linked SOD1 mutant G85R mediates damage to astrocytes and promotes rapidly progressive disease with SOD1-containing inclusions. *Neuron* **18**: 327-338.

Brzustowicz, L M, *et al.* (1990). Genetic mapping of chronic childhood-onset spinal muscular atrophy to chromosome 5q11.2-13.3. *Nature* **344**: 540-541.

Buckingham, M (1992). Making muscle in mammals. *Trends in Genetics* **8**: 144-148.

Burglen, L, *et al.* (1997). The gene encoding p44, a subunit of the transcription factor TFIIH, is involved in large-scale deletions associated with Werdnig-Hoffmann disease. *American Journal of Human Genetics* **60**: 72-79.

Burlet, P, *et al.* (1998). The distribution of SMN protein complex in human fetal tissues and its alteration in spinal muscular atrophy. *Human Molecular Genetics* **7**: 1927-1933.

Calado, A, *et al.* (2002). Exportin-5-mediates nuclear export of eukaryotic elongation factor 1A and tRNA. *The EMBO journal* **21**: 6216-6224.

Campbell, L, *et al.* (2000). Direct interaction of Smn with dp103, a putative RNA helicase: a role for Smn in transcription regulation? *Human Molecular Genetics* **9**: 1093-1100.

Campbell, L, *et al.* (1997). Genomic variation and gene conversion in spinal muscular atrophy: implications for disease process and clinical phenotype. *American Journal of Human Genetics* **61**: 40-50.

Carmeliet, P (2000). Mechanisms of angiogenesis and arteriogenesis. *Nature Medicine* **6**: 389-395.

Carpenter, S and Karpati G (2001). Pathology of Skeletal Muscle. 2nd Edition. Oxford University Press, New York, NY

Carr-Schmid, A, *et al.* (1999). Mutations in a GTP-binding motif of eukaryotic elongation factor 1A reduce both translational fidelity and the requirement for nucleotide exchange. *The Journal of Biological Chemistry* **274**: 30297-30302.

Carter, T A, *et al.* (1997). A multicopy transcription-repair gene, BTF2p44, maps to the SMA region and demonstrates SMA associated deletions. *Human Molecular Genetics* **6**: 229-236.

Carvalho, T, *et al.* (1999). The spinal muscular atrophy disease gene product, SMN: A link between snRNP biogenesis and the Cajal (coiled) body. *Journal of Cell Biology* **147**: 715-728.

Chambers, D M, Peters, J and Abbott, C M (1998). The lethal mutation of the mouse wasted (wst) is a deletion that abolishes expression of a tissue-specific isoform of translation elongation factor 1alpha, encoded by the Eef1a2 gene. *Proceedings of the National Academy of Sciences* **95**: 4463-4468.

Chance, P F, *et al.* (1998). Linkage of the gene for an autosomal dominant form of juvenile amyotrophic lateral sclerosis to chromosome 9q34. *American Journal of Human Genetics* **63**: 633-640.

Charroux, B, *et al.* (1999). Gemin3: A novel DEAD box protein that interacts with SMN, the spinal muscular atrophy gene product, and is a component of gems. *Journal of Cell Biology* **147**: 1181-1194.

Charroux, B, *et al.* (2000). Gemin4. A novel component of the SMN complex that is found in both gems and nucleoli. *Journal of Cell Biology* **148**: 1177-1186.

Chen, W, *et al.* (2006). Lack of association of VEGF promoter polymorphisms with sporadic ALS. *Neurology* **67**: 508-510.

Chou, S M, *et al.* (1998). Advanced glycation endproducts in neurofilament conglomeration of motoneurons in familial and sporadic amyotrophic lateral sclerosis. *Molecular Medicine* **4**: 324-332.

Cifuentes-Diaz, C, *et al.* (2001). Deletion of murine SMN exon 7 directed to skeletal muscle leads to severe muscular dystrophy. *Journal of Cell Biology* **152**: 1107-1114.

Cifuentes-Diaz, C, *et al.* (2002). Neurofilament accumulation at the motor endplate and lack of axonal sprouting in a spinal muscular atrophy mouse model. *Human Molecular Genetics* **11**: 1439-1447.

Clermont, O, *et al.* (1995). SMN gene deletions in adult-onset spinal muscular atrophy. *Lancet* **346**: 1712-1713.

Cole, N and Siddique, T (1999). Genetic disorders of motor neurons. *Seminars in Neurology* **19**: 407-408.

Coleman, M P and Perry, V H (2002). Axon pathology in neurological disease: a neglected therapeutic target. *Trends in Neuroscience* **25**: 532-537.

Collings, D A, *et al.* (1994). Elongation factor 1 alpha is a component of the subcortical actin bundles of characean algae. *Cell Biology International* **18**: 1019-1024.

Comi, G P, *et al.* (1998). Cytochrome c oxidase subunit I microdeletion in a patient with motor neuron disease. *Annals of Neurology* **43**: 110-116.

Condeelis, J (1995). Elongation factor 1 alpha, translation and the cytoskeleton. *Trends in Biochemical Science* **20**: 169-170.

Coovert, D D, *et al.* (1997). The survival motor neuron protein in spinal muscular atrophy. *Human Molecular Genetics* **6**: 1205-1214.

Coovert, D D, *et al.* (2000). Does the survival motor neuron protein (SMN) interact with Bcl-2? *Journal of Medical Genetics* **37**: 536-539.

Corbo, M and Hays, A P (1992). Peripherin and neurofilament protein coexist in spinal spheroids of motor neuron disease. *Journal of Neuropathology and Experimental Neurology* **51**: 531-537.

Corcia, P, *et al.* (2002). Abnormal SMN1 gene copy number is a susceptibility factor for amyotrophic lateral sclerosis. *Annals of Neurology* **51**: 243-246.

Corson, L B, *et al.* (1998). Chaperone-facilitated copper binding is a property common to several classes of familial amyotrophic lateral sclerosis-linked superoxide dismutase mutants. *Proceedings of the National Academy of Sciences* **95**: 6361-6366.

Couillard-Despres, S, *et al.* (1998). Protective effect of neurofilament heavy gene overexpression in motor neuron disease induced by mutant superoxide dismutase. *Proceedings of the National Academy of Sciences* **95**: 9626-9630.

Covault, J, *et al.* (1986). Molecular forms of N-CAM and its RNA in developing and denervated skeletal muscle. *Journal of Cell Biology* **102**: 731-739.

Crawford, G E, *et al.* (2000). Assembly of the dystrophin-associated protein complex does not require the dystrophin COOH-terminal domain. *The Journal of Cell Biology* **150**: 1399-1409.

Crow, J P, *et al.* (1997). Decreased zinc affinity of amyotrophic lateral sclerosis-associated superoxide dismutase mutants leads to enhanced catalysis of tyrosine nitration by peroxynitrite. *Journal of Neurochemistry* **69**: 1936-1944.

Cserjesi, P, *et al.* (1992). MHox: a mesodermally restricted homeodomain protein that binds an essential site in the muscle creatine kinase enhancer. *Development* **115**: 1087-1101.

Cudkowicz, M E, et al. (1998). Limited corticospinal tract involvement in amyotrophic lateral sclerosis subjects with the A4V mutation in the copper/zinc superoxide dismutase gene. *Annals of Neurology* **43**: 703-710.

Dal Canto, M C and Gurney, M E (1994). Development of central nervous system pathology in a murine transgenic model of human amyotrophic lateral sclerosis. *American Journal of Pathology* **145**: 1271-1279.

Das, T, *et al.* (1998). RNA polymerase of vesicular stomatitis virus specifically associates with translation elongation factor-1 alphabetagamma for its activity. *Proceedings of the National Academy of Sciences* **95**: 1449-1454.

Datta, S R, *et al.* (1997). Akt phosphorylation of BAD couples survival signals to the cell-intrinsic death machinary. *Cell* **91**: 231-241.

Davies, K E, *et al.* (1991). Molecular studies of spinal muscular atrophy. *Neuromuscular Disorders* **1**: 83-85.

Davis, R L, *et al.* (1990). The MyoD DNA binding domain contains a recognition code for muscle-specific gene activation. *Cell* **60**: 733-746.

de Belleroche, J, *et al.* (1995). Familial amyotrophic lateral sclerosis/motor neurone disease (FALS): a review of current developments. *Journal of Medical Genetics* **32**: 841-847.

Deckwerth, T L and Johnson, E M Jr (1994). Neurites can remain viable after destruction of the neuronal soma by programmed cell death (apoptosis). *Developmental Biology* **165**: 63-72.

Dedkov, E I, *et al.* (2001). Reparative myogenesis in long-term denervated skeletal muscles of adult rats results in a reduction of the satellite cell population. *Anatomical Records* **103**: 565-574.

Dharmawardhane, S, *et al.* (1991). Compartmentalization and actin binding properties of ABP-50: the elongation factor-1 alpha of Dictyostelium. *Cell Motility and Cytoskeleton* **20**: 279-288.

Dhavan, R and Tsai, L H (2001). A decade of CDK5. *Nature Reviews Molecular Cell Biology* **2**: 749-759.

DiDonato, C J, *et al.* (1997). Deletion and conversion in spinal muscular atrophy patients: is there a relationship to severity? *Annals of Neurology* **41**: 230-237.

Dubowitz, V (1991). Chaos in classification of the spinal muscular atrophies of childhood. *Neuromuscular Disorders* **1**: 77-80.

Duguez, S, et al. (2002). Miochondrial biogenesis during skeletal muscle regeneration. *American Journal of Physiology, Endocrinology and Metabolism* **282**: E802-E809.

Dupuis, L, et al. (2003). Up-regulation of mitochondrial uncoupling protein 3 reveals an early muscular metabolic defect in amyotrophic lateral sclerosis. *The FASEB Journal* 17: 2091-2093.

Echaniz-Laguna, A, *et al.* (2006). Muscular mitochondrial function in amyotrophic lateral sclerosis is progressively altered as the disease develops: a temporal study in man. *Experimental Neurology* **198**: 25-30.

Edmonds, B T, *et al.* (1998). The effect of F-actin on the binding and hydrolysis of guanine nucleotide by Dictyostelium elongation factor 1A. *The Journal of Biological Chemistry* **273**: 10288-10295.

Edmonds, B T, *et al.* (1996). Elongation factor-1 alpha is an overexpressed actin binding protein in metastatic rat mammary adenocarcinoma. *Journal of Cell Science* **109**: 2705-2714.

Edmondson, D G, *et al.* (1992). Analysis of the myogenin promoter reveals an indirect pathway for positive autoregulation mediated by the muscle-specific enhancer factor MEF-2. *Molecular and Cellular Biology* **12**: 3665-3677.

Edmondson, D G and Olson, E N (1989). A gene with homology to the myc similarity region of MyoD1 is expressed during myogenesis and is sufficient to activate the muscle differentiation program. *Genes and Development* **3**: 628-640.

Eftimie, R, *et al.* (1991). Myogenin and MyoD join a family of skeletal muscle genes regulated by electrical activity. *Proceedings of the National Academy of Sciences* **88**: 1349-1353.

Emerson, C P (1990). Myogenesis and developmental control genes. *Current Opinion in Cell Biology* **2**: 1065-1075.

Engel, A G, and Franzini-Armstrong, C (1994). Myology: Basic and Clinical. McGraw-Hill Inc, New York, NY

Engel, W K (1970). Selective and nonselective susceptibility of muscle fiber types. A new approach to human neuromuscular diseases. *Archieve in Neurology* **22**: 97-117.

Engelhardt, J I and Appel, S H (1990). IgG reactivity in the spinal cord and motor cortex in amyotrophic lateral sclerosis. *Archives of Neurology* **47**: 1210-1216.

Engelhardt, J I, *et al.* (1997). Altered calcium homeostasis and ultrastructure in motoneurons of mice caused by passively transferred anti-motoneuronal IgG. *Journal of Neuropathology and Experimental Neurology* **56**: 21-39.

Engelhardt, J I, *et al.* (1993). Lymphocytic infiltrates in the spinal cord in amyotrophic lateral sclerosis. *Archives of Neurology* **50**: 30-36.

Esteban, J, *et al.* (1994). Identification of two novel mutations and a new polymorphism in the gene for Cu/Zn superoxide dismutase in patients with amyotrophic lateral sclerosis. *Human Molecular Genetics* **3**: 997-998.

Estevez, A G, *et al.* (1999). Induction of nitric oxide-dependent apoptosis in motor neurons by zinc-deficient superoxide dismutase. *Science* **286**: 2498-2500.

Evans, S, *et al.* (1987). Muscle acetylcholine receptor biogenesis: regulation by transcript availability. *Journal of Biological Chemistry* **262**: 4911-4916.

Eyer, J, *et al.* (1998). Pathogenesis of two axonopathies does not require axonal neurofilaments. *Nature* **391**: 584-587.

Fan, L and Simard, L R (2002). Survival motor neuron (SMN) protein: role in neurite outgrowth and neuromuscular maturation during neuronal differentiation and development. *Human Molecular Genetics* **11**: 1605-1614.

Ferrante, R J, *et al.* (1997). Increased 3-nitrotyrosine and oxidative damage in mice with a human copper/zinc superoxide dismutase mutation. *Annals of Neurology* **42**: 326-334.

Fidzianska, A (1971). Ultrastructural changes in white and red muscle after denervation. *Acta Medicana Poland* **12**: 181-186.

Figlewicz, D A, *et al.* (1994a). Variants of the heavy neurofilament subunit are associated with the development of amyotrophic lateral sclerosis. *Human Molecular Genetics* **3**: 1757-1761.

Figlewicz, D A, *et al.* (1994b). Identification of flanking markers for the familial amyotrophic lateral sclerosis gene ALS1 on chromosome 21. *Journal of the Neurological Sciences* **124**: 90-5.

Finn, J T, *et al.* (2000). Evidence that Wallerlian degeneration and localized axon degeneration induced by local neurotrophin deprivation do not involve caspases. *Journal of Neuroscience* **20**: 1333-1341.

Fischer, R L, *et al.* (2004). Amyotrophic lateral sclerosis is a distal axonopathy: evidence in mice and man. *Experimental Neurology* **185**: 232-240.

Fischer, U, *et al.* (1997). The SMN-SIP1 complex has an essential role in spliceosomal snRNP biogenesis. *Cell* **90**: 1023-1029.

Flowers, J M, *et al.* (2001). Intron 7 retention and exon 9 skipping EAAT2 mRNA variants are not associated with amyotrophic lateral sclerosis. *Annals of Neurology* **49**: 643-649.

Frey, D, *et al.* (2000). Early and selective loss of neuromuscular synapse subtypes with low sprouting competence in motoneuron diseases. *Journal of Neuroscience* **20**: 2534-2542.

Freyssenet, D, Berthon, P and Denis, C (1996). Mitochondrial biogenesis in skeletal muscle in response to endurance exercises. *Archives of Physiology and Biochemistry* **104**: 129-141.

Frugier, T, *et al.* (2000). Nuclear targeting defect of SMN lacking the C-terminus in a mouse model of spinal muscular atrophy. *Human Molecular Genetics* **9**: 849-858.

Frydenberg, J, *et al.* (1991). Isolation and characterization of the gene encoding EF-1 alpha O, an elongation factor 1-alpha expressed during early development of Xenopus laevis. *Gene* **109**: 185-192.

Galcheva-Gargova, Z, *et al.* (1998). The cytoplasmic zinc finger protein ZPR1 accumulates in the nucleolus of proliferating cells. *Molecular Biology of Cell* **9**: 2963-2971.

Galcheva-Gargova, Z, *et al.* (1996). Binding of Zinc Finger Protein ZPR1 to the Epidermal Growth Factor Receptor. *Science* **272**: 1797-1802.

Gangwani, L, *et al.* (1998). Interaction of ZPR1 with translation elongation factor-1alpha in proliferating cells. *Journal of Cell Biology* **143**: 1471-1484.

Gangwani, L, *et al.* (2001). Spinal muscular atrophy disrupts the interaction of ZPR1 with the SMN protein. *Nature Cell Biology* **3**: 376-383.

Giesemann, T, *et al.* (1999). A role for polyproline motifs in the spinal muscular atrophy protein SMN. Profilins bind to and colocalize with smn in nuclear gems. *The Journal of Biological Chemistry* **274**: 37908-37914.

Goldowitz, D, *et al.* (1985). Longitudinal assessment of immunologic abnormalities of mice with the autosomal recessive mutation, "wasted". *Journal of Immunology* **135**: 1806-1812.

Gomes, M D, *et al.* (2001). Atrogin-1, a muscle-specific F-box protein highly expressed during muscle atrophy. *Proceedings of the National Academy of Sciences* **98**: 14440-14445.

Gonatas, N K, *et al.* (1998). The involvement of the Golgi apparatus in the pathogenesis of amyotrophic lateral sclerosis, Alzheimer's disease, and ricin intoxication. *Histochemistry and Cell Biology* **109**: 591-600.

Gonen, H, *et al.* (1994). Protein synthesis elongation factor EF-1 alpha is essential for ubiquitin-dependent degradation of certain N alpha-acetylated proteins and may be substituted for by the bacterial elongation factor EF-Tu. *Proceedings of the National Academy of Sciences* **91**: 7648-7652.

Grossman, L I and Shoubridge, E A (1996). Mitochondrial genetics and human disease. *Bioessays* **18**: 983-991.

Gubitz, A K, *et al.* (2002). Gemin5, a novel WD repeat protein component of the SMN complex that binds Sm proteins. *The Journal of Biological Chemistry* **277**: 5631-5636.

Gunning, P, *et al.* (1983). Isolation and characterzation of full-length cDNA clones for human α-, β-, and -actin mRNAs: skeletal but not cytoplasmic actins have as amino-terminal cysteine that is subsequently removed. *Molecular and Cellular Biology* **3**: 787-795.

Gunning, P and Hardeman E (1987). Differential patterns of transcript accumulation during human myogenesis. *Molecular and Cellular Biology* **7**: 4100-4114.

Gurney, M E, *et al.* (1994). Motor neuron degeneration in mice that express a human Cu,Zn superoxide dismutase mutation. *Science* **264**: 1772-1775.

Hadano, S, *et al.* (2001a). A gene encoding a putative GTPase regulator is mutated in familial amyotrophic lateral sclerosis 2. *Nature Genetics* **29**: 166-173.

Hadano, S, *et al.* (2001b). Cloning and characterization of three novel genes, ALS2CR1, ALS2CR2, and ALS2CR3, in the juvenile amyotrophic lateral sclerosis (ALS2) critical region at chromosome 2q33-q34: candidate genes for ALS2. *Genomics* **71**: 200-213.

Hahnen, E, *et al.* (1995). Molecular analysis of candidate genes on chromosome 5q13 in autosomal recessive spinal muscular atrophy: evidence of homozygous deletions of the SMN gene in unaffected individuals. *Human Molecular Genetics* **4**: 1927-1933.

Hand, C K, *et al.* (2002). A novel locus for familial amyotrophic lateral sclerosis, on chromosome 18q. *American Journal of Human Genetics* **70**: 251-256.

Hansen, S and Ballantyne, J P (1978). A quantitative electrophysiological study of motor neurone disease. *Journal of Neurology, Neurosurgery and Psychiatry* **41**: 773-783.

Hanzliková, V, Mackova, E V and Hník, P (1975). Satellite cells of the rata soleus muscle in the process of compensatory hypertrophy. *Cell and Tissue Research* **160**: 411-421.

Hatcher, J P, *et al.* (2001). Development of SHIRPA to characterise the phenotype of gene-targeted mice. *Behavioural Brain Research* 125: 261-273.

Hausmanowa-Petrusewicz, I, *et al.* (1980). Is Kugelberg-Welander spinal muscular atrophy a fetal defect? *Muscle Nerve* **3**: 389-402.

Haverkamp, L J, *et al.* (1995). Natural history of amyotrophic lateral sclerosis in a database population. Validation of a scoring system and a model for survival prediction. *Brain* **118**: 707-719.

Hayward, C, *et al.* (1999). Molecular genetic analysis of the APEX nuclease gene in amyotrophic lateral sclerosis. *Neurology* **52**: 1899-1901.

He, B P and Strong, M J (2000). Motor neuronal death in sporadic amyotrophic lateral sclerosis (ALS) is not apoptotic. A comparative study of ALS and chronic aluminium chloride neurotoxicity in New Zealand white rabbits. *Neuropathology and Applied Neurobiology* **26**: 150-160.

Hebert, M D, *et al.* (2001). Coilin forms the bridge between Cajal bodies and SMN, the spinal muscular atrophy protein. *Genes and Development* **15**: 2720-2729.

Hentati, A, *et al.* (1994). Linkage of recessive familial amyotrophic lateral sclerosis to chromosome 2q33-q35. *Nature Genetics* **7**: 425-428.

Hentati, A, *et al.* (1998). Linkage of a commoner form of recessive amyotrophic lateral sclerosis to chromosome 15q15-q22 markers. *Neurogenetics* **2**: 55-60.

Hood, D A, *et al.* (2000). Assembly of the cellular powerhouse: current issues in muscle mitochondrial biogenesis. *Exercise and Sport Sciences Reviews* **28**: 68-73.

Hornberger, T A, *et al.* (2001). Regulation of translation factors during hindlimb unloading and denervation of skeletal muscle in rats. *American Journal of Physiology and Cell Physiology* **281**: C179-C187.

Hosler, B A, *et al.* (2000). Linkage of familial amyotrophic lateral sclerosis with frontotemporal dementia to chromosome 9q21-q22. *Journal of American Medical Association* **284**: 1664-1669.

Hu, J H, *et al.* (2003a). Protein kinase and protein phosphatase expression in the central nervous system of G93A mSOD overexpressing mice. *Journal of Neurochemistry* **85**: 422-431.

Hu, J H, *et al.* (2003b). Protein kinase and protein phosphatase expression in amyotrophic lateral sclerosis spinal cord. *Journal of Neurochemistry* **85**: 432-442.

Huang, F, Chotiner, J K and Stewart, O (2005). The mRNA for elongation factor 1α is localized in dendrites and translated in response to treatments that induce long-term depression. *Journal of Neuroscience* **25**(31): 7199-7209.

Huang, F, *et al.* (1994). Rapid inhibition of myogenin-driven acetylcholine receptor subunit gene transcription. *EMBO Journal* **13**: 634-640.

Huang, F, Neville, C M and Schmidt J (1993). Control of myogenic factor genes by the membrane depolarization/protein kinase C cascade in chick skeletal muscle. *FEBS Letter* **319**: 21-25.

Huang, F and Schmidt, J (1994). Calcium influx blocks the skeletal muscle acetylcholine receptor α-subunit gene *in vivo*. *FEBS Letter* **338**: 277-280.

Huang, F, Tong J and Schmidt, J (1992). Protein kinase C couples membrane excitation to acetylcholine receptor gene activation in chick skeletal muscle. *Neuron* **9**: 671-678.

Hughes, J T (1982). Pathology of amyotrophic lateral sclerosis. *Advances in Neurology* **36**: 61-74.

Iannaccone, S T, *et al.* (1987). Type 1 fiber size disproportion: morphometric data from 37 children with myopathic, neuropathic, or idiopathic hypotonia. *Pediatric Pathology* **7**: 395-419.

Ince, P, *et al.* (1993). Parvalbumin and calbindin D-28k in the human motor system and in motor neuron disease. *Neuropathology and Applied Neurobiology* **19**: 291-299.

Iborra, F J, Jackson, D A and Cook, P R (2001). Coupled transcription and translation within nuclei of mammalian cells. *Science* **293**: 1139-1142.

Inoue, T, *et al.* (1986). Effect of DNA-damaging agents on isolated spleen cells and lung fibroblasts from the mouse mutant "wasted," a putative animal model for ataxia-telangiectasia. *Cancer Research* **46**: 3979-3982.

Iwahashi, H, *et al.* (1997). Synergistic anti-apoptotic activity between Bcl-2 and SMN implicated in spinal muscular atrophy. *Nature* **390**: 413-417.

Jackman, R W and Kandarian, S C (2003). The molecular basis of skeletal muscle atrophy. *American Journal of Physiology, Endocrinology and Metabolism* **287**: C834-C843.

Jackson, M, *et al.* (1997). Copper/zinc superoxide dismutase 1 and sporadic amyotrophic lateral sclerosis: analysis of 155 cases and identification of a novel insertion mutation. *Annals of Neurology* **42**: 803-807.

Jackson, M, *et al.* (1996). Analysis of chromosome 5q13 genes in amyotrophic lateral sclerosis: homozygous NAIP deletion in a sporadic case. *Annals of Neurology* **39**: 796-800.

Jagoe, R T and Goldberg, A L (2001). What do we really know about the ubiquitin-proteasome pathway in muscle atrophy? *Current Opinion in Clinical Nutrition and Metabolics Care* **4**: 183-190.

Janssen, G M, *et al.* (1994). The subunit structure of elongation factor 1 from Artemia. Why two alpha-chains in this complex? *The Journal of Biological Chemistry* **269**: 31410-31417.

Job, C and Eberwine, J (2001). Localization and translation of mRNA in dendrites and axons. *Nature Reviews Neuroscience* **2**: 889-898.

Jones, K W, *et al.* (2001). Direct interaction of the spinal muscular atrophy disease protein SMN with the small nucleolar RNA-associated protein fibrillarin. *The Journal of Biological Chemistry* **276**: 38645-38651.

Kahns, S, *et al.* (1998). The elongation factor 1 A-2 isoform from rabbit: cloning of the cDNA and characterization of the protein. *Nucleic Acids Research* **26**: 1884-1890.

Kandel, E R and Schwartz, J H, Eds. (2000). Principles of neural science, 4th Edition. McGraw-Hill, New York, NY

Kaur, K J and Ruben, L (1994). Protein translation elongation factor-1 alpha from Trypanosoma brucei binds calmodulin. *The Journal of Biological Chemistry* **269**: 23045-23050.

Kawamura, Y, *et al.* (1981). Morphometric comparison of the vulnerability of peripheral motor and sensory neurons in amyotrophic lateral sclerosis. *Journal of Neuropathology and Experimental Neurology* **40**: 667-675.

Kent, M P, Spencer, M J and Koohmaraie, M (2004). Postmortem proteolysis is reduced in transgenic mice overexpressing calpastatin. *Journal of Animal Science* **82**: 794-801.

Khalyfa, A, *et al.* (2001). Characterization of elongation factor-1A (eEF1A-1) and eEF1A-2/S1 protein expression in normal and wasted mice. *The Journal of Biological Chemistry* **276**: 22915-22922.

Khalyfa, A, *et al.* (1999). Toxin injury-dependent switched expression between EF-1 alpha and its sister, S1, in rat skeletal muscle. *Developmental Dynamics* **216**: 267-273.

Khalyfa, A, *et al.* (2003). Changes in protein levels of elongation factors, eEF1A-1 and eEF1A-2, in long-term denervated rat muscle. *Restorative Neurology and Neuroscience* **21**: 47-53.

Kikuchi, S, *et al.* (2000). Detection of an Amadori product, 1-hexitol-lysine, in the anterior horn of the amyotrophic lateral sclerosis and spinobulbar muscular atrophy spinal cord: evidence for early involvement of glycation in motoneuron diseases. *Acta Neuropathologica* **99**: 63-66.

Klocke, R, *et al.* (1994). Role of innervation, excitability, and myogenic factors in the expression of the muscular chloride channel ClC-1. A study on normal and myotonic muscle. *The Journal of Biological Chemistry* **269**: 27635-27639.

Knudsen, S M, *et al.* (1993). Tissue-dependent variation in the expression of elongation factor-1 alpha isoforms: isolation and characterisation of a cDNA encoding a novel variant of human elongation-factor 1 alpha. *European Journal of Biochemistry* **215**: 549-554.

Koch, M C, *et al.* (1992). The skeletal muscle chloride channel in dominant and recessive human myotonia. *Science* **257**: 797-800.

Kong, J and Xu, Z (1998). Massive mitochondrial degeneration in motor neurons triggers the onset of amyotrophic lateral sclerosis in mice expressing a mutant SOD1. *Journal of Neuroscience* **18**: 3241-3250.

Kostic, V, *et al.* (1997). Bcl-2: prolonging life in a transgenic mouse model of familial amyotrophic lateral sclerosis. *Science* **277**: 559-562.

Krainc, D, *et al.* (1998). Synergistic activation of the N-methyl-D-aspartate receptor subunit 1 promoter by myocyte enhancer factor 2C and Sp1. *The Journal of Biological Chemistry* **273**: 26218-26224.

Krieg, P A, *et al.* (1989). The mRNA encoding elongation factor 1-alpha (EF-1 alpha) is a major transcript at the midblastula transition in Xenopus. *Developmental Biology* **133**: 93-100.

Kulkarni, G, *et al.* (2006). Expression of protein elongation factor eEF1A2 predicts favorable outcome in breast cancer. *Breast Cancer Research and Treatment* Aug 9; [Epub ahead of print]

Kunst, C B, *et al.* (2000). Genetic mapping of a mouse modifier gene that can prevent ALS onset. *Genomics* **70**: 181-189.

Lambrechts, D, *et al.* (2003). VEGF is a modifier of amyotrophic lateral sclerosis in mice and humans and protects motoneurons against ischemic death. *Nature Genetics* **34**: 383-394.

LaFramboise, W A, *et al.* (1991). Emergence of the mature myosin phenotype in the rat diaphragm muscle. *Developmental Biology* **144**: 1-15.

Lassar, A B, *et al.* (1989). MyoD is a sequence-specific DNA binding protein requiring a region of myc homology to bind to the muscle creatine kinase enhancer. *Cell* **58**: 823-831.

Lau, J, *et al.* (2006). Identification of elongation factor 1α as a potential associated binding partner for Akt2. *Molecular and Cellular Biochemistry* **286**: 17-22.

Lawlor, M A and Alessi, D R (2001). PKB/Akt: a key mediator of cell proliferation, survival and insulin response? *Journal of Cell Science* **114**: 2903-2910.

Leclerc, N, *et al.* (2001). Selective changes in mitochondria respiratory properties in oxidative or glycolytic muscle fibers isolated from G93AhumanSOD1 transgenic mice. *Neuromuscular Disorders* **11**: 722-727.

Lee, J M (2003). The role of protein elongation factor eEF1A2 in ovarian cancer. *Reproductive Biology and Endocrinology* **1**:69.

Lee, S, Ann, D K and Wang, E (1994). Cloning of human and mouse brain cDNAs coding for S1, the second member of the mammalian elongation factor-1 alpha gene family: analysis of a possible evolutionary pathway. *Biochemical and Biophysical Research Communications* **203**: 1371-1377.

Lee, S, *et al.* (1992). Tissue-specific expression in mammalian brain, heart, and muscle of S1, a member of the elongation factor-1 alpha gene family. *The Journal of Biological Chemistry* **267**: 24064-24068.

Lee, S, *et al.* (1995). Terminal differentiation-dependent alteration in the expression of translation elongation factor-1 alpha and its sister gene, S1, in neurons. *Experimenatal Cell Research* **219**: 589-597.

Lee, S, *et al.* (2004). Regulation of muscle protein degradation: coordinated control of apoptotic and ubiquitin-proteasome systems by phosphotidylinositol 3 kinase. *Journal of American Society of Nephrology* **15**: 1537-1545.

Lee, S, Stollar, E and Wang, E (1993a). Localization of S1 and elongation factor-1 alpha mRNA in rat brain and liver by non-radioactive in situ hybridization. *Journal of Histochemistry and Cytochemistry* **41**: 1093-1098.

Lee, S, Wolfraim, L and Wang, E (1993b). Differential expression of S1 and elongation factor-1 alpha during rat development. *The Journal of Biological Chemistry* **268**: 24453-24459.

Lee, S, *et al.* (1995). Terminal differentiation-dependent alteration in the expression of translation elongation factor-1 alpha and its sister gene, S1, in neurons. *Experimental Cell Research* **219**: 589-597.

Lefebvre, S, *et al.* (1995). Identification and characterization of a spinal muscular atrophy-determining gene. *Cell* **80**: 155-165.

Lefebvre, S, *et al.* (1997). Correlation between severity and SMN protein level in spinal muscular atrophy. *Nature Genetics* **16**: 265-269.

Léger, B, *et al.* (2006). Human skeletal muscle atrophy in amyotrophic lateral sclerosis reveals a reduction in Akt and an increase in atrogin-1. *The FASEB Journal* **20**: 583-585.

Leigh, P N, *et al.* (1988). Ubiquitin deposits in anterior horn cells in motor neurone disease. *Neuroscience Letters* **93**: 197-203.

Li, Q, *et al.* (2004). A syntaxin 1, $G\alpha_o$, and N-type calcium channel complex at a presynaptic nerve terminal: analysis by quantitative immunocolocalization. *Journal of Neuroscience* **24**: 4070-4081.

Lin, C L, *et al.* (1998). Aberrant RNA processing in a neurodegenerative disease: the cause for absent EAAT2, a glutamate transporter, in amyotrophic lateral sclerosis. *Neuron* **20**: 589-602.

Liston, P, *et al.* (1996). Suppression of apoptosis in mammalian cells by NAIP and a related family of IAP genes. *Nature* **379**: 349-353.

Liu, Q. and Dreyfuss, G (1996). A novel nuclear structure containing the survival of motor neurons protein. *EMBO Journal* **15**: 3555-3565.

Liu, Q, *et al.* (1997). The spinal muscular atrophy disease gene product, SMN, and its associated protein SIP1 are in a complex with spliceosomal snRNP proteins. *Cell* **90**: 1013-1021.

Liu, Q, *et al.* (2002). Interaction of elongation factor 1alpha with F-actin and beta-actin mRNA: implications for anchoring mRNA in cell protrusions. *Molecular Biology of the Cell* **13**: 579-592.

Loh, H (2003). Analysis of the role of eukaryotic translation elongation factor1 alpha-2 (EEF1A-2) in the wasted mouse mutant. PhD thesis, The Open University.

Lorkovic, H and Tomanek, R J (1977). Potassium and chloride conductances in normal and denervated rat muscles. *American Journal of Physiology* **232**: C109-C114.

Lorson, C L, *et al.* (1999). A single nucleotide in the SMN gene regulates splicing and is responsible for spinal muscular atrophy. *Proceedings of the National Academy of Sciences* **96**: 6307-6311.

Lu, X A and Werner, D (1989). The complete cDNA sequence of mouse elongation factor 1 alpha (EF 1 alpha) mRNA. *Nucleic Acids Research* **17**: 442.

Ludvigsson, P, *et al.* (1999). Spinal muscular atrophy. Incidence in Iceland. *Neuroepidemiology* **18**: 265-269.

Lund, A, *et al.* (1996). Assignment of human elongation factor 1alpha genes: EEF1A maps to chromosome 6q14 and EEF1A2 to 20q13.3. *Genomics* **36**: 359-361.

Lutsep, H L and Rodriguez, M (1989). Ultrastructural, morphometric, and immunocytochemical study of anterior horn cells in mice with "wasted" mutation. *Journal of Neuropathology and Experimental Neurology* **48**: 519-533.

Lynch, T, *et al.* (1994). Clinical characteristics of a family with chromosome 17-linked disinhibition-dementia-parkinsonism-amyotrophy complex. *Neurology* **44**: 1878-1884.

Lynch, G S (2001). Therapies for improving muscle function in neuromuscular disorders. *Exercise and Sport Science Reviews* **29**: 141-148.

Madsen, H O, *et al.* (1990). Retropseudogenes constitute the major part of the human elongation factor 1 alpha gene family. *Nucleic Acids Research* **18**: 1513-1516.

Mannen, T, *et al.* (1977). Preservation of a certain motoneurone group of the sacral cord in amyotrophic lateral sclerosis: its clinical significance. *Journal of Neurology, Neurosurgery and Psychiatry* **40**: 464-469.

Mansilla, F, *et al.* (2002). Mapping the human translation elongation factor eEF1H complex using the yeast two-hybrid system. *Biochemical Journal* **365**: 669-676.

Marchesi, V T and Ngo, N (1993). In vitro assembly of multiprotein complexes containing alpha, beta, and gamma tubulin, heat shock protein HSP70, and elongation factor 1 alpha. *Proceedings of the National Academy of Sciences* **90**: 3028-3032.

Martin, L J (1999). Neuronal death in amyotrophic lateral sclerosis is apoptosis: possible contribution of a programmed cell death mechanism. *Journal of Neuropathology and Experimental Neurology* **58**: 459-471.

Martin, L J, *et al.* (2000). Mechanisms for neuronal degeneration in amyotrophic lateral sclerosis and in models of motor neuron death (Review). *International Journal of Molecular Medicine* **5**: 3-13.

Martinuzzi, A, *et al.* (1986). Expression of muscle-gene-specific isozymes of phosphorylase and creatine kinase in innervated cultured human muscle. *Journal of Cell Biology*. **103**: 1423-1429.

Martinuzzi, A, *et al.* (1988). Asynchronous regulation of muscle specific isozymes of creatine kinase, glycogen phosphorylase, lactic dehydrogenase and phosphoglycerate mutase in innervated and non-innervated cultured human muscle. *Neuroscience Letters* **89**: 216-222.

Matera, A G and Frey, M R (1998). Coiled bodies and gems: Janus or gemini? *American Journal of Human Genetics* **63**: 317-321.

Matera, A G and Hebert, M D (2001). The survival motor neurons protein uses its ZPR for nuclear localization. *Nature Cell Biology* **3**: E93-E95.

Matsuura, T, *et al.* (1993). Identification of androgen receptor in the rat spinal motoneurons. Immunohistochemical and immunoblotting analyses with monoclonal antibody. *Neuroscience Letters* **158**: 5-8.

McAndrew, P E, *et al.* (1997). Identification of proximal spinal muscular atrophy carriers and patients by analysis of SMNT and SMNC gene copy number. *American Journal of Human Genetics* **60**: 1411-1422.

McClatchy, D B, *et al.* (2002). Novel Interaction between the M4 Muscarinic Acetylcholine Receptor and Elongation Factor 1A2. *The Journal of Biological Chemistry* **277**: 29268-29274.

McClatchy, D B, Fang, G and Levey A I (2006). Elongation factor 1A family regulates the recycling of the M4 muscarinic acetylcholine receptor. *Neurochemical Research* **31**: 975-988.

McGeachie, J and Allbrook, D (1978). Cell proliferation in skeletal muscle following denervation or tenotomy. *Cell and Tissue Research* **193**: 259-267.

McKay, S E, *et al.* (1996). The expression of trkB and p75 and the role of BDNF in the developing neuromuscular system of the chick embryo. *Development* **122**: 715-724.

Merlie, J P, *et al.* (1984). Denervation supersensitivity in skeletal muscle: analysis with a cloned cDNA probe. *Journal of Cell Biology* **99**: 332-335.

Merrick, W C (1992). Mechanism and regulation of eukaryotic protein synthesis. *Microbiology Reviews* **56**: 291-315.

Meyer, T, *et al.* (1999). The RNA of the glutamate transporter EAAT2 is variably spliced in amyotrophic lateral sclerosis and normal individuals. *Journal of the Neurological Sciences* **170**: 45-50.

Meyer, T, *et al.* (1998). The EAAT2 (GLT-1) gene in motor neuron disease: absence of mutations in amyotrophic lateral sclerosis and a point mutation in patients with hereditary spastic paraplegia. *Journal of Neurology, Neurosurgery and Psychiatry* **65**: 594-596.

Midrio, M (2006). The denervated muscle: facts and hypotheses. A historical review. *European Journal of Applied Physiology* **98**: 1-21.

Minella, O, *et al.* (1996). Major intracellular localization of elongation factor-1. *Cellular and Molecular Biology* **42**: 805-810.

Monani, U R, *et al.* (1999). A single nucleotide difference that alters splicing patterns distinguishes the SMA gene SMN1 from the copy gene SMN2. *Human Molecular Genetics* **8**: 1177-1183.

Monani, U R, *et al.* (2000). The human centromeric survival motor neuron gene (SMN2) rescues embryonic lethality in Smn(-/-) mice and results in a mouse with spinal muscular atrophy. *Human Molecular Genetics* **9**: 333-339.

Morales, J, *et al.* (1991). Purification and characterization of a germ cell-specific form of elongation factor 1 alpha (EF-1 alpha) from Xenopus laevis. *Biochimie* **73**: 1249-1253.

Mostacciuolo, M L, *et al.* (1992). Epidemiology of spinal muscular atrophies in a sample of the Italian population. *Neuroepidemiology* **11**: 34-38.

Moulard, B, *et al.* (1998). Association between centromeric deletions of the SMN gene and sporadic adult-onset lower motor neuron disease. *Annals of Neurology* **43**: 640-644.

Mulder, D W, *et al.* (1986). Familial adult motor neuron disease: amyotrophic lateral sclerosis. *Neurology* **36**: 511-517.

Musarò, A, *et al.* (2001). Localized Igf-1 transgene expression sustains hypertrophy and regeneration in senescent skeletal muscle. *Nature Genetics* **27**: 195-200.

Muscat, G E O and Kedes, L (1987). Multiple 5'-flanking regions of the human α-skeletal actin gene synergistically modulate muscle-specific expression. *Molecular and Cellular Biology* **7**: 4089-4099.

Nader, G A (2005). Molecular determinants of skeletal muscle mass: getting the "AKT" together. *The International Journal of Biochemistry and Cell Biology* **37**: 1985-1996.

Nader, G A, Hornberger, T A and Esser, K A (2002). Translational control: implications for skeletal muscle atrophy. *Clinical Orthopedics*: S178-S187.

Nagai, M, *et al.* (1998). Identification of alternative splicing forms of GLT-1 mRNA in the spinal cord of amyotrophic lateral sclerosis patients. *Neuroscience Letters* **244**: 165-168.

Negrutskii, B S and El'skaya, A V (1998). Eukaryotic translation elongation factor 1 alpha: structure, expression, functions, and possible role in aminoacyl-tRNA channeling. *Progress in Nucleic Acid Research and Molecular Biology* **60**: 47-78.

Newbery, H J (2003). The role of eEF1A-2 in the pathogenesis of motor neuron disease. PhD thesis, University of Edinburgh.

Newbery, H J, *et al.* (2005). Progressive loss of motor neuron function in wasted mice: effects of a spontaneous null mutation in the gene for the Eef1A2 translation factor. *Journal of Neuropathology and Experimental Neurology* **64**: 295-303.

Nguyen, M D, *et al.* (2003). Cell cycle regulators in the neuronal death pathway of amyotrophic lateral sclerosis caused by mutant superoxide dismutase 1. *Journal of Neuroscience* **23**: 2131-2140.

Nguyen, M D, Lariviere, R and Julien, J P (2000). Reduction of axonal caliber does not alleviate motor neuron disease caused by mutant superoxide dismutase 1. *Proceedings of the National Academy of Sciences* **97**: 12306-12311.

Nguyen, M D, *et al.* (2001). Deregulation of Cdk5 in a mouse model of ALS: toxicity alleviated by perikaryal neurofilament inclusions. *Neuron* **30**: 135-147.

Nordeen, S K, *et al.* (1984). Evaluations of wasted mouse fibroblasts and SV-40 transformed human fibroblasts as models of ataxia telangiectasia in vitro. *Mutation Research* **140**: 219-222.

Olkowski, Z L (1998). Mutant AP endonuclease in patients with amyotrophic lateral sclerosis. *Neuroreport* **9**: 239-242.

Olson, E N (1990). MyoD family: a paradigm for development? *Genes and Development* **4**: 1454-1461.

Ontell, M (1974). Muscle satellite cells: a validated technique for light microscopic identification and a quantitative study of changes in their population following denervation. *Anatomical Records* **178**: 211-228.

Oosthuyes, B, *et al.* (2001). Deletion of the hypoxia-response element in the vascular endothelial growth factor promoter causes motor neuron degeneration. *Nature Genetics* **28**: 131-138.

Pagliardini, S, *et al.* (2000). Subcellular localization and axonal transport of the survival motor neuron (SMN) protein in the developing rat spinal cord. *Human Molecular Genetics* **9**: 47-56.

Pallafacchina, G, *et al.* (2002). A protein kinase B-dependent and rapamycin-sensitive pathway controls skeletal muscle growth but not fiber type specification. *Proceedings of the National Academy of Sciences* **99**: 9213-9218.

Parton, M J, *et al.* (2002). D90A-SOD1 mediated amyotrophic lateral sclerosis: a single founder for all cases with evidence for a Cis-acting disease modifier in the recessive haplotype. *Human Mutation* **20**: 473-481.

Pasinelli, P, *et al.* (2000). Caspase-1 and -3 are sequentially activated in motor neuron death in Cu,Zn superoxide dismutase-mediated familial amyotrophic lateral sclerosis. *Proceedings of the National Academy of Sciences* **97**: 13901-13906.

Pellizzoni, L, *et al.* (2001a). The survival of motor neurons (SMN) protein interacts with the snoRNP proteins fibrillarin and GAR1. *Current Biology* **11**: 1079-1088.

Pellizzoni, L, *et al.* (2002). Purification of native survival of motor neurons complexes and identification of Gemin6 as a novel component. *The Journal of Biological Chemistry* **277**: 7540-7545.

Pellizzoni, L, *et al.* (2001b). A functional interaction between the survival motor neuron complex and RNA polymerase II. *Journal of Cell Biology* **152**: 75-85.

Pellizzoni, L, *et al.* (1998). A novel function for SMN, the spinal muscular atrophy disease gene product, in pre-mRNA splicing. *Cell* **95**: 615-624.

Pencil, S D, Toh, Y and Nicolson, G L (1993). Candidate metastasis-associated genes of the rat 13762NF mammary adenocarcinoma. *Breast Cabcer Research and Treatment* **25**: 165-174.

Petroulakis, E and Wang, E (2002). Nerve growth factor specifically stimulates translation of eukaryotic elongation factor 1A-1 (eEF1A-1) mRNA by recruitment to polyribosomes in PC12 cells. *The Journal of Biological Chemistry* **277**: 18718-18727.

Pette, D and Vrbovà, G (1985). Neural control of phenotypic expression in mammalian muscle fiber. *Muscle Nerve* **8**: 676-689.

Pfaff, S L, *et al.* (1996). Requirement for LIM homeobox gene Isl1 in motor neuron generation reveals a motor neuron-dependent step in interneuron differentiation. *Cell* **84**: 309-320.

Piette, J, *et al.* (1990). Two adjacent MyoD1-binding sites regulate expression of the acetylcholine receptor alpha-subunit gene. *Nature* **345**: 353-355.

Pollock, R and Treisman, R (1991). Human SRF-related proteins: DNA-binding properties and potential regulatory targets. *Genes and Development* **5**: 2327-2341.

Potter, M, *et al.* (1998). The wst gene regulates multiple forms of thymocyte apoptosis. *Cellular Immunology* **188**: 111-117.

Rabin, B A, *et al.* (1999). Autosomal dominant juvenile amyotrophic lateral sclerosis. *Brain* **122**: 1539-1550.

Reaume, A G, *et al.* (1996). Motor neurons in Cu/Zn superoxide dismutase-deficient mice develop normally but exhibit enhanced cell death after axonal injury. *Nature Genetics* **13**: 43-47.

Reiser, P J, *et al.* (1988). Functional significance of myosin transitions in single fibers of developing soleus muscle. *American Journal of Physiology* **254**: C605-C613.

Reynet, C and Kahn, C R (2001). Unbalanced expression of the different subunits of elongation factor 1 in diabetic skeletal muscle. *Proceedings of the National Academy of Sciences* **98**: 3422-3427.

Reynold, T H IV, Bodine, S C and Lawrence J C Jr (2002). Control of Ser2448 phosphorylation in the mammalian target of rapamycin by insulin and skeletal muscle load. *Journal of Biological Chemistry* **277**: 17657-17662.

Rhodes, S J and Konieczny, S F (1989). Identification of MRF4: a new member of the muscle regulatory factor gene family. *Genes and Development* **3**: 2050-2061.

Ripps, M E, *et al.* (1995). Transgenic mice expressing an altered murine superoxide dismutase gene provide an animal model of amyotrophic lateral sclerosis. *Proceedings of the National Academy of Sciences* **92**: 689-693.

Robertson, J, *et al.* (2003). A neurotoxic peripherin splice variant in a mouse model of ALS. *Journal of Cell Biology* **160**: 939-949.

Rocha, E M, *et al.* (2000). Identification of androgen receptor protein and 5alpha - reductase mRNA in human ocular tissues. *British Journal of Ophthalmology* **84**: 76-84.

Rogers, D C, *et al.* (1997). Bahavioral and functional analysis of mouse phenotype: SHIRPA, a proposed protocol for comprehensive phenotype assessment. *Mammalian Genome* **8**: 711-713.

Rommel, C, *et al.* (2001). Mediation of IGF-1-induced skeletal myotube hypertrophy by PI(3)K/Akt/Mtor and PI(3)K/Akt/GSK3 pathways. *Nature Cell Biology* **3**: 1009-1013.

Rosen, D R, *et al.* (1993). Mutations in Cu/Zn superoxide dismutase gene are associated with familial amyotrophic lateral sclerosis. *Nature* **362**: 59-62.

Rothstein, J D, Martin, L J and Kuncl, R W (1992). Decreased glutamate transport by the brain and spinal cord in amyotrophic lateral sclerosis. *New England Journal of Medicine* **326**: 1464-1468.

Rothstein, J D, *et al.* (1995). Selective loss of glial glutamate transporter GLT-1 in amyotrophic lateral sclerosis. *Annals of Neurology* **38**: 73-84.

Rowland, L P (1982). Diverse forms of motor neuron diseases. *Advances in Neurology* **36**: 1-13.

Rowland, L P (1998). Molecular basis of genetic heterogeneity: role of the clinical neurologist. *Journal of Child Neurology* **13**: 122-132.

Roy, N, *et al.* (1997). The c-IAP-1 and c-IAP-2 proteins are direct inhibitors of specific caspases. *EMBO Journal* **16**: 6914-6925.

Roy, N, *et al.* (1995). The gene for neuronal apoptosis inhibitory protein is partially deleted in individuals with spinal muscular atrophy. *Cell* **80**: 167-178.

Ruest, L-B, et al. (2002). Peptide Elongation Factor eEF1A-2/S1 Expression in Cultured Differentiated Myotubes and Its Protective Effect against Caspase- 3-mediated Apoptosis. *The Journal of Biological Chemistry* **277**: 5418-5425.

Sacheck, J M, *et al.* (2004). IGF-I stimulates muscle growth by suppressing protein breakdown and expression of atrophy-related ubiquitin ligases, atrogin-1 and MuRF1. *American Journal of Physiology, Endocrinology, and Metabolism* **287**: E591-E601.

Sampson, M J, *et al.* (1998). A novel isoform of the mitochondrial outer membrane protein VDAC3 via alternative splicing of a 3-base exon. Functional characteristics and subcellular localization. *The Journal of Biological Chemistry* **273**: 30482-30486.

Sanders, J, *et al.* (1996). Immunofluorescence studies of human fibroblasts demonstrate the presence of the complex of elongation factor-1 beta gamma delta in the endoplasmic reticulum. *Journal of Cell Science* **109**: 1113-1117.

Sandri, M, *et al.* (2004). Foxo transcription factors induce the atrophy-related ubiquitin ligase atrogin-1 and cause skeletal muscle atrophy. *Cell* **117**: 399-412.

Sassoon, D, *et al.* (1989). Expression of two myogenic regulatory factors myogenin and MyoD1 during mouse embryogenesis. *Nature* **341**: 303-307.

Scharf, J M, *et al.* (1998). Identification of a candidate modifying gene for spinal muscular atrophy by comparative genomics. *Nature Genetics* **20**: 83-86.

Schiaffino, S, *et al.* (1989). Three myosin heavy chain isoforms in type 2 skeletal muscle fibres. *Journal of Muscle Research and Cell Motility* **10**: 197-205.

Schlaepfer, W W (1974). Calcium-induced degeneration of axoplasm in isolated segments of rat peripheral nerve. *Brain Research* **69**: 203-215.

Schlaepfer, W W and Micko, S (1978). Chemical and structural changes of neurofilaments in transected rat sciatic nerve. *Journal of Cell Biology* **78**: 369-378.

Schoser, B G, Wehling, S and Blottner, D (2001). Cell death and apoptosis-related proteins in muscle biopsie of sporadic amyotrophic lateral sclerosis and polyneuropathy. *Muscle Nerve* **24**: 1083-1089.

Schuetze, S M and Role, L W (1987). Developmental regulation of nicotinic acetylcholine receptors. *Annual Reviews Neuroscience* **10**: 403-457.

Schweighoffer, F, *et al.* (1986). In vivo developmental modifications of the expression of genes encoding muscle-specific enzymes in rat. *The Journal of Biological Chemistry* **261**: 10271-10276.

Sedehizade, F, Klocke, R and Jockusch, H (1997). Expression of nerve-regulated genes in muscles of mouse mutants affected by spinal muscular atrophies and muscular dystrophies. *Muscle Nerve* **20**: 186-194.

Shaw, C E, *et al.* (1998). Mutations in all five exons of SOD-1 may cause ALS. *Annals of Neurology* **43**: 390-394.

Shepherd, J C, *et al.* (1989). Fruit flies with additional expression of the elongation factor EF-1 alpha live longer. *Proceedings of the National Academy of Sciences* **86**(: 7520-7521.

Shiina, N, *et al.* (1994). Microtubule severing by elongation factor 1 alpha. *Science* **266**: 282-5.

Shirasawa, T, *et al.* (1992). Nucleotide sequence of rat elongation factor-1 alpha cDNA. *Nucleic Acids Research* **20**: 909.

Shultz, L D, et al. (1982). 'Wasted', a new mutant of the mouse with abnormalities characteristic to ataxia telangiectasia. *Nature* **297**: 402-404.

Siddique, T and Deng, H X (1996). Genetics of amyotrophic lateral sclerosis. *Human Molecular Genetics* **5**: 1465-1470.

Siddique, T, *et al.* (1991). Linkage of a gene causing familial amyotrophic lateral sclerosis to chromosome 21 and evidence of genetic-locus heterogeneity. *New England Journal of Medicine* **324**: 1381-1384.

Siddique, T, *et al.* (1996). Molecular genetic basis of familial ALS. *Neurology* **47**: 27S-34S.

Siklos, L, *et al.* (1998). Intracellular calcium parallels motoneuron degeneration in SOD-1 mutant mice. *Journal of Neuropathology and Experimental Neurology* **57**: 571-587.

Sjalander, A, *et al.* (1995). The D90A mutation results in a polymorphism of Cu,Zn superoxide dismutase that is prevalent in northern Sweden and Finland. *Human Molecular Genetics* **4**: 1105-1108.

Slobin, L I (1980). The role of eucaryotic factor Tu in protein synthesis. The measurement of the elongation factor Tu content of rabbit reticulocytes and other

mammalian cells by a sensitive radioimmunoassay. *European Journal of Biochemistry* **110**: 555-563.

Smeitink, J, *et al.* (2001). The genetics and pathology of oxidative phosphorylation. *Nature Reviews Genetics* **2**: 342-352.

Smith, D S, *et al.* (2001). Cdk5 on the brain. *Cell Growth and Differentiation* **12**: 277-283.

Smith, R G, *et al.* (1996). Autoimmunity and ALS. *Neurology* **47**: S40-S50.

Snow, M H (1983). A quantitative ultrastructural analysis of satellite cells in denervated fast and slow muscles of the mouse. *Anatomical Records* **207**: 593-604.

Sommer, B, *et al.* (1991). RNA editing in brain controls a determinant of ion flow in glutamate-gated channels. *Cell* **67**: 11-19.

Spencer, M J, *et al.* (2002). Stable expression of calpain 3 from a muscle tarnsgene in vivo: immature muscle in transgenic mice suggests a role for calpain 3 in muscle maturation. *Proceedings of the National Academy of Sciences* **99**: 8874-8879.

Spencer, M J and Mellgren, R L (2002). Over-expression of a calpastatin transgene in mdx muscle reduces dystrophic pathology. *Human Molecular Genetics* **11**: 2645-2655.

Spencer, P S, *et al.* (1987a). Cycad use and motor neurone disease in Kii peninsula of Japan. *Lancet* **2**: 1462-1463.

Spencer, P S, *et al.* (1987). Cycad use and motor neurone disease in Irian Jaya. *Lancet* **2**: 1273-1274.

Steinmeyer, K, *et al.* (1991). Primary structure and functional expression of a developmentally regulated skeletal muscle chloride channel. *Nature* **354**: 301-304.

Stitt, T N, *et al.* (2004). The IGF-1/PI3K/Akt pathway prevents expression of muscle atrophy-induced ubiquitin ligases by inhibiting FOXO transcription factors. *Molecular Cell* 14(3): 395-403.

Stone, J, *et al.* (1987). Definition of regions in human c-myc that are involved in transformation and nuclear localization. *Molecular and Cellular Biology* **7**: 1697-1709.

Strasswimmer, J, *et al.* (1999). Identification of survival motor neuron as a transcriptional activator-binding protein. *Human Molecular Genetics* **8**: 1219-1226.

Subramaniam, J R, *et al.* (2002). Mutant SOD1 causes motor neuron disease independent of copper chaperone-mediated copper loading. *Nature Neuroscience* **5**: 301-307.

Swerdlow, R H, *et al.* (1998). Mitochondria in sporadic amyotrophic lateral sclerosis. *Experimental Neurology* **153**: 135-142.

Taanman, J W, *et al.* (1992). Steady-state transcript levels of cytochrome c oxidase genes during human myogenesis indicate subunit switching of subunit VIa and co-expression of subunit VIIa isoforms. *Biochimica et Biophysica Acta* **1139**: 155-162.

Tachibana, M, *et al.* (2000). Expression of Androgen Receptor in Mouse Eye Tissues. *Investigative Ophthalmology and Vision Science* **41**: 64-66.

Takahashi, A, *et al.* (2002). Myogenic Akt signaling regulates blood vessel recruitment during myofiber growth. *Molecular Cell Biology* **22**: 4803-4814.

Takuma, H, *et al.* (1999). Reduction of GluR2 RNA editing, a molecular change that increases calcium influx through AMPA receptors, selective in the spinal ventral gray of patients with amyotrophic lateral sclerosis. *Annals of Neurology* **46**: 806-815.

Tanabe, Y and Jessell, T M (1996). Diversity and pattern in the developing spinal cord. *Science* **274**: 1115-1123.

Tanaka, E and Sabry, J (1995). Making the connection: cytoskeletal reaarrangements during growth cone guidance. *Cell* **83**: 171-176.

Tapscott, S J, *et al.* (1988). MyoD1: a nuclear phosphoprotein requiring a Myc homology region to convert fibroblasts to myoblasts. *Science* **242**: 405-411.

Tatsuka, M, *et al.* (1992). Elongation factor-1 alpha gene determines susceptibility to transformation. *Nature* **359**: 333-336.

Terro, F, *et al.* (1998). Mild kainate toxicity produces selective motoneuron death with marked activation of CA(2+)-permeable AMPA/kainate receptors. *Brain Research* **809**: 319-324.

Tezuka, H, *et al.* (1986). Evaluation of the mouse mutant "wasted" as an animal model for ataxia telangiectasia. I. Age-dependent and tissue-specific effects. *Mutation Research* **161**: 83-90.

Thayer, M J, *et al.* (1989). Positive autoregulation of the myogenic determination gene MyoD1. *Cell* **58**: 241-248.

Thieme, A, *et al.* (1993). Epidemiological data on Werdnig-Hoffmann disease in Germany (West-Thuringen). *Human Genetics* **91**: 295-297.

Thisse, B, *et al.* (1988). Sequence of the twist gene and nuclear localization of its protein in endomesodermal cells of early Drosophila embryos. *EMBO Journal* **7**: 2175-2183.

Toker, A (2000). Protein kinases as mediators phosphoinositide 3-kinase signaling. *Molecular Pharmacology* **57**: 652-658.

Tomlinson, V A, *et al.* (2005). Translation elongation factor eEF1A2 is a potential oncoprotein that is overexpressed in two-thirds of breast tumours. *BMC cancer* **5**: 113.

Troy, C M, *et al.* (1990). Regulation of peripherin and neurofilament expression in regenerating rat motor neurons. *Brain Research* **529**: 232-238.

Tsokas, P, *et al.* (2005). Local protein synthesis mediates a rapid increase in dendritic elongation factor 1A after induction of late long-term potentiation. *Journal of Neuroscience* **25**(24): 5833-5843.

Tu, P H, *et al.* (1996). Transgenic mice carrying a human mutant superoxide dismutase transgene develop neuronal cytoskeletal pathology resembling human amyotrophic lateral sclerosis lesions. *Proceedings of the National Academy of Sciences* **93**: 3155-3160.

Uetsuki, T, *et al.* (1989). Isolation and characterization of the human chromosomal gene for polypeptide chain elongation factor-1 alpha. *The Journal of Biological Chemistry* **264**: 5791-5798.

Vielhaber, S, *et al.* (2003). Is there mitochondrial dysfunction in amyotrophic lateral sclerosis skeletal muscle? *Annals of Neurology* **53**: 686-687.

Vielhaber, S, *et al.* (2000). Mitochondrial DNA abnormalities in skeletal muscle of patients with sporadic amyotrophic lateral sclerosis. *Brain* **123**: 1339-1348.

Vielhaber, S, *et al.* (1999). Visualization of defective mitochondrial function in skeletal muscle fibers of patients with sporadic amyotrophic lateral sclerosis. *Journal of the Neurological Sciences* **169**: 133-139.

Viguie, C A, et al. (1997). Quantitative study of the effects of long-term denervation on the extensor digitorum longus muscle of the rat. *Anatomical Records* **248**: 346-354.

Villares, R and Cabrera, C V (1987). The achaete-scute gene complex of D. melanogaster: conserved domains in a subset of genes required for neurogenesis and their homology to myc. *Cell* **50**: 415-424.

Voytik, S L, *et al.* (1993). Differential expression of muscle regulatory factor genes in normal and denervated adult rat hindlimb muscles. *Developmental Dynamics* **198**: 214-224.

Wagey, R, *et al.* (1998). Phosphatidylinositol 3-kinase: increased activity and protein level in amyotrophic lateral sclerosis. *Journal of Neurochemistry* **71**: 716-722.

Waldvogel, H J, *et al.* (1991). Differential sensitivity of calbindin and parvalbumin immunoreactive cells in the striatum to excitotoxins. *Brain Research* **546**: 329-335.

Wang, C H, *et al.* (1996). Characterization of survival motor neuron (SMNT) gene deletions in asymptomatic carriers of spinal muscular atrophy. *Human Molecular Genetics* **5**: 359-365.

Wang, Q, *et al.* (2001). Comparative studies on the expression patterns of three troponin T genes during mouse development. *Anatomical Records* **263**: 72-84.

Wang, Z, *et al.* (2004). Endothelial and hematopoietic cell fate of human embryonic stem cells originates from primitive endothelium with hemangioblastic properties. *Science* **304**: 1164-1166.

Weintraub, H, *et al.* (1991). Muscle-specific transcriptional activation by MyoD. *Genes and Development* **5**: 1377-1386.

Whiteman, E L, Cho H and Birnbaum M J. Role of Akt/protein kinase B in metabolism. *Trends in Endocrinology and Metabolism* **13**: 444-451.

Wickham, L A, *et al.* (2000). Identification of androgen, estrogen and progesterone receptor mRNAs in the eye. *Acta Ophthalmologica Scandinevica* **78**: 146-153.

Wiedemann, F R, *et al.* (1998). Impairment of mitochondrial function in skeletal muscle of patients with amyotrophic lateral sclerosis. *Journal of the Neurological Sciences* **156**: 65-72.

Wilkes, J J and Bonen, A (2000). Reduced insulin-stimulated glucose transport in denervated muscle is associated with impaired Akt-alpha activation. *American Journal of Physiology, Endocrinology, and metabolism* **279**: E912-E919.

Williams, B Y, *et al.* (2000). The survival motor neuron protein interacts with the transactivator FUSE binding protein from human fetal brain. *FEBS Letters* **470**: 207-210.

Williams, B Y, *et al.* (1999). Differential subcellular localization of the survival motor neuron protein in spinal cord and skeletal muscle. *Biochemistry and Biophysics Research Communications* **254**: 10-14.

Williams, T L, *et al.* (1997). Calcium-permeable alpha-amino-3-hydroxy-5-methyl-4-isoxazole propionic acid receptors: a molecular determinant of selective vulnerability in amyotrophic lateral sclerosis. *Annals of Neurology* **42**: 200-207.

Williamson, T L, *et al.* (1998). Absence of neurofilaments reduces the selective vulnerability of motor neurons and slows disease caused by a familial amyotrophic lateral sclerosis-linked superoxide dismutase 1 mutant. *Proceedings of the National Academy of Sciences* **95**: 9631-9636.

Wischmeyer, E, *et al.* (1993). Development of electrical myotonia in the ADR mouse: role of chloride conductance in myotubes and neonatal animals. *Neuromuscular Disorders* **3**: 267-274.

Witzemann, V, *et al.* (1989). Developmental regulation of five subunit specific mRNAs encoding acetylcholine receptor subtypes in rat muscle. *FEBS Letters* **242**: 419-424.

Wong, P C, *et al.* (1995). An adverse property of a familial ALS-linked SOD1 mutation causes motor neuron disease characterized by vacuolar degeneration of mitochondria. *Neuron* **14**: 1105-1116.

Wong, P C, *et al.* (1998). The genetic and molecular mechanisms of motor neuron disease. *Current Opinion in Neurobiology* **8**: 791-799.

Wright, W. E., D. A. Sassoon, *et al.* (1989). "Myogenin, a factor regulating myogenesis, has a domain homologous to MyoD." Cell **56**(4): 607-617.

Yanagihara, R, *et al.* (1984). Calcium and vitamin D metabolism in Guamanian Chamorros with amyotrophic lateral sclerosis and parkinsonism-dementia. *Annals of Neurology* **15**: 42-48.

Yang, F, *et al.* (1990). Identification of an actin-binding protein from Dictyostelium as elongation factor 1a. *Nature* **347**: 494-496.

Yang, Y, *et al.* (2001). The gene encoding alsin, a protein with three guanine-nucleotide exchange factor domains, is mutated in a form of recessive amyotrophic lateral sclerosis. *Nature Genetics* **29**: 160-165.

Young, P J, *et al.* (2000). The relationship between SMN, the spinal muscular atrophy protein, and nuclear coiled bodies in differentiated tissues and cultured cells. *Experimental Cell Research* **256**: 365-374.

Younger, D S, *et al.* (1991). Lymphoma, motor neuron diseases, and amyotrophic lateral sclerosis. *Annals of Neurology* **29**: 78-86.

Yu, Y T, *et al.* (1992). Human myocyte-specific enhancer factor 2 comprises a group of tissue-restricted MADS box transcription factors. *Genes and Development* **6**: 1783-1798.

Yutzey, K E, *et al.* (1990). Differential trans activation associated with the muscle regulatory factors MyoD1, myogenin, and MRF4. *Molecular and Cellular Biology* **10**: 3934-3944.

Appendix 1

Sequence of the *HSA-EEF1A2* fragment of the pUC19-HSA-EEF1A2 plasmid (*HSA* sequence is indicated in blue, and its first exon is in bold; Sequences of Exon 2 to Exon 8 of human *EEF1A2* are indicated in bold; Underlines denote *Hind*III and *Kpn*I sites used to remove the *HSA-EEF1A2* fragment.).

5'

```
gacgaaagggcctcgtgatacgcctatttttataggttaatgtcatgataataatggttt   60
cttagacgtcaggtggcacttttcggggaaatgtgcgcggaacccctatttgtttatttt   120
tctaaatacattcaaatatgtatccgctcatgagacaataaccctgataaatgcttcaat   180
aatattgaaaaaggaagagtatgagtattcaacatttccgtgtcgcccttattccctttt   240
ttgcggcattttgccttcctgtttttgctcacccagaaacgctggtgaaagtaaaagatg   300
ctgaagatcagttgggtgcacgagtgggttacatcgaactggatctcaacagcggtaaga   360
tccttgagagttttcgccccgaagaacgttttccaatgatgagcacttttaaagttctgc   420
tatgtggcgcggtattatcccgtattgacgccgggcaagagcaactcggtcgccgcatac   480
actattctcagaatgacttggttgagtactcaccagtcacagaaaagcatcttacggatg   540
gcatgacagtaagagaattatgcagtgctgccataaccatgagtgataacactgcggcca   600
acttacttctgacaacgatcggaggaccgaaggagctaaccgctttttgcacaacatgg   660   pUC19
gggatcatgtaactcgccttgatcgttgggaaccggagctgaatgaagccataccaaacg   720
acgagcgtgacaccacgatgcctgtagcaatggcaacaacgttgcgcaaactattaactg   780
gcgaactacttactctagcttcccggcaacaattaatagactggatggaggcggataaag   840
ttgcaggaccacttctgcgctcggcccttccggctggctggtttattgctgataaatctg   900
gagccggtgagcgtgggtctcgcggtatcattgcagcactggggccagatggtaagccct   960
cccgtatcgtagttatctacacgacggggagtcaggcaactatggatgaacgaaatagac  1020
agatcgctgagataggtgcctcactgattaagcattggtaactgtcagaccaagtttact  1080
catatatactttagattgatttaaaacttcatttttaatttaaaaggatctaggtgaaga  1140
tccttttgataatctcatgaccaaaatcccttaacgtgagttttcgttccactgagcgt  1200
cagaccccgtagaaaagatcaaaggatcttcttgagatccttttttttctgcgcgtaatct  1260
gctgcttgcaaacaaaaaaaccaccgctaccagcggtggtttgtttgccggatcaagagc  1320
taccaactctttttccgaaggtaactggcttcagcagagcgcagataccaaatactgttc  1380
ttctagtgtagccgtagttaggccaccacttcaagaactctgtagcaccgcctacatacc  1440
tcgctctgctaatcctgttaccagtggctgctgccagtggcgataagtcgtgtcttaccg  1500
ggttggactcaagacgatagttaccggataaggcgcagcggtcgggctgaacgggggttt  1560
cgtgcacacagcccagcttggagcgaacgacctacaccgaactgagatacctacagcgtg  1620
agctatgagaaagcgccacgcttcccgaagggagaaaggcggacaggtatccggtaagcg  1680
gcagggtcggaacaggagagcgcacgagggagcttccagggggaaacgcctggtatcttt  1740
atagtcctgtcgggtttcgccacctctgacttgagcgtcgatttttgtgatgctcgtcag  1800
gggggcggagcctatggaaaaacgccagcaacgcggccttttacggttcctggccttttt  1860
```

gctggccttttgctcacatgttctttcctgcgttatcccctgattctgtggataaccgta 1920
ttaccgcctttgagtgagctgataccgctcgccgcagccgaacgaccgagcgcagcgagt 1980
cagtgagcgaggaagcggaagagcgcccaatacgcaaaccgcctctccccgcgcgttggc 2040
cgattcattaatgcagctggcacgacaggtttcccgactggaaagcgggcagtgagcgca 2100
acgcaattaatgtgagttagctcactcattaggcaccccaggctttacactttatgcttc 2160
cggctcgtatgttgtgtggaattgtgagcggataacaatttcacacaggaaacagctatg 2220
accatgattacgccaagcttctctgtaaggaaaggtaagagttgaactgagcaagagtttt 2280 *Hind*III
gaaaaatagtgacaatcccattctcctttggaatgcgcacaaatattgaggtatccagtg 2340
aacggcagcaaatttcctaccttcaaggcccaaatgtaagctagtccccttacgttacat 2400
gcagctcatttgctaagtggtttttttctagtatctccactactcgctgacacaggagga 2460
cacaggatgttaaaaaggaaatacagttctgtcaattattcacttactctccaaaatact 2520
tggaagaactaaatatggaaccataggagactttatcctcaccgcatagtccctatacta 2580
gtcaaactccttatttttaattgatcattttaggaaggtagcattttattcactagaa 2640
cattttgttaatacttgtttatttttgggatgaactgccatgatgtgggctacagagga 2700
gggtcgcatatgcttccatccccctttagagaatccacacctgtcccagttgctgggtt 2760
ccactaccaaaagtgaattgcaactattttaggagcacttaagcacatccgaaaaatgag 2820
tgattctgttctggcccacaccacatcactgatgtacccccttaaagcatgtccctgagt 2880
tcatcacagaagactgctcctcctgtgccctccacaaggttagaactgtccttgtcttag 2940
ggaaaaaggagagagagagagagagagagagagagagagagagagagagagagagaggg 3000
gacaggcaccaactgggtaacctctgctgacccccactctactttaccataagtagctcc 3060
aaatccttctagaaaatctgaaaggcatagccccatatatcagtgatataaatagaacct 3120 HSA
gcagcaggctctggtaaatgatgactacaaggtggactgggaggcagcccggccttggca 3180 promoter
ggcatcatcctctaaatataaagatgagtttgttcagcctttgcagaaggaaaaactgcc 3240
acccatcctagagtgccgcgtccttgtccccccacccccctccaatttattgggaggaagg 3300
accagctaagcctcatctaggaagagcccctcacccatctccacctccactccaggtcta 3360
gccagtcctgggttgtgacccttgtctttcagccccaggagagggacacacatagtgcca 3420
ccaaagaggctgggggagggcctcagcccaccaaaacctggggccagtgcgtcctacagg 3480
aggggaaccctcacccctttcaatccctttaggagacccaagggcgctgcgcgtccctgag 3540
gcggacagctccgtgtgctcaggctttgcgcctgacaggcctatccccgggagcccccgc 3600
gcctcctccccggcgctccgccctcgcctcccccgccagttgtctatcctgcgacagct 3660
gcgcgccctccggccgccggtggccctctgtgcggtgggggaaggggtcgacgtggctca 3720
gctttttggattcagggagctcgggggtgggaagagagaaatggagttccaggggcgtaa 3780
aggagagggagttcgccttccttcccttcctgagactcaggagtgactgcttctccaatc 3840
ctcccaagcccaccactccacacgactccctcttcccggtagtcgcaagtgggagtttgg 3900
ggatctgagcaaagaacccgaagaggagttgaaatattggaagtcagcagtcaggcacct 3960
tcccgagcgcccagggcgctcagagtggacatggttggggaggcctttgggacaggtgcg 4020
gttcccggagcgcaggcgcacacatgcacccaccggcgaacgcggtgaccctcgccccac 4080
cccatcccctccggcgggcaactgggtcgggtcaggaggggcaaacccgctagggagaca 4140
ctccatatacggcccggcccgcgttacctgggaccgggccaacccgctccttctttggtc 4200
aacgcaggggacccgggcgggggcccaggccgcgaaccggccgagggaggggctctagt 4260

gcccaacacccaaatatggctcgagaagggcagcgacattcctgcggggtggcgcggagg 4320

gaatgcccgcgggctatataaaacctgagcagagggacaagc**GGCCACCGCAGCGGACAG** 4380 Exon 1 of

CGCCAAGTGAAGCCTCGCTTCCCCTCCGCGGCGACCAGGGCCCGAGCCGAGAGTAGCAGT 4440 HSA

TGTAGCTACCCGCCCAGgtagggcaggagttgggaggggacaggggacagggcactacc 4500 promoter

gaggggaacctgaaggactccggggcagaacccagtcggttcacctggtcagccccaggc 4560

ctgcgccctgagcgctgtgcctcgtctccggagccacacgcgctttaccggtctccccac 4620

caccactggccccacagaatcactgcagccccctcgccctgagccagagcaccccgggt 4680

cccgccagcccctcacactcccagcaaa**atgggcaaggagaagacccacatcaacatcgt** 4740 Exon 2 of

ggtcatcggccacgtggactccggaaagtccaccaccacgggccacctcatctacaaatg 4800 EEF1A2

cggaggtattgacaaaaggaccattgagaagttcgagaaggaggcggctgaggtgagctc 4860

cccaggctatggtcttggcccctgagaaggaacccccaactcccgtggtggccaggctt 4920

ggcatctcccagccccagggcatggggctcaggtgacctcctccagggcaggagggaccc 4980

ccgctgtggggcactcaggcctcagagggtctggtggggcagcctctctcttaggggag 5040

cttggtgggggaggggtggccatcgagctgccggacttgccctgtggtgagggaggtgac 5100

ctgggagggtctgcagaaggctctggaactctgccatgttgagctggggctggagggcgc 5160

tggagccttacccccttcccccccagggccaaggctggggctggagatggtactgccctca 5220

cttgtcctagggccctgccagggcacacgctactattaatagctgattgatgggcagccg 5280

gcccgtctgctccatttttcttgtgctgggctgtggagggctgctgtccagggcagccctg 5340

gggtgggggtcctggatgaggtgacctcctagctgacctttgaagcgatttctctttgg 5400

tggctgagacggtggtggggagcggtcatgagacggggtctgctctctgatccccatccc 5460

ccacccaggactctggggagaagcccactcctgggagggcctgtgggagctctcacctgg 5520

atgatgagggcggaggccagggcccaaggtgggggcactcgctgtcctgggctgagcctc 5580

tgccctggcggggttgggggtgctctgagctgcacccctgagtttgggctgcatcaccct 5640

ttacctggccttgtcaggaggaggcgggggtttcagagggccgctgtttcaggccccagc 5700

tgggtcccatctgggtctgctccagactgggcagcctcctggagggcagagtcctgtctg 5760

tgcgaggccctggcgaggagttctgcccagctgggtagtgaccgccgctgctgccctgac 5820

tgaagcccgtccccttctgtgggggtctcactggccgaggcccccagcttcccgtgtcc 5880

ggcagagcgaggaaggggaggagaagcctcagagggatggggaggctggagcagcgggaa 5940

ggagctgcgtggccaggccctcctcctgacctcattcagttttcctttctccttacctta 6000

aaaaaacacacacacacagagggttatttatctgacagccccaaacacggtggtattatt 6060

ggcctctggttgaggaagggatctgggggcgtccgcagcttcagataaaggggagccctc 6120

gcccgggaggggtttatcccatctggcggcttcgctcgtagagcgagcgactcccaggcc 6180

cttgcgccacctgctggtggacctgcgtagccgcgcccatttcggagcaggtgcggaggc 6240

cggccctgggggcagggtctgggtgtggggtcccgacggaggggccggcgtcccagga 6300

ccccgacggagagcaaggggtgctggagcccatctcccgcctctcgcggccactctgct 6360

gtaacaagcagctcgcaccaccagggactcctgggtcccgggtcccgccctcagccgtga 6420

ccctcacccgctccag**atggggaagggatccttcaagtatgcctgggtgctggacaagct** 6480 Exon 3 of

gaaggcggagcgtgagcgcggcatcaccatcgacatctccctctggaagttcgagaccac 6540 EEF1A2

caagtactacatcaccatcatcgatgccccggccaccgcgacttcatcaagaacatgat 6600

cacgggtacatcccaggtgagcagggcacagcaggcggggctgggggagaggccgctgca 6660

ccttcaagggacactgggggcccctggggtcactgggatggtagggtctcctgtgcttc 6720
ctgtgagggcaggggacccctcacctgggccaccctcacccagtctggctcagagccccc 6780
ctaaggatgaatccagtgctctggcatctgaaccagtgcctgtgaaggcatccagccagt 6840
gtcagagtccccagatagatgggggcagatggggacgtggacacaccttcatacatggag 6900
gggttggaggccaggatgggagagtgagcagtgggcagaggtgccacccgccaggtgta 6940
gactgtatgacatttcagggcactcacagagacgcacggacaccccagacacagcaccct 7000
gcagacagcaggacacatgccaccacctccaaactgctttgataactgtgacttctatcc 7060
gtcctcaagtgaggaacaggagcagataggctgagtgacttgtccagggacacacagccc 7120
actggtggtggagccagggctgaacctcggtcccctgacccagggcctggcgatgagccc 7180
ccatgctgcccttgaagtggggacccccatgcctccctccccaaggccccagtgggctgc 7240
tcaggccccagcccgctgcctggagaggcctggaagtgaggtggggccaggctcgctctg 7300
tcccctgccaggcaggcggggcagggctcactgtgtcccctgccgggcag**gcggactgcg** 7360
cagtgctgatcgtggcggcgggcgtgggcgagttcgaggcgggcatctccaagaatgggc 7420
agacgcgggagcatgccctgctggcctacacgctgggtgtgaagcagctcatcgtgggcg 7480
tgaacaaaatggactccacagagccggcctacagcgagaagcgctacgacgagatcgtca 7540
aggaagtcagcgcctacatcaagaagatcggctacaacccggccaccgtgccctttgtgc 7600
ccatctccggctggcacggtgacaacatgctggagccctcccccaacgtgagtggcggct 7660
agggcggggcgggccacgggagctggctggacccccctggcccagagcgaggcaccggcag 7720
gtggcacggggaggtcgagggcctgtccccgggaaatgcaggttcccctcgaaacctgct 7780
gggtttccctaactggctcagggcccggcggggagccccatgcccctcagcaccgggctt 7940
tgctcctacactcagcctcccacgcggctggccggggccagggcccatctacgatgtcaa 9000
cacagcaggggcagcggcctccagcaccaggcccatgtgcttggtctccagagccctgcc 9060
atgggggcggtcggtttcatctctgccaggccattgtcctggtcctggacaccgtgcagg 9120
ggctttgggctgggccgtgggggcctccttggctgcctcccctgggatcttggagcaggg 9180
ttgggctttgggaagtgtgcatgcttctgggcttgctgggatggccaagggttggctctt 9240
ggccggtcacctgggagctcaacgtgcgaacagtctgtagcccagggactctgccttggc 9300
tggaggtgacgcgtggagacacttgcagaacctgagactgttcccagggttctccaagcc 9360
agaggagaccccagaatggccaccactaggctctgccagcactgtcgctgcccacagtga 9420
gggtgcaggtgtggagtctagagacagcagggagacagaccagcagcactgagcctggag 9480
ctgaggtctggggacagaactgggagggactcccccagctccgcctccatctcacgaggc 9540
tcggtgttgtttacctgtgatggcgttttcctcatggggtatcatgtggcgaacgccact 9600
ctcccctccccagggaggcctccagccatcagggaccctgcactcccctctggcctgagc 9660
tgctaggtggctcgtgcttacacaggccctgggggctggggcactgtgctgccggcccc 9720
ctcccctgctccctgtttgtggcaggtggcccagagggaggcttcatgggatgggagtgg 9780
gggccacactaggagaagctccggacaaggctgggccaagctcggaggcagcacggtgtc 9840
cagaagctagggtggggcgaggctcctccagctctgtccctggcctggcccttggccaga 9900
ctcagcatcctcctagtcaagtcatctgccctgcctggagctgatggtcaggggcccggg 9960
gtttcggggacttggggctggactggggatttgttcacagtgtcagcaactcctgagcag 10020
cctgggctgggaagggtgctttccctctttgtcctcctccttttaagagggatctccttc 10080
ccagagtccctgtgatgctggggctatgggctggggaggagcagggtggggaaattcctc 10140

Exon 4 of EEF1A2

atctcaaagggcacgaggcaagtttagcctgaacagcagtactcctggaagcaccctggg 10200

gaggcctgagggtggggaggccaccaatgtctcttaacggattgattttctccctttggt 10260

ccag**atgccgtggttcaagggctggaaggtggagcgtaaggagggcaacgcaagcggcgt** 10320 Exon 5 of

gtcctgctggaggccctggacaccatcctgccccccacgcgccccacggacaagcccct 10380 EEF1A2

gcgcctgccgctgcaggacgtgtacaagattggcggtgagcaagggcgctgtgctggagc 10440

tcctgcctggccagctctgcctgccctagaccaggggcccctacaaggcatctcaagact 10500

gggctgtctccaatctctcccttaccacacactttctgtgggacagtccatcccacatc 10560

catccatccatccacccacctccccacccatccatcctctgtccatccatccacccatcc 10620

atctatccacctctccatccatctatctatccatccatccatccatcgatccatccatct 10680

ccccacccatccatccttcactccatccatccatccatccattgtcccatccatccttct 10740

ctctatcgaaccatccctccatctctccatctatccacctccccacccatccatccttct 10800

gtccatcaatccatccatccatccatccatccacctctccatccatccatccatctcccc 10860

acccatccatccttctctctatccatccatccatccatccattgattgtcccaccc 10920

atccatccttctctctatccctccatccatccatccatgcatccatccatccattgtccc 10980

acccatccatccttctctctatccatccatccatccttccatccatccatccacctcccc 11040

acccatccatccttctgtccatccatccatccatccatctctccatccatccatccatcc 11100

atccattgtctcaaccatccatccttctctctatccatccatccatccatccatccatct 11160

acccacccatccatccttctctctatccatccatctattgacccacccatccatccttct 11220

atctatccatccatccattcatccactcacccacctacccacccatccatccttctgtac 11280

atccatccatccatccatccacccacctacctatccatccatccttccatccatccattt 11340

atccatccatccatccatccatctatccacccacctacccacccatacatccatccatcc 11400

acctccccatccatccacttccccatccatccatccatccatccatctccccatccaccc 11460

atccacctctctatccatccatctccccacccagccatccttccctccatcatccatcca 11520

tccatctcatccatccgttcatctcctcatccatccatccatccatccatccatccatcc 11580

atccatccatccacctccccatccgtccgtccatccatccatccatctatcccccc 11640

atccatccatccatccatccatccatccatctatccatccacctccccatccatcc 11700

attcatccacccaccttcctacccatccatccttctgtccatccactcatctacctcctc 11760

atccatccatccatccatccatccaccaatccatccatccatctccctactcatccatct 11820

ccccacccatccttctgtccatccacctccccatccatctaccaccccattcatacatcc 11880

atccatccatccacccacctccccatccatccgtccatccatccatccatcccaccaaga 11940

agagaaaccataaacaaatctgagaccctagagaagggcactgataggagacccccagcc 12000

agtgggctgcagccaaagatgttgcaggcatctctgtgtgcactgtgggggcatcatgct 12060

caccccagcacagagcacagccactggcctcagtgaagttggctggaggctacaacaggc 12120

ctccctcacagccctgggaggtgagggtggagacccagtagcctgggggggggacaagacc 12180

cccatgtggcagctgcacaattggtttaagtagatccatgagaaatgccagggacgctca 12240

tgtgccgctgtgcctgtgctgcatctggctgagaggccccttttagtgatagagacctgca 12300

gcatccaagtggggcccagagagcctgcagggagcagggagcagggcctgcagggagcag 12360

ggagcagggccaccaggccccaggcagaagcagtcagtcgccccgcccacactcacaggg 12420

aggagtcctcagacaaaggaggggtcccatagtgcctcctttgagggaaagtgctctccg 12480

ggggcaaggatgggaccccaggttcagacagcccctctctgcccatcctcccgcttctct 12540

gtccctgtggcttttccgtgggttcctgggagctctgctgctcagcctcttatttcccca 12600
gctgggtgggagagcccccacttcccttggaatctctgtgtctgcccttgtccctggcct 12660
cccttcccctgcactccgcccatgtggccccaaccccccaggcctgtcgggggggatccagt 12720
cccaggctttgttggtttccaggctctgtccccgaatatcctgccccagcatcccctcgg 12780
gccccaccttcccctcacacccccctcccctctgcag**gcattggcacggtgcccgtgggcc** 12840
gggtggagaccggcatcctgcggccgggcatggtggtgacctttgcgccagtgaacatca 12900 Exon 6 of
ccactgaggtgaagtcagtggagatgcaccacgaggctctgagcgaagctctgcccggcg 12960 EEF1A2
acaacgtcggcttcaatgtgaagaacgtgtcggtgaaggacatccggcggggcaacgtgt 13020
gtggggacagcaagtctgacccgccgcaggaggctgctcagttcacctcccaggtggggg 13080
gctgcgctgggtccaggggctggcgcctgctggacagcagcaggactgtcctgggtgag 13140
gctgctgtcggcaggtggcctggcgtggggagaaaaccagaccctcaggctgggcgcagt 13200
ggttcacgcctgtaatcccagcactttgagaggccgaggcgggcagatcacgaggtcaag 13260
agatcaagtccatcctggtcaacatggtgaaaccccgtctctactaaaaatacaaaaatt 13320
agccaggcgtggtggcacgtgcctgtagtcccagctatcaggaagctgaggcaggagaat 13380
cgcttgaacctgggaggcggaggttgcagtgagccgagattgcgccactgcactccagcc 13440
tgcgtgacagagcgagacttcgtctcaaaagaaaaaaaaaaaaaagaaaagggacccgcat 13500
accaccgaggggccaccgagcactcaacgaggggatcaatcagttctgggaggggtgca 13560
ggccctgtggctcccagcctgtgtgcaatcgcgggtctgtcttccacgctgcactgctgg 13620
gatgcccagcctttgaggtcctacattcgtcctagaaaaacgcttttgttaacttactgt 13780
ctgagacatctctgtcatacttttattctctacagtcttcattgcccctctttgctggcc 13840
tcttcatatgatttatttatttttttttgagacggagtctcgctctgttgcccaggctg 13900
gagtgcagtggtgcgatctcggctcactgcaacctccgcctcccgggttcaagtgattct 13960
cctgcctcagcctcccaagtaggtaagattacaggcatgtgccaccacgcctggctaatt 14020
tttgtattattagtagatacggggtttcaccatgttggccaggccggtctcgaactcctg 14080
acctcaagtgatccacgtgcgtcagcctcccaaagtactgggatgacaggtgtgagccac 14140
cgtgcctggcctcttcatatgatttttaaaagtggctttattgagatacaactgaaacac 14200
aggaattgaggtccagttttgtcacccccccgccttagttccagctggggttggccgtgt 14260
aagtgctgcccctgcccccttcgaaacaatgaatctcagttgtttatcttttgcttaatga 14320
ggatgttgaggttcaggtctgggggctgggtcctcagagcctgagccccctccagtcagc 14380
actccgggcccaggagcccgtgcaggggcgccggtgactgggcctcccagccccgctctg 14440
gcgccctcccggtgcccaccgccgatgtgcctgatggccgcctgtggctccgctcgcag**g** 14500
tcatcatcctgaaccacccggggcagattagcgccggctactccccggtcatcgactgcc 14560
acacagcccacatcgcctgcaagtttgcggagctgaaggagaagattgaccggcgctctg 14620 Exon 7 of
gcaagaagctggaggacaaccccaagtccctgaagtctggagacgcggccatcgtggaga 14680 EEF1A2
tggtgccgggaaagcccatgtgtgtggagagcttctcccagtacccgcctctcggtgagc 14740
cggggtggtccggggaggtgcagcccccaggctgtggctgatccaggctgagggcagagg 14800
actgcggggatggggcgctggggacagcagtgggccccctttcctgcggagcttggccca 14860
gagcatggcaggagagccacggcctccgtgtcactgagtgcaggtgaccctgcccagacg 14920
agctggggtgggccctgtgtgcagacgaggccccgaaagtgagggaggccccgcgagtga 14980
ggaaggcccgcggtcgcccagtggcagcgttagggctgcccccgccccgtggccgccccg 15040

cagaccgtggagcagccgcccaggcaggactcccgcgaggccggccgtcttcacaggggc 15100
gcgctctgcgctaagcgtgttccgaggacattcccgacgcggttgcgcccccgcccggcc 15160
agagccctggggttgggggggtcaagtcctccggccccgcccacacgccgccccccgcc 15220
ccccag**gccgcttcgccgtgcgcgacatgaggcagacggtggccgtaggcgtcatcaaga** 15280 Exon 8 of
acgtggagaagaagagcggcggcgccggcaaggtcaccaagtcggcgcagaaggcgcaga 15340 EEF1A2
aggcgggcaagtgaagcgcgggcgcccgcggcgcgaccctccccggcggtgccgcgctcc 15400
gaaccccgggcccgggcccccgccccgcccccgcccccgcgcgccggtccggcgccccgca 15460
cccccgccaggcgcatgtctgcacctccgcttgccagaggccctcggtcagcgactggat 15520
gctcgccatcaaggtccagtggaagttcttcaagaggaaaggcgccccgccccaggctt 15580
ccgcgcccagcgctcgccacgctcagtgcccgttttaccaataaactgagcgaccccaga 15640
gccgtgtgcgcctgctgctgggggggtgggccccgcgccccccggaccccctccctgccca 15700
agtggccggcccagcatccttcactccctgcccggggaccccagggtgggcggtgggcct 15760
gcaagagtggtcccctgcgctgcacagggtgagcgctgagcgctcgctgaggagggcctg 15820
gtgtcccccaggccgtggcccagcagcaagaccccatccgaaggccaggtggcctgggtg 15880
gctttgaggggcttctccatggctactcagggcagagaatggtgccttcagatccacaga 15940
accaggctgcgggttttgggatctctgggggccgcatgagagctgagggctcctccaccg 16000
cgagtgactgtcacacacacactcattcttcccctggccccgcacacctggtctcactct 16060
cctgctaagccggtcacctgtggctgcagcctgtacctatccatcctgctcccaggtcca 16120
ggccctctgtacgtggttgtaggaactccagcccccgaacccgggaggctggtgacttca 16180
gtcagtgggctgggggctttgggtcttccctagtctctctgggctagaacctgccccgac 16240
cttggctgggaagagtggaggggtggggagaggggaggacagctcctttccacccctccc 16300
tgctctgggaaagcggccccggcccacagccagtcatgctgcagcaggtgaaggtcgggg 16360
tggagggtgagcaggttccctgaggatgcagaggagggtcagggtggagggtgggcagct 16420
tccttgaggatgcagaggagggtcagggtggagggtgggcagcttccctgaggatgcgga 16480
ggagggtggggtggagggtgggcaggttccctgaggatgcagaggagggttgggtggagg 16540
atgggcaggttccctgaggatgcagaggagggtggggtggaggatgggcaggttccctga 16600
ggatgcagaggagggtggggtggaggttgggcagcttccctgaggatgcagaggagggtc 16660
tgggtggagggtgggcaggctccctgaggatgcggaggagggtggggtggagggtgggca 16720
ggttccctgaggatgcggaggagggtggggtggagggtgggcaggttccctgaggatgca 16780
ggtgaggtcagggtggaggatgggcaggttccctgaggatgcagggagggtggggtggag 16840
ggtgggcaggttccctgaccctgtacacagcactgaggcaggcctctctgtcgcccagcc 16900
cccagctcccagcctgcagccgggtaccgagctcgaattcactggccgtcgttttacaac 16960 *Kpn*I
gtcgtgactgggaaaaccctggcgttacccaacttaatcgccttgcagcacatccccctt 17020
tcgccagctggcgtaatagcgaagaggcccgcaccgatcgcccttcccaacagttgcgca 17080
gcctgaatggcgaatggcgcctgatgcggtattttctccttacgcatctgtgcggtattt 17140
cacaccgcatatggtgcactctcagtacaatctgctctgatgccgcatagttaagccagc 17200
cccgacacccgccaacacccgctgacgcgccctgacgggcttgtctgctcccggcatccg 17260
cttacagacaagctgtgaccgtctccgggagctgcatgtgtcagaggttttcaccgtcat 17320
caccgaaacgcgcga 3' 17335

Appendix 2

Photographs comparing sizes of bodies, hindlimbs, and spleens of non-transgenic wild-type, transgenic wasted, and non-transgenic wasted mice.

WT tg, wasted non-tg, wasted

Bodies

WT tg, wasted non-tg, wasted

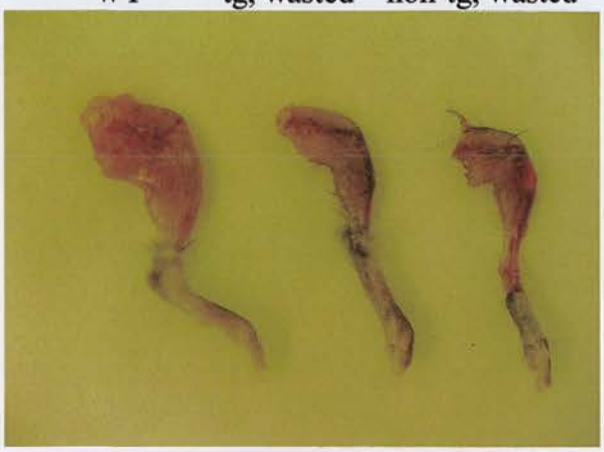

Hindlimbs

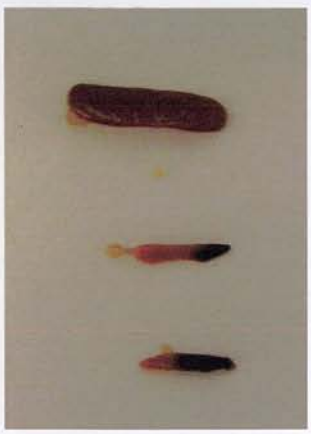

Spleen

WT

Tg, wasted

Non-tg, wasted